STUDIES OF ADSORPTION AND STABILIZATION OF SILICA SUSPENSIONS USING WELL-DEFINED POLYMERIC DISPERSANTS

by

Chiahong Chen

Dissertation submitted to the Faculty of the
Virginia Polytechnic Institute and State University
in partial fulfillment of the requirements for the degree of
Doctor of Philosophy
in
Chemical Engineering

Approved by:

Richey M. Davis, Chairman

James P. Wightman

Eva Marand

Judy S. Riffle

G. Alan Schick

June, 1994

Blacksburg, Virginia

Studies of Adsorption and Stabilization of Silica Suspensions Using Well-Defined Polymeric Dispersants

by
Chiahong Chen
Richey M. Davis, Chairman
Department of Chemical Engineering

Abstract

Solutions of poly(2-ethyl-2-oxazoline) and poly(2-methyl-2-oxazoline) in water and several alcohols were characterized by light scattering and cloud point measurements. The second virial coefficients in water were found to decrease with increasing temperature, reflecting lower critical solution behavior, which is consistent with the cloud point measurements. The temperature dependence of the second virial coefficients revealed that specific interactions between polymer and water dominated the free energy of mixing. The Flory-Huggins χ parameter determined from light scattering was in the range 0.48 - 0.49 in water and 0.32 - 0.41 in ethanol. The Kuhn length for PEOX was determined to be 0.77 nm which corresponds to less than two monomer units, indicating relatively flexible chains of PEOX.

The segmental adsorption energy, χ_s^{po}, of PEOX was measured using a desorption/displacement technique. PEOX was desorbed from silica with five low molecular weight organic displacers in two solvents - water and ethanol - to obtain values of the critical volume fraction of the displacer at which desorption was complete, ϕ_{cr}. The high adsorption energy parameters are consistent with the polymer adsorbing principally by hydrogen bonding between the carbonyl groups on the polymer and surface silanol groups. The difference in adsorption energies in water and ethanol reflect specific solvent effects that may be related to the formation of hydrogen bond bridges between PEOX and silanol groups in water.

Adsorption of PEOX from water, alcohols and chlorobenzene onto silica was investigated by measuring PEOX adsorption isotherms using a depletion method. A

linear relationship of the plateau adsorption amount, Γ_p, vs. *log* (molecular weight) was obtained, which agreed qualitatively with the Scheutjens-Fleer (S-F) mean field adsorption theory. The values of Γ_p varied significantly with solvent type as well as with pH and electrolyte concentration in water. These variations in Γ_p were due to changes of the polymer solvency and the silanol density on the silica particles.

Competitive adsorption experiments of PEOX with various polymers were performed, including poly(ethylene oxide) (PEO), poly(propylene oxide) (PPO) poly(vinyl methyl ether) (PVME), and poly(dimethyl siloxane) (PDMS). PEOX showed a higher affinity to the silica surface than other polymers. This suggested that PEOX had good potential for serving as an anchor block for diblock copolymer stabilizers for metal oxides in water.

The solubility of homopolymers PEOX, PEO, PPO, PVME, and PDMS and copolymers PEOX-PDMS and PEOX-PVME was investigated in water, alcohols, and chlorobenzene using static light scattering (SLS). The steric stabilization effect of silica dispersions in chlorobenzene by PEOX-PDMS was measured by dynamic light scattering (DLS). The stability was qualitatively related to the average particle hydrodynamic diameter against time.

The adsorbed amount and layer thickness of diblock copolymer poly(dimethyl amino ethyl methacrylate-*b*-n-butyl methacrylate) (DMAEM-BMA) on silica surfaces from isopropanol was measured. The linear dependence of the adsorbed amount and thickness with respect to the tail block length was obtained. This is consistent with the Marques-Joanny model.

ACKNOWLEDGMENT

Acknowledgement

First of all, I would like to thank Dr. Richey M. Davis, the Chairman of the Committee, for his guidance and financial support in the graduate study in the Department of Chemical Engineering. Without his patience and instructions, I could never finish this project in this period. Many thanks also go to Drs. J. P. Wightman, E. Marand, J. S. Riffle and G. A. Schick for serving on my committee and for coping with the short notice on my dissertation defense. Special thanks to Dr. J. S. Riffle and those people in her group for providing a series of polymers which were used in most of my research. In addition, I thank Drs. D. T. Wu and A. Yokoyama for kindly sending us the copolymers which we can proceed our experiments, and also for the helpful discussions.

I would also like to thank Dr. John E. Wilson of the University of Bristol, England, for his previous work on this subject when he was a Research Scientist in our group, and for the continuous knowledgeable discussions. Also, my deep appreciations are sent to Dr. Wen Chen of Hewlett Packard Co., CA., for his suggestions which lead to a great progress in the steric stabilization when he was a Research Scientist here.

Many thanks go to Dr. G. Chen, Dr. C. C. Chiu and my laboratory colleague A. Gaynor for their helps in TEM. The work containing in this dissertation benefitted greatly from these people.

I would like to express my sincere appreciation to the late Dr. J.M.H.M. Scheutjens in the Netherlands. With his advice and suggestions, we are able to continue our work with more confidence.

Finally, I would like to thank my parents. Without their encouragement, I can not finish this study here.

TABLE OF CONTENTS

Title	Page
Table of Contents	i
List of Figures	vi
List of Tables	ix
Abstract	
Chapter 1. Introduction	
General	1
Water Soluble Polymer in Solution	4
Polymer Adsorption	12
Polymer Stabilizers	18
Modified DLVO Theory	19
Applications of This Work	27
Goals of the Study	28
Thesis Organization	29
References	35
Chapter 2. Solution Properties of Poly(2-alkyl-2-oxazoline)s: Light Scattering, Cloud Point and Viscosity Studies	
Abstract	38
Introduction	38
Experimental	41
Materials and Solution Preparation	41
Partial Specific Volume	42
Light Scattering	42
GPC Analysis	44
Intrinsic Viscosity	44
Cloud Point	44
Results and Discussion	46
Molecular Weight Measurement	46
Second Virial Coefficient (A_2) Measurement	49
Effect of Temperature and Molecular Weight	49
Effect of Polymer Structure	53
Effect of Solvent Type	53

Chain Stiffness 53
Cloud Point 54
Conclusions 58
Appendices 60
References 62

Chapter 3. Nonionic Water-Soluble Polymer Segmental Adsorption Energy on a Silica Surface

Abstract 65
Introduction 65
Theoretical Background 70
Experimental 75
Materials 75
Displacer Adsorption Isotherms 76
Adsorption Isotherms of PEOX 78
Displacement Isotherms 78
Thin Layer Chromatography 79
Results and Discussion 79
Displacer Isotherm 79
PEOX Adsorption Isotherm 82
Displacement Isotherm for PEOX 84
Critical Displacer Energy 87
Calculation of χ_s^{po} 88
Comparison with PVP 93
Effect of the Lattice Parameter 95
Comparison with Polymers in Non-polar Solvents 95
Effect of Substrate Chemistry 96
Conclusions 96
References 98

CHAPTER 4. Adsorption Studies of Poly(ethyl-2-oxazoline)

Abstract 101
Introduction 101
Polymer Adsorption and Chain Conformation 102
Effect of Polymer Solubility 103
Competitive Adsorption 104
Chapter Outline 107

Adsorption Review 107
Scheutjens-Fleer Mean-Field Theory 108
Molecular Weight and Solvency Dependence 112
Concentration Dependence of the Adsorbed Amount 118
Adsorption Energy Dependence 119
Adsorbed Layer Thickness and Tails 119
Experimental 123
Materials 123
Solvents 123
Polymers 123
Adsorbent 123
Procedures 124
Solubility and MW 124
Adsorption Isotherm 125
Competitive Adsorption 125
Results and Discussion 127
Polymer Solution Properties 127
Adsorption Studies 129
Rate of Adsorption 129
Molecular Weight Dependence 129
Solvent Type Effect 136
pH Effect 137
Salt Effect 141
Competitive Adsorption 143
Conclusions 149
Appendix 150
References 151

CHAPTER 5. The Solubility and Adsorption of PEOX-PVME and PEOX-PDMS in Organic Solvents

Abstract 154
Introduction 154
Effect of Block Solubility on Stabilization 156
Effect of Block Structure on Adsorption 157
Chapter Outline 158
Theoretical Background 159
Copolymer Adsorption Theory 159
Effect of chain composition 161
Effect of solubility 164

Steric Stabilization 165
Coagulation Process 171
Experimental 173
Materials 173
Polymers 173
Solvents 174
Silica 175
Procedure 176
Light Scattering 176
Static Light Scattering 178
Dynamic Light Scattering 178
Adsorption Isotherm 180
Results and Discussion 182
Solution Properties 182
Homopolymers 182
Copolymers 184
Copolymer in Mixed Solvents 184
Adsorption Studies 185
Silica Characterization 186
Adsorption Isotherms 186
PEOX adsorption 187
Competitive Adsorption 187
PEOX/PDMS 191
PEOX/PVME 193
PEOX-PDMS Copolymer 195
Steric Stabilization 197
Stability Ratio in Chlorobenzene 197
Conclusions 205
Appendix 206
References 207

CHAPTER 6. Adsorption of Diblock Copolymer DMAEM-BMA on Silica from Isopropanol

Abstract 211
Introduction 211
Chapter Goal 213
Scaling Theory for Non-selective Solvents 213
Reviews of Adsorption Experiments 215

Experimental 217
Materials 217
Copolymers 217
Adsorbent 217
Procedure 220
Dynamic Light Scattering 220
Adsorption Isotherm 222
Results and Discussion 222
Hydrodynamic Thickness 222
Adsorption Isotherms 223
Conclusions 228
References 229

CHAPTER 7. Conclusions and Future Work

Summary 230
Future Work 232

Vita

LIST OF FIGURES

Figure		page
1.1	Effects of polymer chains on colloidal dispersions	2
1.2	(a) Polymer phase diagram versus polymer volume fraction (b) Cloud points of water-soluble polymers.	5
1.3	Polymer adsorption configuration at solid/liquid interface (a) Homopolymers, (b) Diblock copolymers, (c) Grafted Copolymer	14
1.4	The energy diagram for three stabilization mechanisms	24
1.5	(a) Dependence of the suspension viscosity on shear stress (b) Effect of the particle interactions on the suspensions	26
1.6	The chemical structures of homopolymers used in this study	30
1.7	The chemical structures of copolymers used in this study	31
1.8	The poly(alkyl oxazoline) synthesis process	32
2.1	Chemical structures of the repeat units of (a) Poly(2-ethyl-2-oxazoline) (b) Poly(2-methyl-2-oxazoline)	40
2.2	Typical static light scattering plot of PEOX in ethanol	45
2.3	Reduced excess thermodynamic dilution functions enthalpy of mixing and entropy of mixing for PEOX and PMOX in water	52
2.4	The cloud points of PEOX in water	56
2.5	The cloud points of PEOX against molecular weights	57
3.1	Displacer displaces solvent molecules from particle surface	71
3.2	Displacer displaces macromolecules in the presence of solvent	72
3.3	Adsorbed amount of displacers vs. displacer from water	80
3.4	Adsorbed amount of displacers vs. displacer from ethanol	81
3.5	Adsorbed amount of PEOX as a function of PEOX concentration	83
3.6	(a) Desorption isotherms of PEOX on silica from water (b) The adsorbed amount of PEOX as a function of retention determined by thin layer chromatography (TLC)	85 85

	(c) Desorption isotherms of PEOX on silica from ethanol	86
3.7	Thermodynamic properties of PEOX adsorption from water solution	90
3.8	Adsorption mechanism of PEOX from water and ethanol	91
4.1	Typical conformation of adsorbed polymer in S-F theory	109
4.2	(a) The adsorbed amount Γ against chain length	113
	(b) Fraction of adsorbed polymer, in trains, loops, and tails	114
4.3	(a) Total surface coverage as a function of chain length.	116
	(b) The Γ_{ex} as a function of ϕ^* at $\chi=0.5$ and $\chi=0$.	117
4.4	(a) The theoretical adsorbed amount Γ vs. χ_s	120
	(b) the direct surface coverage vs. χ_s	120
4.5	Theoretical hydrodynamic thickness δ_h vs. adsorbed amount	122
4.6	UV-vis spectroscopy of PEOX solution absorbance	126
4.7	Second virial coefficient of PEO in water	128
4.8	PEOX(60K) adsorption isotherm curve as a function of time	130
4.9	PEOX adsorption isotherms (a) from water (b) from ethanol	
	(c) from isopropanol and n-butanol	131
4.10	PEOX plateau adsorption amount vs. *log* MW from water and ethanol	135
4.11	PEOX(60K) adsorption isotherms from water and dioxane	138
4.12	The dependence of pH values on PEOX adsorption amount	139
4.13	Dependence of electrolyte concentration on PEOX adsorption amount	142
4.14	The comparison of χ_s and χ of PEOX and several polymers	146
4.15	Competitive adsorption of PEOX and PEO	148
5.1	A typical copolymer model for S-F theory	160
5.2	(a) Adsorbed amount of copolymer vs. anchor block composition	162
	(b) Adsorbed layer thickness vs. tail block length at different χ	162
5.3	Schematic representation of steric stabilization of suspensions	166
5.4	Schematic representation of the total energy vs. particle distance	167
5.5	Transmission electron micrograph of a typical silica dispersion	177

5.6	PEOX-PVME hydrodynamic diameter vs. water composition	185
5.7	(a) Adsorption isotherms of PEOX and PDMS from isopropanol	188
	(b) Adsorption isotherms of PEOX from chlorobenzene and water	189
5.8	Illustration of competitive adsorption	190
5.9	Competitive adsorption at different PDMS/PEOX chain ratios	192
5.10	Summary of the competitive adsorption of PEOX and other polymers with χ_s and χ	196
5.11	(a) PEOX-PDMS adsorption isotherm from Cab-O-Sil and Stöber silica	198
	(b) The adsorption isotherm of PEOX-PDMS from chlorobenzene	199
5.12	(a) Aggregation of silica in chlorobenzene	201
	(b) Steric stabilization of silica by PEOX-PDMS in chlorobenzene	202
6.1	A model of AB block in non-selective solvent	214
6.2	Chemical structure of DMAEM-BMA repeat unit	218
6.3	Transmission electron micrograph of a typical silica dispersion	221
6.4	Adsorbed layer thickness of DMAEM-BMA against block length	224
6.5	Adsorption Isotherms of DMAEM-BMA from isopropanol	225
6.6	(a) Linear relationship of surface coverage σ vs. $1/N_A$	227
	(b) Surface coverage compared with Wu's data	227

List of Tables

Table	Caption	Page
1.1	Applications of steric stabilization	3
1.2	Hamaker constants for various materials	21
2.1	Refractive index increments for poly(2-alkyl-oxazolines) at 510 nm	47
2.2	Second virial coefficients and molecular weights for poly(2-alkyl -2-oxazolines) as a function of temperature and solvent type	48
2.3	Molecular weight characterization data for poly(2-alkyl-2-oxazolines)	49
2.4	Effect of temperature on A_2 for poly(2-alkyl-2-oxazolines)	50
3.1	Summary of the PEOX molecular weight in this study	76
3.2	Structure and molecular volumes of solvents and displacers	77
3.3	Initial slopes of displacer adsorption isotherms on silica	82
3.4	Critical displacer volume fractions for PEOX 30K	87
3.5	Segmental adsorption energy (χ_s^{Po}) and combined solvency parameter	92
4.1	A summary of MW and χ parameter of the polymers	124
4.2	The plateau adsorbed amount of PEOX on Cab-O-Sil silica	134
4.3	A_2 coefficient and χ parameter of PEOX 17K in aqueous solutions	141
4.4	Summary of the competitive adsorption of PEOX with other polymers	144
4.5	The calculated polar and hydrogen bonding parameters of monomers	145
5.1	Summary of copolymer molecular weights	174
5.2	Summary of polymer solubility and molecular weight	183
5.3	Summary of polymer plateau adsorption amount	186
5.4	Competitive adsorption of PEOX and other polymers	194
5.5	The stability ratio of silica by copolymer	203
6.1	Characterization of DMAEM-BMA copolymer	217
6.2	Hydrodynamic thickness of DMAEM-BMA on silica surface	223
6.3	Adsorbed amount of DMAEM-BMA on silica surface	226

CHAPTER 1
Introduction

GENERAL

The adsorption of polymer chains at an interface is a complex phenomenon of considerable scientific and technological interest. When the interface consists of the surface of a colloidal particle in suspension, the state of aggregation of the suspension can be affected in several ways. The effects of polymer, whether free or attached, on the stability of colloidal dispersions are represented schematically in a greatly simplified manner in Figure 1.1.[1,2] At very low free polymer concentrations (~a few ppm), the adsorption of polymer chains onto more than one particle can induce bridging flocculation. The effects of attached polymer on the stability of colloids with respect to aggregation, *i.e.* steric and electrostatic stabilization, have been the subject of many experimental and theoretical studies. At higher adsorbed polymer concentrations corresponding to near or complete surface coverage, steric stabilization can result when the adsorbed chains are in a good solvent. Steric stabilization occurs due to mutual repulsion between adsorbed chains on different particles. Increasing the free polymer concentration further may result in depletion flocculation, although stabilization may be observed again at even higher polymer concentrations. When the adsorbed chains are charged, electrostatic repulsion between particles is enhanced.

The control of suspension aggregation with adsorbed polymers is critical to a wide range of applications.[3-7] For example, concentrated suspensions of colloidal ceramic particles are typically used in casting operations. At typical particle volume fractions of 0.5 and higher, the suspension viscosity abruptly increases by several orders when particles aggregate. This presents severe processing problems.[8] Some other applications of concentrated suspensions where control of particle aggregation is important are listed

Polymer Stabilization and Flocculation

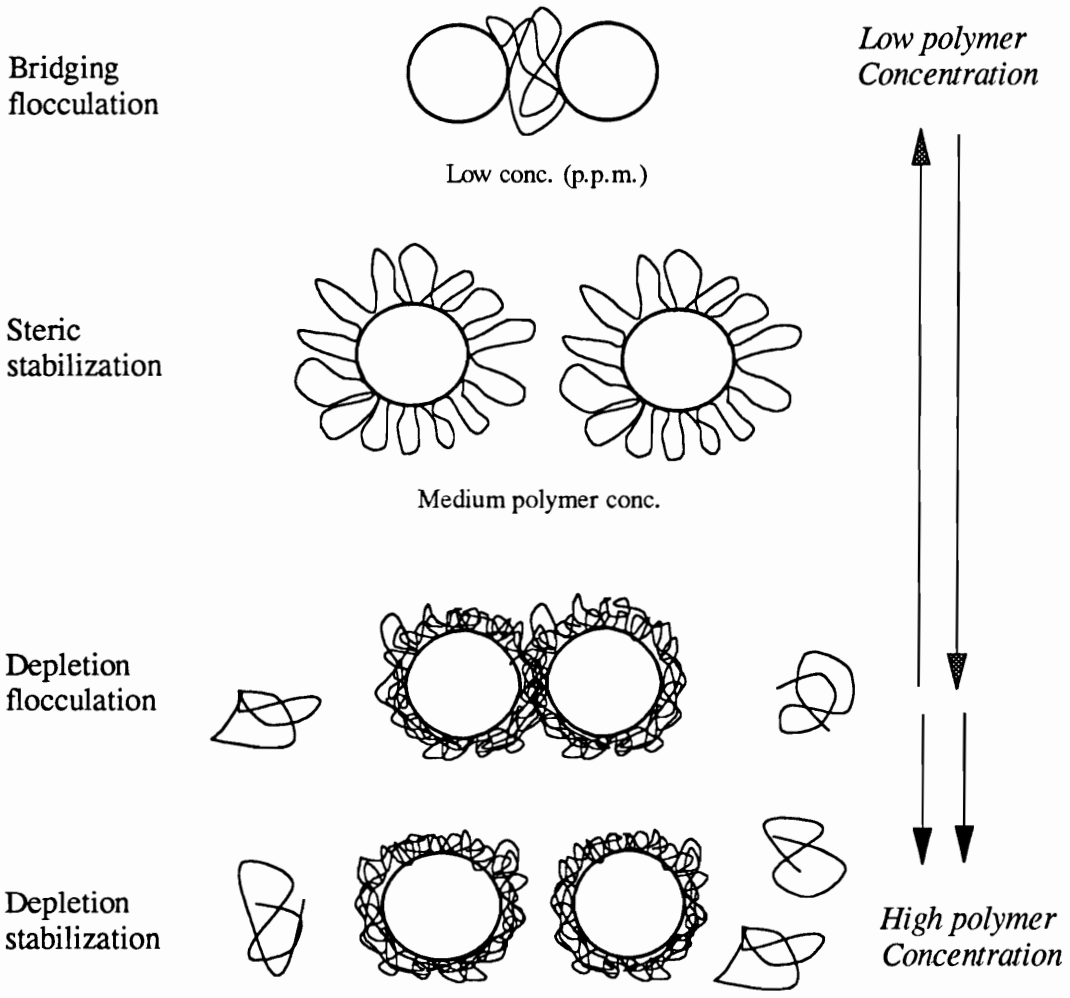

Figure 1.1 Polymer stabilization and flocculation effects on dispersions as a function of polymer concentration. [2]

in Table 1.1.

Table 1.1 Applications of steric stabilization by polymers.[6]

(1)	paints, inks, and adhesives
(2)	emulsions, for pharmaceutical, food, agricultural
(3)	detergents and laundry products
(4)	oils and lubricants
(5)	ceramic particle processing
(6)	paper coating.

Recently, the use of water-soluble polymers as stabilizers has attracted much attention due to environmental concerns.[1] Many applications in aqueous suspensions such as ceramics and paper coatings involve polyelectrolyte stabilizers which work by adsorbing onto a colloid particle, thus increasing the repulsive electrostatic forces between the particles.

Steric stabilization has several advantages over electrostatic stabilization. Steric stabilization is feasible in both aqueous and organic solvents whereas electrostatic stabilization is most effective in water. Steric stabilization is efficient in both high and low solid concentrations whereas electrostatic stabilization is most effective at low concentrations. Sterically stabilized suspensions have better freeze/thaw properties than electrostatically stabilized suspensions. This is important for storage of suspensions. Finally, sterically stabilized suspensions tend to be much less sensitive to electrolyte concentration than are electrostatically stabilized suspensions. Given the growing importance of environmental issues and the need for convenient usage of polymers, the stabilization of suspensions by adsorbed polymers will be done increasingly in aqueous media.[9]

An understanding and control of steric stabilization requires a knowledge of the properties of polymer solutions, the adsorption behavior of homo- and copolymers, and

the subsequent effects of the adsorbed layers on interparticle forces. The following sections will briefly introduce each of these topics. These will be followed by a brief description of the objectives of this research and an outline of this thesis.

Water Soluble Polymers in Solution. Considerable attention to water-soluble polymers (WSP) has been paid in both academia and industry due to their applications in biological systems, foods, and industrial products where the advantage and low cost of water as a solvent can be employed. Recently, environmental concerns in the chemical process industry have greatly promoted this interest. The production rate of WSP's is estimated to be more than 5 million tons per year.[9] Of this total, 80-90% were starches and natural gums (biopolymers[9]). A relatively small portion of WSP production are synthetic polymers (mainly as poly(vinyl alcohols) and polyacrylamides), which can be used either as homopolymers or can be converted to random copolymers. The synthetic polymers are especially valuable for ceramics, coatings, textile sizing, detergent production, and oil-well drilling.[10-14]

Despite its great economic importance, the physical chemistry of WSP's is not as well understood as is that of polymers soluble in organic solvents. This is due to the complex specific interactions between WSP's and water, primarily by hydrogen bonding and strong dipole-dipole interactions. A rigorous equation of state that fully explains polymer solution properties in aqueous solutions still does not exist. Thus, nonionic water-soluble polymers constitute an important but still poorly understood class of polymers. Non-ionic water-soluble polymers generally exhibit solution properties which significantly differ from those of polymers soluble in organic solvents. For example, the entropy of mixing of water dominates the thermodynamic properties of aqueous polymer solutions, resulting in phase separation as temperature increases. This results in the phase diagram typically observed for WSP's. These solutions exhibit both upper critical solution temperature (UCST) and lower critical solution temperature (LCST), respectively, shown in Figure 1.2(a). Measurements of the thermodynamic properties[9,15]

(a)

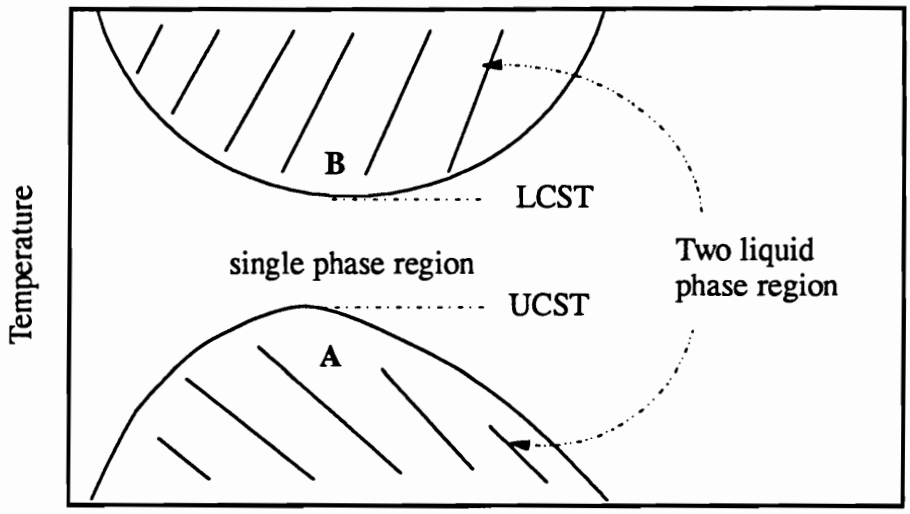

(b)

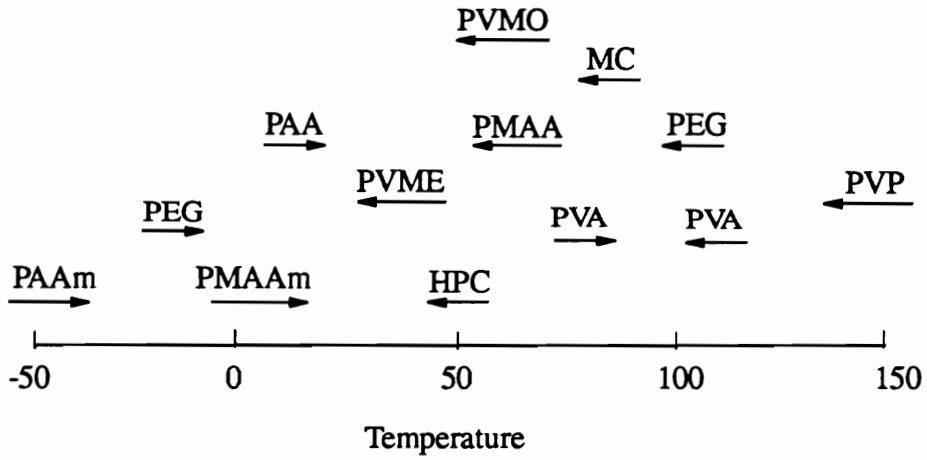

Figure 1.2 (a) A diagram illustrating two types of phase boundaries commonly encountered in polymer solutions; A, the two phase region characterized by the upper critical solution temperature (UCST); and B the two-phase region giving the lower critical solution temperature (LCST), commonly seen in aqueous solution. Between A and B, single-phase region. (b) The cloud points of several WSP's at 25 °C, → phase separation occurs upon cooling, ← phase separation upon heating. [9]

of water in solutions of WSP's, such as the excess chemical potential ($\Delta\mu^{ex}$), excess entropy (Δs^{ex}) and excess enthalpy (Δh^{ex}) of the solvent, have started to reveal how the repeat unit structure is related to the solution behavior in water. WSP's are complex in that a given repeat unit has both hydrophilic and hydrophobic character. The structuring of water around a repeat unit reflects this complex character. Thus, the architecture as well as the chemical composition of a repeat unit affects the solubility in water. The structure of water around a WSP chain profoundly influences the polymer solution properties, such as the second virial coefficient, radius of gyration, and effective molecular weight.

The solution properties of polymer are controlled by intramolecular interactions between segments and by the thermodynamic interactions between different macromolecules. The thermodynamic parameters relevant to polymer adsorption and steric stabilization can be characterized using various techniques, including:

(1) *Light Scattering*: Dynamic light scattering (DLS) can be used to measure polymer hydrodynamic diameter and characterize the polymer conformation in solution. Static light scattering (SLS) measures polymer weight-average molecular weight (M_w) and second virial coefficient (A_2) in dilute solution, according to Equation (1.1a):

$$K\cdot c/\Delta R(\theta) = M_w^{-1}(1+(qR_g)^2/3) + 2A_2\cdot c \qquad (1.1)$$

where c is the polymer concentration and q is the scattering vector, defined as

$$q = 4\pi n_o\cdot\sin(\theta/2)/\lambda_0 \qquad (1.2a)$$

In Equation (1.2a), n_o is the refractive index of the solvent, θ is the scattering angle, λ_0 is the wavelength of the light *in vacuo*. $\Delta R(\theta)$ is the excess Rayleigh ratio of scattering to primary beam intensities. The optical constant K is defined as:

$$K = \frac{(2\pi\ n_0)^2}{N_a \lambda_0}\left(\frac{\partial n}{\partial c}\right)^2 \qquad (1.2b)$$

where N_a is the Avogadro number and $\partial n/\partial c$ is the specific refractive index increment. In this study, $(qR_g)^2/3$ is much less than unity due to the low molecular weight of polymers and therefore this term is neglected.

An important experimental value from light scattering is the second virial coefficient, A_2, which is related to Flory-Huggins coefficient χ and the excess chemical potential ($\Delta\mu_1$) of the solvent. A_2 is related to χ by:

$$A_2 = \left(\frac{1}{2}-\chi\right)\left(\frac{v_2^2}{V_1}\right) h(z) \qquad (1.3)$$

where v_2 is the partial specific volume of polymer, and V_1 is the molar volume of the solvent. The term $h(z)$ is a function of excluded volume z that accounts for inter-chain interactions. At the θ-state, *i.e.*, as $z \rightarrow 0$, $h(z) \rightarrow 1$.[16] For good solvents, the factor $h(z)$ is larger than one. Although the Flory-Huggins (FH) lattice theory fails to describe rigorously the behavior of dilute polymer solutions in several aspects, the theory still provides a framework for understanding polymer solution properties.

Classical thermodynamics provides another approach to analyze solution properties. The chemical potential of mixing of the solvent can be expressed as:

$$\begin{aligned} \Delta\mu_1 &= \Delta\mu_1^{id} + \Delta\mu_1^{ex} \qquad (1.4a) \\ &= \Delta h_1 - T\Delta s_1 \end{aligned}$$

Similarly, the enthalpy and entropy terms can be expressed as:

$$\Delta h_1 = \Delta h_1^{id} + \Delta h_1^{ex}$$
$$\Delta s_1 = \Delta s_1^{id} + \Delta s_1^{ex} \qquad (1.4b)$$

and $\Delta h_1^{id} = 0$.[15] The energy of mixing $\Delta \mu_1^{id} = - A_2 \cdot c V_1 \cdot RT/M_n$ is always negative if the polymer is soluble in the solvent, M_n is the number-average polymer molecular weight.

The chemical potential of the solvent $\Delta \mu_1$ can be related to the osmotic pressure Π according to:

$$\mu_1 - \mu_1^0 = - V_1 \cdot \Pi \qquad (1.5a)$$

Thus, the correlation of excess chemical potential and the second virial coefficient A_2 in dilute solutions can be expressed as:

$$\Delta \mu_1 = - [\frac{RT}{M} c + RT \cdot A_2 c^2] V_1 \qquad (1.5b)$$

Furthermore, the excess heat and entropy of dilution of the solvent can be obtained from the dependence of temperature upon $\Delta \mu_1$, which are expressed as:

$$\Delta h_1^{ex} = \partial \Delta \mu_1 / \partial (1/T) = (B_2' T - B_2) c^2 V_1 \qquad (1.5c)$$
$$\Delta s_1^{ex} = \partial \Delta \mu_1 / \partial T - \Delta s_1^{id} = B_2' c^2 V_1 \qquad (1.5d)$$

where $\Delta s_1^{id} = RT \cdot \ln X_1$ is the ideal entropy of dilution of the solvent, and X_1 (= $n_1/(n_1+n_2)$) is the mole fraction of the solvent.[9] In addition, $B_2 = RT \cdot A_2$ and $B_2' = dB_2/dT$. Thus, the excess thermodynamic properties of solvent can be obtained from values of A_2 as a function of temperature. This is discussed in more detail in Chapter 2.

The Flory-Huggins solution theory is limited in describing the properties of WSP solutions. Flory-Huggins theory assumes all polymer/solvent interactions are non-specific, such as van der Waals or electrostatic forces. It does not account for specific association of solvent molecules with the polymer chain such as in hydrogen bonding.

This association leads to a highly negative entropy of dilution of the solvent which typically is greater than the positive combinatorial entropy of mixing of the solvent with the polymer chain.[9]

As a consequence, the FH theory cannot predict the LCST which is typically observed in WSP's. From the FH theory, χ parameter is predicted to increase as temperature decreases until a UCST is reached. This relation is given by

$$\chi = \beta_0 + \beta_1/T \tag{1.6}$$

where positive β_0 is related to negative excess entropy of dilution ($\Delta s_1^{ex} < 0$) and positive β_1 corresponds to the endothermic solution ($\Delta h_1 > 0$), respectively. The classical FH theory predicts that both β's are positive for non-polar solvents. Equation (1.6) is qualitatively correct in predicting phase separation upon cooling in the organic solvents. However, experimental data for WSP's usually show that β_1 is negative indicating an exothermic heat of mixing. Also, the entropy of mixing of water in solutions of WSP's is quite negative. These effects are due to the hydrogen bonding between polymer and water, and hydrophobic nature in the polymer repeat units.[9] As a consequence, the solution reaches the θ-condition (*i.e.*, $A_2=0$) upon heating.

Another unique solution property of WSP's is aggregation in water solution. Based on Franks[9], the aggregation phenomenon, *i.e.* hydrophobic hydration, is dominated by the negative excess entropy of mixing ($\Delta s_1^{ex} < 0$), and not by the enthalpic repulsion. Because of the combination of hydrophobic and hydrophilic nature in the WSP's repeat units, the polymer conformation is very sensitive to interactions of polymers with water by hydrogen bonding.

(2) *Cloud point*: The cloud point is the temperature corresponding to the onset of turbidity in a polymer solution due to phase separation. Phase separation measurements over a wide range of molecular weights gives useful information on the

dependence of the $\Delta\mu_1$ or the χ parameter on temperature and concentration. Water-soluble polymers typically exhibit a phase diagram shown in part (B) of Figure 1.2(a). There is a range of temperature and composition in which a single phase regime exists between curves A and B. When the temperature is raised or lowered, the solvent becomes thermodynamically poorer for the polymer. Finally a temperature is reached beyond which the polymer and solvent are no longer miscible in all proportions. The maximum point of the lower curve (A) for the phase separation is designated the UCST. For water-soluble polymers the phase separation normally occurs when the temperature is raised until a LCST is reached, as shown in the lowest point of the upper curve in Figure 1.2 (a). In addition, Figure 1.2(b) shows the cloud point results of several WSP's in the aqueous solutions. The direction of the arrow indicates the type of θ behavior: '→' means demixing or phase separation on cooling, and '←' indicates demixing on heating. For sufficiently high M_w, the FH theory relates the cloud temperature T_c to the θ-temperature, θ, by:

$$\frac{1}{T_c} \sim (\frac{1}{\theta})(1+M^{-1/2}) \qquad (1.7)$$

where T_c is the critical temperature, the lowest cloud point of each polymer molecular weight at various concentrations.

(3) *Viscosity*: An isolated linear macromolecule with sufficiently high molecular weight tends to assume a random coil configuration. For sufficiently low MW or stiff chains, a rigid rod conformation can result. Intrinsic viscosity measurements can be used to determine the dimensions of the random coil and estimate the chain configuration at a specific temperature.

The intrinsic viscosity $[\eta]$ is related to the molecular weight M by the Mark-Houwink-Sakurada relation[12,17], expressed as:

$$[\eta] = K \cdot M^a \qquad (1.8)$$

K and a are empirical constants for a given polymer under specified solution conditions. The limit $a=0.5$ corresponds to a Gaussian coil which is typically observed for flexible polymers at the θ-state. At the θ-condition, the unperturbed chain radius of gyration $<R_g^2>_0^{1/2}$ is related to $[\eta]_\theta$ by:

$$[\eta]_\theta = K_\theta \cdot M^{1/2} = 6^{3/2} \cdot \Phi_0 <R_g^2>_0^{3/2}/M \qquad (1.9)$$

where Φ_0 is a universal constant $\sim 2.87 \times 10^{23}$ mole^{-1} for the non-draining case, determined from the Kirkwood-Riseman theory[18].

Special Problems with WSP's. In summary, the thermodynamic properties of the non-ionic water-soluble polymers in water are very different from those of polymers in organic solvents where specific association of the solvent with the polymer does not occur. These differences include (i) strong specific association of solvent (water with polymer chains), (ii) the phase separation behavior (LCST) in water which is a consequence of (i), (iii) the failure of mean field theories which makes a precise description of solution properties in terms of χ parameter or the excluded volume effect impossible, (iv) commonly observed aggregation of water-soluble polymer in water. A quantitative theory of these effects does not yet exist.

The above thermodynamic properties of polymer solutions are needed especially in the studies of polymer adsorption at solid/liquid interfaces. Recently, de Gennes[19] proposed a general form of the free energy function which attempts to account for at least some of the specific solvent association effects. The results suggest that the adsorption behavior may depend on the polymer configuration in solution. The configuration is related to the polymer-solvent interactions and polymer segment-segment

interaction.[20] Two phase equilibrium concentration regimes were proposed for poly(ethylene oxide) (PEO) in water. At low concentration, the polymer forms the coils and at high concentrations, helix configuration responds to the formation of microgel. The author speculated that the adsorption of the helical configuration of PEO will be inhibited.[9,19]

Polymer Adsorption. Self consistent field (SCF) theories[1,3,21,22] for polymer solutions have served as the starting point for theories of polymer adsorption, most notably the lattice theory (S-F) of Scheutjens *et al.*[23] and scaling theory by de Gennes[24]. The scaling theory seeks to correlate the polymer adsorbed amount and layer thickness with the molecular weight, solubility, and, in the case of diblock copolymers, the ratio of the block length between anchor and tail blocks. Our current studies focus on how polymer adsorption is affected by polymer molecular weight, polymer solubility, solvent composition in binary solvent systems, and competitive adsorption from mixtures of polymers.

According to S-F lattice theory, the adsorption behavior of a polymer is affected by two energetic parameters: the segmental adsorption energy parameter χ_s, and polymer-solvent interaction parameter χ. As defined by Silberberg[25], $\chi_s kT$ is the net free energy change associated with the transfer of a polymer segment from a bulk site to a surface site minus that of a solvent molecule. This change includes breaking some solvent-polymer contacts in solution and some solvent-surface contacts when the polymer segment adsorbs. Adsorption occurs when χ_s is greater than χ_{sc}, the critical adsorption energy parameter which is the minimum change in free energy that a polymer segment has to overcome the loss of entropy upon adsorption. Typical values of χ_{sc} are less than 1 kT [26].

In addition to the interaction considerations such as polymer-surface, polymer-solvent and solvent-surface, one of the principal problems still to be adequately resolved is the conformation of the polymer chains on the surface. Jenckel and Rumbach[27] in 1952

suggested that adsorbed polymer chains can have segments arranged in loops (Figure 1.3(a)), flat sequences in contact with the surface are defined as 'trains', and the free ends of the molecule extending into solution, defined as 'tails'. This has been verified for adsorbed homopolymer chains.[3,34,41] In a study by Barnett *et al.*[34], the estimation of the segment density profiles of poly(vinyl acetate) on polystyrene latex particles from water have been carried out using solid-state NMR and small angle neutron scattering (SANS) techniques.

If the polymer molecule is composed of two blocks with different affinities for the surface, *i.e.*, the AB diblock copolymer (in Figure 1.3(b)), then the anchor block may preferentially adsorb in a loop-train conformation (with small loops) while the soluble block or B segments remain in solutions with one long tail. One of the most significant advantages of copolymer stabilizers over homopolymers stabilizers is the copolymer tail blocks can extend into the medium to form a relatively thick steric layer. Several studies[20,28,29] have shown that the extension is a function of polymer molecular weight and the block length ratio of tail to anchor. This present work is focused on designing criteria for such a diblock system since this can result in a very efficient colloid stabilizer.

Adsorption Theories. The adsorption of polymer is different from the adsorption of small molecules or low molecular weight surfactants. There are at least three qualitative differences:

(1) The conformation of the adsorbed polymer chains differ from that in bulk solutions, due to the complex interactions between surfaces and polymer chains, surfaces and solvents, and solvents and polymer chains. There is no such change in conformation upon adsorption of low molecular weight compounds. The conformation of the chains is strongly dependent upon the added polymer concentration and the molecular weight of polymer chains.

(2) The chain character of polymer chains leads to high affinity isotherms that are

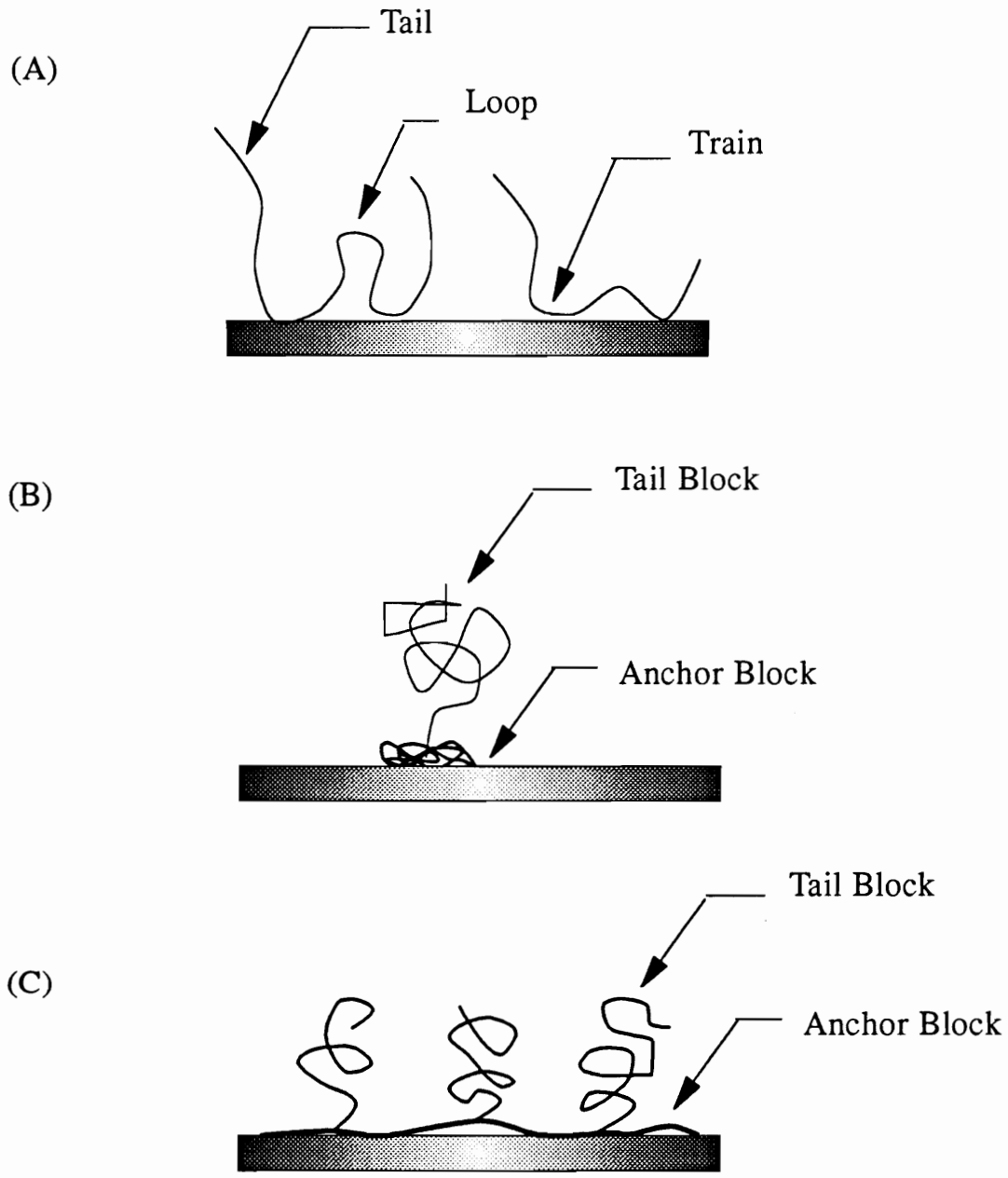

Figure 1.3 Schematic representation of polymer adsorption conformation on solid surface. (A) Homopolymer; (B) Diblock Copolymer; (C) Grafted Copolymer. [34]

not predicted rigorously by the Langmuir adsorption theory, which has been proven to work well with low MW species. The chain character of polymers leads to competitive (or displacement) adsorption between polymers resulting from differences in the molecular weights of the polymer chains and their chemical structures.

(3) The translational entropy loss during adsorption is more significant than that for small molecules, due to the large mass of the polymer.

Homopolymer Adsorption Since the 1960's, several theories have attempted to explain the behavior of polymer adsorption on a surface.[3,9,30] A model, proposed by Perkel and Ullman[30], connected the plateau adsorbed amount (Γ_p), *i.e.*, the amount of adsorbed polymer at full surface coverage, and polymer molecular weight (Mw):

$$\Gamma_p = \beta \cdot Mw^{\alpha} \qquad (1.10)$$

where β is an adjustable parameter that increases with the polymer adsorption affinity. Attempts have been made to relate the empirical exponent α with polymer conformations on the surface. However, this simplified relation was criticized by Fleer[3], who pointed out that the Perkel-Ullman model did not consider the lateral interactions between the adsorbed polymer chains.

More recently, the scaling theory of de Gennes[24] and the mean lattice theory (S-F) developed by Scheutjens and Fleer[23], have had some success in describing polymer adsorption at the solid/liquid interface. The S-F lattice theory takes into account all possible chain conformations on and near the surface. The theory predicts that polymer adsorption strongly depends on several factors: molecular weight (Mw), polymer volume fraction in solution in equilibrium with surface (ϕ^*), polymer segment-solvent interaction parameter (χ), and segmental adsorption energy parameter (χ_s).[23] According to the S-F mean field theory, polymer adsorption increases with χ_s (greater polymer-solvent attraction) and χ (less solubility). The polymer adsorption process is sometimes regarded

as an irreversible process in which the adsorbed polymer cannot be displaced by dilution with solvent. However, Cohen Stuart *et al.*[31] showed that pre-adsorbed polymer can be displaced using small organic compounds. This displacement process can be used to measure χ_s, as discussed in Chapter 3.

The competitive adsorption of a mixture of two polymers in a solution is a direct probe of their relative adsorption affinities. This is important for designing copolymers for stabilization applications. The block with the higher adsorption affinity for the surface will act as the anchor block, while the block with lesser affinity will serve as the tail block. This is discussed in Chapters 4 and 5.

Diblock Copolymer Adsorption Extending the homopolymer lattice model to diblock copolymer systems, Scheutjens and Fleer[29] developed a model to account for tail and anchor block effects. For an AB block copolymer where block A is the anchor block and block B is the non-adsorbing block, the fraction of the anchor block in a polymer chain, ν_A, is defined as:

$$\nu_A = \frac{N_A}{N_A+N_B} \tag{1.11}$$

where N_A and N_B are the degrees of polymerization of the anchor blocks and tail blocks, respectively. At low ν_A, the total adsorbed amount of the copolymer (θ^a) is also low because of the small total adsorption energy. As the fraction of A-segments increases, the adsorption amount increases until a maximum adsorbed amount is reached. As the adsorbed amount increases, the B block extends into the medium and forms the steric layer. The composition ν_A corresponding to this maximum will be referred to as the 'optimal composition', ν_A^{opt}. At and near the optimal composition, later interactions between the tethered tail chains lead to chain extension of the tail blocks away from the surface. This is highly desirable for steric stabilization. Beyond ν_A^{opt}, the adsorbed

amount gradually decreases because most of the adsorption sites on the surface are occupied by flat A-segments. The theory introduces a correlation of the copolymer adsorbed amount (θ^a) and chain composition (ν_A) by

$$\theta^a = \theta_{hA}{}^a \cdot (1 + \alpha \cdot N_B/N_A) \tag{1.12a}$$

where θ_{hA} is the adsorbed amount of the homopolymer A having the same degree of polymerization as the copolymer, α is related to the difference of the adsorption energy parameter between blocks A and B, and expressed as:

$$\alpha = \lambda_1 \cdot [(\chi_s{}^{po})_{anchor} - (\chi_s{}^{po})_{tail}] \tag{1.12b}$$

where λ_1 is the lattice parameter. The S-F theory also predicts the optimum chain ratio ($\nu_A{}^{opt}$), at which $\theta_A{}^a = 1$ monolayer is assumed. Thus, Equation (1.12a) leads to the maximum adsorbed amount of copolymers and to the thickest adsorbed layer by

$$\nu_A^{opt} \approx \frac{\theta_{hA}^{-1} - \alpha}{1 - \alpha} \tag{1.13}$$

Based on Equation (1.13), $\nu_A{}^{opt}$ decreases with increase of total chain length, due to the reverse relationship between θ_{hA} and $\nu_A{}^{opt}$.

The scaling approach is another way to model polymer adsorption. Marques and Joanny (MJ)[28] adapted scaling theory to explain diblock copolymer adsorption. When both blocks are dissolved in a good solvent, a characteristic asymmetry ratio β can be defined in terms of the Flory radii of the component polymers, $\beta = (R_A/R_B)^{3/5} \sim (N_A/N_B)^{3/5} a'$, where a' is the monomer length ratio of tail blocks to anchor blocks, R_A and R_B are the Flory radii of gyration of the anchor and the brush segments, respectively. It was found that the adsorbed hydrodynamic layer thickness was larger than the

dimension of the molecule in bulk solution, implying the deformation of the polymer coil on adsorption.

According to the MJ theory, the adsorbed layer thickness (L) can be related to the degree of polymerization of the tail block (N_B) and adsorbed surface density (σ) by:

$$L \sim N_B \cdot \sigma^{1/3} \tag{1.14}$$

since surface density $\sigma \equiv (\Gamma_p \cdot N_a/Mw) \cdot 10^{-21} \sim N_A^{-1}$,[32] where Γ_p is the adsorbed amount of copolymer at full surface coverage and N_a is the Avogadro's number. Thus

$$L \sim N_B N_A^{-1/3} \qquad \text{for } \beta < N_A^{1/2}, \tag{1.15}$$

and

$$L \sim N_B^{3/5} N_A^{2/5} \qquad \text{for } \beta > N_A^{1/2}. \tag{1.16}$$

An optimum block ratio of polymer adsorption was predicted by the MJ theory at $\beta = N_A^{1/2}$, at which both the adsorbed amount (Γ) and thickness (L) reach a maximum. This is very useful for designing diblock copolymers to function as steric stabilizers in a non-selective solvent. Wu and co-workers[33] verified the S-F theory (Equations 1.12-1.13) and MJ model (Equations 1.15-1.16) with experiments measuring the adsorption of poly(dimethyl amino ethyl methacrylate-*b*-butyl methacrylate) (DMAEM-BMA) on silica from isopropanol. The optimum block ratio and adsorbed layer thickness were qualitatively consistent with both theories. Guzonas *et al.*[32] also measured the surface forces and adsorbed amount of the diblock copolymer PEO-PS on mica from toluene. They found that the scaling theory correlated with the adsorption data very well.

Polymeric Stabilizers. Adsorbed polymer can lead to flocculation or stabilization of colloid suspensions and thus is important in controlling the rheology and other properties of ceramic suspensions, emulsions, and coatings. In order for a polymer to be an

effective steric stabilizer, several requirements need to be met:[1] (i) the segmental energy χ_s must be larger than the critical adsorption energy χ_{sc}; (ii) polymer chains should cover the surface, *i.e.*, reach the plateau adsorption region; (iii) the tails should be soluble in the liquid phase *i.e.*, $\chi<0.5$, and (iv) the adsorbed layer must be sufficiently thick to generate repulsive steric forces to prevent aggregation or coagulation. Typical values of the adsorbed layers required for steric stabilization lie in the range 2-20 nm. Based on the above criteria, adsorbed homopolymers do not have the optimum structure for steric stabilization because of the combined requirements for strong binding and thick layers.

Amphiphilic polymer molecules are generally more effective stabilizers. Examples of amphipathic stabilizers are the diblock and graft copolymers comprising distinct stabilizing and anchoring chains, Figure 1.3(b,c). Several studies have shown that diblock copolymers can serve as better stabilizers than homopolymers.[33-35] Lower concentrations of copolymer are needed for steric stabilization, relative to homopolymers.[23] The thickness of the steric layer can be controlled by adjusting the MW of tail block. This is particularly useful in light of the chain extension effect. Adsorbed diblock copolymers generate a near hard-sphere interparticle potential leading to minimum viscosity at higher particle volume fractions than those attainable by electrostatic stabilization.[2] Therefore, for the purpose of steric stabilization in the present work, we are principally concerned with the design of diblock copolymers for steric stabilization in aqueous suspensions.

Modified DLVO Theory To control the properties of dispersions, it is necessary to control the interaction forces between the particles. A useful model for the forces is the Deryagain-Landau-Verwey-Overbeek (*DLVO*) theory[1] which was modified to take into account the effects of steric forces by incorporating a steric repulsive term $V_S(h)$ into the expression for the total pair potential interaction energy $V_T(h)$:

$$V_T(h) = V_A(h) + V_E(h) + V_S(h) \qquad (1.17)$$

where h is the minimum distance between particle surfaces, V_S, V_A and V_R are the polymer steric repulsive, van der Waals attraction and electrostatic repulsive potentials respectively.

The potential energy of attraction $V_A(h)$ between two spherical particles of material (1) in a liquid medium (3) can be expressed in the form:

$$V_A = -\frac{A_{131}}{12}\left[\frac{1}{x^2+2x} + \frac{1}{x^2+2x+1} + 2\ln\left(\frac{x^2+2x}{x^2+2x+1}\right)\right] \qquad (1.18)$$

where $x=h/(2\cdot R)$, R is the particle radius. The composite Hamaker constant is given by:

$$A_{131} = (\sqrt{A_{11}} - \sqrt{A_{33}})^2 \qquad (1.19)$$

where A_{11} and A_{33} are the Hamaker constants of the particles and the medium, respectively. The Hamaker constant is directly related to the nature of the material by:[35]

$$A_{jj} = 3\pi^2 h_p \nu_j \alpha_j^2 q_j^2/4 \qquad (1.20)$$

where h_p Planck's constant, ν_j the dispersion frequency of the material, α_j the static polarizability, and q_j the number of atoms or molecules per unit volume. Note that the Hamaker constant $A_{jj} \propto \alpha^2$. The Lorenz-Lorentz equation is a relationship between material refractive index (n) and polarizability:

$$\frac{\alpha}{4\pi\varepsilon_o} = \left(\frac{n^2 - 1}{n^2 + 2}\right)\left(\frac{3\nu}{4\pi}\right) \qquad (1.21)$$

where ν is the frequency, and ϵ_o is the static dielectric constant of the molecules in the liquid state. The Lorenz-Lorentz equation shows that A_{jj} increases with the refractive

index n. Several common values of Hamaker constants are listed in Table 1.2.

Table 1.2 Hamaker constants for various materials

Material	$A_{11}(10^{-20}$ J)	Ref.
water	3.0 - 6.1	36
Poly(styrene)	5.6 - 6.4	36
Poly(methyl methacrylate)	7.11	34
Silica (SiO_2)	8.6	36
Titanium oxide (TiO_2)	11 - 31	44
Alumina (Al_2O_3)	14.8 - 15.5	44

Based on Equation (1.18), the van der Waals attraction force increases with the composite Hamaker constant. Thus, poly(styrene) latex particles can be stabilized in water rather easily due to the small difference of the Hamaker constants between poly(styrene) and water, which results in relatively weak van der Waals force. However, metal oxides such as TiO_2 or Al_2O_3 are relatively difficult to stabilize in water due to the stronger attraction force resulting from large values of the composite Hamaker constant.

Electrostatic repulsive forces are created when two particles with the same charge approach each other. The range of the electrostatic forces depends on the thickness of the electrostatic double-layer, κ^{-1}, and is expressed as:

$$\kappa^{-1} = (\varepsilon \cdot kT/2e^2I)^{1/2} \qquad (1.22)$$

where ε=the dielectric constant of solution; k=Boltzmann's constant; T=temperature; e=electronic charge. The ionic strength $I=\frac{1}{2}\cdot\Sigma n_i(z_i)^2$, where n_i=molarity of ionic species in solution, z_i=valence of ionic species in solution, and the summation is over all the low Mw ionic species in solution. The electrostatic interactions between two spherical particles can be expressed quantitatively in the forms:

$$V_E(h) = 2\pi\epsilon_r\epsilon_0\psi_s^2 \cdot \ln[1+\exp(-\kappa h)] \qquad \text{for } \kappa \cdot R > 10 \qquad (1.23a)$$

$$V_E(h) = 4\pi\epsilon_r\epsilon_0\psi_s^2 \cdot R \cdot \exp(-\kappa h)/(h+2R) \qquad \text{for } \kappa \cdot R < 3 \qquad (1.23b)$$

where ϵ_r and ϵ_0 are the relative permittivity of the solution phase and that of free space. V_E is often ignored where the ionic strength of the medium is high or where the dielectric constant of the medium is low such that it will not support ionization.

The steric interaction (V_S) contains two components: an osmotic (enthalpic) component which may either be attractive or repulsive depending upon the solubility, and an elastic (entropic) component which is purely repulsive. The evaluation of these two contributions requires a knowledge of the polymer segment-density distribution between the surfaces.

Steric stabilization with well-defined adsorbed layers generates a potential approaching the hard sphere case. As the particles separates at a distance of h larger than twice of the adsorbed layer thickness, 2δ, there is no steric repulsion. As particles approach further, steric repulsion[1] occurs when the adsorbed chain layers interpenetrate for $\delta \leq h \leq 2\delta$. In general, the elastic interaction in the interpenetration domain is negligible, *i.e.*, the osmotic effect dominates in this region. If the segment density distribution is assumed to be constant, the steric potential can be expressed as:

$$\frac{V_S(h)}{kT} = \frac{4\pi R\delta^2}{v_1}\left[f^2\left(\frac{1}{2}-\chi_1\right) + 1.5\, f^3\left(\frac{1}{3}-\chi_2\right)\right]\left(1-\frac{h}{2\delta}\right)^2 \qquad \delta \leq h \leq 2\delta \qquad (1.24)$$

$$V_S(h) = 0 \qquad h > 2\delta$$

where v_1 is the molecular volume of the solvent, f is the volume fraction of the polymer in the adsorbed layer, χ_2 is the concentration dependence of the Flory-Huggins interaction parameter χ, and $\chi = \chi_1 + \chi_2 \cdot f$. Repulsive interparticle forces thus increase with the solubility of the tail block (decreasing χ). When particles further approach such that

$h < \delta$, an elastic factor is significant and dominates the repulsion forces.

From the expression in Equation (1.24), the steric repulsive potential V_S is primarily related to the adsorbed layer thickness (δ), segment-density function (f), and polymer solubility (χ). Cosgrove *et al.*[3,37,41,42] measured the segment-density distribution to calculate the fractions of trains, loops, and tails. The polymers include several homopolymers such as PEO, poly(vinyl acetate)(PVA), block copolymers such as triblock PEO-PPO-PEO and diblock poly(styrene-vinyl pyrrolidone)(PS-PVP)), random copolymers such as poly(ethylene/vinyl acetate), and poly(dimethyl amino ethyl methacrylate-methyl methacrylate) on different surfaces (such as mica, latex particle, and silica) by solid-state NMR and small angle neutron scattering (SANS) techniques. The results show monotonic decay of the polymer density distribution away from the surface. Thus, using solid-state NMR and SANS techniques for segment-density function measurements, and combining photon correlation spectroscopy (PCS) for the adsorbed layer thickness measurements and solubility measurements by static light scattering from our research, the steric energy can be estimated using the above expression. In addition, the surface force apparatus developed by Israelachvili *et al.*[20] has been used to directly measure interactions of polymers on various surfaces. Based on the measurements by Israelachvili *et al.*[20] and Tirrel *et al.*,[37] the results are applied to verify the polymer adsorbed conformation with the scaling theory.

Different particle interactions as a function of distance are shown in Figure 1.4. In Figure 1.4(a), two minima and one maximum are seen for a suspension stabilized by electrostatic forces. For very small particle separations, a strong attraction occurs in the *primary minimum* (V_{min}). Particles in this attractive well are coagulated. At a larger separation flocculation may occur into the *secondary minimum* (V_{sm}). At this stage, the particles can be re-dispersed by shearing the suspension. The *primary maximum* (V_{max}) serves as a barrier to coagulation.

For effective stabilization, the primary maximum V_{max} in the $V_T(h)$ should be sufficiently high to prevent particles from aggregation. The stability ratio W is used to

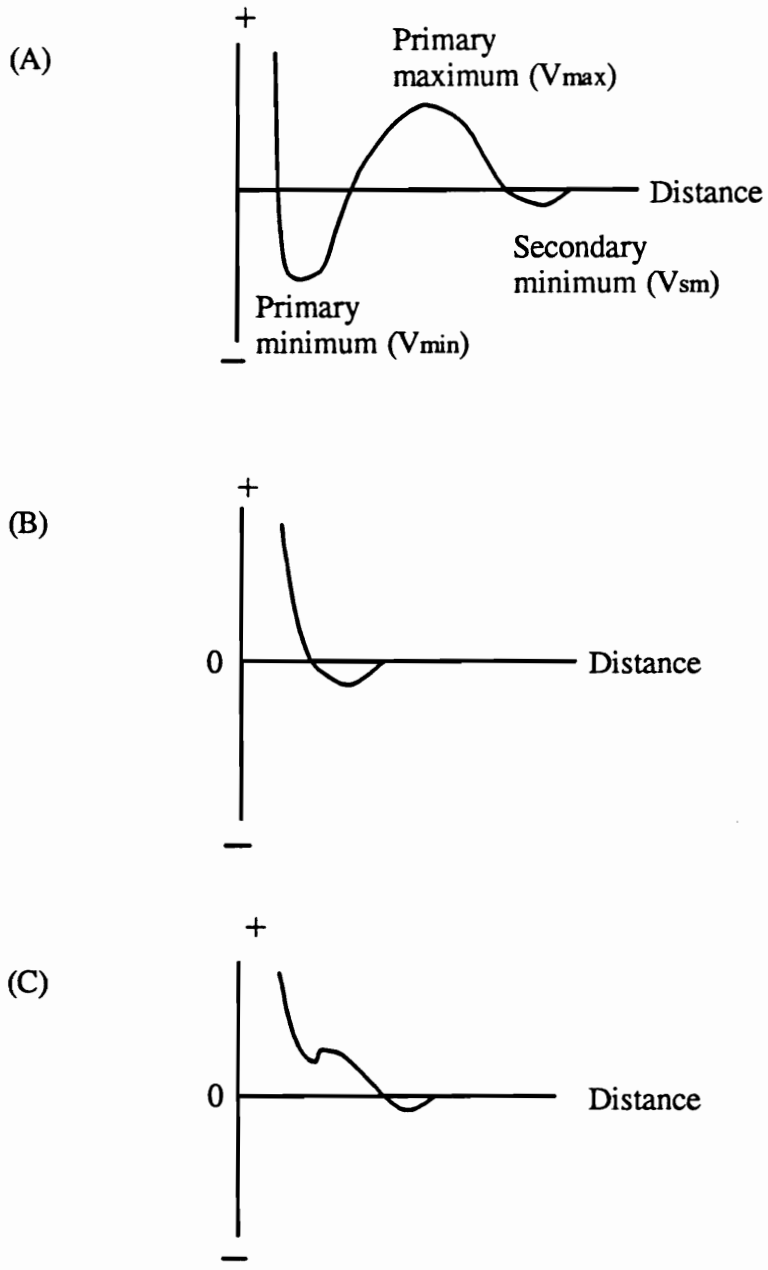

Figure 1.4 Total energy-distance curves for three different stabilization mechanisms. (A) Electrostatic; (B) Steric (polymers); (C) Electrostatic + steric (polyelectrolytes).[1]

characterize the suspension stability, and defined as:

$$W = \frac{\textit{No. of particle collisions}}{\textit{No. of collisions inducing coagulation}}$$

The ratio W value can also be expressed in terms of the total energy $V_T(h)$ by:

$$W = 2R\int_0^{\infty} \frac{\exp(V_T\,(h)/kT)\;dh}{(h + 2R)^2} \qquad (1.25)$$

In the absence of an energy barrier, *i.e.* $V_T=0$, $W=1$, the particles aggregate rapidly. For large V_T, W increases and the rate of coagulation slows down. For V_{max} is greater than 15 kT, $W \sim 10^5$. For $V_{max}=25\ kT$, $W \sim 10^9$ and suspensions can be stable for several months.[2]

Suspension Rheology. The interparticle potential directly affects the rheology of suspensions. Figure 1.5(a) is a representative plot of viscosity versus stress for two suspensions - one sterically stabilized and one flocculated. The stabilized suspension reaches a low and constant viscosity with decreasing stress. However, the flocculated suspension has a higher viscosity and exhibits a yield stress due to the formation of a network of aggregated particles. Similarly, Figure 1.5 (b) shows representative cases of suspension viscosity as a function of volume fraction. All curves except curve D show a steeply increasing viscosity with increasing particle concentration. The different critical volume fractions (*i.e.*, at which viscosity abruptly increases) indicates different stabilization conditions: curve A - coagulated particles, curve B - electrostatically-stabilized particles, curve C - weakly flocculated particles, and curve D - the hard-sphere base line with steric stabilization.

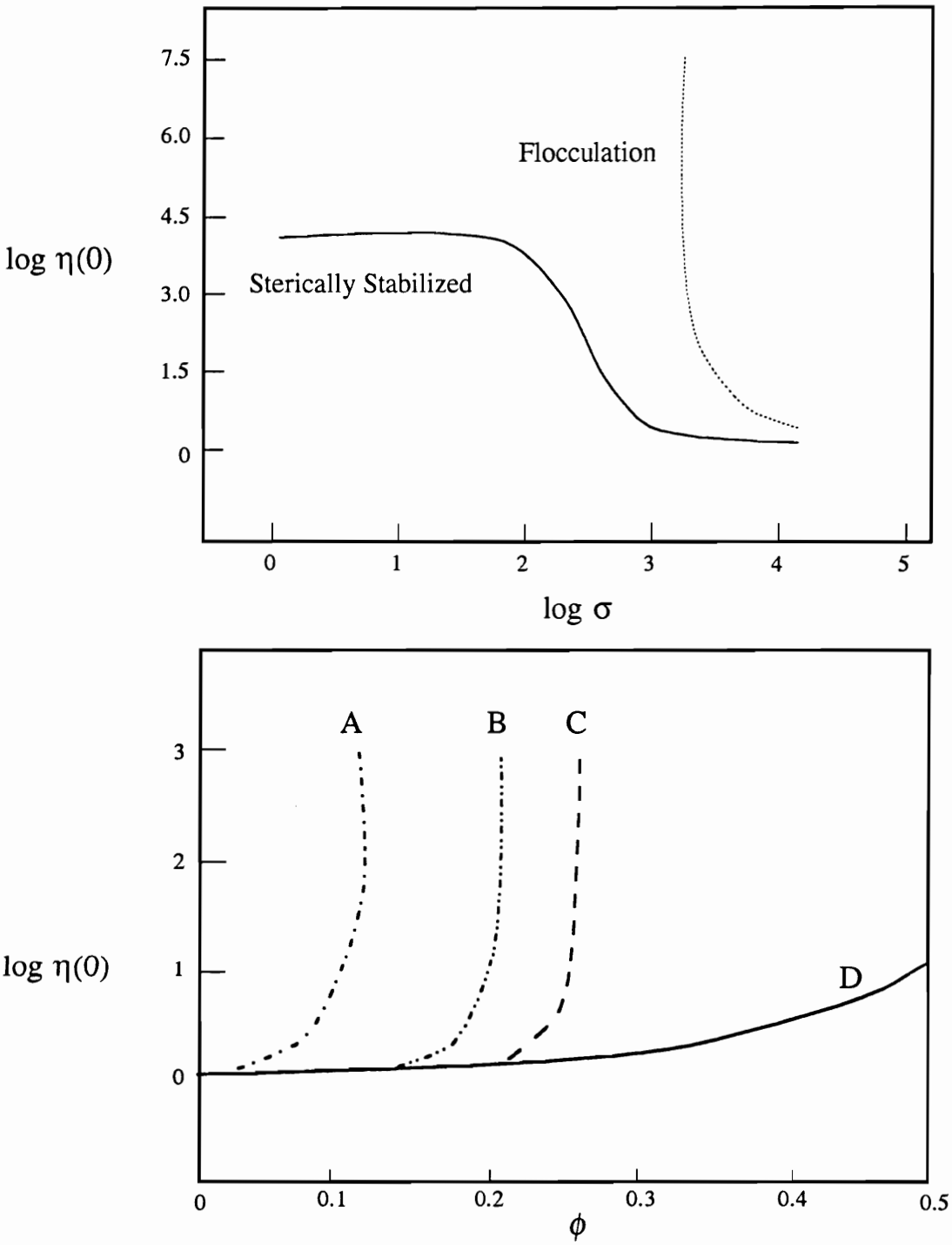

Figure 1.5 (A) Dependence of the suspension viscosity on shear stress for sterically stabilized material (——), and flocculated material (.....). (B) Effect of particle interactions on the low shear viscosity of suspensions relative to that of the solvent volume fraction. Curve A, coagulated particles; B, small stable and charged particles, electrostatic stabilization; C, weakly flocculated large particles, and D, hard-sphere base line with steric stabilization. [8]

APPLICATIONS OF THIS WORK

In processing colloidal ceramic suspensions by casting techniques - slip, pressure, or tape - the rheological behavior of the suspensions is critically important. Control of the interparticle potential can improve ceramic processing significantly.[8] Advanced ceramics require defect- (void-) free components for high mechanical strength, uniformly packed green microstructures, fine powder size (~ 0.01 - $0.1\ \mu m$) with a narrow particle size distribution.[38] Manufacturing such components requires rapid formation of dispersed and in some instances, flocculated suspensions at high particle volume fractions, $\phi > 50\%$. Highly aggregated suspensions can lead to voids in the green body, which will generate voids in the final product unless removed by long and costly high temperature sintering. These voids lead to structural ceramics with weak strengths and to premature dielectric breakdown in electronic ceramics.

Colloidal stabilization is also important in the paper-coating industry. Paper-coatings are concentrated aqueous suspensions of pigment particles and polymer latex binders. A major problem of paper-coating performance arises from aggregation of the pigment and binder particles which make up the coating. Aggregation results in un-acceptable streaks and scratches on the final coated paper. Thus, it is important to employ water-soluble polymers as stabilizers for the pigment and binder particles in order to suppress particle aggregation, thus leading to greatly improved coating performance.[43]

Water-soluble polyelectrolyte dispersants have been used for some time to control aqueous suspension aggregation and rheology. Steric stabilization has been used less often to control aggregation in concentrated suspensions because only homopolymers have been readily available and these have not functioned as well in general as polyelectrolytes. The relation between polymer structure and dispersant performance is still poorly understood.[43] This deficiency lies first in the difficulty of describing the water-soluble polymers in aqueous solutions. The Flory-Huggins solution theory can not rigorously explain water-soluble polymer solution behavior, such as the LCST and negative entropy

of dilution of the water. Any quantitative theory for steric stabilization must rest on a proven theory for polymer solution thermodynamics. Thus, in addition to the need for designing diblock copolymers that will function as steric stabilizers in aqueous suspensions, it is important to better understand the thermodynamics of water-soluble homopolymers.

GOALS OF THE STUDY

The ultimate goal of this work is the development of water-soluble diblock copolymers which possess dispersion and rheological characteristics superior to current technology. The principal scientific objective was to determine the relationships between the structures of different functional groups comprising water-soluble polymers and their effect on polymer adsorption. Several problems were addressed:

(1) Characterization of the solution properties of water-soluble polymers in aqueous solutions and related polymer solvents - For polymers that can be synthesized as either tail or anchor blocks in a diblock system, their solution properties are measured that relate to adsorption and stabilization. These properties are primarily A_2, Δs^{ex}, Δh^{ex}. The goal is to relate these properties to segment structure.

(2) Determination of the relationships between the structures of different polymeric functional groups and their effect on polymer adsorption - The questions we seek to answer include:

(i) What functional groups of a polymer such as siloxane, ether, or carbonyl groups lead to the strongest adsorption onto the metal oxide surfaces, such as silica?
(ii) How is the structure of the adsorbed polymer layer on a particle, in terms of the extent of adsorbed amount and the effective thickness of the adsorbed layer, related to

molecular weight and type of functional group?

(3) Relation of the diblock copolymer structure to colloidal suspension and particle aggregations that concern the steric stabilization performance.

In this study, silica was chosen as the adsorbent because well-characterized polydisperse SiO_2 is readily obtainable and because near-monodisperse SiO_2 can be synthesized in a wide size range from 0.05 to 0.3 μm by the Stöber method.[39] Thus, silica is a good model adsorbent to test the adsorption theories. However, the current work can be extended to other ceramic metal oxide particles, such as TiO_2, and Al_2O_3. The polymers used in this study include poly(2-ethyl-2-oxazoline) (PEOX), poly(2-methyl-2-oxazoline) (PMOX), poly(dimethyl siloxane) (PDMS), poly(vinyl methyl ether) (PVME), poly(ethylene oxide) (PEO) and poly(propylene oxide) (PPO). The chemical structures are shown in Figure 1.6. In addition, copolymers of PEOX-PDMS and PEOX-PVME were prepared. The poly(dimethyl amino ethyl methacrylate-*b*-butyl methacrylate) (DMAEM-BMA) were generously donated by Dr. D. T. Wu in the Du Pont Chemical Co.. The structures of copolymers are shown in Figure 1.7. A unique feature of this work is that we were able to obtain a relatively wide variety of chemical structures with well-defined homopolymers and block copolymers from Professor R. S. Riffle's group. A simple scheme is illustrated in Figure 1.8 which shows the synthesis of PEOX via the ring-opening polymerization (via an S_N2 reaction) of 2-ethyl-2-oxazoline initiated by benzyl iodides in chlorobenzene at 110°C.[40]

THESIS ORGANIZATION

Chapters 2 to 6 are written in a manuscript format. Each chapter has its own introduction, literature review, experimental procedure, results and discussions, conclusions, and references.

Poly(ethyl oxazoline):PEOX

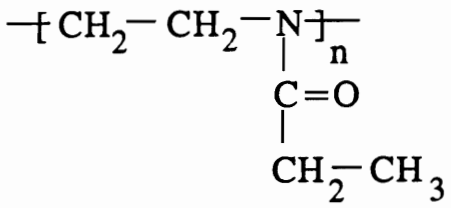

Poly(vinyl methyl ether):PVME

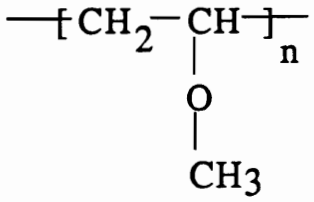

Poly(dimethyl siloxane):PDMS

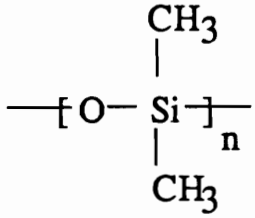

Poly(ethylene oxide):PEO

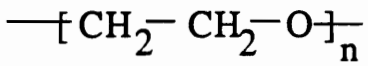

Poly(propylene oxide):PPO

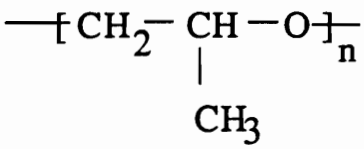

Figure 1.6 The chemical structure of homopolymers used in this study.

Copolymer: PEOX-PVME

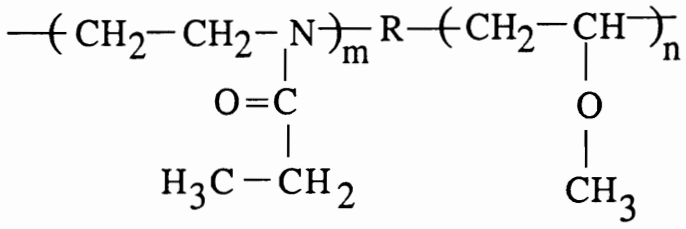

Copolymer: PEOX-PDMS

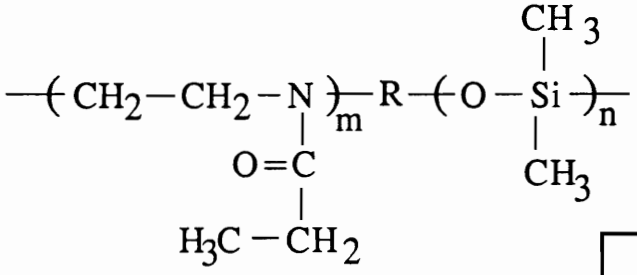

R = alkyl, benzyl

poly(dimethyl amino ethyl methacrylate-*b*-butyl methacrylate) (DMAEM-BMA):

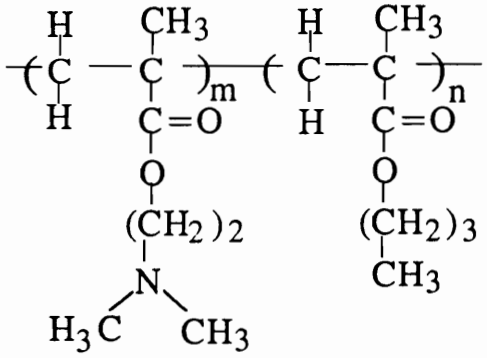

Figure 1.7 The chemical formula of copolymers used in this study.

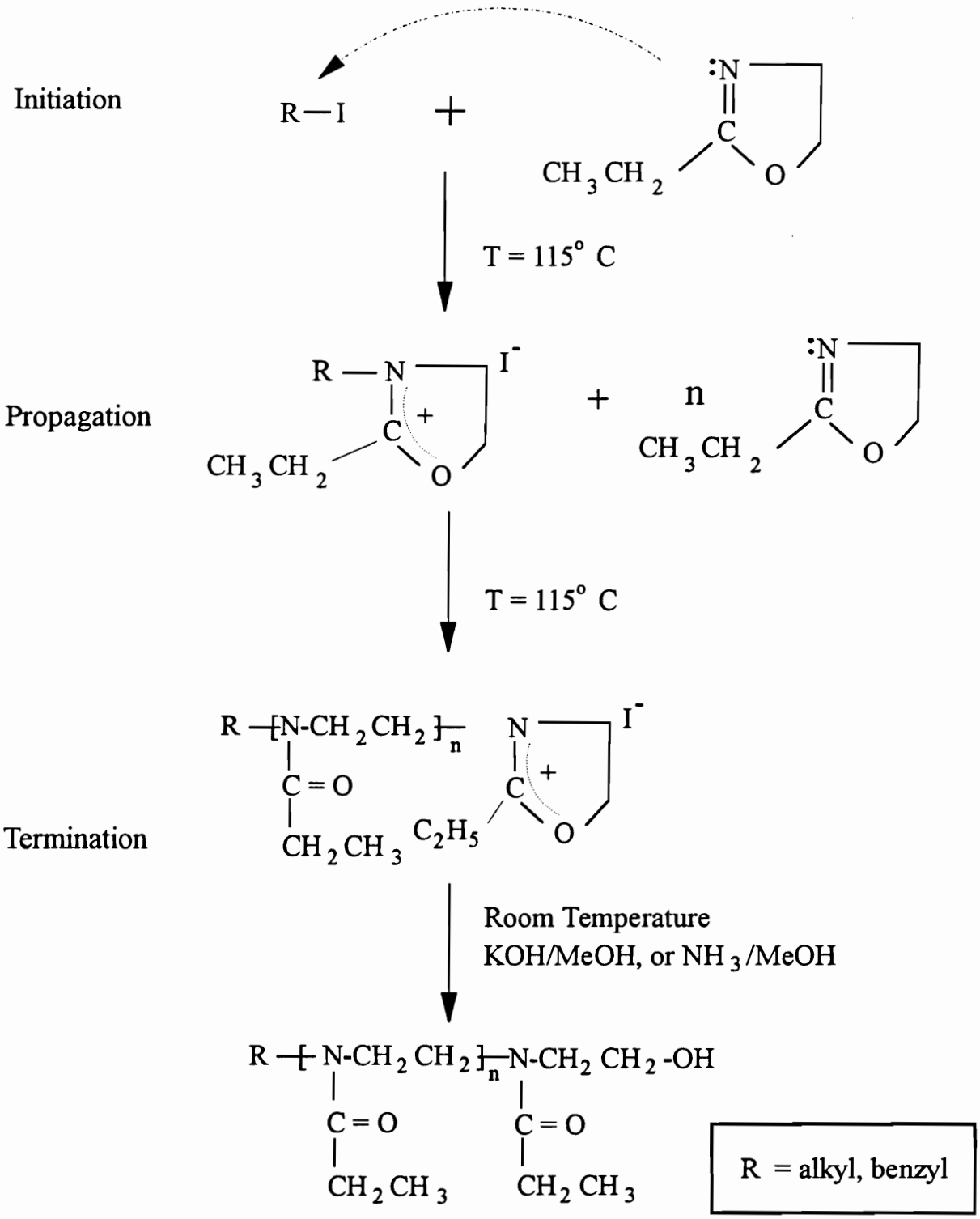

Figure 1.8 An schematic illustration of the Poly(alkyl oxazoline) ring-opening polymerization process.

Chapter 2 primarily concerns the properties of solutions of poly(2-ethyl-2-oxazoline) in water and alcohols using light scattering, GPC, viscosimetry and cloud point measurements. From this, the molecular weights of PEOX, the Kuhn length of PEOX segments, the second virial coefficients of PEOX in solvents, and the enthalpy and entropy of dilution of water in PEOX-water solution were measured.

Chapter 3 concerns the segmental adsorption energy parameter, χ_s^{po}, of PEOX on silica from water and ethanol. This parameter is directly related to polymer adsorption affinity since the adsorbed amount increases with χ_s according to the Scheutjens-Fleer lattice model. The measurement of χ_s was accomplished using the desorption/displacement technique developed by Cohen Stuart *et al.*[31]. This approach is based on the mean field lattice theory of Scheutjens and Fleer which provides a useful framework for interpreting experimental adsorption results. From the high segmental adsorption energy values of PEOX in water and ethanol, different adsorption mechanisms of PEOX on silica surfaces from water and ethanol were postulated. The contribution of the water's entropy on the adsorption of PEOX is also discussed.

Chapter 4 focuses further on the adsorption behavior of PEOX on silica from various solvents, including water and several alcohols. The adsorbed amount data were interpreted qualitatively with the Scheutjens and Fleer mean-field lattice theory. In addition, the influences of pH value and salt concentration on the adsorption of PEOX were measured. It was found that the solubility of polymer played an important role in the adsorption. The competitive adsorption of several polyethers with PEOX from different solvents was studied to relate the relative adsorption affinity to polymer structure. These results provide guidelines for the design of water-soluble diblock systems.

Chapter 5 deals with the solution properties and the adsorption behavior of PEOX-PDMS and PEOX-PVME copolymers on silica. The solution properties (presence or absence of micellization) were mainly related to their solubility in different solvents. In addition, monodisperse Stöber silica was synthesized and used in the adsorption

experiments. Competitive adsorption experiments established that PEOX should serve as an effective anchor block for all of the diblocks studied. The PEOX-PDMS diblock copolymer effectively stabilized the silica dispersions in chlorobenzene. A quantitative estimation of the particle stability was observed by the DLS technique.

In **Chapter 6**, the measurements of the adsorbed layer thickness and the adsorbed amount of DMAEM-BMA diblock copolymers in isopropanol were performed. The Stöber and Cab-O-Sil silica served as the adsorbents for thickness and adsorption isotherm, respectively. Isopropanol is a good solvent for two blocks. The results of Wu *et al.* and ours were combined to compare with the scaling theory, which showed that the Marques-Joanny scaling theory could explain copolymer adsorption in our system very well.

REFERENCES

(1) Napper, D. H., *"Polymeric Stabilization of Colloidal Dispersion,"* N.Y. 1983.

(2) Hunter, R.J., *"Foundation of Colloid Science,"* Vol I, Oxford, London, 1986.

(3) Tadros, Th. F., in *"The Effect of Polymers on Dispersion Properties,"* Academic Press, London, 1982.

(4) Fontana, N.J., in *"Chemistry of Biosurfaces,"* Hair, M.L.(Ed.) vol.I, Dekker, New York, 1971.

(5) Ives, K.J., *"The scientific Basis of Flocculation,"*, Sijthoff and Noordhoff, Alphenaan den Rijn, Netherlands, 1978.

(6) Patric, R.L., *"Treatise on Adhesion and Adhesives,"* vol.I Dekker, N.Y. 1967.

(7) Kraus, G., *"Reinforcement of Elastomers,"* Wiley, N.Y. 1965.

(8) Goodwin, J.W. *Ceramic Bulletin*, **69**, 1694 (1990); Ring, T.A. *Material Research Sci. Bull.* 34, **January** (1990).

(9) Finch, C.A. (Ed.), *"Chemistry and Technology of Water-Soluble Polymers,"* Plenum Press, Chapters 1,7,9 New York, 1981.

(10) Chiu, T.T., Thill, B.P., Fairchok, W.J. in *"Water-Soluble Polymers, Beauty with Performance,"* Glass, J.E. (Ed.), Advances in Chemistry Series, vol. 213, Washington, D.C., 1986.

(11) Stahl, G.A., Schulz, D.N., *"Water-Soluble Polymers for Petroleum Recovery,"* Plenum Press, New York, 1987.

(12) Molyneux, P., *"Water-Soluble Synthetic Polymers: Properties and Behavior,"* Vol. I & II, CRC Press, 1983.

(13) Shalaby, S.W., McCormic, C.L., Butler, G.B., *"Water-Soluble Polymers, Synthesis, Solution Properties and Applications,"* ACS Symposium Series 467, Washington, D.C., 1991.

(14) Glass, J.E., *"Polymers in Aqueous Media, Performance Through Association,"* Advances in Chemistry Series 223, ACS Press, Washington, D.C., 1989.

(15) Chen, F.P., Ames, A.E., and Taylor, L.D., *Macromolecules* **23**, 4688 (1990).

(16) Koningsveld, R. Stockmayer, W.H., Kennedy, J.W., Kleintjens, L.A., *Macromolecules* **7**, 73 (1974).

(17) Flory, P.J., *"Principles of Polymer Chemistry,"* Cornell Press, Ithaca, 1953.

(18) Patterson, D., Delmas, G., *Trans Faraday Soc.*, **65**, 708 (1969).

(19) de Gennes, P.G., *Pure & Appl. Chem.* **64**, 1585 (1992).

(20) Israelachvili, J., Tandon, R., White, L. *J. Colloid Interface Sci.* **78**, 430 (1980); Klein, J., Luckham, P., *Macromolecules* **17**, 1041 (1984).

(21) Howard, G.J., in *"Interfacial Phenomena in Apolar Media,"* Surfactant Science Series; vol. 21, Eicke, H.-F., Parfitt, G.D. (Ed.) Marcel Dekker, Inc. New York, 1987.

(22) Goddard, E.D., Vincent, B., *"Polymer Adsorption and Dispersion Stability,"* ACS Symposium Series 240, ACS Washington, D.C. 1984.

(23) Scheutjens, J.M.H.M., Fleer G.J., *J. Phys. Chem.* **83**, 1619 (1979); **84**, 178 (1980).

(24) de Gennes, P.G., *J. de Phys.* **36**, 1199 (1975); **37**, 1445 (1976).

(25) Silberberg, A., *J. Chem. Phys.* **48**, 2835 (1968).

(26) Cohen Stuart M.A., Cosgrove, T., Vicent, B. *Adv. Colloid Interface Science* **24**, 143 (1986)

(27) Jenckel, E. and Rumbach, R., *A. Elecktrochem.* **55**, 612 (1952).

(28) Marques, C.M., Joanny, J.F. *Macromolecules* **22**, 1454 (1989).

(29) Fleer G.J., Scheutjens, J.M.H.M. *Colloids and Surface* **51**, 281 (1990).

(30) Perkel, R., Ullman, R., *J. Polym. Sci.* **54**, 127 (1961).

(31) Cohen Stuart, M.A., Fleer, G.J. and Scheutjens, J.H.H.M., *J. Colloid Interf. Sci.* **97**, 526 (1984); **90**, 310; 321 (1982).

(32) Guzonas, D., Hair, M.L., Cosgrove, T,, *Macromolecules* **25**, 2777 (1992); Guzonas, D.,Boils, D., Hair, M.L. *Macromolecules* **24**, 3383 (1991).

(33) Wu, D.T., Yokoyama, A., Settlerquist, R.L. *Polymer* **23**, 709 (1991).

(34) Buscall, R., Corner, T., Stageman, J.F. *"Polymer Colloids"* Elsevier Applied Science Publishers, New York, 1985.

(35) Cosgrove, T., Phipps, J.S., Richardson, R.M., Hair, M.L., Guzonas, D.A. *Macromolecules* **26**, 4363 (1993).

(36) Shaw, D. J., *"Introduction to Colloid and Surface Chemistry"* Butterworths, Boston, 1980.

(37) Tadros, Th. F., *"Polymers in Colloid Systems, Adsorption, Stability and Flow"* Academic Press, London, 1988.

(38) Kerkar, A.V., Henderson, R.J.M., Feke, D.L., *J. Am. Ceram. Soc.* **73(10)**, 2879, 2886 (1990).

(39) Stöber, W., Fink, A., Bohn, E., *J. Collod. Interface Sci.* **26**, 62 (1968).

(40) (a) Liu, Q., Konas, M., Riffle, J.S., *Macromolecules* **26**, 5572, (1993); (b) Liu, Q., Konas, M., Davis, R.M., Riffle, J.S., *J. Polymer Science: Part (A), Polymer Chemistry* **31**, 1709 (1993); (c) Liu, Q., Wilson, G.R., Davis, R.M., Riffle, J.S., *Polymer* **34**, 3030 (1993).

(41) Barnett, K., Cosgrove, T., Crowley, Tadros, Th. F., Vincent, B. in *"The Effect of Polymers on Dispersion Properties,"* Tadros, Th. F. (Ed.) Academic Press, London, 1982.

(42) (a) Cosgrove, T., Heath, T.G., Phipps, J.S., Richardson, *Macromolecules* **24**, 94 (1991) (b) Cosgrove, T., Finch, N.A., Webster, R.P. *Macromolecules* **23**, 3353 (1990).

(43) Davis, R.M., *TAPPI Journal* **74(4)**, 99 1987.

(44) Visser, J. *Adv. Colloid and Interf. Sci.* **3**, 331 (1972).

Chapter 2

Solution Properties of Poly(2-alkyl-2-oxazoline)s: Light Scattering, Cloud Point and Viscosity Studies

ABSTRACT

Solutions of poly(2-ethyl-2-oxazoline) and poly(2-methyl-2-oxazoline) in water and several alcohols were characterized by light scattering, cloud point and capillary viscometry. The second virial coefficients in water were found to decrease with increasing temperature, reflecting lower critical solution behavior due to hydrogen bonding. This was consistent with the cloud point measurements. This resulted in negative values of the excess enthalpy Δh^E and entropy of dilution of the solvent Δs^E for PEOX and PMOX in water. The magnitudes of Δh^E and Δs^E were higher for PMOX than for PEOX. The magnitudes of Δh^E and Δs^E for PEOX increased with molecular weight. The second virial coefficients of PEOX in water were systematically lower than in ethanol, isopropanol, and n-butanol. The Flory-Huggins χ parameter determined from light scattering was in the range 0.48-0.49 in water and in the range 0.32-0.41 in ethanol. The Kuhn length for PEOX was determined from intrinsic viscosity measurements to be 0.77 nm which corresponds to less than two monomer units.

INTRODUCTION

There is considerable interest in water-soluble polymers because of their importance in controlling the colloid stability and rheology of ceramic suspensions, emulsions, and coatings. Environmental concerns in the chemical process industry have heightened this interest. Nonionic water-soluble polymers constitute an important and still poorly understood class of polymers due to the lack of a rigorous equation of state

relating polymer and solvent structure to solution properties. Polymer adsorption is typically described in terms of a polymer-solvent interaction parameter, either in the form of a Flory χ parameter[1-3] or an excluded volume term[4,5], and a polymer segment-surface interaction term χ_s [3]. This paper focuses on the characterization of the polymer-solvent interactions in various solvents for poly(2-alkyl-2-oxazolines) as part of a program to develop diblock copolymer steric stabilizers. Poly(2-ethyl-2-oxazoline), PEOX, has been used in the synthesis of two novel diblock systems - poly(dimethyl siloxane-2-ethyl-2-oxazoline)[6] and poly(methyl vinyl ether-2-ethyl-2-oxazoline)[7]. A corresponding study of the segmental adsorption free energy of PEOX on silica from water and ethanol is the subject of Chapter 3.

PEOX, and poly(2-methyl-2-oxazoline), PMOX, are amorphous, nonionic, tertiary amide polymers with repeat units illustrated in Figure 2.1. There is reason to believe that the PEOX block will function as an effective anchor block on surfaces with hydrogen bonding groups such as hydroxyl groups on metal oxides. Thus, we have characterized PEOX homopolymer samples with relatively narrow molecular weight distributions by capillary viscometry, static and dynamic light scattering, and gel permeation chromatography (GPC). Second virial coefficients were also measured for PMOX to study the effects of polymer structure on polymer-solvent interactions. We report values of intrinsic viscosity $[\eta]$ at θ-condition, second virial coefficient A_2, Kuhn length L_k, and the Flory χ parameter for PEOX samples over the range of molecular weights in which PEOX should function most effectively as an anchor block. The molecular weight distribution affects solution and adsorption behavior. Control of the molecular weight distribution is essential in testing adsorption theories.[1]

In the most comprehensive study to date of the solution properties of PEOX, Chen *et al.* characterized a polydisperse sample of PEOX by static and dynamic light scattering as well as by osmotic pressure measurements of PEOX in water and ethanol[8]. Phase separation measurements demonstrated that PEOX exhibits lower critical solution temperature (LCST) behavior in water with the θ-temperature=56°C. The temperature

(a)

Poly(ethyl oxazoline):PEOX

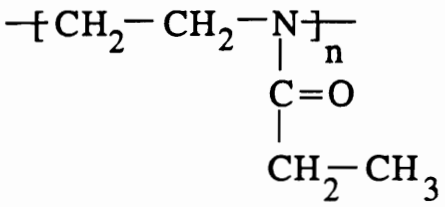

(b)

Poly(methyl oxazoline):PMOX

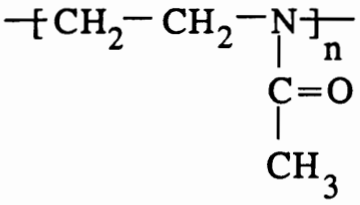

Figure 2.1 Chemical formula of the repeat units of (a) Poly(2-ethyl-2-oxazoline), PEOX, and (b) Poly(2-methyl-2-oxazoline), PMOX.

dependence of the second virial coefficient revealed that the excess enthalpy of dilution of the solvent, Δh^E, was negative due to hydrogen bond formation between the carbonyl (-C=O) group on the polymer and water. FTIR spectroscopy demonstrated that hydrogen bonds formed between PEOX and deuterium oxide. The excess entropy of dilution, Δs^E, was negative as well due to the specific association of the water molecules with the PEOX chain. PEOX was found to be more soluble in ethanol than in water. PEOX is soluble in a variety of solvents, particularly those capable of forming hydrogen bonds[10]. PEOX is compatible with a number of polymers for the same reason[9-11]. Nothing has been reported on the solution properties of PMOX.

In this chapter, we studied well-defined PEOX homopolymer samples by static light scattering in water and several alcohols. We report values of the excess enthalpy and entropy of dilution for PEOX in water for molecular weights in the range $\approx$ 20-60 kg mole^{-1} as part of our work to understand how the behavior of PEOX in solution is related to its adsorption behavior[12]. Second virial coefficients were also measured for PMOX to study the effects of polymer structure on polymer-solvent interactions.

Experimental

Materials and Solution Preparation

PEOX and PMOX were synthesized over a range of molecular weights using a cationic living polymerization process which has been described by Saegusa *et al.* previously[13-14] and Liu *et al.*[6-7,15]. The living nature of the polymerization makes it possible to prepare di- and tri-block copolymers from these monomers[14] and allows for functional termination[15-17]. Liu *et al.* established that the M_n of PEOX increased linearly with monomer conversion, suggesting that chain transfer reactions were not occurring[15]. In that same study, gel permeation chromatography showed that PEOX homopolymer samples with $M_n \leq 40$ kg mole^{-1} had $M_w/M_n \approx 1.3$.[15] Those measurements were not straightforward due to the adsorption of PEOX onto components in the GPC system. The typical M_w/M_n values, 1.3, were somewhat larger than expected for a living

polymerization system. This might be explained by slight aggregation of the PEOX in the mobile phase (85/15 v/v THF/MeOH). In this chapter, it is shown that PEOX aggregates in water and n-butanol. Samples of PEOX were stored in a desiccator chamber prior to use since PEOX is very hygroscopic. Deionized water with a resistivity of $17x10^6$ ohm-cm was obtained from a Barnstead NANOPURE II™ water purification system. Ethanol (200-proof, Aaper Alcohol and Chemical Company) was further dried by vacuum distillation from CaH_2. Solutions for light scattering were filtered typically with 0.22 micron Acrodisk filters. The solvents were purchased from Aldrich Chemical Company. Isopropanol (anhydrous, 99+%), n-butanol (HPLC grade), and benzene (Spectrophotometric grade, 99%) were used.

Partial Specific Volume

The partial specific volume v_p of PEOX was determined from density measurements of PEOX in water and anhydrous ethanol using a Mettler KEM DA-300 density meter that is accurate to within ± 0.0001 g cm^{-3} at temperatures over the range 5-45°C $\pm$ 0.01°C. The values of v_p were independent of temperature with v_p = 0.87 cm^3g^{-1} for water and v_p = 0.86 cm^3g^{-1} for ethanol. This compares with the value of v_p = 0.877 cm^3g^{-1} for an ideal solution of PEOX at 25°C derived from the density of solid PEOX of 1.14 g cm^{-3} [9]. The values of v_p will be used in calculating approximate Flory χ parameters for study of PEOX adsorption on silica[12].

Light Scattering

Static light scattering experiments were performed with a Brookhaven model 2030AT instrument. The light source was an argon ion laser operated at a wavelength of 514.5 nm. Refractive index increments $\partial n/\partial c$ were measured at a wavelength of 510 nm with a Model 60/ED refractometer made by Bellingham & Stanley, Ltd. equipped with a differential cell.

The angular dependent scattering intensity, $I(\theta)$, was used to calculate the

Rayleigh ratio, $R(\theta)$ for polarized light according to[18]

$$R(\theta)=C_R I(\theta)\sin(\theta)(n_s/n_c)^2/I_o \qquad (2.1)$$

where I_0 is the incident beam intensity, C_R is an instrumental constant, and n_s and n_c are the refractive indices of the scattering solution and the calibration liquid, respectively. Benzene was used as a scattering reference to determine the constant C_R. The Rayleigh ratio for benzene measured with vertically polarized incident light at a scattering angle of 90° is $R_V(90°) = 30.4\times10^{-6}$ cm^{-1}.[18] The effect of temperature on the Rayleigh ratio was taken into account using the method recommended by Chu[19] which corrects the ratio at a given temperature using the scattering intensity of benzene and the refractive index at that temperature[20,21]. The excess Rayleigh ratio, $\Delta R(\theta)$, ($= R(\theta)_{solution} - R(\theta)_{solvent}$) is related to the weight-average molecular weight M_w, the second virial coefficient A_2, and the radius of gyration R_g by[22]:

$$Kc/\Delta R(\theta) = M_w^{-1}(1+(qR_g)^2/3) + 2A_2c \qquad (2.2)$$

where c is the polymer concentration and q is the scattering vector defined as

$$q= 4\pi n_0\sin(\theta/2)/\lambda_0 \qquad (2.3)$$

and n_0 is the solvent refractive index. In equation (2.2), K is defined for vertically polarized light by

$$K = (2\pi n_0(\partial n/\partial c))^2/N_a\lambda_0^4. \qquad (2.4)$$

For all light scattering experiments from 5° - 45°C, $\Delta R(\theta)$ was independent of the scattering angle within experimental error, *i.e.* $qR_g << 1$ due to the relatively low molecular weights employed and due to the relatively low degree of chain expansion of

the PEOX. Thus, equation (2.2) can be simplified as:

$$Kc/\Delta R(\theta) = M_w^{-1} + 2A_2c. \qquad (2.5)$$

All measurements of the second virial coefficient, A_2, were made at a scattering angle of 90° with dilute solutions with polymer concentration $c \leq 0.01$ g cm^{-3}. A representative scattering intensity plot for the samples PEOX 20K and 30K in ethanol is shown in Figure 2.2.

GPC Analyses.

The molecular weight and molecular weight distributions of the PEOX samples were measured with a gel permeation chromatograph equipped with a refractive index detector and a VISCOTEK intrinsic viscosity detector which permitted the use of a universal calibration curve.[22] PERMAGEL columns were used with a column packing size of 10 microns. Details of this procedure have been reported previously.[7] The mobile phase was an 85/15 v/v mixture of tetrahydrofuran and methanol and the measurements were performed at 25°C.

Intrinsic Viscosity Experiments.

Viscosities of dilute solutions of PEOX in water were measured with a Cannon Ubbelohde L-50 viscometer in a water bath over the temperature range 25-56°C. The temperature was regulated to within $\pm$ 0.1°C.

Cloud Point.

PEOX solutions in water were prepared at different concentrations for cloud point measurement. The phase separation was observed visually while the solution was heated. The solutions were contained in glass vials and were placed in a temperature bath containing silicone oil. Solutions were heated at a rate of 1.0 °C/min.

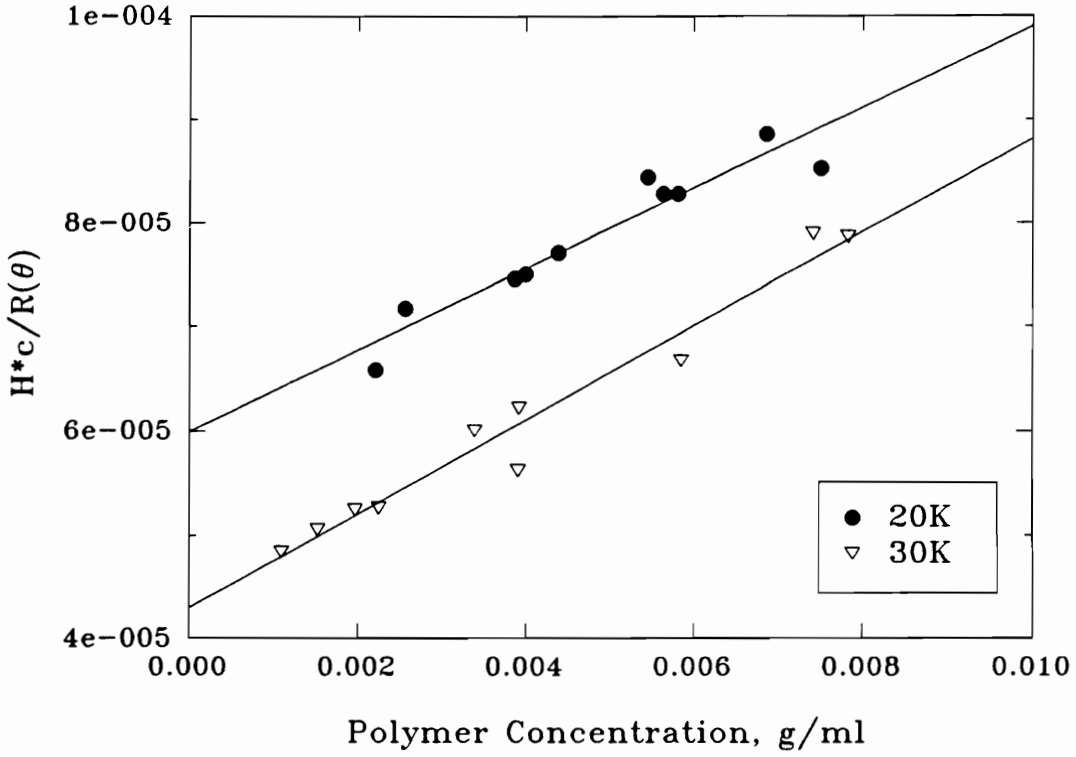

Figure 2.2 Representative static light scattering plot of PEOX(20K) and PEOX(30K) in ethanol at 25°C; • PEOX(20K); ▽ PEOX(30K).

RESULTS AND DISCUSSION

Molecular Weight Measurements

Table 2.1 lists values of the refractive index increment, $\partial n/\partial c$ for PEOX and PMOX at different temperatures and in different solvents. The values of M_w in Table 2.2 for PEOX 20K and PEOX 30K in ethanol and isopropanol agreed reasonably well. The calculation of standard deviation for molecular weight measurements is cited in Appendix I, according to the least squares method. In addition, Table 2.3 summarizes the molecular weights of PEOX from static light scattering and gel permeation chromatography. The M_w measurements in water for PEOX 20K, 30K, and 60K were somewhat higher than in alcohols. We believe this is due to some aggregation of PEOX in water. Indeed, a PEOX sample with a number average M_n = 2 kg mole^{-1} as determined from monomer conversion data formed aggregates in water with an apparent $M_w \approx 57$ kg mole^{-1}. Aggregation of nonionic water soluble polymers in water was reviewed by Burchard[23] for several polymers including poly(ethylene oxide), PEO, and poly(vinyl pyrrolidone), PVP. In one study, PEO with an approximate molecular weight 20 kg mole^{-1} had an apparent $M_w \approx 260$ kg mole^{-1} as determined by light scattering. The aggregation of PEO in water has been attributed to hydrophobic interactions between the nonpolar regions of the polymer chain[24]. PVP, whose structure is similar to PEOX, also has been found to aggregate in water but little, if any in ethanol[23]. The higher value of M_w for PEOX in n-butanol than in ethanol and isopropanol may be due to some slight aggregation. In future work, this will be explored using experiments at other molecular weights. Thus, the values of M_w in water and n-butanol are apparent or extrapolated values while the true values of M_w were determined in ethanol and isopropanol.

Table 2.1. Refractive Index Increments, $\partial n/\partial c$, for Poly(2-alkyl-oxazolines) at 510 nm

Polymer/Solvent	$\partial n/\partial c$, cm^3g^{-1}		
	5°C	25°C	45°C
PEOX/Water	0.184±0.002	0.176±0.002	0.174±0.002
PEOX/Ethanol	--	0.155±0.002	--
PEOX/Isopropanol	--	0.155±0.003	0.159±0.001
PEOX/n-Butanol	--	0.110±0.001	--
PMOX/Water	0.180±0.002	0.172±0.002	0.172±0.002

The effect of aggregation on the interpretation of light scattering results has been discussed in detail by Elias[25]. Several cases of aggregation are possible, most of them resulting in highly nonlinear plots of $Kc/\Delta R(\theta)$ versus c (see equation (2.5)). In Elias' nomenclature, the results for PEOX correspond to the Type IVB case where the polymer is in a good solvent and the scattering plot of $Kc/\Delta R(\theta)$ versus c is linear but the extrapolated M_w depends upon the solvent used. In this case, the magnitude of the second virial coefficient exceeds the effect of the intermolecular association which, by itself, would lead to nonlinearity. Good linearity was observed for the scattering experiment shown in Figure 2.2 over the PEOX concentration range 0.001-0.008 g cm^{-3}. All of the scattering experiments were conducted in the concentration range 0.001-0.01 g cm^{-3}. We found no systematic curvature over these concentrations in any of the scattering experiments.

In water and possibly n-butanol, there is likely a distribution of unimers (single chains) and multimers (associated chains). For open association, all types of multimers can form whereas, for closed association, only two species are present - unimers and multimers with a single, fixed degree of association. It is not clear whether the association of PEOX is open or closed. Type IVB behavior is exhibited by polymers undergoing both open and closed association[25]. In view of this, the A_2 values of PEOX in water and n-butanol represent effective averages over the associated states in solution.

TABLE 2.2. Second Virial Coefficients and Molecular Weights for Poly(2-alkyl-2-oxazoline) as a function of temperature and solvent type.

Sample	Solvent	T °C	M_W[a] kg mole^{-1}	Second Virial Coefficient, A_2 mole cm^3 g^{-2} x 10^4
PEOX 20K	Water	5	22.9±0.9	12.2±1.4
		25	23.1±0.8	10.8±1.0
		45	23.2±0.7	9.4±1.1
	Ethanol	25	16.6±0.6	19.5±2.1
	Isopropanol	25	14.4±0.5	29.1±1.9
		45	16.5±0.4	33.8±1.2
	n-Butanol	25	20.2±0.3	20.4±1.2
PEOX 30K	Water	5	32.0	9.56
		25	34.0	7.41
		45	33.8	5.92
	Ethanol	25	23.2±1.2	22.6±1.6
	Isopropanol	25	22±0.9	30.9±1.9
		45	22.3±0.4	25.8±0.8
PEOX 60K	Water	5	67.1±0.4	8.8±0.7
		25	66.9±4.7	7.5±0.8
		45	62.1±2.3	4.2±0.5
	Isopropanol	25	47.0±0.1	9.87±0.6
		45	46.0±0.1	10.8±0.8
PMOX 20K	Water	25	21.8±1.1	17.1±1.9
PMOX 30K	Water	5	24.3	17.3
		25	23.7	13.7
		45	21.7	11.2

[a] From light scattering at scattering angle = 90°.

This is analogous to the interpretation of A_2 measurements for solutions of single chains with some polydispersity[26].

Molecular Weight Dependence.

The samples with the three lowest molecular weights - PEOX 2K, 5K, and 7K - aggregated in water due most probably to interchain hydrogen bonding. The approximate number of PEOX chains per aggregate, $(M_W)_{aggregate}/(M_W)_{single\ chain}$ ranged from 14 for PEOX 2K to 2 for PEOX 7K. These ratios are based on the value of $(M_W)_{single\ chain}$ obtained by GPC and listed in Table 2.3. It is believed that the PEOX chains aggregate through hydrogen bond bridges formed by water molecules.

TABLE 2.3 Molecular Weight Characterization Data for Poly(2-alkyl-oxazolines)

Sample	M_n(GPC) kg mole^{-1}	M_w (GPC)	M_w/M_n(GPC)	M_w (SLS)[a]
PEOX 2K	3.7	4.1	1.10	~57[c]
PEOX 5K	7.3	8.1	1.11	~34[c]
PEOX 7K	6.1	7.4	1.21	~13[c]
PEOX 20K	19.4	29.0	1.50	22.6[a]
PEOX 30K	36.8	43.8	1.19	33.2[a]
PEOX 60K	54.0	83.2	1.54	63.5[a]
PMOX 20K				21.8[b]
PMOX 30K				23.2[b]

[a] Average values from static light scattering at 5°, 25°, and 45°C in water at scattering angle = 90°.
[b] From static light scattering at 25° in water with scattering angle = 90°.
[c] Aggregated

Second Virial Coefficients

Effect of Temperature and Molecular Weight. The second virial coefficients of PEOX and PMOX are summarized in Table 2.2. The standard deviations for A_2, σ_{A2}, are

also shown in Appendix I. The decrease of A_2 with increasing temperature reflects the lower critical solution behavior of PEOX and PMOX in water. The magnitude of dA_2/dT, summarized in Table 2.4 for various polymers in water, generally increased with molecular weight. The analysis of the temperature dependence of the values of A_2 for PEOX in water is simplified by the lack of systematic variation of the extrapolated M_w with temperature. The variations that do occur generally fell within the error bars for the experiments. Thus, the A_2 measurements as a function of temperature are probing the interactions of solvent with associated chains whose effective molecular weight distributions do not change very much with temperature.

Table 2.4 Effect of Temperature on Second Virial Coefficients for Poly(2-alkyloxazolines)

Polymer/Solvent	M_w kg mole^{-1}	dA_2/dT mole cm^3 g^{-2} °K x 10^5	B_2'[a] cal cm^{3}g^{-2} °K^{-1} x 10^3
PEOX 20K/water	23.1[b]	-0.7±0.01	-1.99±0.16
PEOX 30K/water	33.3[b]	-0.91±0.09	-3.85±0.35
PEOX 60K/water	65.4[b]	-1.15±0.28	-5.5±1.9
PEOX(Chen)/water	116[c]	-3.3	-19.0
PMOX 30K/water	23.2[b]	-1.52±0.1	-6.2±0.2

[a] $B_2' = d(RTA_2)/dT = \Delta s^E/c^2V_1$, reduced excess entropy of dilution, from equation (2.7).
[b] Average values from static light scattering at 5°, 25°, and 45°C in water with angle 90°.
[c] From static light scattering by Chen *et al.*, reference (8).

To quantify further the effect of temperature on A_2, we follow the approach of Schulz *et al.*[27] who decomposed the temperature dependence of A_2 into a contribution from the excess enthalpy of dilution of the solvent, Δh^E, and a contribution from the excess entropy of dilution of the solvent, Δs^E. This analysis can be applied to aggregating

systems as long as the second virial coefficient dominates the aggregation effect as shown by the linearity of the scattering plots. The excess enthalpy of dilution is given by

$$\Delta h^E = (B_2' \, T - B_2)c^2 \, V_1 \qquad (2.6)$$

where $B_2 = RTA_2$, $B_2' = dB_2/dT$, and V_1 is the partial molar volume of water. The excess entropy of dilution is given by

$$\Delta s^E = B_2' c^2 \, V_1. \qquad (2.7)$$

The excess chemical potential of the solvent is then given by

$$\Delta \mu^E = \Delta h^E - T\Delta s^E. \qquad (2.8)$$

For solutions of PEOX and PMOX in water, the excess enthalpy Δh^E and the excess entropy Δs^E were negative due to hydrogen bonding between PEOX and water. The reduced quantities $T\Delta s^E/c^2 \, V_1$ ($= T \, B_2'$) and $\Delta h^E/c^2 \, V_1$ for PEOX in water at 45°C, shown in Figure 2.3, became more negative with increasing molecular weight. The data from Chen *et al.* for a relatively polydisperse sample of PEOX with higher M_w (M_w = 116 kg mole^{-1}, M_w/M_n=2.4) are also shown in Figure 2.3 and are consistent with the molecular weight trend[9]. The magnitude of the enthalpic contribution to the excess chemical potential, $|\Delta h^E|$, was always greater than the entropic contribution, $T|\Delta s^E|$ in the temperature range 5°-45°C. While the molecular weight dependence of Δh^E and Δs^E cannot be explained definitively, the results suggest that the availability of the carbonyl groups in the PEOX chain to form hydrogen bonds with water increases with the molecular weight.

It has been suggested that the temperature dependence of χ be decomposed into an enthalpic term χ_H and an entropic term χ_S or equivalently, the terms κ and ψ from the

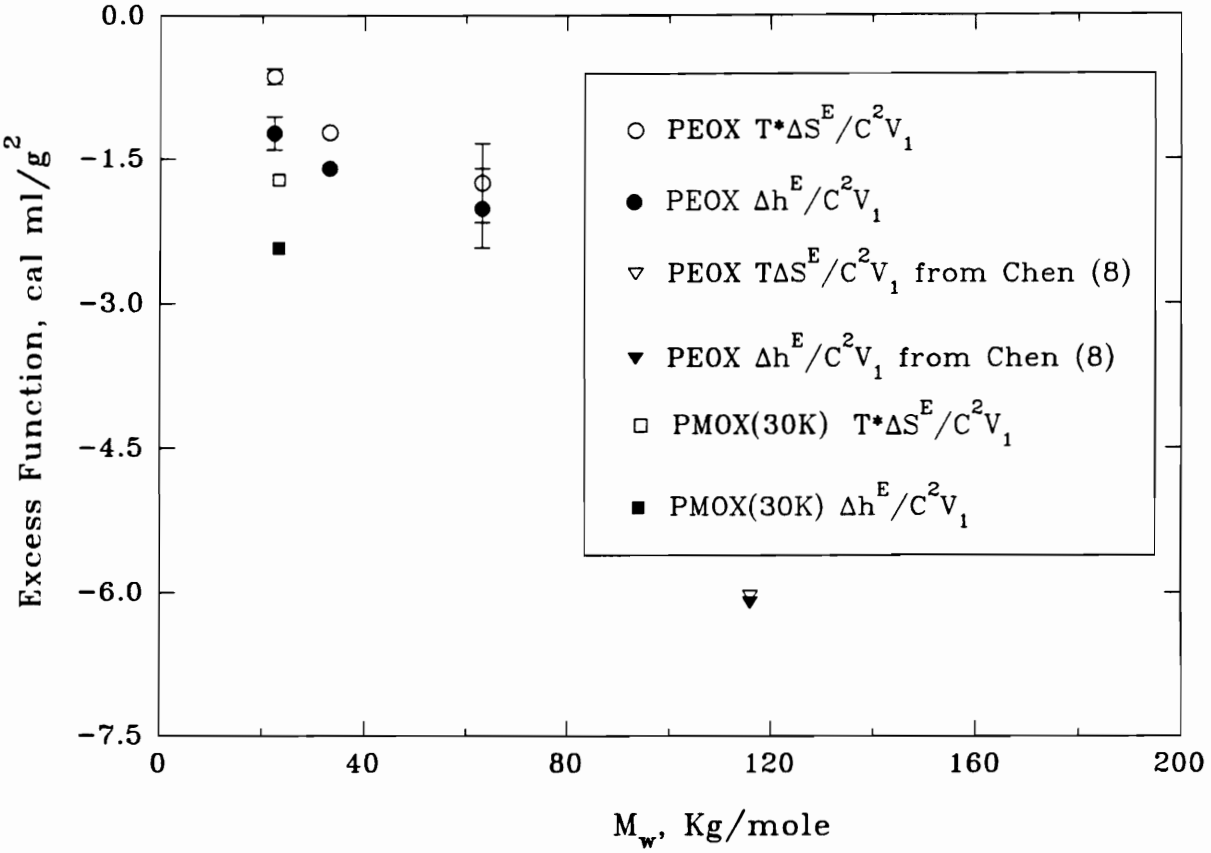

Figure 2.3 Reduced excess thermodynamic dilution functions enthalpy of mixing, $\Delta h^E/C_p^2V_1$ (equation (2.6)), and entropy of mixing $T\Delta s^E/C_p^2V_1$ (equation (2.7)) for PEOX and PMOX in water for 45°C plotted as a function of weight-average molecular weight. Also plotted are data from Chen *et al.*, reference (8).

original Flory-Huggins theory solution theory[28]. However, this approach fails to account for specific interactions such as hydrogen bonding between the polymer chain and solvent molecules.

Effect of Polymer Structure. Both Table 2.3 and Figure 2.3 show that the magnitude of the reduced excess entropy of mixing, B_2', was about 40% higher for PMOX 30K than for PEOX 20K which had a comparable value of M_w in water. This suggests water molecules form more highly ordered structures around PMOX. The methyl group shows more polar than the ethyl group due to less number of carbon. Thus, the carbonyl group in PEOX is less polar than the carbonyl group in PMOX and should form a weaker hydrogen bond with water. In addition, the more bulky and hydrophobic ethyl group probably interferes more with the formation of structures of water molecules around the PEOX backbone than does the methyl group in PMOX.

Effect of Solvent Type. At a given temperature, the values of A_2 for PEOX 20K, 30K, and 60K in different alcohols were higher than the values of A_2 in water as seen in Table 2.2. The trends are also qualitatively consistent with estimated solubility parameters for PEOX and the solvents. The Hansen solubility parameters for water, ethanol, isopropanol and butanol are 48.0, 26.3, 23.6, 23.2 $J^{1/2}/cm^{3/2}$, respectively. The solubility parameter of PEOX was estimated as $\approx$ 26 $J^{1/2}/cm^{3/2}$ by the group contribution method using values of functional groups by Fedors[29]. Better solubility and hence higher second virial coefficients are expected for polymer-solvent combinations where their solubility parameters match more closely.

Chain Stiffness. The Kuhn length L_k characterizes the chain stiffness. The ratio (R_{go}^2/M) is primarily a function of chain structure and is related to L_k by[22]

$$L_k = (6M_{mon}/L_{mon})(R_{go}^2/M) \qquad (2.9)$$

where M_{mon} is the monomer molecular weight (= 0.099 kg/mole) and L_{mon} is the monomer length (= 0.46 nm) for PEOX. The number of Kuhn segments N_k, *i.e.* the number effectively stiff segments in the polymer chain, then follows from

$$N_k = L_c/L_k \tag{2.10}$$

where L_c is the contour length, defined as the product of the degree of polymerization and monomer length L_{mon}.

Another estimate of (R_{go}^2/M) comes from the values of $[\eta]_\theta$ using the Flory-Fox equation[22]

$$(R_{go}^2/M)^{3/2} = [\eta]_\theta/(6^{3/2}M_w^{1/2}\Phi_o) \tag{2.11}$$

This gives an average value of $(R_{go}^2/M) = 5.95\text{x}10^{-4}$ nm^2 mole g^{-1} which leads L_k to be 0.77 nm of PEOX in study. The range of the Kuhn length L_k corresponds to less than twice the monomer length. Thus, PEOX is a relatively flexible polymer.

Cloud Point Measurement. Figure 1.2(a) in Chapter 1 shows typical phase diagrams for water-soluble polymers. The phase separation of polymer solutions over a wide range of molecular weights and concentrations gives useful information that is complementary to the second virial coefficient data. The temperature dependence of χ was discussed by Patterson *et al.*[30] and Flory *et al.*[31] and reviewed in Chapter 1. Based on the Flory-Huggins (FH) theory for organic solutions (non-polar solvents), the χ parameter increases as the temperature decreases until phase separation occurs. However, for water-soluble polymers phase separation also occurs when the temperature is raised to the lower critical solution temperature (LCST). In FH theory, the temperature at which phase separation occurs is given by

$$\frac{1}{T_c} = (\frac{1}{\Theta})[1+(\frac{1}{\Psi_1})(\frac{1}{\sqrt{x_n}}+\frac{1}{2\,x_n})] \qquad (2.12)$$

where T_c is the critical temperature, x_n is the degree of polymerization (number-average), Θ is the theta temperature and Ψ_1 is an entropy term, which is defined from equation (2.13):[12]

$$\Delta s_1^E = R\Psi_1\phi_2^2 \qquad (2.13)$$

in modified Flory-Huggins theory.[12,31] The intercept of Equation (2.12) provides the information of the theta temperature, Θ.

Figure 2.4 shows the cloud point measurements of PEOX in water at different molecular weights. All curves exhibit the concave shapes, which are typical for water-soluble polymers.[23,32] The cloud points decrease as polymer molecular weights increase. More analyses for the thermodynamic properties of PEOX in water are obtained from a plot of T_c associated with PEOX molecular weight, following Equation (2.12). A plot of the reciprocal critical temperature (T_c^{-1}) against the molecular weight function, $x_n^{-1/2} + (2x_n)^{-1}$, is plotted in Figure 2.5. The number-average molecular weights measured by GPC were used for this calculation. A negative slope of $1/(\Theta\cdot\Psi)$ and a positive intercept of $(1/\Theta)$ were obtained. By extrapolation of the cloud point to infinite molecular weight, the θ-temperature of PEOX in water is obtained at 60 ± 2 °C, which is relatively close to the value of 56 °C reported earlier by Chen *et al.*[8].

Also from Figure 2.5, the negative slope indicates that $\Psi_1 < 0$. This demonstrates a negative entropy of dilution of water. It is known that this slope is generally positive for polymers in non-polar organic solvents.[33] The negative sign in water results from the specific association of the water molecules with the PEOX chains.

The FH theory cannot predict the LCST which is typically observed in WSP's. In this theory, the χ parameter is predicted to increase as temperature decreases until a UCST is reached. This relation is given by[23]

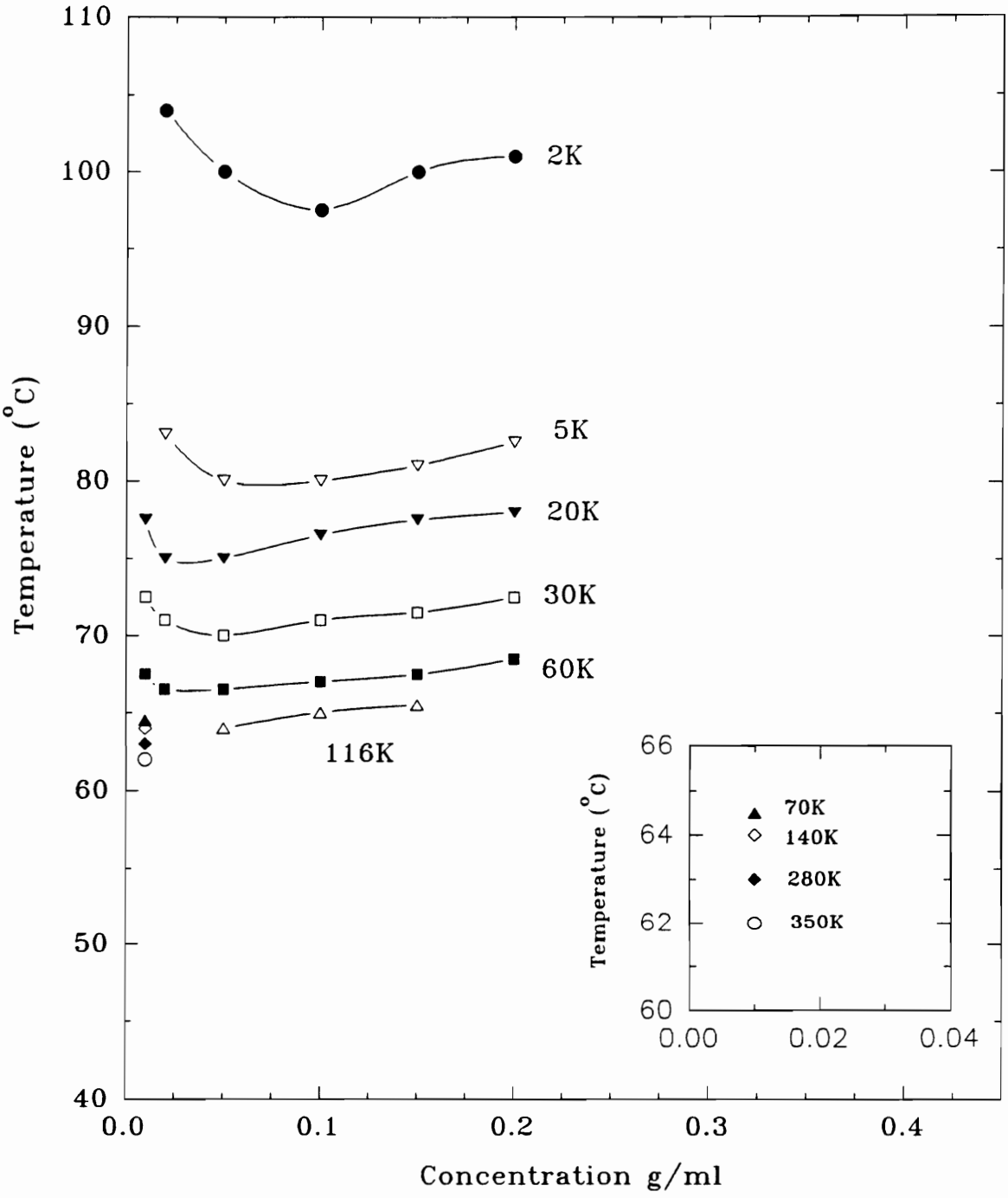

Figure 2.4 The cloud point measurements of PEOX in the dilute range at different molecular weights in water as a function of concentration. The cloud points of PEOX at high molecular weights, shown in the insert, are from reference (9).

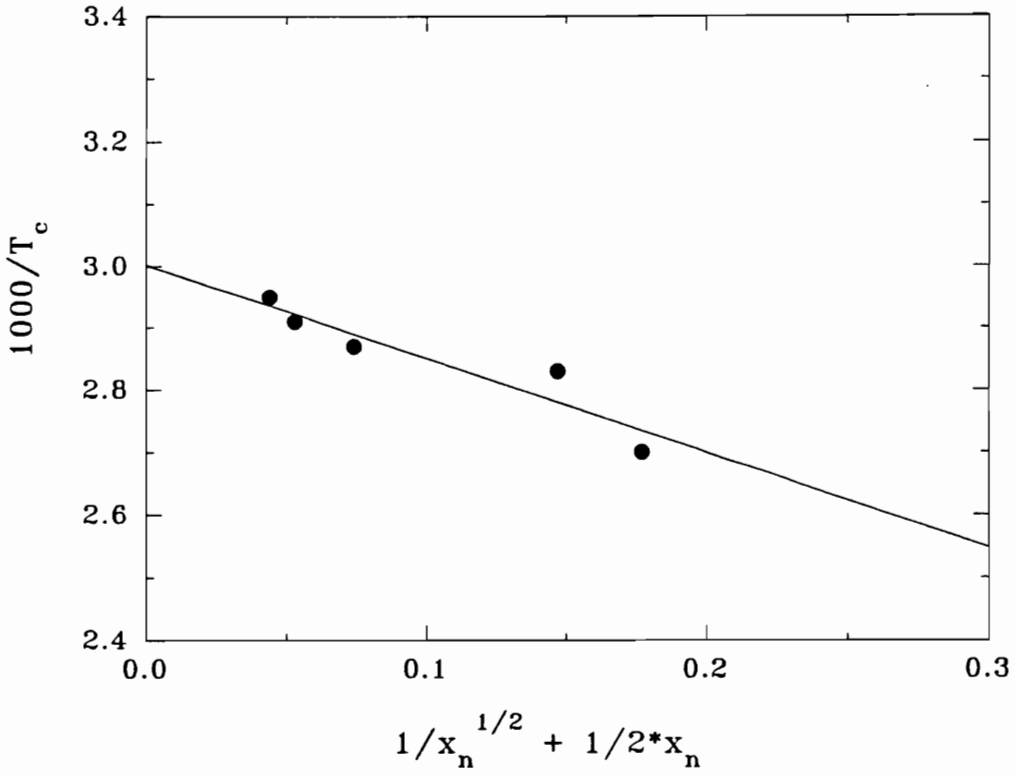

Figure 2.5 Cloud Point extrapolation to infinite molecular weight.

$$\chi = \beta_0 + \beta_1/T \qquad (2.14)$$

where positive β_0 represents a negative excess entropy of dilution of the solvent ($\Delta s_1^{ex} < 0$) and positive β_1 corresponds to an endothermic heat of dilution ($\Delta h_1 > 0$), respectively.[23] The classical FH theory predicts that both β's are positive. Equation (2.14) correctly predicts that phase separation occurs upon cooling in organic solvents. However, the experimental results of WSP's usually show a different trend that β_1 is negative indicating an exothermic heat of dilution ($\Delta h_1 < 0$). From Equation (2.8), it is seen that the entropic factor ($T \cdot \Delta s^E$) dominates the solubility behavior as temperature increases leading to $\Delta\mu_1^E = 0$ at the cloud point. As a consequence, the solution reaches the θ-condition (*i.e.*, $A_2 = 0$) upon heating. This effect is due to specific interactions, such as hydrogen bonding between polymer and water, and to the hydrophobic nature of the polymer repeat units.

CONCLUSIONS

A series of samples of poly(2-ethyl 2-oxazoline), PEOX, and poly(2-methyl 2-oxazoline), PMOX, were characterized by static light scattering, viscosity, and cloud point measurements. Both PEOX and PMOX displayed lower critical solution temperature behavior in water. Measurements of the excess enthalpy and entropy of dilution of the water, Δh^E and Δs^E, respectively, provide valuable insight into solvent structuring effects around polymer segments. The excess enthalpy of dilution of the water was negative due to hydrogen bond formation between the carbonyl group (-C=O) on the polymer chain and water. The excess entropy of dilution was also negative due to the ordering of water molecules around the polymer chains. The magnitudes of Δh^E and Δs^E increased with molecular weight, suggesting that the availability of the carbonyl groups to form hydrogen bonds with water increased. The magnitude of Δs^E and Δh^E for PMOX were higher than those for PEOX in keeping with the view that PMOX was generally

more hydrophilic than PEOX. The values of A_2, Δh^E, and Δs^E will be used in Chapter 3 which is a study of the adsorption of PEOX on silica. Some aggregation of PEOX in water was observed which may be related to aggregation reported for other water-soluble polymers. The possibility of aggregation of PMOX in various solvents will be studied in future work. PEOX was more soluble in ethanol, isopropanol, and n-butanol than in water. In future work, Δh^E and Δs^E for PEOX and PMOX will be measured in various alcohols to relate solvent structuring effects to polymer structure. Similar experiments are also planned with poly(ethylene oxide) and poly(vinyl pyrrolidone) to allow further comparisons with polymer structure.

The Kuhn length of PEOX in water was determined from the intrinsic viscosity measurements at θ-temperature. The Kuhn length stayed in the range of 0.77 nm, corresponding to less than two monomer units. This showed that PEOX was quite flexible. The final part of this chapter discussed the concentration and molecular weight dependence of the LCST in the PEOX/water system. The LCST was caused by specific interactions between the PEOX segments and water molecules. These specific interactions are related to the structure of water molecule around the PEOX chain.

Appendix I. Error Analysis for Light Scattering

(a) The weight-average molecular weight and second virial coefficient were obtained from light scattering data which were analyzed using the least-squares fitting method.[34] The standard deviations of molecular weight (σ_{MW}) and second virial coefficient (σ_{A2}) are calculated according to:

Assume that $y_i = a \cdot c_i + b$

$$\sigma_a^2 = \frac{\sigma^2 \sum c_i^2}{\Delta}$$
$$\sigma_{M_w} = M_w^2 \sigma_a \qquad \text{(A1)}$$

$$\sigma_{slope}^2 = N\frac{\sigma^2}{\Delta}$$
$$\sigma_{A_2} = (\frac{1}{2})\sigma_{slope} \qquad \text{(A2)}$$

where

$$\sigma^2 = \frac{1}{N-2}\sum_{i=1} (y_i - a - bc_i)^2$$

$\Delta = N \cdot \Sigma c_i^2 - (\Sigma c_i)^2$,

$y_i = K \cdot c_i / \Delta R_\theta$,

N = number of samples.

(b) The standard deviation of Δh_1^{ex} is calculated.

$$H = \Delta h_1^{ex}/c^2 V_1 = B_2'T - B_2 \qquad (2.7)$$

$$\sigma_H^2 = T^2 \sigma_{B2'}^2 + \sigma_{B2}^2 + 2T \sigma_{B2'B2}^2 \qquad \text{(A3)}$$

Appendix II. Intrinsic viscosity [η] (cm^3/g) of PEOX at different temperature

PEOX	M_w	25°C	35°C	45°C	56°C
20K	22.3	16	14.5	13.5	8
30K	33.2	31	23	17	13
60K	63.5	38	32	28	16

REFERENCES

(1) Scheutjens, J. M. H. M.; Fleer, G. J. *J. Phy. Chem.* 1979, **83**, 1619; 1980, **84**, 178.

(2) Cohen Stuart, M.A.; Scheutjens, J. M. H. M.; Fleer, G.J. *J. Polym. Sci., Polym. Phys. Ed.* 1980, **18**, 559.

(3) Cohen Stuart, M. A.; Fleer, G. J.; Scheutjens, J. M. H. M. *J. Coll. and Inter. Sci.* 1984, **97**, 515; 526.

(4) Ploehn, H.J.; Russel, W.B. *Macromol.* 1989, **22**, 266.

(5) Ploehn, H.J.; Russel, W.B *Adv. Chem. Engr.* 1990, **15**, 137.

(6) Liu, Q.; Wilson, G.R.; Davis, R.M.; Riffle, J.S. *Polymer* 1993, **34**, 3030.

(7) Liu, Q.; Konas, M.; Davis, R.M.; Riffle, J.S.,, *J. Poly. Sci., Poly. Chem.*, 1993, **31**, 1709.

(8) Chen, F. P.; Ames, A. E.; Taylor, L. D. *Macromol.* 1990, **23**, 4688.

(9) Chiu, T. T.; Thill, B. P.; Fairchok, W. J. in *'Water-Soluble Polymers'*, Glass, J.E., ed.; Advances in Chemistry 213; American Chemical Society: Washington, DC, 1986; pp 425-433.

(10) Keskkula, H.; Paul, D. R. *Proc. Div. PMSE ACS Meeting, St. Louis, MO*, 1984, p.11.

(11) Lichkus, A. M.; Painter, P. C.; Coleman, M. M. *Macromol.* 1988, **21**, 2636.

(12) Cowie, J.M.G. *"Polymers: Chemistry & Physics of Modern Materials"* Chapman & Hall, New York, 1991.

(13) Kabayashi, S.; Kaku, M.; Sawada, S.; Saegusa, T. *Polym. Bull.*, 1985, **13**, 447.

(14) Saegusa, T.; Ikeda, H.; Fujii, H. *Polymer J.* 1973, **4(1)**, 87.

(15) Liu, Q.; Konas, M.; Riffle, J.S. *Macromol.* 1993, **26**, 5572.

(16) Miyamoto, M.; Sawamoto, M.; Higashimura, T. *Macromol.* 1984, **17**, 2228.

(17) Miyamoto, M.; Sawamoto, M.; Higashimura, T. *Macromol.* 1985, **18**, 123.

(18) Instruction Manual for Laser Light Scattering Goniometer, Brookhaven

Instruments Co. Holtsville, New York, 1987.

(19) Chu, B. in *'Laser Light Scattering'* Academic Press, New York, 1974.

(20) Kratohvil, J. P.; Dezelic, G.J.; Kerker, M.; Matijevic, E. *J. Polym. Sci.* 1962, **57**, 59.

(21) Johnson, B.L.; Smith, J. *'Light Scattering From Polymer Solutions'*, M.B. Huglin, ed., Academic Press, London, 1972, p.27.

(22) Hiemenz, P. C. in *'Polymer Chemistry The Basic Concepts'* Marcel Dekker Inc., New York, 1984, p.709.

(23) Burchard, W. in *'Chemistry and Technology of Water-Soluble Polymers'*, C.A. Finch, Ed., Plenum Press, New York, 1981.

(24) Vink, H. *European Polymer Journal,* 1971, **7**, 1411.

(25) Elias, H.-G., *'Light Scattering from Polymer Solutions'*, M.B. Huglin, ed., Academic Press, London, 1972, p.397.

(26) Yamakawa, H., *'Modern Theory of Polymer Solutions'*, Harper and Row, New York, 1971, p.221.

(27) Schulz, G.V., Cantow, H.-J. *Elektrochem. Z.*, 1956, **60**, 517.

(28) Napper, D. H., *'Polymeric Stabilization of Colloidal Dispersions' Academic Press, New York,* 1983, p.49.

(29) van Krevelen, D. W. *'Properties of Polymers, Their Estimation and Correlation with Chemical Structure'*, Elsevier Scientific Publishing Co., New York, 1976, p.129.

(30) (a) Patterson, D., Delams, G. *Trans. Faraday Soc.* **65**, 708 (1969); (b) Patterson, D., Delams, G. *Disscussion Faraday Soc.* **49**, 98 (1970).

(31) Flory, P.J., Ottewell, R.A. and Vrij, A. *Journal of American Chemical Society*, **86**, 3507, 3515 (1964).

(32) Saeki, S., Kuwahara, N., Nakata, M., Kaneko, M. *Polymer* **17**, 685 (1976)

(33) Koningsveld, R. Staverman, A.J., *Journal of Polymer Science* A-2, **6**, 349 (1968).

(34) Bevington, R. P. *'Data Reduction and Error Analysis for the Physical Sciences'* McGraw-Hill Co., New York, p.60 (1969).

Chapter 3

Measurement of the Segmental Adsorption Energy of Poly(2-ethyl-2-oxazoline) on Silica in Water and Ethanol

ABSTRACT

The segmental adsorption energy parameter, χ_s^{po}, was measured for poly(2-ethyl-2-oxazoline), PEOX, using a desorption/displacement technique. PEOX was desorbed from silica with four low molecular weight organic displacers in two solvents - water and ethanol - to obtain values of the critical volume fraction of the displacer at which the desorption was complete, ϕ_{cr}. The segmental adsorption energy for PEOX was 5.1 kT and 3.2 kT in water and ethanol, respectively. These values are consistent with the polymer adsorbing principally by hydrogen bonding between the carbonyl groups on the polymer and surface silanol groups. The difference in adsorption energies in water and ethanol reflect specific solvent effects that may be related to the negative excess entropy of mixing for water in PEOX solutions as well as due to the formation of hydrogen bond bridges between PEOX and silanol groups in water. The relatively high values of χ_s^{po} for PEOX in both solvents suggest that PEOX may serve as an effective anchor block in block copolymers adsorbing on surfaces by hydrogen bonding.

INTRODUCTION

The adsorption of nonionic, water-soluble polymers at an interface has significant scientific and technological importance. In recent years, considerable efforts have focused on understanding the factors controlling the structure of adsorbed homopolymer and

copolymer layers on surfaces and how that structure affects interfacial behavior such as colloid stability, emulsification, wetting, and tribology.[1,2] Steric stabilization of concentrated colloidal suspensions, particularly with well-defined block copolymers, is important as a method for controlling the state of aggregation and hence the rheology and sedimentation behavior of concentrated ceramic slips, paints, and coatings.[3] Theoretical and experimental studies have focused recently on block copolymers[4-11] which can form self-assembled layers that hold great promise for tailoring interfacial properties. However, the development of water-soluble steric stabilizers has lagged behind that of polymer stabilizers soluble in organic solvents due to the complex structure of water and its interactions with polymers.

Polyelectrolytes with low molecular weights are frequently used to stabilize aqueous colloid suspensions. However, steric stabilization offers several advantages over electrostatic stabilization. Steric stabilization can be more effective than at very high particle volume fractions. Sterically stabilized suspensions are also not as sensitive to added salt as are electrostatically stabilized suspensions.[3] Moreover, steric stabilization can be equally effective in both aqueous and non-aqueous solution.[3,9,10]

This work concerns a study of the adsorption of the nonionic polymer poly(2-ethyl-2-oxazoline), PEOX, on silica from water, ethanol, and from binary mixtures. This polymer is especially interesting because it can be made with relatively narrow molecular weight distributions and because it can be incorporated in diblock copolymers with narrow molecular weight distributions. In recent work, Riffle *et al.* synthesized two new diblock systems - poly(dimethyl siloxane-2-ethyl-2-oxazoline)[12] and poly(ethyl vinyl ether-2-ethyl-2-oxazoline) with relatively narrow molecular weight distributions.[13] These polymers are model systems for studying steric stabilization.

The solution properties of PEOX were described in Chapter 2. PEOX homopolymer samples with relatively narrow molecular weight distributions were characterized by light scattering. At 25°C, second virial coefficients gave values of the Flory polymer-solvent interaction parameter, χ^{po}, in water in the range 0.48-0.49 for M_w

in the range 20-60 kg mole^{-1} while χ^{po} in ethanol lay in the range 0.32-0.35. A previous study had shown that the solubility of PEOX in water was due to the formation of hydrogen bonds with the carbonyl (C=O) group in the polymer chain[15] while another study had shown that PEOX was soluble in a variety of polar organic solvents, particularly those capable of forming hydrogen bonds.[16] These solubility characteristics make PEOX particularly attractive since it is desirable to use copolymer stabilizers in solvents where micelles do not form since micelles can complicate copolymer adsorption and hinder stabilization.[4,5] At present, there is no block copolymer available in narrow molecular weight distributions in which both blocks are soluble in water.

The segmental adsorption energy parameter χ_s^{po} and the χ^{po} parameter describe the energetic aspects of polymer adsorption in the context of the mean field lattice theory developed by Scheutjens and Fleer.[17,19,20] The segmental adsorption energy, χ_s^{po} kT, is defined as the change in free energy when a polymer segment adsorbs on a surface thereby breaking contacts with solvent molecules and displacing solvent molecules from the surface.[17] In this paper, we report for the first time values of χ_s^{po} for PEOX on silica from water and ethanol. We follow the notation of Scheutjens *et al.* in which the superscript "p" denotes the polymer and the superscript "o" denotes the solvent in which the polymer is dissolved.[20] By definition, χ_s^{po} is positive if the polymer adsorbs preferentially from the solvent. The relatively high values of χ_s^{po} for PEOX in water and ethanol obtained in this work suggest the polymer has promise as an anchor block component in a block copolymer adsorbing onto surfaces such as metal oxides that possess hydrogen bonding groups.

The χ_s^{po} and χ^{po} parameters along with molecular weight determine the mass of adsorbed polymer per unit area, Γ, and the structure of the adsorbed layer in terms of the fraction of segments in trains, tails, and loops, *i.e.* the segment distribution function. For a fixed value of molecular weight and χ^{po}, Γ and the fraction of segments adsorbed in flat trains increases with χ_s^{po}, up to $\chi_s^{po} \approx 2$, with a subsequent reduction in the fraction of segments adsorbed as loops or tails. This is important for polymeric

dispersants since the interparticle potential is governed by the fraction of segments in tails.[20] For $\chi_s^{po} > 2$, Γ and the train fraction become essentially independent of χ_s^{po}.[21b]

The two principal methods for estimating the segment adsorption energy χ_s^{po} kT are microcalorimetry[22,23] and desorption by displacers.[20,24] Microcalorimetry is suitable for systems where the principal contribution to the free energy of adsorption is enthalpic since it does not measure entropic contributions to the free energy. However, when there is a large change of entropy of the solvent upon adsorption of the polymer chain, such as in aqueous solutions where water associates strongly with the polymer chain, microcalorimetry may not provide accurate measurements of χ_s^{po}.[20]

Cohen Stuart *et al.*[25] used microcalorimetry to measure χ_s^{po} for the adsorption of poly(vinylpyrrolidone), PVP, on silica in water and dioxane. Good agreement was found between this method and the displacement technique used in the present study. In general, entropic contributions to the free energy of adsorption could be significant for polymers that associate strongly with solvent molecules, leading to a negative excess entropy of mixing of the solvent which overshadows the conventional combinatorial entropy of mixing of solvent with polymer in lattice theories for solutions.[23]

Cohen Stuart *et al.* have shown that a low molecular weight displacer with a sufficiently strong affinity for a surface may completely desorb a polymer chain at a critical displacer volume fraction ϕ_{cr} and that measurements of ϕ_{cr} for a series of displacers with various strengths permits a calculation of χ_s^{po}.[20,24] In addition to the importance of χ_s^{po} in the lattice theory for adsorption, the ability of a polymer to displace another polymer in a given solvent at a given degree of polymerization correlates with their relative values of χ_s^{po}. A polymer with a higher value of χ_s^{po} will displace a polymer with a lower value. This is important because many applications of polymeric dispersants occur in media where several soluble polymers are present in solution. For a diblock copolymer adsorbed at an interface, the solvated tail block is anchored to the surface by the anchor or head block. For efficient stabilizer performance, it is essential that χ_s^{po} for the anchor block be sufficiently larger than that for the tail block so that the tail is

completely displaced.

Aside from the determination of values of χ_s^{po}, measurements of polymer adsorption from mixed solvents and the subsequent are important for other reasons. In many industrial processes, it is important to understand what types of low molecular weight species will affect the adsorption of a polymer.

There are relatively few studies of the adsorption energy for polymers with all but one of them focusing on polymers adsorbing onto metal oxides from relatively nonpolar organic solvents.[25-310] A series of papers by Cohen Stuart *et al.* on the adsorption of poly(vinylpyrrolidone), PVP, from water and dioxane is the only study to date on a water soluble polymer in water.[21,24] This work is especially relevant to the present study of PEOX adsorption given the similarities of PEOX and PVP, *i.e.* both have an amide group with similar polarity and the solution properties in water are similar - $\chi^{PEOX,w}$ = 0.48-0.49 while $\chi^{PVP,w}$ = 0.47. It was shown that PVP adsorbed on silica principally through hydrogen bonding of the carbonyl C=O on the polymer to silanol groups on the surface.[21,32] Low molecular weight, organic displacers were used to desorb poly(vinylpyrrolidone), PVP, from silica in water and dioxane.[24] The experimental values of χ_s^{po}, ~ 4.0 in both water and dioxane, correlated well with the relatively high fraction of adsorbed segments in trains detected by NMR. These values will be compared in the Results and Discussion section to the values of χ_s^{po} for PEOX measured in this study.

A recent study by van der Beek *et al.*[25-27] employed a variety of techniques including FTIR, thin-layer chromatography, microcalorimetry, and displacement processes to determine χ_s^{po} for a variety of polymers containing different functional groups adsorbing onto various metal oxides from various organic solvents. Values of χ_s^{po} ranging from 0.5 to 5.1 were measured depending on the polymer structure, solvent type, and substrate chemistry. All of these studies illustrate the complex relation between polymer adsorption and the structures of the polymer, solvent, and substrate. A deeper understanding of these interactions is essential for the systematic design of polymeric stabilizers.

This paper is organized as follows. The next section describes the theoretical basis for measuring χ_s^{po} developed by Cohen Stuart *et al.*.[20] The experimental procedures used in the adsorption/displacement experiments are then described, followed by the discussion of results.

THEORETICAL BACKGROUND

The displacement method is based on an approximate form of the mean field lattice theory of Scheutjens and Fleer which describes the conformations of polymer chains on and near the surface as sequences of segments in a lattice.[20,24] In the one-layer approximation, it is assumed that the adsorbed polymer segment density close to the point of complete desorption, *i.e.* $\phi=\phi_{cr}$, differs from the bulk solution concentration only in the lattice layer next to the surface. The χ_s^{po} parameter of the polymer adsorbing on the surface can be separated into two terms - the χ_s^{do} parameter of the displacer adsorbing in the presence of solvent (o) (as depicted in Figure 3.1), and the segmental adsorption energy parameter χ_s^{pd} of the polymer adsorbing from the pure displacer (d) (Figure 3.2),

$$\chi_s^{po} = \chi_s^{pd} + \chi_s^{do}. \tag{3.1}$$

The χ_s^{pd} parameter of the polymer adsorbing from pure displacer is related to the critical displacer volume fraction ϕ_{cr} by:

$$\chi_s^{pd} = \ln\phi_{cr} + \chi_{sc} - \lambda_1\chi^{pd} + (1-\phi_{cr})(1-\lambda_1)\Delta\chi^{do} \tag{3.2}$$

where $\chi_{sc}\,kT$ is the minimum critical adsorption energy that a polymer segment must have to adsorb since the segment loses entropy upon adsorption, λ_1 is the lattice parameter (= 0.25 for a hexagonal lattice), and $\Delta\chi^{do}$ is the solvency parameter, defined as

$$\chi_s^{po} = \chi_s^{pd} + \chi_s^{do}$$

(Cohen-Stuart et al. JCIS(1984))

Displacers Adsorption Isotherms

$$\chi_s^{do}$$

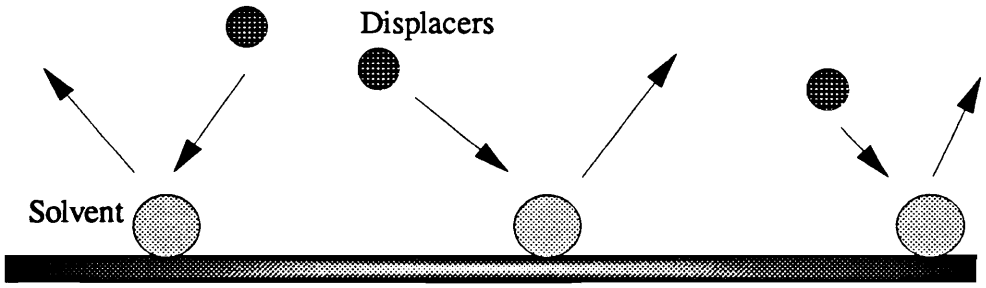

Figure 3.1 A schematic representation of organic compounds displacing solvent molecules from a substrate surface. The plot is not drawn to scale.

Polymer Desorption Isotherms

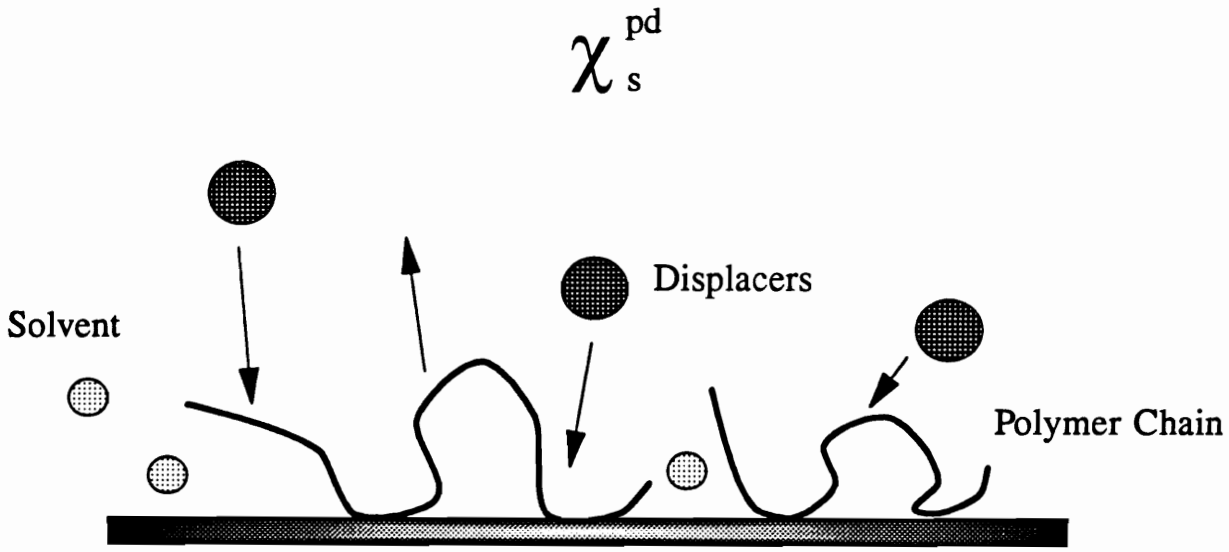

Figure 3.2 Schematic illustration of the organic compounds (displacers) displacing macromolecules from a surface in the presence of solvent.

$$\Delta\chi^{do} = \chi^{pd} + \chi^{do} - \chi^{po} \qquad (3.3)$$

where χ^{pd} and χ^{do} are the polymer-displacer and displacer-solvent interaction parameters, respectively. The critical volume fraction ϕ_{cr} is determined experimentally as the volume fraction of displacer which completely displaces the polymer from the surface. The χ_s^{do} parameter is obtained from the initial slope, S, of the displacer adsorption isotherm since this part of the isotherm contains information on the displacement of solvent molecules from active surface adsorption sites in the absence of displacer-displacer interactions. This part of the isotherm is also relatively insensitive to surface heterogeneities. The initial slope is defined as

$$S = \lim_{\phi_*^d \to 0} (\Gamma/\phi_*^d) \qquad (3.4)$$

where Γ is the adsorbed amount of displacer in moles per unit area and ϕ_*^d is the volume fraction of displacer in the bulk solution. From regular solution theory, the surface concentration of displacer, ϕ_1^d, is related to the bulk concentration of displacer, ϕ_*^d, in the limit $\phi_*^d \to 0$ by,

$$\lim_{\phi_*^d \to 0} (\phi_1^d/\phi_*^d) = \exp(\chi_s^{do} + \lambda_1 \chi^{do}) \qquad (3.5a)$$

Combining equations (3.3) and (3.4), Cohen Stuart *et al.* showed that S is related to a dimensionless slope s by

$$s = \exp(\chi_s^{do} + \lambda_1 \chi^{do}) \qquad (3.5b)$$

$$= \Gamma_{mon}^{-1} (v_d/v_o) S \qquad (3.5c)$$

where v_d and v_o are the molecular volumes of the displacer and solvent, respectively, and

Γ_{mon} is the site density of isolated silanol groups on the silica surface. Substituting equations (3.2) and (3.5) into equation (3.1) results in an equation relating χ_s^{po} to ϕ_{cr}:

$$\chi_s^{po} = \ln\phi_{cr} + \ln s + \chi_{sc} - \lambda_1\chi^{po} + [(1-\phi_{cr})(1-\lambda_1)-\lambda_1]\Delta\chi^{do}. \qquad (3.6)$$

Adsorption will not occur if $\chi_s^{po} < \chi_{sc}$. The χ_{sc} parameter is obtained experimentally by measuring ϕ_{cr} for a displacer that is a low molecular weight analog of the polymer repeat unit. In this case, $\chi^{pd} = 0$ and $\chi^{po} = \chi^{do}$ so that $\Delta\chi^{do} = 0$ from equation (3.3). In addition, $\chi_s^{pd} = 0$ since the contact free energy of adsorption on the surface for both is approximately the same. Equation (3.2) then reduces to

$$\chi_{sc} = -\ln(\phi_{cr})_{analog}. \qquad (3.7)$$

If there is some solvency effect with the displacer, *i.e.* if χ^{pd} is not quite zero, then equation (3.7) is still a good approximation of equation (3.2) for relatively large values of $(\phi_{cr})_{analog}$. The experimental values of χ_{sc} from equation (3.7) can be compared to the analytical result from the lattice model which accounts for the loss of conformational entropy of the polymer segment upon adsorption

$$\chi_{sc} = -\ln(1-\lambda_1). \qquad (3.8)$$

Values of χ_{sc} from equations (3.7) and (3.8) will be compared in a later section.

An inspection of equation (3.6) shows that the calculation of the segmental adsorption energy χ_s^{po} requires values for the solvency parameter $\Delta\chi^{do}$ in addition to values of ϕ_{cr}, s, and χ^{po} which can be measured directly. Values of $\Delta\chi^{do}$ can be obtained by evaluating equation (3.2) for polymer displacement experiments for a given displacer "d" carried out from the solvents water (w) and ethanol (EtOH). Subtracting the two resulting equations gives

$$\ln(\phi_{cr}^{d,w}/\phi_{cr}^{d,EtOH})+0.75(1-\phi_{cr}^{d,w})\Delta\chi^{d,w} - 0.75(1-\phi_{cr}^{d,EtOH})\Delta\chi^{d,EtOH}=0. \quad (3.9)$$

In a similar fashion, equation (3.6) can be evaluated for a common solvent "o" with two displacers d1 and d2:

$$\ln(\phi_{cr}^{d1,o}/\phi_{cr}^{d2,o})+\ln(s^{d1,o}/s^{d2,o})+(0.5-0.75\phi_{cr}^{d1,o})\Delta\chi^{d1,o} - (0.5-0.75\phi_{cr}^{d2,o})\Delta\chi^{d2,o}=0. \quad (3.10)$$

For a given pair of displacers d1 and d2 and for the two solvents water and ethanol, equations (3.9) and (3.10) generate four independent, linear, algebraic equations with the solvency parameters $\Delta\chi^{d,o}$ as the four unknowns. These are solved to obtain values of χ_s^{po} as discussed below.

EXPERIMENTAL

Materials. Samples of poly(2-ethyl-2-oxazoline), PEOX, were synthesized by cationic ring-opening polymerization using procedures described earlier by Riffle *et al.*.[12] Values of the weight-average molecular weight M_w for several samples, listed in Table 3.1, were measured by static light scattering and were reported in Chapter 2. Values of the polydispersity index M_w/M_n, measured by gel permeation chromatography, were less than 1.3 for $M_n \leq 40$ kg mole^{-1}.[33] Cab-O-Sil EH-5 silica, manufactured by G. L. Cabot Inc., was used for the adsorption experiments. The surface area is 380 ± 30 m^2/g.[34] The silica powder was dried by heating at 100°C-115°C for 4 hours and then stored in a desiccator prior to use.[37] Pyridine (PYR), N-ethyl acetamide (NET), dimethyl sulfoxide (DMSO), and furfuryl alcohol (FUR) were selected as the displacers because of their ability to act as Lewis bases or proton-acceptors. Their structures are shown in Table 3.2. These displacers were expected to interact strongly with the acidic silanol (Si-OH) groups on the silica surface. The displacer chosen as a low molecular weight analog for

PEOX was N,N-dimethylpropionacetamide, DMP, which is a precise analog of PEOX. DMP was obtained from Aldrich with a stated purity higher than 99.7%. All other displacers (HPLC grade) were purchased from Aldrich Chemical Co. and used as received. Deionized water and ethyl alcohol (Aaper Co., 200 Proof) were used as the solvents. Care was taken to avoid exposure of the displacers and ethanol to atmospheric moisture. The deionized water had a resistivity of 17×10^6 ohm-cm and was obtained from a Barnstead NANOPURE II™ water purification system.

TABLE 3.1 Molecular Weight Characterization Data for Poly(2-ethyl-2-oxazolines)

Sample	M_w* kg mole^{-1}
PEOX 20K	23.1
PEOX 30K	33.3
PEOX 60K	65.4

*Measured by static light scattering in water at 25°C; M_w/M_n was approximately 1.19-1.54 as determined by gel permeation chromatography, reference (13).

Displacer Adsorption Isotherms. Adsorption isotherms for the four displacers on silica were measured in water and ethanol. The adsorption isotherms were determined by the conventional solution depletion method. Typically, an initial solution of approximately 2.5% (w/w) was prepared for each displacer in two solvents. Approximately 0.2 g silica were mixed with 10 g of solution. The mixtures were gently rotated end-over-end for 24 hours at ~25°C. The suspensions were then centrifuged at 2250 g's for 10 minutes. The supernatants were carefully transferred to quartz cuvettes where the UV absorbance was measured with a Hitachi U-2000 UV/vis spectrophotometer at a low wavelength in the range of 220-250 nm, according to different displacers, to determine the unadsorbed displacer concentrations. The amount

Table 3.2. Structure and Molecular Volumes of Solvents and Displacers

Name	Formula	Abbreviation	Molecular Volume (nm^3)
Dimethyl Sulfoxide	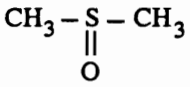	DMSO	0.118
Pyridine	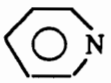	PYR	0.135
N-Ethyl Acetamide	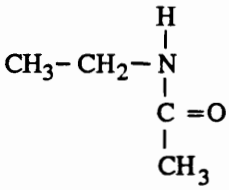	NET	0.157
Furfuryl Alcohol	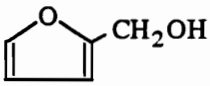	FUR	0.144
N,N-dimethylpropionamide	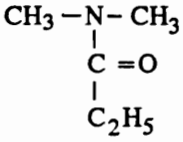	DMP	0.183
Ethanol		EtOH	0.097
Water		w	0.030

of adsorbed displacer was then calculated through the comparison of the absorbance change. The measurement precision was $\pm 2\%$.

Adsorption Isotherms of PEOX. Adsorption isotherms of PEOX on silica from water and ethanol were also determined by the solution depletion method very similar to that used for the displacer isotherms. The polymer concentration in the supernatant was measured at a wavelength of 238 nm. All experiments were carried out at $\sim 25°C$. The measurement precision was $\pm 2\%$.

Displacement isotherms. Displacement isotherms were measured for the PEOX 30K (degree of polymerization DP $\approx$ 330) sample to determine the critical displacer volume fraction ϕ_{cr} in water and in ethanol for the four different displacers. Only one molecular weight was used since Cohen Stuart *et al.* demonstrated that the value of ϕ_{cr} was essentially independent of the molecular weight of the polymer for DP $>$ 100.[18] The PEOX displacement measurements were performed with a modification of the solution depletion technique. Approximately 0.2 g silica were mixed with 10 g of solutions of PEOX 30K dissolved in mixtures of a given solvent and displacer at various concentrations of displacer. The added PEOX concentration was controlled at 1.6 g/l, well in the plateau regions of the individual PEOX adsorption isotherms. After equilibration for 24 hours, the dispersions were centrifuged and the supernatants were withdrawn. Since the displacers and PEOX absorbed at similar wavelengths, the residual displacers had to be first removed from the supernatant before measuring the concentration of PEOX. The solvents and displacers were first vaporized by heating at 100°C in air followed by drying in a vacuum oven at 100°C for 24 hours. Deionized water was then added to the dry polymer and the entire heating cycle was repeated at least twice. In the final step, deionized water was added to the dry polymer and the polymer concentration was measured spectrophotometrically.

Thin Layer Chromatography. Thin layer chromatography (TLC) was performed to provide an independent measurement of ϕ_{cr} for pyridine in water. TLC has been shown to be a very sensitive method for determining ϕ_{cr}.[26] Whatman K5F silica gel TLC plates, purchased from Alltech Associates Inc. (Deerfield, IL), with a silica layer of 0.25 mm were used for the thin-layer chromatographic experiments. The plates were dried in air at 120°C for 12 hours prior to use. Spots of PEOX were deposited along a start line with 2 cm from the lower edge of the plate. The plate was then placed above the eluent of the appropriate composition in a closed glass development tank for 45 minutes in order to establish equilibrium between the vapor phase, the liquid phase, and the adsorbed phase on the silica. The upward elution was started by lowering the plate just into the eluent. After elution the plates were dried, then sprayed with a 2% iodine aqueous solution and dried again. A dark spot would appear indicating the position of PEOX on the plate, from which the R_f values, defined as the ratio of the distance from the polymer spot to the start line to that from liquid front to the start line, were measured.

RESULTS AND DISCUSSION

Displacer Isotherm. The displacer adsorption isotherms in water, Figure 3.3, and in ethanol, Figure 3.4, were measured at sufficiently low displacer concentrations to obtain values of the slope "S" in the initially linear part of the isotherm. The slopes were determined by least squares regression. These slopes are relatively insensitive to surface heterogeneities and to interactions between adsorbed displacer molecules. From equation (3.5c), the scaled slope "*s*" was calculated using a value of the site density of active silanol groups cited by Kiselev for silica heated to 700°C, $\Gamma_{mon}=2.33\times10^{-6}$ mole m^{-2}.[35] This value was recommended by Cohen Stuart *et al.* based on a previous study of the adsorption of the related polymer PVP on silica which showed that only isolated silanols that persist upon heating to elevated temperatures were the active sites for hydrogen bonding with PVP.[23] Values of the dimensional slope "S" and the natural log of the scaled slope "*s*" are listed in Table 3.3. Relative standard deviations of S were typically

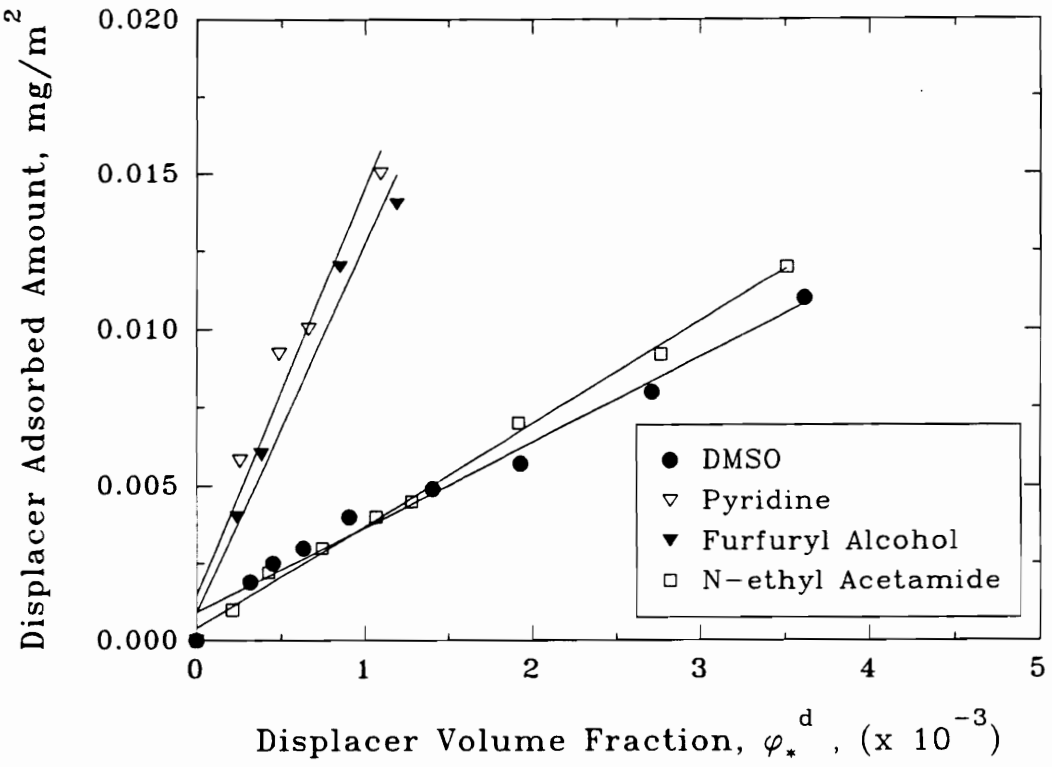

Figure 3.3 Adsorbed amount of displacers, mg m^{-2}, against the displacer volume fraction ϕ^d from water onto Cab-O-Sil EH-5 silica. (•) dimethyl sulfoxide; (▽) pyridine; (▼) furfuryl alcohol; (□) N-ethyl acetamide.

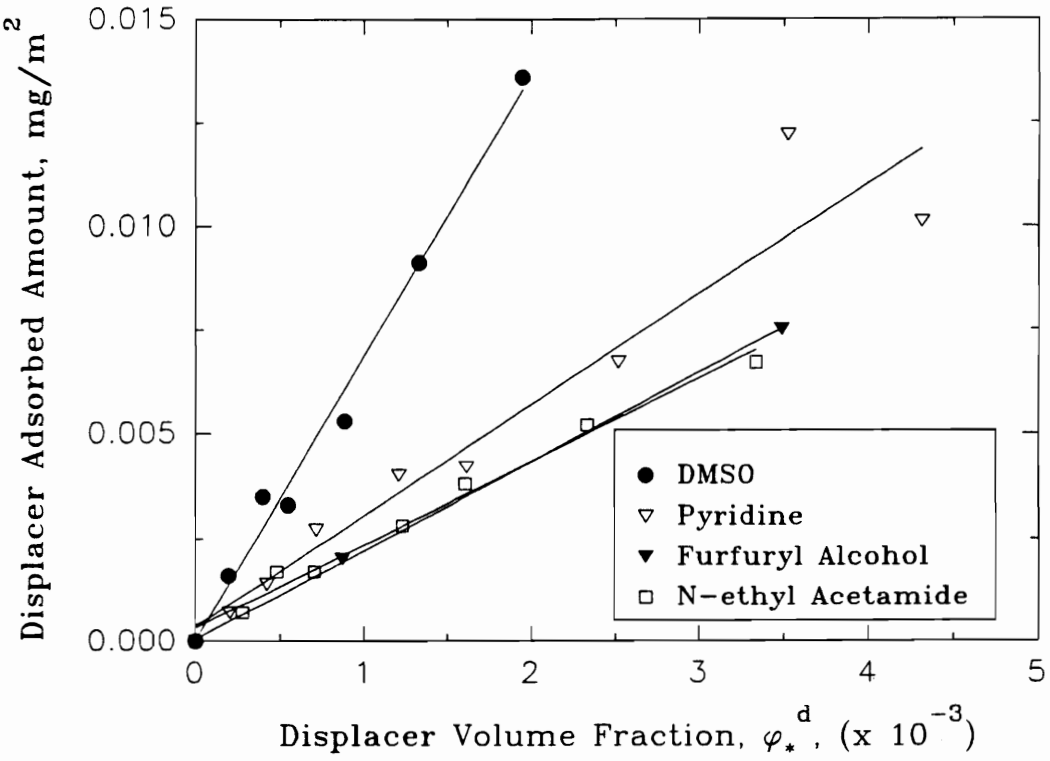

Figure 3.4 Adsorbed amount of displacers, mg m^{-2}, as a function of displacer volume fraction ϕ^d from ethanol onto Cab-O-Sil EH-5 silica.

5-10%. This led to less than ±2% variation in the calculated values of χ_s^{po}.

TABLE 3.3 Initial slopes of displacer adsorption isotherms on silica

Displacers[a]	Initial slope, S x 10^5, mole m^{-2}		ln s^b	
	water	ethanol	water	ethanol
DMSO	3.46	8.72	4.07	3.82
PYR	11.8	3.41	5.43	3.02
NET	3.79	2.30	4.44	2.77
FUR	12.0	2.14	5.51	2.61

[a] Abbreviations are same as in Table 3.2.
[b] s obtained from equation (3.5c) where Γ_{mon} = 2.33 x 10^{-6} mol m^{-2} and values of molecular volumes V_o and V_d are listed in Table 3.2.

Cohen Stuart *et al.*[23] also measured values of S_{PYR} and S_{DMSO} for Cab-O-Sil M5 in water which are somewhat lower than our corresponding values - $S_{PYR}=5.3x10^{-5}$ mole m^{-2} as compared to our value of $11.8x10^{-5}$ mole m^{-2} and $S_{DMSO}=2.8x10^{-5}$ mole m^{-2} as compared to our value of $3.46x10^{-5}$ mole m^{-2}. The differences may be due to the range of displacer volume fraction used in our study, $0 \leq \phi_*^d \leq 0.005$, whereas the slopes reported by Cohen Stuart *et al.* appear to have been calculated over the range $0 \leq \phi_*^d \leq 0.01$. Some curvature in the isotherm in that range may have led to somewhat lower slopes. The slopes in Table 3.3 were always calculated with a minimum of four data points and usually with as many as six to eight points. The differences in "S" lead to differences of 5% in $\ln(s)_{DMSO}$ and 15% in $\ln(s)_{PYR}$. Given the limited comparison of slopes available, it is difficult to assess the effect that these differences may have on the comparison of our values of χ_s^{po} for PEOX and those for PVP.

PEOX Adsorption Isotherm. Figure 3.5 depicts the adsorption isotherms of PEOX samples on the silica surface from water for three molecular weights and from ethanol for PEOX 30K. The adsorption isotherms tended to rise steeply with increasing

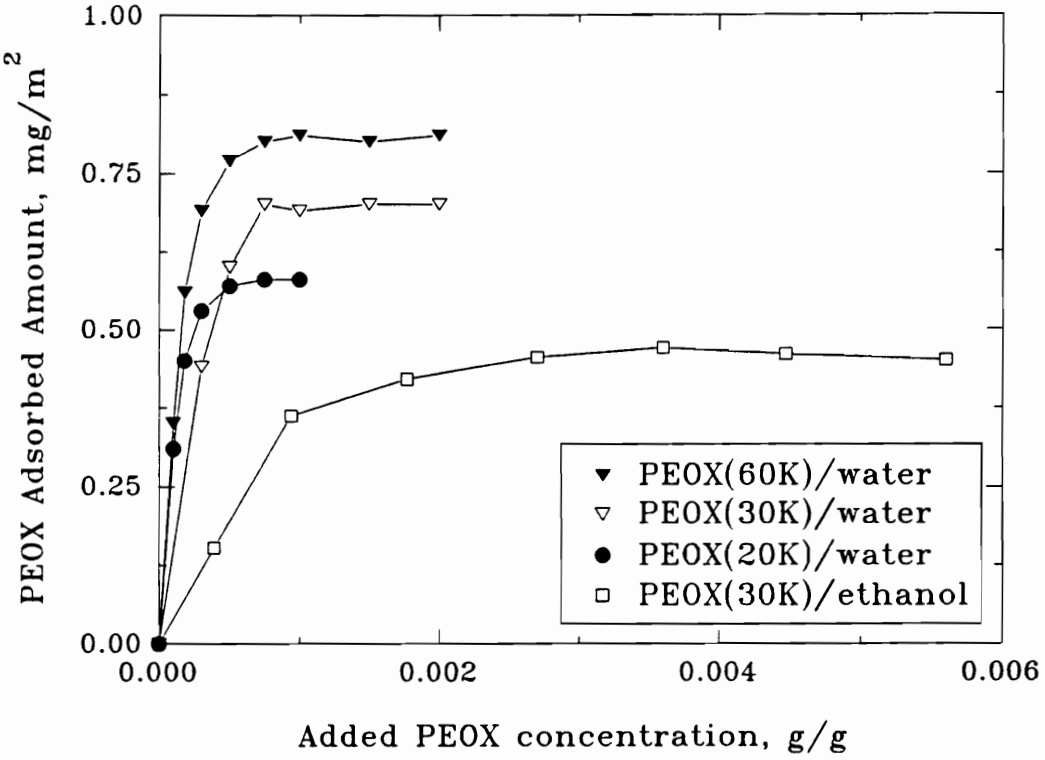

Figure 3.5 Adsorbed amount of PEOX, mg m^{-2}, as a function of added PEOX concentration, g PEOX/g solution. Three different molecular weights (defined in Table 4.1) are shown in different solvents. (•) 20K/water; (▽) 30K/water; (▼) 60K/water; (□) 30K/ethanol.

polymer concentration, especially for PEOX 20K and 60K and all reached a plateau, indicating saturation of the surface. The adsorption isotherms are of the high-affinity type which is characteristic for high polymers. The plateau adsorption amounts of PEOX in water increased steadily with molecular weight, ranging from 0.57 to 0.80 mg m^{-2}. The plateau adsorption amount of PEOX 30K in ethanol, 0.46 mg m^{-2}, was significantly less than the corresponding value in water, 0.70 mg m^{-2}. This is related to the greater solubility of PEOX in ethanol, *i.e.* $\chi^{po}=0.32$ in ethanol compared to $\chi^{po}=0.48$ in water[14], and to the different values of χ_s^{po} in water and ethanol that will be discussed later.

Displacement Isotherms for PEOX. The displacement isotherms in Figure 3.6 for PEOX 30K in water show that all five displacers were capable of completely displacing PEOX. The adsorbed mass of PEOX per unit area, Γ, decreased with increasing volume fraction of displacer in equilibrium with the silica, ϕ_*^d, reaching zero at the critical displacer concentration ϕ_{cr}. Similar displacement curves were found for PEOX 30K in ethanol. In those instances where the displacement curve did not drop abruptly to zero, ϕ_{cr} was obtained by interpolation as illustrated for pyridine and furfuryl alcohol in Figure 3.6(a). Excellent agreement was found between the interpolated value for pyridine in water and the value obtained by thin layer chromatography as shown in Figure 3.6(b).

Two significant features of the displacement isotherms were their shapes and the relative orders of ϕ_{cr} for the displacers in ethanol (in Figure 3.6(c)) and water, summarized in Table 3.4. The curves in water and ethanol do not exhibit minima, indicating relatively strong displacer effects. The order of ϕ_{cr} , *i.e.* the relative strengths of the displacers, was not the same in water and in ethanol. The displacer strength in water as given by the order of ϕ_{cr} increased in the order DMSO < NET < FUR < PYR. In ethanol, the displacer strength increased in the order FUR < NET < PYR < DMSO. This suggests the importance of nonzero values of the solvency parameter $\Delta\chi^{do}$ since for athermal solutions, *i.e.* $\Delta\chi^{do}=0$, the order of displacer strength is independent of solvent

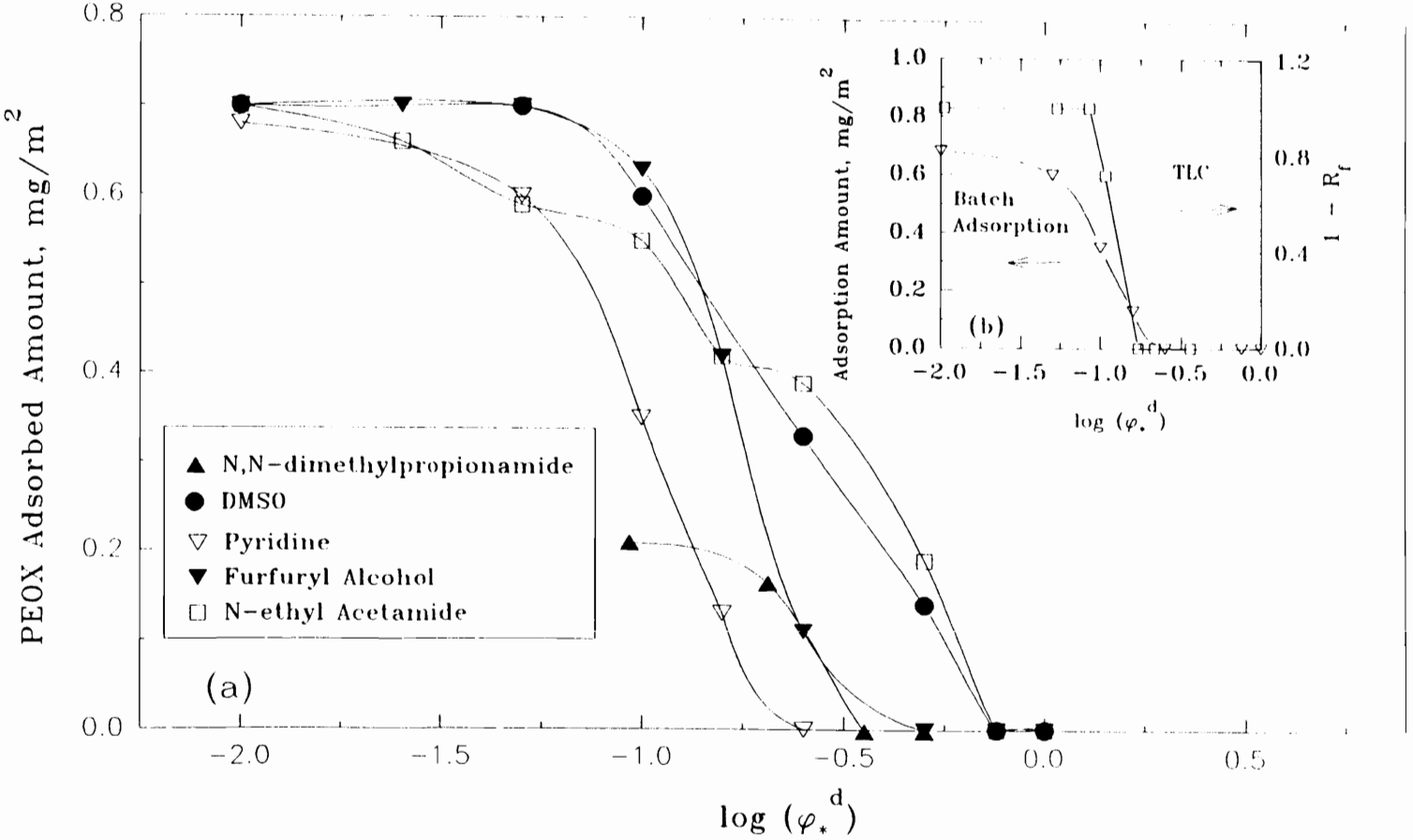

Figure 3.6(a & b), see next page.

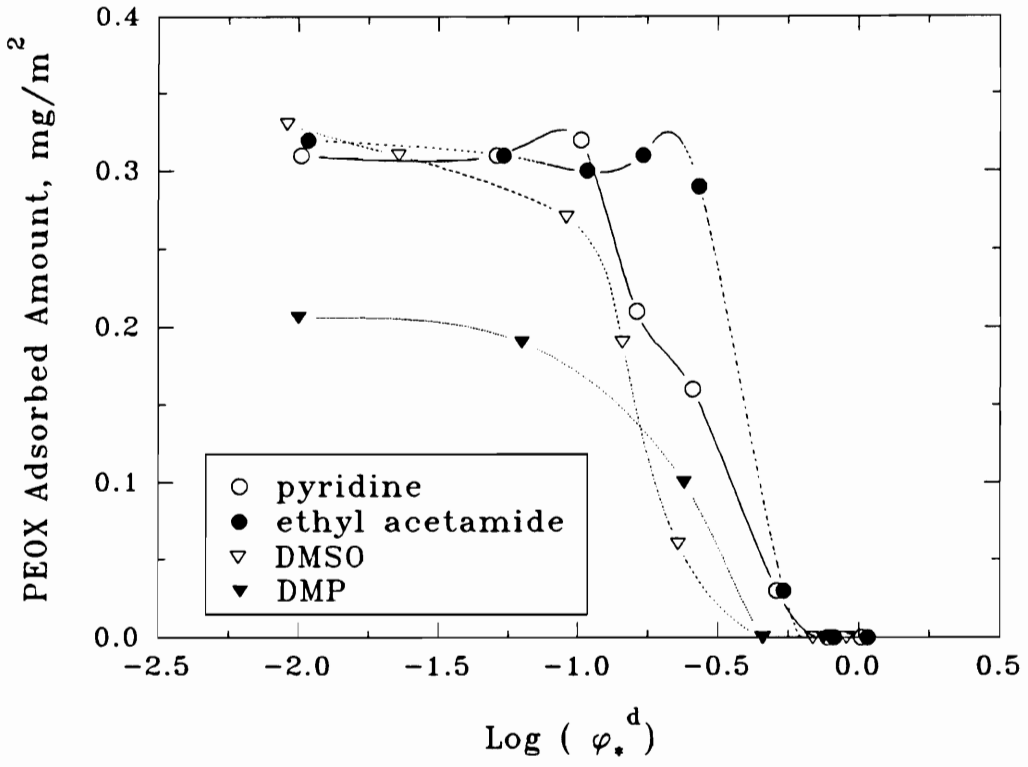

Figure 3.6 (a) Desorption isotherms of PEOX on silica from water. The ϕ_{cr} are obtained from the interpolation of each curve to zero adsorbed amount.
(b) The adsorbed amount of PEOX, mg m^{-2}, as a function of retention determined by thin layer chromatography (TLC), expressed as ($1-R_f$) for PEOX in the solvent mixture water-pyridine and batch desorption process as a function of the volume fraction ϕ^d of pyridine.
(c) Desorption isotherms of PEOX on silica from ethanol. The adsorbed amount of PEOX as a function of displacer concentration.

type.

These displacement results can be compared to the results of Cohen Stuart *et al.* for the displacement of PVP from silica by DMSO and pyridine.[23] DMSO is a stronger displacer for PEOX than it is for PVP since $(\phi_{cr})_{DMSO}=0.75$ for PEOX whereas PVP was not completely desorbed even in pure DMSO. Pyridine is also a stronger displacer for PEOX than it is for PVP with $(\phi_{cr})_{PYR}=0.21$ for PEOX whereas $(\phi_{cr})_{PYR}=0.35$ for PVP.

TABLE 3.4 Critical Displacer Volume Fractions for PEOX 30K

Solvent	Displacer*	$\ln(\phi_{cr})$	ϕ_{cr}
Water	PYR	-1.54	0.21
	PYR (TLC)**	-1.56	0.21
	FUR	-1.0	0.37
	NET	-0.46	0.63
	DMSO	-0.28	0.76
	DMP	-0.99	0.37
Ethanol	PYR	-0.69	0.50
	FUR	-0.30	0.74
	NET	-0.58	0.56
	DMSO	-1.15	0.32
	DMP	-0.78	0.46

* Abbreviations are same as in Table 3.2.
** Determined by thin layer chromatography (TLC).

Critical Displacer Energy. The critical adsorption energy parameter, χ_{sc}, can be estimated from the lattice model using equation (3.8) and can be estimated from equation (3.7) with desorption experiments where the displacer is chosen to match the repeat unit of the polymer so that $\chi_s^{pd}=0$ and $\Delta\chi^{do}=0$. For a hexagonal lattice with the lattice parameter $\lambda_1=0.25$, $\chi_{sc}=0.288$. Equation (3.7) is valid when χ_s^{po} is not too small, *i.e.*

$\chi_s^{po} > 2$ [27] which is satisfied in this study. Given the values of $(\phi_{cr})_{NET}$ listed in Table 3.4, $\chi_{sc}=0.99$ in water and $=0.78$ in ethanol. These are somewhat higher than the theoretical value of 0.288 most likely because the lattice theory assumes no specific interactions between the polymer, solvent, and surface. This is not the case with the present system where hydrogen bonding is important. Additional effects of specific interactions will be seen below in the calculations of the solvency parameter $\Delta\chi^{do}$. The experimental values of χ_{sc} were used in the subsequent calculations of χ_s^{po} to maintain self-consistency.

Calculation of χ_s^{po}. The solvency parameters $\Delta\chi^{do}$ were calculated from equations (3.9) and (3.10) for various combinations of the two solvents and four displacers. This was done with the values of ln s and ϕ_{cr} listed in Tables III and IV, respectively, along with the values of χ^{po} for PEOX at 25°C noted earlier - $\chi^{po}=0.48$ in water and $\chi^{po}=0.41$ in ethanol. Values of χ_s^{po} were then calculated from equation (3.6) and are summarized along with values of $\Delta\chi^{do}$ in Table 3.5. To test the self consistency of the data, calculations were made for the three different combinations of displacers resulting in 6 independent values of χ_s^{po} and 3 independent values of $\Delta\chi^{do}$ in a given solvent. These values should be independent of the particular pair of displacers used. The values of χ_s^{po} were quite self-consistent, with an average value of 5.1 in water and 3.2 in ethanol. The relative standard deviations of the averages for χ_s^{po} were 4% and 9% for water and ethanol, respectively. There was considerably more scatter in the values of $\Delta\chi^{do}$ due to an accumulation of experimental errors and to effects neglected by the lattice model such as specific association of water molecules with the PEOX chain. Given this latter point, the experimental values of $\Delta\chi^{do}$ cannot be interpreted strictly in terms of the regular solution theory. However, it is noted that the term in equation (3.6) that contains $\Delta\chi^{do}$ was typically $\leq 15\%$ of the calculated value of χ_s^{po} for a given combination of displacers in a given solvent. Only for the displacer combination of furfuryl alcohol/dimethyl sulfoxide in ethanol did the term containing $\Delta\chi^{do}$ reach 34% of the value of χ_s^{po}. There is no significant change in the average value of χ_s^{po} in ethanol if this set of displacers is

ignored.

The higher adsorption energy of $\chi_s^{p,water}$ is due to solvent effects. Two mechanisms of PEOX adsorption on silica surface from water and ethanol are proposed, as shown in Figures 3.7 and 3.8. One possible solvent effect is the participation of water in forming hydrogen bond bridges between the polymer and surface silanol groups since a water molecule can form two hydrogen bonds at once as shown in Figure 3.7. This bridging would be in addition to direct hydrogen bond formation between the carbonyl oxygen on PEOX and surface hydroxyl groups. In ethanol, only direct hydrogen bonding is possible since ethanol itself can only form one hydrogen bond at a time. This bridging might circumvent steric hindrances to direct hydrogen bond formation between a given carbonyl group and silanol group.

Another possible solvent effect, which was previously discussed in Chapter 2, that the excess entropy of mixing, Δs^E, of water in PEOX solutions was negative due to specific association between water and the polymer (in Figure 3.8), *i.e.* by hydrogen bonding.[14,15] The adsorption of segments in trains may partially disrupt hydrogen bonding between water and those segments, leading to a decrease in specific association of water with the chains and thus an increase in the entropy of water molecules. Thus, the adsorption of segments in trains would be favored by the increase of entropy of the water.

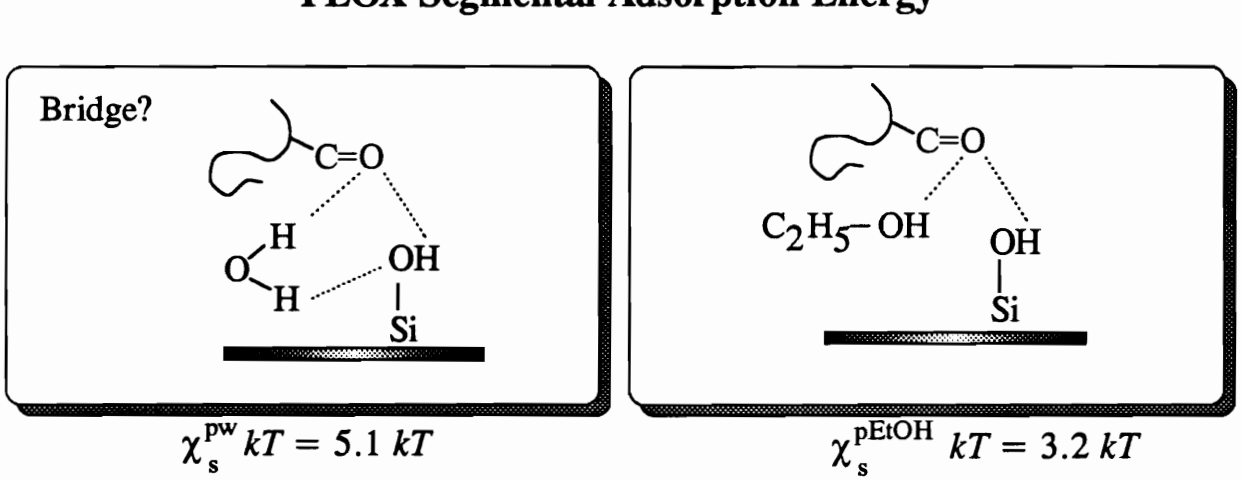

Figure 3.7 Proposed water bridging adsorption mechanism of PEOX on silica surface from water and ethanol, based on the segmental adsorption energy measurements.

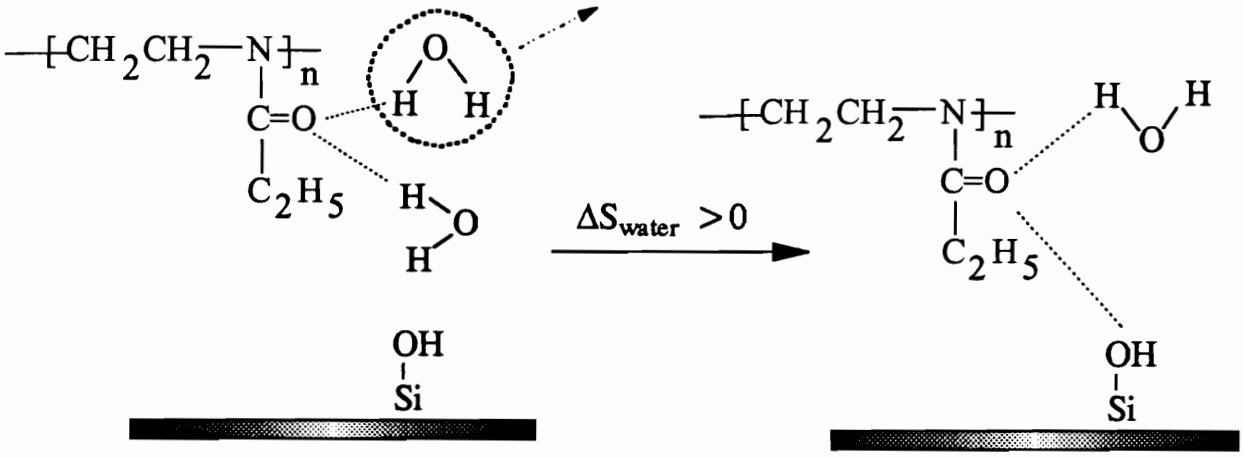

Figure 3.8 Thermodynamic properties of the PEOX adsorption on silica surface from water.

TABLE 3.5 Segmental Adsorption Energy, χ_s^{po}, and Combined Solvency Parameter, $\Delta\chi^{do}$, for Poly(2-ethyl-2-oxazoline) on Silica for Various Combinations of Solvents and Displacers.

	$\Delta\chi^{do}$		χ_s^{po}	
	water	ethanol	water	ethanol
PYR	2.13	1.07	5.5	3.1
FUR	0.41	-2.59		
DMSO	-5.29	-1.94	5.0	3.3
NET	5.93	5.34		

	$\Delta\chi^{do}$		χ_s^{po}	
	water	ethanol	water	ethanol
DMSO	-3.02	0.63	4.9	3.5
FUR	-2.34	-9.03		
PYR	0.11	-2.10	4.9	2.7
NET	-2.30	-1.57		

	$\Delta\chi^{do}$		χ_s^{po}	
	water	ethanol	water	ethanol
PYR	1.40	-0.08	5.2	3.0
DMSO	-8.52	-1.35		
FUR	-1.48	-7.22	5.1	3.4
NET	7.38	6.55		
		Average =	5.1 ± 0.2*	3.2 ± 0.3*

* standard deviation of the average value of χ_s^{po}

Comparison with PVP

By comparison, Cohen Stuart *et al.* measured χ_s^{po} for PVP adsorbed onto silica from water and dioxane to be approximately 4 *kT* using the displacement technique.[23] This agreed quite well with the value obtained by microcalorimetry where the monomer analog N-ethylpyrrolidone was adsorbed on silica from both water and dioxane[21b] Solvent entropic effects were presumed to be negligible since both methods agreed well. Support for this interpretation comes from measurements by Vink of the osmotic pressure of solutions of PVP in water.[35] Values of the total entropy of mixing of water were reported for PVP with M_n=27.9 kg mole^{-1} at 25°C. Conversion of these data at a polymer concentration $C_p \sim 0.02$ g ml^{-1} to the excess entropy of mixing gave $\Delta s^E = 2 \times 10^{-4}$ cal mole^{-1} °K^{-1} whereas PEOX 30K with roughly the same molecular weight had $\Delta s^E = -4.8 \times 10^{-5}$ cal mole^{-1} °K^{-1}. This supports the hypothesis that solvent entropic effects favor PEOX adsorption from water. However, further work is needed to make a definitive conclusion about the nature of the solvent effects.

An unresolved issue here is the effect of polymer concentration on the magnitude and sign of Δs^E. For PVP solutions with $C_p \geq 0.052$ g ml^{-1}, Vink reports negative values of the total entropy of mixing of water and hence negative values of Δs^E, that increase in magnitude with C_p. No corresponding data are available for PEOX solutions in water and so it is not clear how Δs^E for PEOX in water at these higher concentrations compares with values for PVP. This concentration effect could be important since the polymer concentration in an adsorbed layer is typically appreciably higher than that in bulk solution.[18]

If bridging plays a role in the adsorption of PEOX on silica in water, one might expect that PVP would exhibit a similar increase in water compared to dioxane since dioxane cannot form a bridge between PVP and surface silanol groups. This was not the case given the essentially equal values of χ_s^{po} for PVP in water and dioxane. However, this does not necessarily rule out the possibility of water bridging for PEOX since structural differences between PEOX and PVP probably lead to differences in their

ability to form hydrogen bonds. PVP possesses a ring structure which may sterically hinder hydrogen bonding of the polymer carbonyl group to solvent molecules and to surface silanol groups.

The excess enthalpy of mixing, Δh^E was negative as required for solubility. For PEOX in water at 25°C, $|\Delta h^E|$ exceeded $|T\Delta s^E|$ by about 30%. PEOX has a Θ-temperature of 56°C which is also a lower critical solution temperature (LCST).[15] Indeed, many nonionic water-soluble polymers exhibit LCST behavior.[36] Mean field lattice theories for polymer solutions and adsorption do not account rigorously for LCST behavior. Thus the neglect of the LCST behavior of PEOX in analyzing the adsorption data with the lattice theory must be regarded as a further approximation.

The higher value of the plateau adsorption amount of PEOX 30K in water, 0.70 mg m^{-2} compared to 0.46 mg m^{-2} in ethanol is a consequence of the lower solubility of the polymer in water. The differences in the segmental adsorption energy parameters in water and ethanol are probably not important here since both values are higher than 2. In this range, the plateau adsorption amount Γ_p is relatively insensitive to further increases in χ_s^{po}.

In an earlier study, Cohen Stuart *et al.*[21b] noted that the solvent molecular volume correlated with the adsorption behavior of PVP from water and dioxane. The plateau adsorption amount in dioxane was typically twice that of PVP in water even though their values of χ_s^{po} and χ^{po} were virtually identical. This was explained in terms of the higher free energy of mixing of polymer per unit volume, ΔG_{mix}, in water because the molecular volume of water is only one-fifth that of dioxane's. For PEOX in water and ethanol, where the molecular volume of ethanol is roughly three times larger than that of water, this size effect is overshadowed by the considerably higher solubility of PEOX in ethanol compared to water. It is clear that a comprehensive description of adsorption must take into account a variety of factors including specific solvent interactions with polymer and surface, molecular volume of the solvent and chain segments, and chain stiffness.

The difference of 1.1 *kT* between our average value for PEOX in water and Cohen Stuart's value for PVP in water may be accounted for given the differences in the structures of the two polymers, the approximations in the lattice theory, and possibly the differences in displacer isotherm slopes noted earlier. Van der Beek reported significant differences in values of χ_s^{po} for polymers with closely related structures. For example, the adsorption energy of poly(ethylene oxide), PEO, $[-(CH_2)_2-O-]_x$ on silica from carbon tetrachloride, 5.1 *kT*, exceeded that of poly(tetrahydrofuran), PTHF, $[-(CH_2)_4-O-]_x$ by 1.2 *kT*.[26] The adsorption energy of poly(methyl methacrylate), PMMA, 4.3 *kT*, exceeded that of the more bulky poly(butyl methacrylate), PBMA, by ~ 1.4 *kT* also on silica from carbon tetrachloride. These two polymers have carbonyl groups in side groups. For polymers adsorbing onto silica from organic solvents, it was generally found that χ_s^{po} decreased with an increase in the number of methylene groups in the main chains or with increasing size of alkyl side groups.[25]

Effect of the Lattice Parameter

Throughout this study, a hexagonal lattice structure of the adsorbed polymer was assumed, *i.e.* $\lambda_0=1/2$ and $\lambda_1=1/4$. If a simple cubic lattice structure is assumed, the lattice parameters $\lambda_0=4/6$ and $\lambda_1=1/6$ need to be used in the calculations for χ_s^{po}.[18,19] The resulting χ_s^{po} values decrease to 2.0 and 4.0 in ethanol and in water, respectively. However, the difference between the χ_s^{po} values in ethanol and in water is still effectively 2 *kT* as in the case of the hexagonal lattice.

Comparison with Polymers in Non-polar Solvents

Finally, it is noted that the magnitudes of the χ_s^{po} values for PEOX in water and ethanol are relatively high compared to those for polymers that interact with surfaces by means other than hydrogen bonding. For example, van der Beek *et al.* measured values of $\chi_s^{po}=1.0$ and 1.9 for polystyrene (PS) adsorbing onto silica from carbon tetrachloride and cyclohexane, respectively.[27] IR analysis showed that the PS adsorbed primarily due

to interaction between the basic phenyl group and acidic surface groups on the oxides.

In a separate study, Kawaguchi *et al.* obtained approximate values of $\chi_s^{po}=0.42$ for PS adsorbing onto silica from trichloroethylene[28] and 1.23 from carbon tetrachloride[29]. However, Kawaguchi's findings in his papers[30,31] are doubtful because: (i) the displacer adsorption isotherms were not measured, (ii) the displacer chosen as a monomeric analog for polystyrene did not precisely match the repeat unit, (iii) incorrect choice of dioxane for monomeric analog for PEO, and (iv) the Scatchard-Hildebrand equation was used to estimate χ^{po}, χ^{pd}, and χ^{do}. A low value of PS adsorption energy ($\chi_s^{po}=1.23$ from carbon tetrachloride) is regarded as the weak adsorption function group of PS, and no H-bonding existence between polymer/solid interface. van der Beek *et al.*[25,26] found that χ_s^{po} for PEO on silica was always greater than χ_s^{po} for PS on silica due to hydrogen bonding between PEO and silanol groups.

Effect of Substrate Chemistry

While all of the adsorption experiments in this work were done with silica, it is useful to briefly describe related work which concerned the effect of substrate chemistry on χ_s^{po}. van der Beek *et al.*[27] reported that, from the solvent of carbon tetrachloride, $\chi_s^{po}=5.1$ for PEO on silica was greater than on alumina by 1. With the same solvent, the adsorption energy of PS on silica was $\chi_s^{po}=1.1$ whereas the adsorption energy of PS on alumina from carbon tetrachloride was lower, $\chi_s^{po}\approx 0.5$. These differences are most likely due to the greater acidity of silica. The high value of 5.1 *kT* for PEO on silica from carbon tetrachloride was attributed to the relative accessibility of the ether groups to surface hydroxyl groups.

CONCLUSIONS

The adsorption of poly(2-ethyl-2-oxazoline), PEOX, was studied using the displacement technique developed by Cohen Stuart *et al.*. The addition of various low

molecular weight displacer molecules from two different solvents - water and ethanol - gave values of the critical displacer volume fraction ϕ_{cr}. The positive values of the critical segmental adsorption parameter χ_{sc} - 0.99 in water and 0.78 in ethanol - are consistent with the predicted value of 0.288 from the lattice theory with the quantitative differences due to approximations in the lattice theory. The average values of the segmental adsorption energy parameter χ_s^{po} were 5.1 and 3.2 in water and ethanol, respectively. These relatively high values are attributed to hydrogen bonding between carbonyl groups on the polymer and surface silanol groups. The difference in adsorption energies in water and ethanol reflects specific solvent effects that may be related to the negative excess entropy of dilution for water in PEOX solutions as well as due to the formation of hydrogen bond bridges between PEOX and silanol groups in water. The relatively large magnitude of χ_s^{po} for PEOX in water and ethanol suggests that PEOX may serve as an effective anchor block in block copolymeric stabilizers.

The solvent effects point to the need for further work to separate the effect of solvent enthalpic and entropic effects in polymer adsorption. Microcalorimetry experiments can measure the enthalpy of adsorption of DMP on silica from water and ethanol which will be compared with the values of χ_s^{po}. Machine simulation of solvent-segment interactions should also prove useful in gaining a qualitative understand of the role that polymer structure plays in structuring solvent molecules, particularly water, around chain segments.

References

(1) Milner, S.T. *Science*, **1991**, *251*, 905.

(2) Buscall, R.; Ottewill, R.H. "Stability of Polymer Latices", Chapter 5 in *Polymer Colloids*; Elsevier Applied Science Publishers; R. Buscall, T. Corner, and J.F. Stageman, eds., 1985.

(3) Napper, D. A. *Polymeric Stabilization of Colloidal Dispersions*; Academic Press: New York, 1983.

(4) Gast, A. P.; Munch, M.R. *Colloids and Surfaces*, **1988**, *31*, 47.

(5) Gast, A. P.; Munch, M.R. *Macromolecules*, **1988**, *21*, 1366.

(6) Marquess, C.M.; Joanny, J.F. *Macromolecules*, **1989**, *22*, 1451.

(7) Ploehn, H. J.; Russel, W. B. *Adv. Chem. Eng.* **1990**, *15*, 137.

(8) Patel, S.; Tirrel, M. *Colloid Surf.* **1988**, *31*, 157.

(9) Hair, M. L.; Guzonas, D. A.; Boils, D. *Macromolecules*, **1991**, *24*, 341.

(10) Guzonas, D. A.; Hair, M. L. *Macromolecules*, **1992**, *25*, 2777.

(11) Wu, D.T.; Yokoyama, A.; Setterquist, R.L. *Polymer Journal*, **1991**, *23*, 709.

(12) Liu, Q.; Wilson, G.R.; Davis, R.M.; Riffle, J.S. *"Preparation and Properties of Poly(dimethylsiloxane-2-ethyl-2-oxazoline) Diblock Copolymers", Polymer,* **1993,** *34*, 3030.

(13) Liu, Q.; Konas, M.; Davis, R.M.; Riffle, J.S. *J. Poly. Sci.:Part A: Polymer Chemistry*, **1993**, *31*, 1709.

(14) Chen, C. H.; Wilson, J. E.; Chen, W.; Davis, R. M.; Riffle, J. S. *"A Light Scattering Study of Poly(2-alkyl-2-oxazoline)s: Effect of Temperature and Solvent Type", Polymer*, accepted, 1994.

(15) Chen, F. P.; Ames, A. E.; Taylor, L. D. *Macromolecules* **1990**, *23*, 4688.

(16) Lichkus, A. M.; Painter, P. C.; Coleman, M. M. *Macromolecules* **1988**, *21*, 2636.

(17) Silberberg, A. *J. Chem. Phys.* **1968**, *48*, 2835.

(18) Scheutjens, J.M.H.M.; Fleer, G.J. *J. Phys. Chem.*, **1979**, *83*, 1619.

(19) Scheutjens, J.M.H.M.; Fleer, G.J. *J. Phys. Chem.*, **1980**, *84*, 178.

(20) Cohen Stuart, M. A.; Fleer, G. J.; Scheutjens, J. M. H. M. *J. Colloid Interface Sci.* **1984**, *97*, 515.

(21) Cohen Stuart, M. A.; Fleer, G. J.; Bijsterbosch, B. H. *J. Colloid Interface Sci.* **1982**, *90*, (a) 310, (b) 321.

(22) Trens, P.; Denoyel, R. *Langmuir*, **1993**, *8*, 519.

(23) Lafuma, F.; Wong, K.; Cabane, B. *J. Colloid Surf*, **1991**, *143*, 9.

(24) Cohen Stuart, M. A.; Fleer, G. J.; Scheutjens, J. M. H. M. *J. Colloid Interface Sci.* **1984**, *97*, 526.

(25) van der Beek, G. P., *"Displacement of Adsorbed Polymers"*, Ph.D. dissertation, Department of Physical and Colloid Chemistry, Wageningen Agricultural University, Wageningen, The Netherlands, 1991.

(26) van der Beek, G. P.; Cohen Stuart, M. A.; Fleer, G. J. *Macromolecules* **1991**, *24*, 6600.

(27) van der Beek, G. P.; Cohen Stuart, M. A.; Fleer, G. J.; Hofman, J. E. *Langmuir*, **1989**, *5*, 1180.

(28) Kawaguchi, M.; Yamagiwa, S.; Takahashi, A.; Kato, T. *J.Chem. Soc. Faraday Trans.*, **1990**, *86*, 1383.

(29) Kawaguchi, M. *Adv. Colloid Interface Sci.* **1990**, *32*, 1.

(30) Kawaguchi, M.; Chikazawa, M.; Takahashi, A. *Macromolecules*, **1989**, *22*, 2195.

(31) Kawaguchi, M.; Hada, T.; Takahashi, A. *Macromolecules*, **1989**, *22*, 4045.

(32) Korn, M.; Killmann, E. *J. Colloid Interface Sci.* **1980**, *76*, 19.

(33) Liu, Q.; Konas, M.; Riffle, J.S. *Macromolecules* **1993**, *26*, 5572.

(34) *CAB-O-SIL Fumed Silica Properties and Functions*, G. L. Cabot Co. Cab-O-Sil Division, 1992.

(35) Vink, H. *European Polymer Journal*, **1971**, *7*, 1411.

(36) Finch, C.A. in *Chemistry and Technology of Water-Soluble Polymers*; Plenum Press: New York, C.A. Finch, ed., 1983.

(37) Kiselev, A.; Lygin, V. I. In *Infrared Spectra of Surface Compounds*; Halsted Press/Wiley: New York, 1975.

CHAPTER 4

The Solution Properties and Adsorption Behavior of Poly(2-ethyl-2-oxazoline) on Silica

ABSTRACT

The adsorption of poly(2-ethyl-2-oxazoline)(PEOX) from water and alcohols (ethanol, isopropanol, and n-butanol) on Cab-O-Sil silica was investigated by measuring PEOX adsorption isotherms using the depletion method. A linear relationship of the plateau adsorption amount, Γ_p, vs. log(molecular weight, MW) was obtained, which agreed qualitatively with the Scheutjens-Fleer (S-F) mean field adsorption theory. The values of Γ_p varied significantly with solvent type as well as with pH and electrolyte concentration in water. These variations in Γ_p were due to changes of the polymer solubility and the silanol density on the silica particles. The final part of this chapter deals with the competitive adsorption of PEOX with other polymers, which include poly(ethylene oxide)(PEO) and poly(propylene oxide)(PPO) in several alcohols and water. PEOX shows a higher affinity for the silica surface than these other polymers. This suggests that PEOX has good potential for serving as an anchor block for diblock copolymer stabilizers for metal oxides in water. This has important implications in designing diblock copolymer stabilizers.

INTRODUCTION

Polymer adsorption on solid/solution interfaces differs in several aspects from the adsorption of small molecules and has attracted much attention recently due to its applications in ceramic processing, paper coating[1], and biochemistry.[2] There are numerous theoretical studies of polymer adsorption, including the mean-field theory[3,4] and

the scaling model[5]. These approaches characterize the polymer-surface interaction in terms of a phenomenological energy of adsorption of a single segment, $\chi_s kT$ and the polymer-solvent interaction in terms of the Flory χ parameter. This approach has been generalized to account for polyelectrolytes[6] and copolymers[7].

Polymer Adsorption and Chain Configuration

The adsorption of low molecular weight species can be described well by a Langmuir-type adsorption isotherm with a low affinity, as expected for relatively low adsorption energies compared to polymer adsorption. Attractive forces leading to adsorption can be due to van der Waals forces, dipole-dipole interaction, hydrogen bonding, and, in the case of charged species, electrostatic attraction. With long chains, adsorption isotherms typically show an abrupt rise at low concentrations of dissolved polymer chains followed by a plateau at higher concentration, corresponding to saturated surface coverage. This is described as a high affinity isotherm. An adsorbed flexible polymer chain can assume a combination of loop-train-tail conformations, where parts of an adsorbed polymer chain make direct contact with the surface as trains, while the remaining segments extend into the solution as loops and tails which lead to a thick adsorbed layer. The polymer conformation on the surface at very low concentrations is not strongly affected by adsorbed chain-chain interactions and tends to adsorbed largely as flat trains.[8b] As coverage increases, interactions between adsorbed polymer molecules lead to an increase in the fraction of loops and tails.

The magnitude of the adsorbed mass of polymer per particle surface area at the plateau Γ_p and its dependence on MW and solvent conditions provide crucial information about the polymer behavior on the surface. In this region, any further polymer added to the solution does not adsorb onto the surface. The area per adsorbed molecule and fraction of train segments attain their minimum values, and adsorbed thickness reaches its maximum value. According to the Scheutjens-Fleer (S-F) mean-field theory,[9] the magnitude of Γ_p from a polymer is generally affected by molecular weight (MW),

volume fraction (ϕ^*) of polymer in solution equilibrium with surface, χ, and χ_s. Scheutjens and Fleer[9] also noted that the adsorbed amount at high polymer concentrations is only a weak function of χ_s for $\chi_s > 2$.

The influences of molecular weight on Γ_p have been widely studied. Howard *et al.*[10] early studied the pronounced effect of MW dependence on the adsorption of PEO (MW from 0.39 to 190.0 kg/mole) on aerosil silica from solvents including water, methanol, benzene and dioxane. All of the results could be correlated with the relation $\Gamma_p = K \cdot MW^{\alpha}$ at high MW region, proposed by Perkel and Ullman.[11] The adsorbed amount depended upon the polymer solubility (determined by the intrinsic viscosity), and also on the competition between solvent molecules and polymer segments onto the surface sites. Dawkins *et al.*[12] investigated the molecular weight dependence of the adsorption of polystyrene (PS), poly(dimethyl siloxane)(PDMS) and poly(ethylene oxide)(PEO) on silica in trichloroethylene. The homopolymers all showed a linear relationship of *log* Γ_p versus *log* MW. Based on the values of α in the above relationship and the experimental measurements of fraction of the train segments, the authors concluded that the PDMS and PS chain form a great portion of loops whereas PEO mostly adsorbed in flat trains on the surface. Fleer[12] criticized these analyses of the adsorbed conformation because this ignored chain-chain interactions on the surface and because the equation by Perkel-Ullman equation lacks a physical basis.

More recently, Cohen Stuart *et al.*[13] studied the effects of molecular weight, molecular weight distribution, and adsorption time of poly(vinyl pyrrolidone)(PVP), in water and in dioxane on silica. A linear relationship of Γ_p and *log* MW for fractionated PVP qualitatively followed the S-F lattice theory for viscosity-average molecular weight M_v in the range 2.77 - 515.0 kg/mole. The difference of PVP adsorbed amount in two solvents was attributed to the difference in the volumes of the solvent molecules.

Effect of Polymer Solubility

Other investigations studied the effect of electrolyte concentration and pH on the

adsorption of water-soluble non-ionic polymer. Barker *et al.*[14] showed that sodium sulfate increased the adsorption of poly(vinyl alcohol)(PVA), MW=45.0 kg/mole onto polystyrene (PS) latex from water. The increase of Γ_p with salt concentration was correlated with the decrease of solubility of the polymer. A similar electrolyte effect was recently reported by Einarson *et al.*[15] concerning the adsorption of triblock copolymers of poly(ethylene oxide)/poly(propylene oxide) on PS latex in water. The PS latex stability was consistent with the decrease of the second virial coefficients (by intrinsic viscosity) of the polymers at high concentrations of $BaCl_2$ and NaCl. Van der Beek *et al.*[16] studied the effects of pH on the adsorption/displacement of PEO (MW from 1.0 to 300 kg/mole) and PVP (MW=10 and 24 kg/mole) on Ludox silica from water. Proton NMR revealed that pre-adsorbed PVP could not be desorbed simply using dimethyl sulfoxide (DMSO) and N,N dimethylformamide (DMF). However, PEO could be desorbed in the same condition. This suggested that PVP exhibited a stronger affinity to silica than PEO in water, *i.e.*, $(\chi_s)_{PVP} > (\chi_s)_{PEO}$.

Competitive Adsorption. Competitive adsorption[10,13,17-23] between polymers has been studied to understand the reversibility of polymer adsorption and the adsorption behavior of polydisperse polymers. The affinity of the polymer for the surface is directly related to the adsorption energy $\chi_s kT$.[8,24] Polymer adsorption can be described in terms of three types of binary interactions acting among adsorbent surface (s), solvent molecule (1), and polymer chain (2), which are designated as the interaction free energies ϵ_{12}, ϵ_{1s}, and ϵ_{2s}. As defined by Silberberg[25], $\chi_s kT$ is the free energy change associated with the transfer of a polymer segment in polymer from a bulk site to a surface site, minus the corresponding energy of a solvent molecule in pure solvent. The adsorption energy parameter of a homopolymer can be expressed as:

$$\chi_s \propto \frac{[\epsilon_{2s} - \epsilon_{1s} + 1/2(\epsilon_{11}-\epsilon_{22})]}{kT} \qquad (4.1)$$

If the interaction ϵ_{2s} is greater than the interaction ϵ_{1s}, polymer adsorption can take place. A theoretical basis for this parameter is provided by the S-F lattice theory which is described in a later section.

Furusawa *et al.*,[17] measured the effect of MW on the competitive adsorption of polydisperse PS from cyclohexane at theta condition. PS chains with higher molecular weights preferentially adsorbed on the silica surface at equilibrium. Shorter PS chains which adsorbed initially were replaced by long PS chains on the surface at longer times.

Another type of competitive adsorption is that between different polymers. Thies[26] reported that poly(methyl methacrylate) (PMMA) (M_v=1900 and 368 kg/mole) preferentially adsorbed over PS (M_v=246 and 39 kg/mole) on silica surface in trichloroethylene using infrared spectroscopy (IR). Schick and Harvey[27] performed competitive adsorption experiments using PS and PMMA on Graphon carbon black in 2-butanone, a poor solvent for PS but a good solvent for PMMA. In contrast to the results of Thies[26], they found that PS adsorbed over preferentially with respect to PMMA. The value of Γ_p for PS in the mixture was lowered by the presence of PMMA. However, Γ_p for PS was only weakly dependent on the MW of PMMA. This preferential adsorption of PS over PMMA was attributed to both the relative solubilities of the polymers in 2-butanone and the non-polar graphite surface. Recently, Kawaguchi *et al.* systematically studied the mixture of PMMA and PS adsorbing on aerosil silica.[19,23] PMMA exhibited a higher affinity toward silica surface in trichloroethylene due to hydrogen bonding between the carbonyl group in the PMMA and the silanol groups on silica surface, which was consistent with the work by Thies.[26] A similar explanation was given by Liptov and coworkers[18], who found poly(butyl methacrylate) (PBMA) competitively adsorbed with respect to PS on silica in carbon tetrachloride.

Botham and Thies[20] measured the competitive adsorption between poly(butadienes) (PBD) and PS from perchloroethylene on two Cab-O-Sil silica surfaces. They found that PS preferentially adsorbed over PBD due to the π electrons from the phenyl groups interacting with the surface more strongly the than π electrons from the C=C group (in PBD) with the surface. Further competitive adsorption experiments with PS/PBD/PS triblock (M_n=105 kg/mole 18.9 mole% PS) and with PS/PBD diblock copolymers (M_n= 88 kg/mole 14.7 mole% PS) showed that PBD was rapidly displaced by the copolymers. However, the copolymers were displaced by PS homopolymers (M_n=38 and 498 kg/mole).

van der Beek *et al.*[28] have also noted a similar strong adsorption of PS on silica and attributed it to the π electrons of the phenyl groups interacting with the protons of the silanol groups. This interpretation was also applied to PS adsorption on other metal oxides, *e.g.* TiO_2 and Al_2O_3. Moreover, Leonhardt *et al.*[22] compared the adsorption affinity of protio- (*-p*) and deutero- (*-d*) PS onto silica in cyclohexane at 30°C, a theta solvent for PS-*d* but a good solvent for PS-*p*. At equilibrium, no PS-*p* was found on the surface which indicated the PS-*d* segregated at the surface. The same result was obtained in low MW (DP=66) of PS-*d* and higher MW of PS-*p* (DP=92) at a 1:1 weight mixture. Since molecular weight did not influence the results, this significant adsorption difference was due to lesser solubility of PS-*d* compared to PS-*p*.

The replacement of PS by PEO was studied by Kawaguchi *et al.* on a nonporous silica in carbon tetrachloride using IR and UV spectroscopy.[21] PS was replaced by PEO due to strong hydrogen bonding between the ether oxygen in the polymer and surface silanol groups. The degree of displacement of PS by PEO depended upon (1) the fraction of the PS segments in trains and (2) the relative MW of the PS and PEO homopolymers. The authors concluded that the chains with conformations extending more into solution could be desorbed more easily than could chains segments adsorb as trains. The results agreed well with the calculations of χ_s by van der Beek[41] who found that $(\chi_s)_{PEO}$ $(=5.1) > (\chi_s)_{PS}$ $(=1.1)$ on silica surface from carbon tetrachloride.

CHAPTER OUTLINE

In this chapter, the adsorption of PEOX on silica from various solvents and as a function of molecular weight is presented. The adsorption isotherms of PEOX were compared qualitatively with the Scheutjens-Fleer theory. An important criterion for a diblock copolymeric stabilizer is that the anchor block must have a stronger affinity to the surface than the tail block.[1] Consequently, the competition of PEOX adsorption with other polymers onto silica was studied. We chose polyethers to compete with PEOX because of the possibility of incorporating polyethers into diblock copolymers with PEOX while controlling the MW of both blocks. We first present a brief review of adsorption theories and their most relevant findings for our work.

ADSORPTION REVIEW

Theoretical models for polymer adsorption have progressed rapidly in recent years.[5,7,8,29] It is now understood that the adsorption of polymer differs qualitatively from the adsorption of small molecules. This difference is attributed to the large number of configurations that a macromolecule can assume, both in the bulk solution and at an interface. For flexible polymers, the entropy loss per molecule upon adsorption is greater than for small molecules or for stiff polymer chains. The decrease in total free energy is also much higher for flexible chains owing to the much larger number of possible attachment points per chain.

In this section, the current state of the art on polymer adsorption is discussed, discussion restricted to nonionic homopolymers. Two main groups of theories can be distinguished, commonly referred to as "scaling" [5] and "mean-field" [4,7,9,10]. Both approaches are extensions of earlier Flory polymer solution theories.[30] The mean-field theory will be briefly outlined in this chapter. The mean-field model can provide more detailed information of the adsorbed layers on surface than scaling, particularly for the

high concentrations usually encountered in the adsorbed layers.[8a]

Scheutjens-Fleer Mean-Field Theory. An early version of a mean field theory of polymer adsorption was proposed by Silberberg[25] in 1968. The theory was greatly modified and extended by Scheutjens and Fleer (S-F)[24] to account for all possible adsorbed polymer configurations on the surface. The S-F lattice theory is an extension of the Flory-Huggins model for an inhomogeneous system. The distribution of segments as a function of distance from the surface and, consequently, end effects (tails) are taken fully into account. The S-F theory successfully predicted adsorption trends for several experimental systems,[13,16,19] especially when segment-solvent interactions are weak, *i.e.* close to the theta condition.

In the S-F theory,[4] all possible chain conformations on the surface are considered in the segment density profile. The following discussion closely follows their treatment.[4] This model assumes that the polymer chains occupy the lattice, where each lattice site is weighted with an entropy factor to account for the local entropy of mixing and an energy factor to account for the nearest neighbor interactions. The lattice is divided into M layers and each layer is parallel to the surface with indices $i = 1,2,\ldots,i,\ldots,M$. The layer index at which polymer chains directly contact with the surface is $i=1$. The index $i=M$ corresponds to a layer far from the surface and in the bulk solution, as illustrated in Figure 4.1. Each layer has L lattice sites. Each lattice site by either a polymer segment or a solvent molecule. The weighting factor P_i for any segment in layer i depends on the number of neighboring occupied sites in layer i and in the adjacent layers of i - 1 and $i+1$. The most serious drawback of this approach is that excluded volume interactions with neighboring polymer segments only roughly accounted for. A lattice site has z nearest neighbors which are expressed by the bond weighting factors λ_0 and λ_1. The factor λ_0 is the fraction of neighboring segments in the same layer and λ_1 is the fraction of segments in the adjacent layers, such that $\lambda_0+2\cdot\lambda_1 =1$. In a simple cubic lattice, $\lambda_0=4/6$ and $\lambda_1=1/6$ and in a hexagonal lattice, $\lambda_0=6/12$ and $\lambda_1=3/12$. The volume

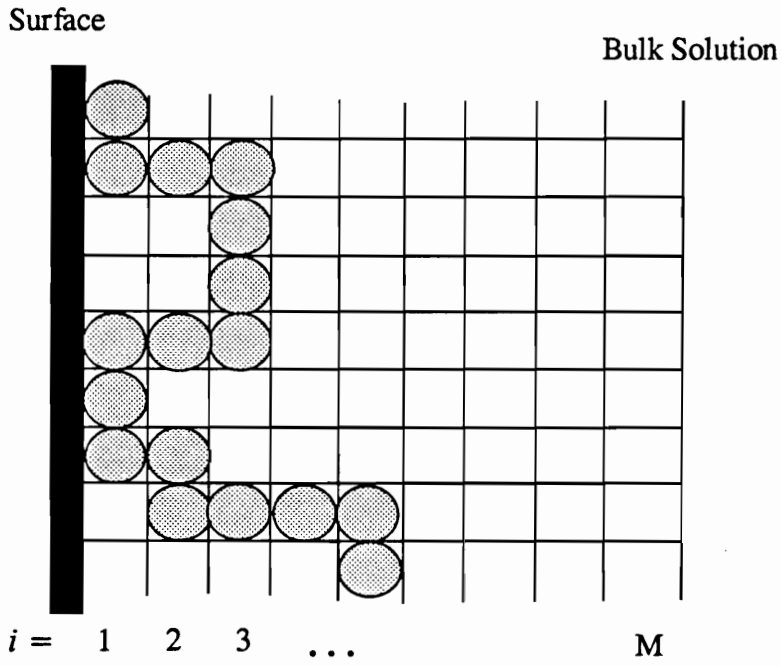

Figure 4.1 A typical conformation of an adsorbed homopolymer chain in a lattice. The layer $i = 1$ is the chain contacting with the surface while $i = M$ represents the bulk solution.

fractions in each layer are defined as $\phi_i = n_i/L$ and $\phi_i^0 = n_i^0/L$, where n_i and n_i^0 are the number of segments and solvent molecules in layer i, respectively. Thus, $\phi_i + \phi_i^0 = 1$.

The lattice theory calculates the probability of every conformation in this lattice. A conformation is defined as the sequence of layers in which the successive segments of a chain are situated. Interactions between adsorbed chain segments are accounted for by a mean field approximation. Each segment in a given layer i has the same interaction energy, dependent on several factors, including the volume fractions (in $i - 1$, i, and $i+1$), the solubility parameter χ, segmental adsorption energy parameter, χ_s (if $i=1$), and the lattice parameters λ_0 and λ_1. The total polymer-solvent interaction energy, u_{sol}, in the lattice is given by

$$u_{sol} = kT\chi \sum_{i=1}^{M} n_i^o \langle \phi_i \rangle \tag{4.2}$$

where k is the Boltzmann constant and T is the absolute temperature. The adsorption energy is calculated as

$$u_{ads} = - kT \cdot n_1 \chi_s \tag{4.3}$$

where n_1 is the number of segments in the layer $i=1$, *i.e.* in trains, and the average polymer volume fraction, $\langle \phi_i \rangle$, is defined as

$$\langle \phi_i \rangle = \lambda_1 \phi_{i-1} + \lambda_0 \phi_i + \lambda_1 \phi_{i+1}. \tag{4.4}$$

An important parameter in the theory is the free segment probability, P_i, defined as the probability of finding a free segment (*e.g.* repeat unit) in layer i. An equation for P_i as a function of the local segment concentrations, is obtained from the partition function and is given by

$$P_i = \phi_i^0 \cdot \exp\{\chi(<\phi_i> - <\phi_i^0>)\} \cdot \exp\{\chi_s \cdot \delta(1,i)\} \qquad (4.5)$$

The Kronecker delta, $\delta(1,i)$, equals unity for $i=1$ and zero for $i \neq 1$. The solvent volume fraction ϕ_i^0 accounts for the entropy of mixing in a layer where a fraction ϕ_i^0 of lattice sites is occupied by the solvent such that $\Delta S_{mix} \propto k \cdot ln\ \phi_i^0$ per segment. The Boltzmann factor containing χ arises from the polymer-solvent interaction and the Boltzmann factor containing χ_s is related to the net adsorption energy per segment.

The end segment probability, P(i,r), *i.e.*, the probability that the end segment of a chain of r segments is in layer i, is calculated from:

$$P(i,r) = P_i \cdot [\lambda_1 P(i\text{-}1, r\text{-}1) + \lambda_0 P(i,r\text{-}1) + \lambda_1 P(i+1, r\text{-}1)] \qquad (4.6)$$

For chains that are r segments long there is the following recurrence relation,

$$P(i,r) = P_i \cdot <P(i,r\text{-}1)> \qquad (4.7)$$

where the angular brackets have the same meaning as in equation (4.4). Equation (4.7) implies that step reversals are allowed, *i.e.* segments r and r - 2 may simultaneously be in the same lattice site. This is one of the largest drawbacks of the theory. By repeated application of equation (4.7), P(i,r), the end dangling segments in layer i, may be calculated based on the distribution P(i,1), ($=P_i$), according to equation (4.5).

Theoretical predictions. In terms of the S-F mean field lattice model, adsorption is a function of: 1) the polymer volume fraction in the bulk equilibrium solution, ϕ^*, 2) the length of the chains, *i.e.* the number of segments, r, 3) the segment-solvent interaction parameter, χ, and 4) the adsorption energy parameter χ_s.

A. Molecular weight and solvency dependence of the adsorbed amount

All adsorption theories[3,4,29] that include interactions between adsorbed chains predict that the plateau adsorbed amount Γ_p increases with the chain length r and also varies inversely with solubility. However, the quantitative descriptions are different with each theory. Silberberg's theory[25] predicts that at very high chain length, a plot of Γ_p against polymer molecular weight in a θ-solvent reaches an upper limiting value, whereas in Hoeve's theory[3], $\Gamma_p \propto MW^{1/2}$. In the S-F theory for a θ-solvent, Γ_p increases linearly with *log* r without bound, but both the slope ($d\Gamma_p/dMW$) and Γ_p are smaller in better (athermal, $\chi=0$) solvents, as illustrated in Figure 4.2(a).

The fractions of segments in loops is the main difference in the adsorbed configurations between good and poor solvents, as seen in Figure 4.2(b). As the solvent becomes poorer, there is a significant increase in the fraction of loops whereas the fraction of tail segments changes only slightly. This is important because the measured hydrodynamic layer thickness, δ_h, is primarily a function of the tail fraction. Because the tail fraction only weakly depends upon χ, δ_h is predicted to be a weaker function of χ than is Γ_p (refer to Figures 4.3 and 4.5).[8]

The adsorbed amount can be expressed in several ways. The excess adsorbed amount (Γ_{ex}) is defined as the difference between the excess concentration of segments in each layer (ϕ_i) and the bulk concentration (ϕ^*):

$$\Gamma_{ex} = \sum_{i=1}^{M} (\phi_i - \phi_i^*) \qquad (4.8a)$$

The adsorbed amount Γ, which is the experimentally measured amount, is defined as the number of adsorbed molecules per surface site.

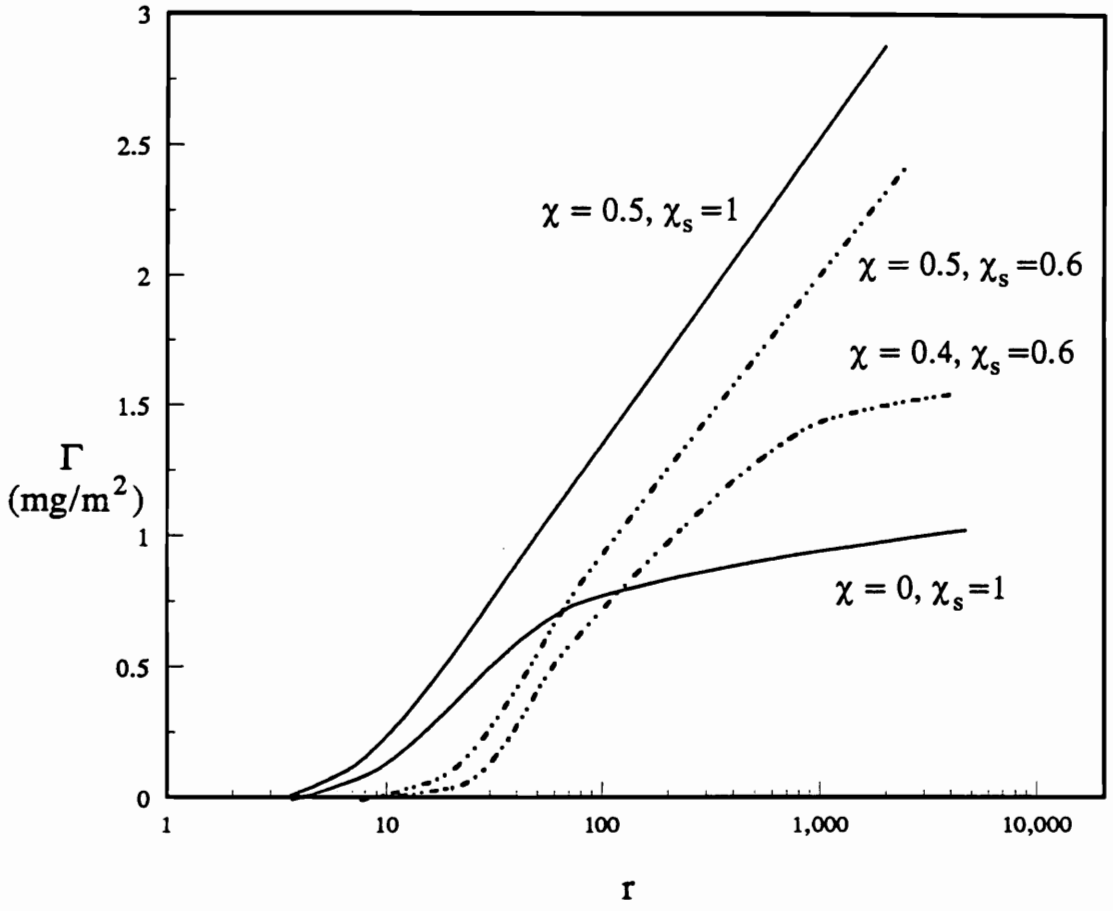

Figure 4.2 (a) The plateau adsorbed amount (Γ) is predicted by Scheutjens and Fleer lattice theory as a function of chain length r, at different χ and χ_s .[8(b)]

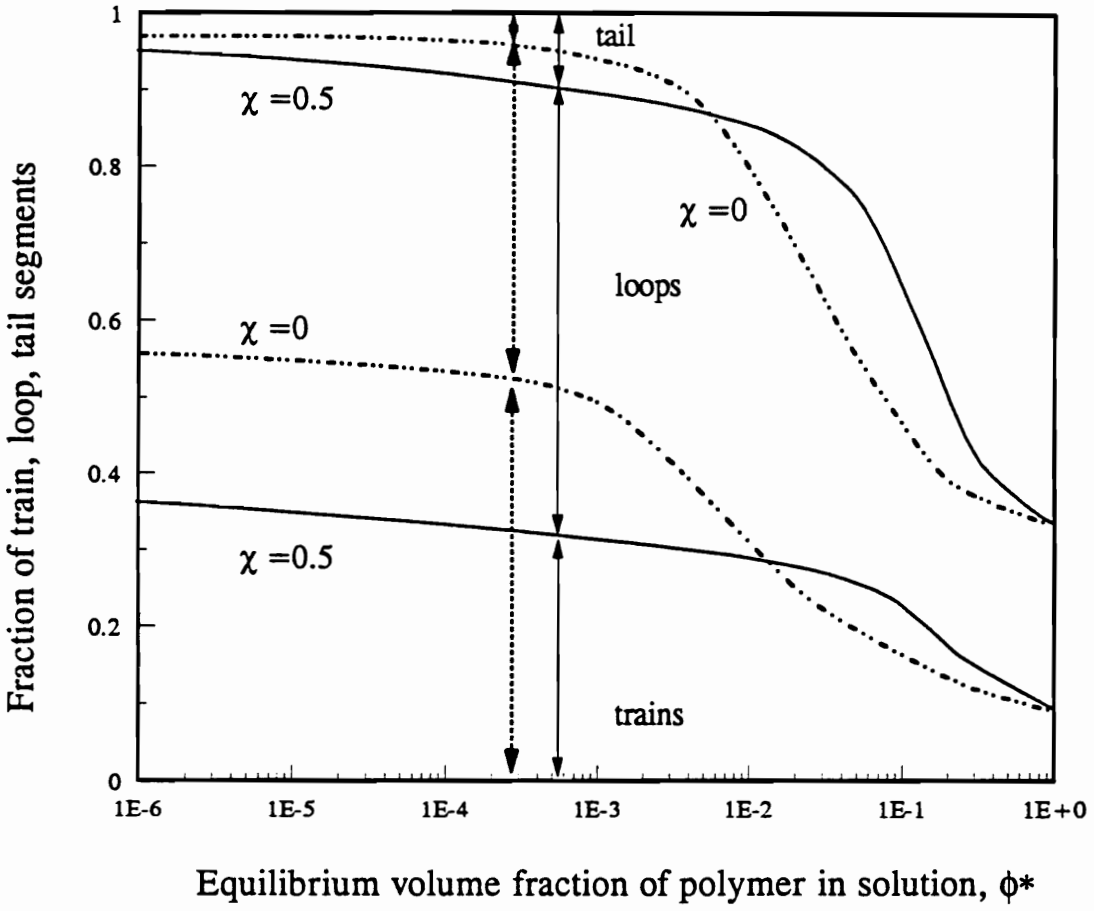

Figure 4.2(b) Fraction of trains (bottom), loops (center) and tails (top) for $\chi = 0$ and 0.5, as a function of ϕ^*, r = 1000, $\chi_s = 1$. [8(a)]

$$\Gamma = \sum_{i=1}^{M} (\phi_i - \phi_i^f) \qquad (4.8b)$$

where ϕ_i^f is the volume fraction of free chains in each layer, *i.e.* those that do not contact the surface. In the surface layer, $\phi_1^f=0$, and for other layers $\phi_i^f \leq \phi^*$. The surface coverage $\theta=1$ means that one equivalent monolayer is adsorbed, *i.e.* all surface sites are occupied by an adsorbed segment. Thus, equation (4.8a) underestimates the adsorbed amount. Γ and Γ_{ex} are related to each other by

$$\Gamma = \Gamma_{ex} + \Gamma_d \qquad (4.8c)$$

where Γ_d is the depletion adsorbed amount. This can be rewritten in terms of the equivalent monolayers, $\theta=\Gamma/\Gamma^{mon}$, where Γ^{mon} represents the monolayer adsorption. There are two contributions to θ, the excess adsorbed amount θ_{ex} and the depletion adsorbed amount θ_d, shown in equation (4.8d) and illustrated in the insert of Figure 4.3(a).

$$\theta = \theta_{ex} + \theta_d \qquad (4.8d)$$

The dependence of θ on the degree of polymerization is illustrated in Figure 4.3(a). The values of θ increase with r at different concentrations. At $\chi=0.5$, the results of the theory can be expressed by two approximate equations for θ_{ex} and θ_d as:

$$\theta_{ex} \sim (1-\phi^*)(a+b\cdot log\ r) \qquad (4.9a)$$

$$\theta_d \sim \phi^*\cdot(0.64+0.562\cdot r^{1/2}) \qquad (4.9b)$$

These equations are valid only for polymer chains with $r \geq 50$.[8b] For shorter chains ($r<50$), θ_d is negligible relative to θ_{ex}. The parameter '*b*' in equation (4.9a) is a function

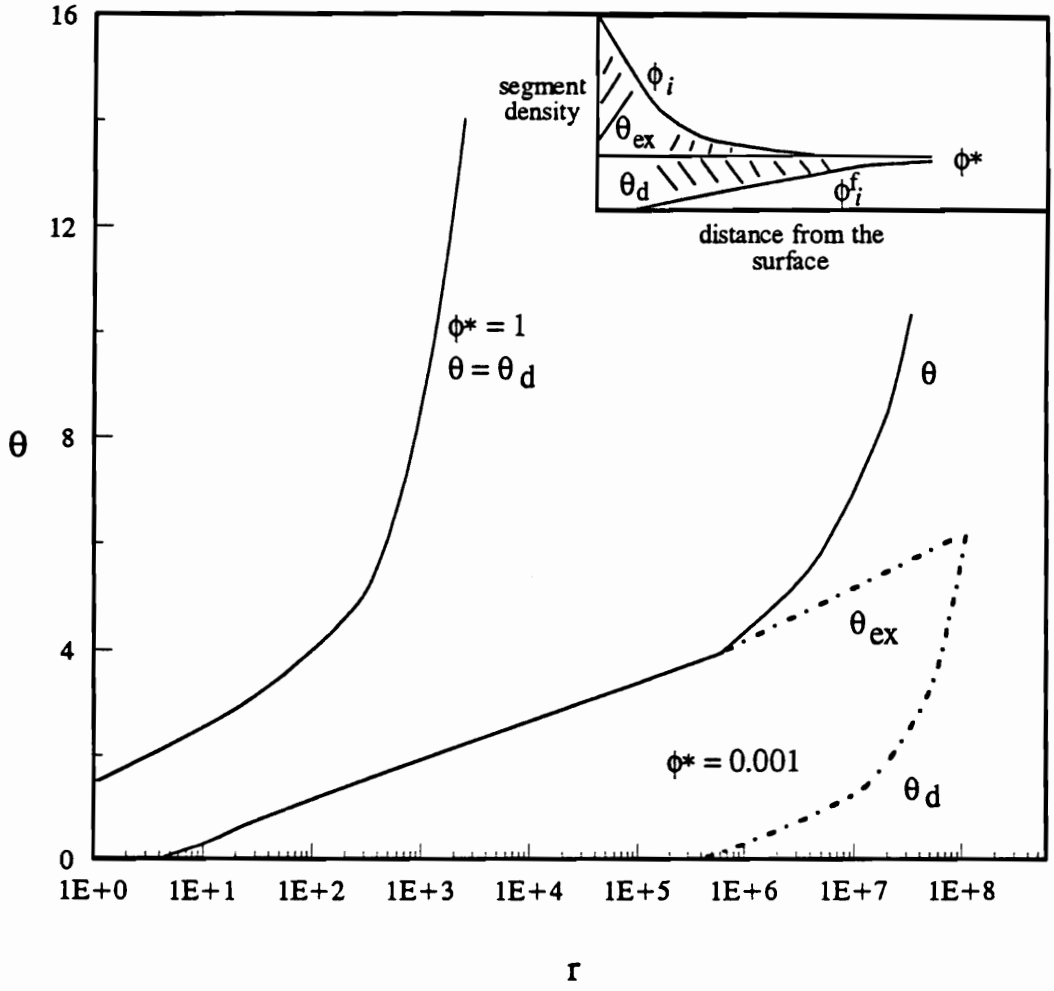

Figure 4.3 (a) The total surface coverage θ as a function of chain length r, for $\phi^*=1$ (bulk polymer) and $\phi^*=0.001$. The inset qualitatively illustrates the segment concentration profile in the adsorbed layer. The integration under the hatched areas corresponds to θ ($=\theta_{ex}+\theta_d$)[8(b)]. According to hexagonal lattice ($\lambda_0=0.5$), $\chi_s=1$, $\chi = 0.5$.

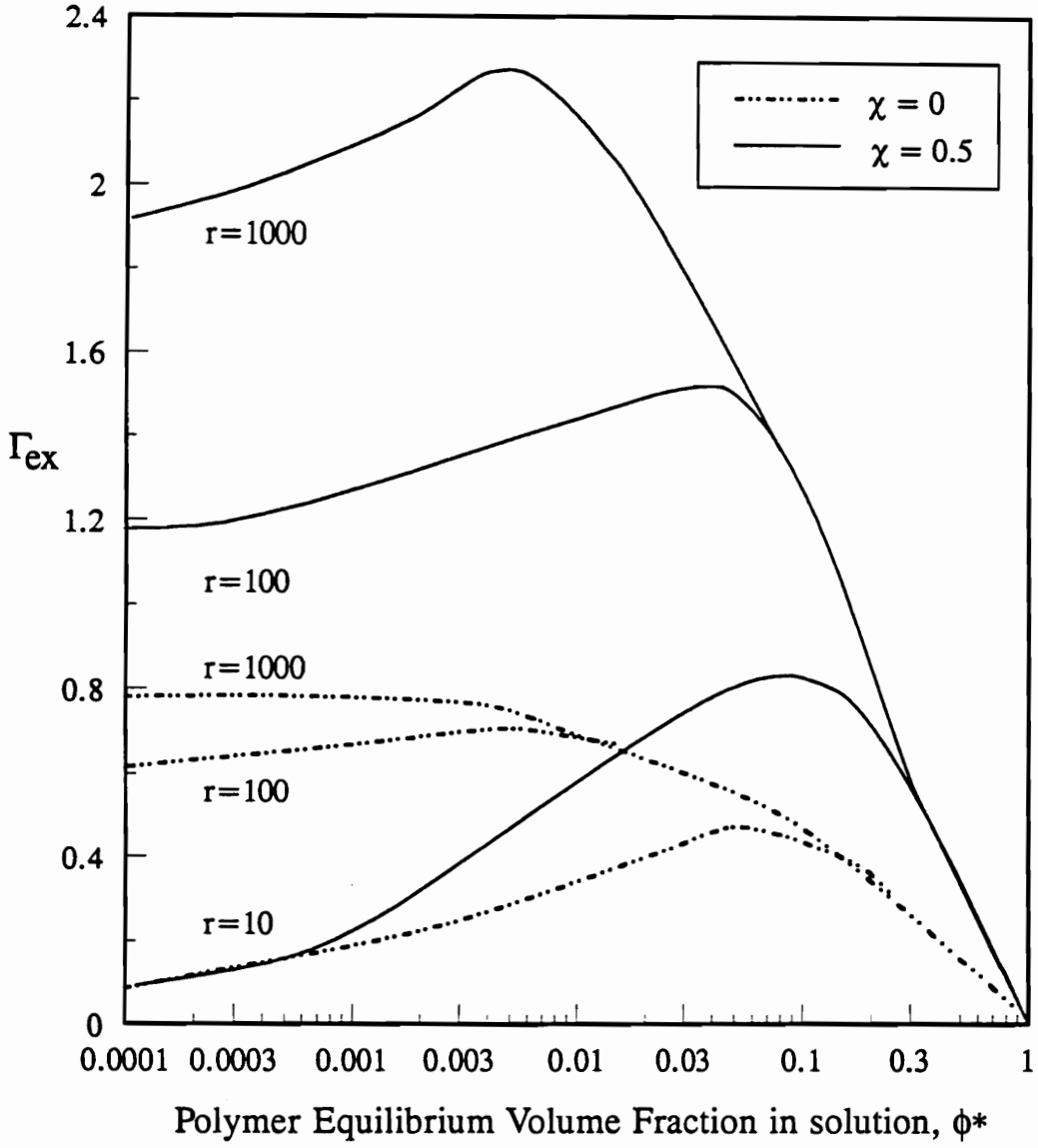

Figure 4.3(b) The polymer adsorbed amount Γ_{ex} as a function of ϕ^* at χ=0.5 and χ=0; where χ_s =1 and hexagonal lattice λ_o=0.5 [8(b)].

of χ, whereas 'a' is affected by ϕ^* and χ_s. Therefore, θ_{ex} is a function of r, χ, χ_s and ϕ^*. The numerical coefficients in equation (4.9b) are not influenced by ϕ^*, χ, and χ_s. Thus, θ_d is only a function of ϕ^* and r. Note that for low ϕ^* typical in the adsorption experiments, $\theta_d << \theta_{ex}$ and $\theta \approx \theta_{ex}$. Equations (4.9a and b) suggest that at $\chi=0.5$, $\theta_{ex} \rightarrow 0$ and $\theta \rightarrow \theta_d$ as $\phi^* \rightarrow 1$. At high concentrations (where $\phi^* \rightarrow 1$ and $\theta \rightarrow \theta_d$), $\theta \propto r^{-0.5}$, which implies that polymer chains have a Gaussian distribution configuration near the interface, in accordance with the chains in the bulk behaving as undisturbed Gaussian coils. This is expected since, under θ-condition and high concentration, only entropy factors play a role. For $\phi^* \rightarrow 1$, the adsorption energy parameter χ_s is not important because θ is only a weak function of θ_{ex} as seen in Equation 4.9 (a). In conclusion, both θ_{ex} and θ_d are related to the polymer volume fraction ϕ^* and polymer chain length.

B. Concentration dependence of the adsorbed amount

In the dilute region, isolated adsorbed chains tends to lie flat on the surface. Under this concentration, an expression describes the relation between θ and other parameters,[8b]

$$\theta \propto \phi^* \cdot \exp[r \cdot (\chi_s + \lambda_1 \cdot \chi)]. \qquad (4.10)$$

Experimental adsorption isotherms for polymers with monodisperse polymers are usually of the so-called high-affinity type, *i.e.*, for very low concentrations ($\phi^* < 10^{-6}$) the isotherm rises rapidly with increasing ϕ^* and then levels off to a plateau (or semi-plateau) region once the concentration in solution is measurable. The S-F model is applicable to the entire concentration range, from extremely dilute solutions (isolated polymer chains, $\phi^* < 10^{-30}$) up to $\phi^* = 1$ (bulk polymer). The value of θ linearly increases with ϕ^* in the extremely dilute region, based on Equation (4.10). As soon as the surface becomes covered to an extent of more than a few per cent, excluded volume effects of adsorbed chains become more significant and the dependence of θ with increasing ϕ^* becomes much weaker. In this region, an adsorption plateau is commonly observed.

Polymer desorption may occur only at an extremely dilute concentration ($\phi^* < 10^{-20}$), which is hardly ever reached in most experiments. This is the reason that polymer adsorption is sometimes described in the literature as an irreversible process by dilution. Alternatively, polymer desorption can occur by changing the solvent composition or quality as described in Chapter 3. Moreover, in Figure 4.3(b) the excess adsorbed amount increases strongly at low ϕ^*, passes through a maximum at intermediate ϕ^*, and decreases at higher ϕ^*, until at $\phi^*=1$ ($\Gamma_{ex}=0$).

C. Dependence of Γ_p on adsorption energy

In the S-F theory, adsorption occurs only when $\chi_s > \chi_{sc}$, where χ_{sc} is the *'critical adsorption energy'*, defined analytically in Chapter 3 by $\chi_{sc} = -\ln(1-\lambda_1)$. From Equation (3.8), $\chi_{sc}=0.29$ for a hexagonal lattice. As shown in Figure 4.4, the value of χ_s did not significantly affect Γ value for $\chi_s \leq 0.3$.[8a] The segmental adsorption energy parameter, χ_s indeed affects the adsorbed amount, especially for $0.3 < \chi_s < 2$ (Figure 4.4). Depending upon the value of χ, Γ increases linearly with χ_s over a narrow range before reaching a plateau region. For high values of χ_s (≥ 2), Γ is only weakly dependent (or even independent) of the adsorption energy. It is important to note that θ' in Figure 4.4(b) is the direct surface coverage, as given as $\theta' = p \cdot \Gamma$, where p is the bound fraction of the chains. The factors θ' and Γ have similar dependence on χ_s, as seen in Figure 4.4(b). If the adsorption energy is in the moderate range ($0 < \chi_s < 2$), the adsorbed amount decreases with decreasing χ_s due to less portion of trains and loops in the adsorbed chains.

D. Dependence of Adsorbed layer thickness and tails on χ and χ_s

For a given solvent quality, S-shaped curves of δ_h against θ are found[8a], shown in Figure 4.5. The adsorbed thickness increases with r and rather weak with solvent quality. In the dilute ($\phi^* \rightarrow 0$) region, $\theta << 1$ (based on Equation (4.10)), the chains lay flat so that δ_h is small and independent of chain length. As the polymer concentration

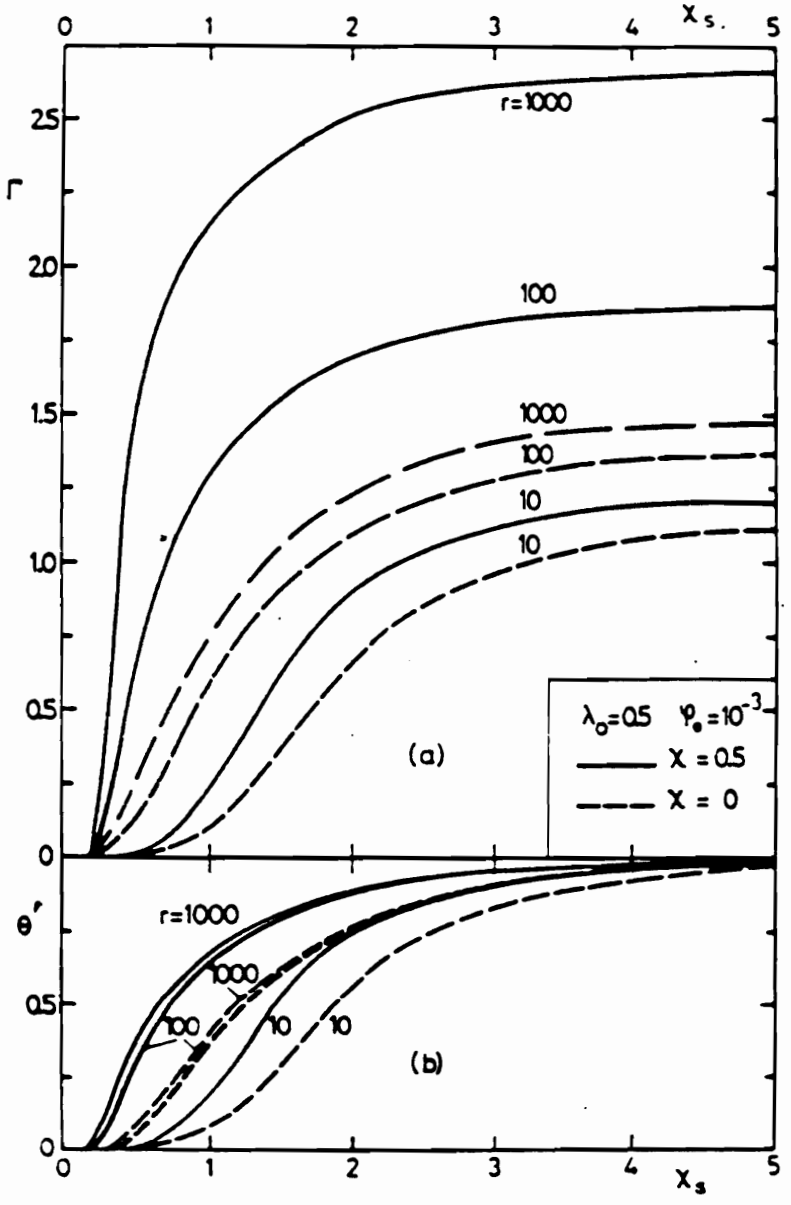

Figure 4.4 (a) The adsorbed amount Γ and (b) the direct surface coverage $\theta'(=p\cdot\Gamma)$, against the adsorption energy parameter χ_s, for $\chi=0.5$ and $\chi=0$. Hexagonal lattice, $\phi^*=0.001$.[4]

increases ($10^{-3} < \phi^* < 10^{-1}$), loops and tails develop and δ_h increases steeply in good solvents but more gradually in poor solvents.

An interesting aspect of the S-F theory is that the layer thickness δ_h depends only weakly on χ and χ_s, despite the fact that these parameters have a much greater effect on θ (or Γ). In the S-F theory, the adsorbed layer thickness is dominated by the tail fraction while the earlier Silberberg theory[25] did not take tails into account. The tail fraction is not a strong function of χ, whereas the loop fraction greatly increases as the solvency decreases (Figure 4.2(b)). This is logical because the increase of θ in poor solvents is due to the increasing fraction of the loops of the adsorbed chains. The loops locate in the inner part of the adsorbed layers and thus do not affect the thickness significantly.

The value of χ_s did not significantly affect δ_h value for $\chi_s \geq 0.3$.[8a] The weak dependence of δ_h upon χ_s is experimentally confirmed by van der Beek[31], who found a similar value for δ_h (at saturation) of PEO on different silica surfaces and Millipore filters (made from cellulose esters[32]) from water. This could be very important for future experiments in that δ_h measured on model colloid systems such as monodisperse SiO_2 could be used to provide accurate estimates of δ_h on polydisperse ceramic particles typically used in processing.

The adsorbed thickness is strongly dependent upon the chain length. At dilute and semi-dilute solutions, the tail fraction does not change appreciably with ϕ^*, as seen in Figure 4.5. The increase of the δ_h is mainly attributed to the increase of molecular weight.

In addition, the δ_h is not a function of concentration as $\phi^* \leq 10^{-3}$. In this regime, the tail fraction is primarily constant, as seen in Figure 4.2b. However, in the higher concentration range of $10^{-3} \leq \phi^* \leq 10^{-1}$,[8b] the δ_h abruptly increases due to the increase of tail fraction.[8a]

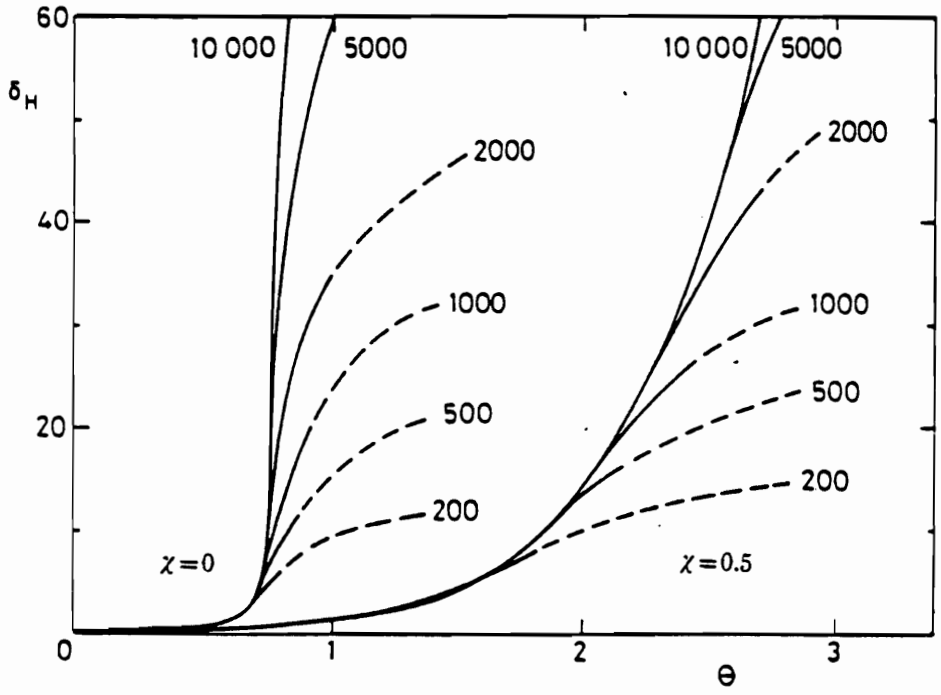

Figure 4.5 Theoretical hydrodynamic thickness δ_h as a function of adsorbed amount (θ) for an athermal ($\chi=0$) and a theta-solvent ($\chi=0.5$) at various chain lengths r. $\phi^*=10^{-2}$ and $\chi_s=1$.[8(a)]

EXPERIMENTAL

Materials

Polymers. Poly(ethyl-oxazoline) (PEOX) was synthesized by Professor Riffle[44] in the Department of Chemistry at Virginia Tech using an anionic ring-opening polymerization technique. The linear PEOX chains exhibited a relatively narrow molecular weight distribution (MWD) with the polydispersity indices less than 1.5 for all PEOX, based on gel permeation chromatography (GPC).[33a] PEOX was dried at 55 - 60°C in a vacuum oven for 24 hours prior to use in the adsorption experiment. The weight-average MW values of PEOX, listed in Table 4.1, were measured by static light scattering. PEO and PPO were purchased from the Aldrich Chemical Co. and ARCO, respectively.

Solvents. Water, ethanol, isopropanol and n-butanol were used as solvents. Deionized water from a NanoPure II deionize system was used with a resistance about 17 megohm-cm. 200 proof grade ethanol from Aaper Chemical Co. was used. Isopropanol and n-butanol (both with HPLC grade, Aldrich Chemical Co.) were distilled once for purification. All distilled solvents were stored in flasks sealed with rubber septa.

Adsorbent. Cab-O-Sil silica, grade L-90, supplied by Cabot Co. (Mass.) served as the adsorbent. The nonporous silica had an equivalent spherical diameter of about 0.27μm, and the surface area was reported by the manufacturers to be 100 ± 15 m^2/g. Prior to use, the silica powder was dried in a convection oven at 110 - 115°C for at least 4 hours.

Table 4.1. A summary of MW and χ[b] measured by static light scattering unless otherwise noted.

Polymer	MW kg/mole	Solvent	χ
PEOX(3K)	2.1[f]	water	<0.46[f]
PEOX(17K)	18.5[a]	water	0.46[a]
		isopropanol	0.20
PEOX(20K)	22.3[a]	water	0.48
		ethanol	0.35
		isopropanol	0.21
		n-butanol	0.25
PEOX(30K)	33.2[a]	water	0.48
		ethanol	0.32
		isopropanol	0.19
PEOX(60K)	63.5[a]	water	0.49
		isopropanol	0.40
PEO(2K)	2.0[c]	water	<0.45[d]
PEO(8K)	8.0[c]	water	<0.45[d]
PEO(12K)	12.5	water	0.41
PPO(20K)	19.9[e]	isopropanol	0.36[e]

[a] Water was used as the solvent for the MW measurement.
[b] χ values for PEOX from Chapter 2.
[c] MW was provided by the manufacturer; polydispersity index <1.1.
[d] Based on reference (34).
[e] Polydispersity index <1.2 from Professor Riffle.
[f] MW was measured by SLS from isopropanol, χ is based on PEOX(17K) in water.

Procedures

Solubility and MW. Static light scattering was used to measure the polymer molecular weight and the solubility from the specific solvent. The procedure was described in Chapter 2. The results are again summarized in Table 4.1. In addition, the value of PEOX *dn/dc* in water was measured to be 0.135 ± 0.005 ml/g using an Abbe refractometer at a wavelength of 510 nm at 25°C, as described in Chapter 2. The *dn/dc* value for PPO in isopropanol was 0.110 ml/g.

Adsorption isotherm. Approximately 0.1 g of SiO_2 particle were mixed with a series of PEOX solutions with different concentrations to make solutions of 10 g total. The solutions were rotated end-over-end for 24 hours. The adsorbed suspensions were centrifuged at 2250 g's for 10 minutes using a MARATHON 21K centrifuge. The supernatant was carefully withdrawn and detected by Hitachi U-2000 UV/vis spectrophotometer in the wavelength range 238 - 245 nm, because in this range UV/vis absorbance obeys Beer's law, *i.e.*, absorbance was linearly proportional to the polymer concentration in the entire experimental concentrations (up to $4.0x10^{-3}$ g/g). The spectra exhibited a sharp absorbance peak corresponding to the carbonyl group (C=O) absorbance. A typical absorbance plot is shown in Figure 4.6. The polymer adsorbed amount, Γ (mg/m^2), was calculated from the change of the carbonyl absorbance before and after adsorption, according to:

$$\Gamma = M_a \cdot (1 - I_s/I_0)/A_s \qquad (4.11)$$

where M_a is the added weight of the polymer in the solution, I_0 is the absorbance of the bulk polymer solution, I_s is the absorbance of the supernatant in the same wavelength with the bulk solution and A_s is the total surface area of the adsorbent.

The adsorption of PEOX on SiO_2 from aqueous solutions was also measured as a function of pH by adjusting the pH with NaOH and HCl (Aldrich Chemical Co.). The added concentrations of PEOX in the solutions in these experiments all reached the plateau region at $2x10^{-3}$ g/ml (see Appendix A), from the single component adsorption isotherm. The HCl and NaOH were used without further purification. The pH was measured with an Orion Model SA 720 pH meter.

Competitive Adsorption. The competitive adsorption procedure was similar to that used in the adsorption isotherm experiment. A solution of 10 g containing PEOX mixing with another polymer was added in vials. All PEO and PPO solutions were mixed

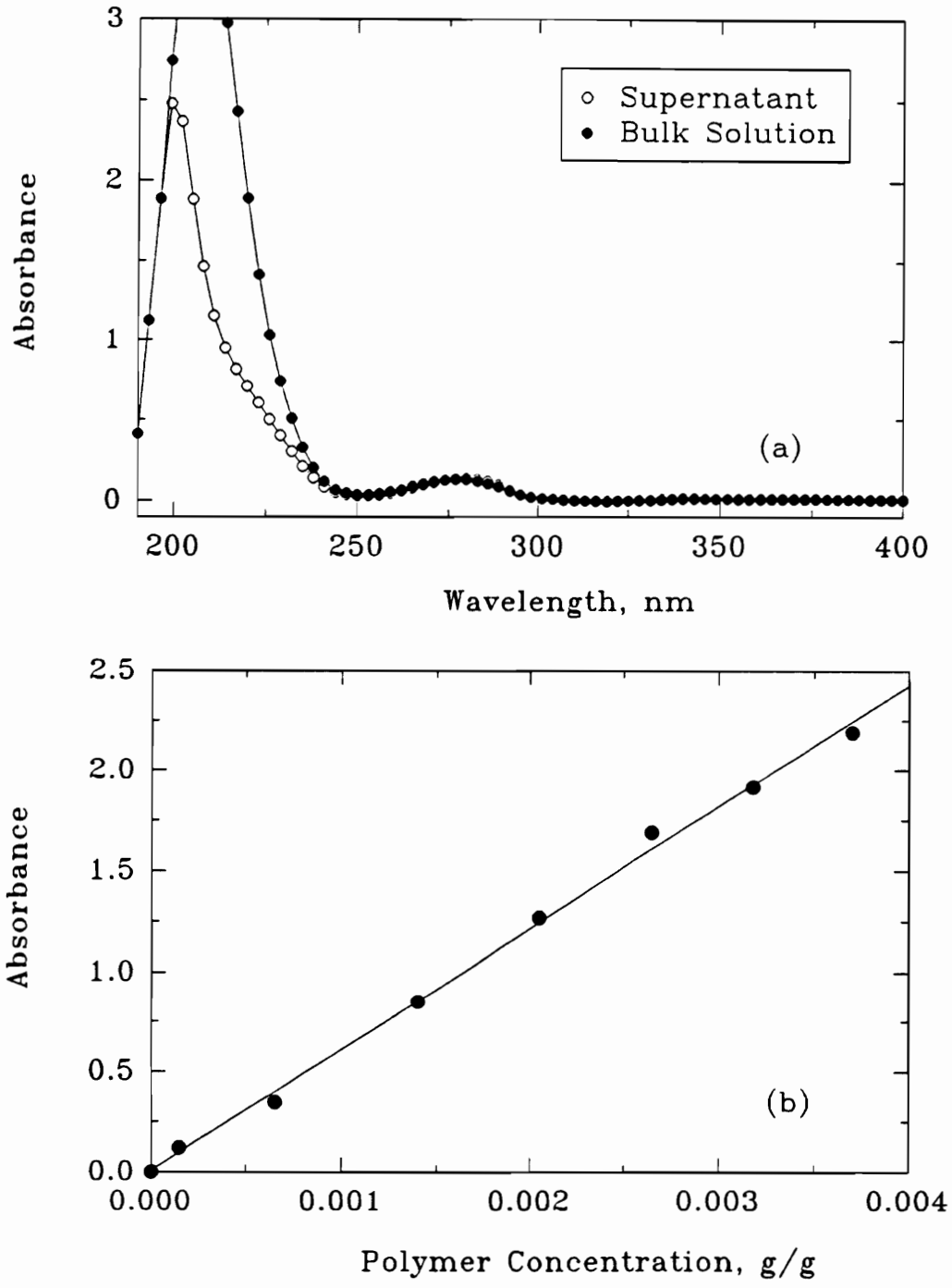

Figure 4.6 (a) Absorbance as a function of wavelength for PEOX solution. The concentration is 9.4×10^{-4} g/g of PEOX 30K in ethanol. (b) The linear relationship of Absorbance vs. polymer concentration at 238 nm.

with PEOX according to a 1:1 weight ratio, unless otherwise noted. The concentration of PEOX in the solution was chosen to be in the adsorption plateau region based on the single component PEOX experiments.

RESULTS AND DISCUSSION

Polymer Solution Properties

The measurements of MW and second virial coefficients of PEOX in water and alcohols were already reported in Chapter 2. Table 4.1 summarizes the Flory-Huggins parameters of polymer used in this chapter. All are cited at 25°C in different solvents.

PEO. Poly(ethylene oxide)(PEO) ($-CH_2CH_2O-$) is one of the most commonly used water-soluble homopolymers. Recent work by Professor Riffle at Virginia Tech suggests it is possible to synthesize PEO-PEOX diblock copolymer with controlled block lengths. Therefore, it is important to understand the relative adsorption affinity of PEOX and PEO for metal oxides in water. It is characterized in this chapter by competitive adsorption experiments. To account for the effects of polymer-solvent interactions, the second virial coefficient of PEO in water was measured by SLS to obtain values of MW and A_2, seen in Figure 4.7. Values of χ are obtained from the second virial coefficient according to the relationship:[30]

$$A_2=(1/2 - \chi)\nu_p^2/V_1 \qquad (4.12)$$

where ν_p is the partial specific volume of PEO ($=0.75$ cm^3/g)[21] and V_1 is the molar volume of the solvent.

PPO. PPO ($-CH_2CH_3CH_2O-$) is another common polyether. It is not soluble in water but is soluble in alcohols. The polymer specific volume (ν_p) used to convert the second virial coefficient to χ value is 0.91 cm^3/g.[24] We studied the competitive adsorption of PPO and PEO with PEOX to learn how polymer structure affects χ_s and to provide

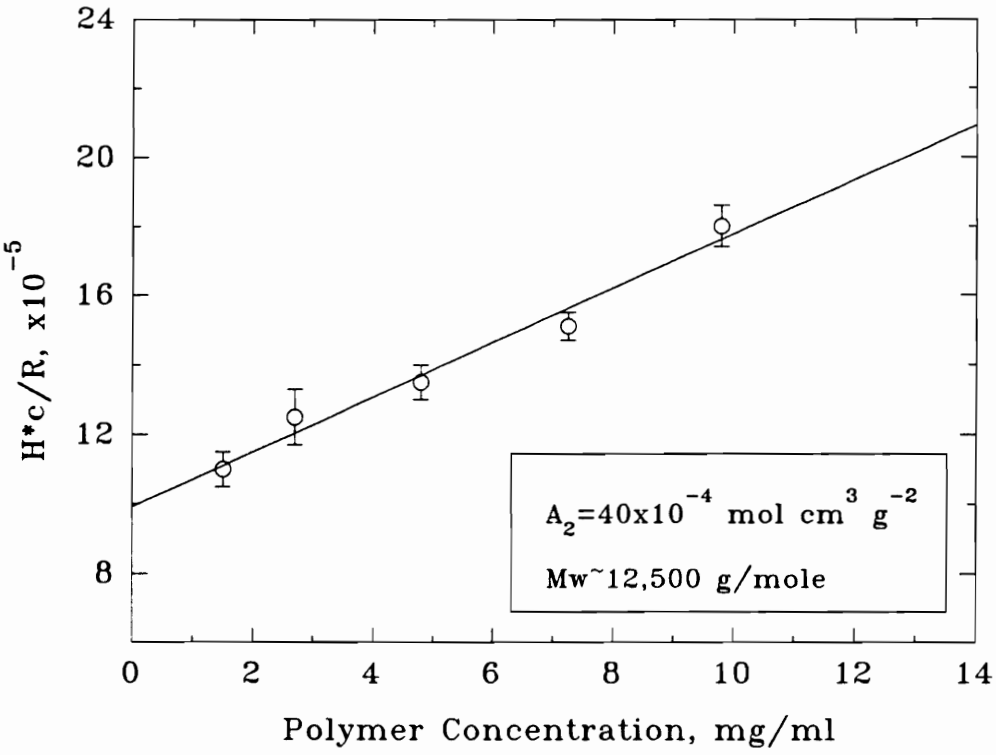

Figure 4.7 The second virial coefficient and M_w measurement of PEO in water at 25°C.

a comparison with poly(vinyl methyl ether) that will be discussed in the next chapter.

Adsorption Studies

Rate of adsorption. General observations indicate that the time to reach an apparent equilibrium adsorption depends markedly on the nature of the adsorbent. Planar surfaces or nonporous particles dispersed in a polymer solution may reach equilibrium adsorption within a few minutes to a few hours while it may take longer for the porous surface if the pore size is sufficiently small.[35] In most cases, polymer samples are polydisperse, *i.e.*, with broad molecular weight distributions. Thus, equilibration of adsorption can involve the displacement of the shorter chains that adsorbed first by longer chains that have a higher net adsorption energy. The time required to reach the equilibrium condition of adsorption depends on the MW of polymer and the solubility of polymer in the particular solvent. According to Cohen Stuart *et al.*,[13] polymers with higher MW and wider molecular weight distribution exhibit a slower adsorption rate due to their lower diffusion coefficients and the replacement time. Therefore, we chose the highest MW available to us, *i.e.*, PEOX 60K, to determine the equilibration time. Also, this polymer showed the widest molecular weight distribution (~ 1.54) from GPC measurement. The measured value of Γ_p on the silica surface in water as a function of time is illustrated in Figure 4.8. The result shows that the amount of adsorption rose rapidly in the first 6 hours, after which a virtually constant amount of adsorption, 0.81 mg/m^2, was reached. On the basis of this result we determined that adsorption equilibrium is essentially established after 6 hours. As the standard for further experiments an adsorption time of at least 24 hours was selected. Similar results were obtained for PEOX adsorption in the different alcohols.

The dependence of Γ_p on Molecular Weight. Figures 4.9(a-c) illustrate several adsorption isotherms of PEOX in water, ethanol, isopropanol and n-butanol, respectively.

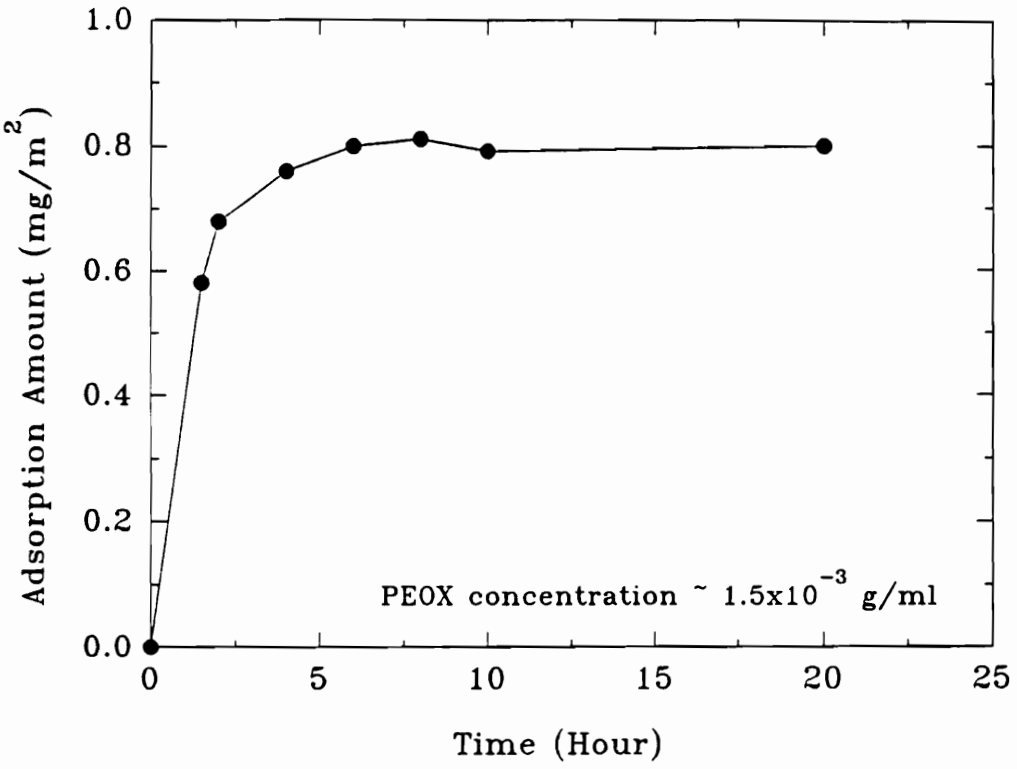

Figure 4.8 PEOX(60K) adsorption isotherm curve as a function of time.

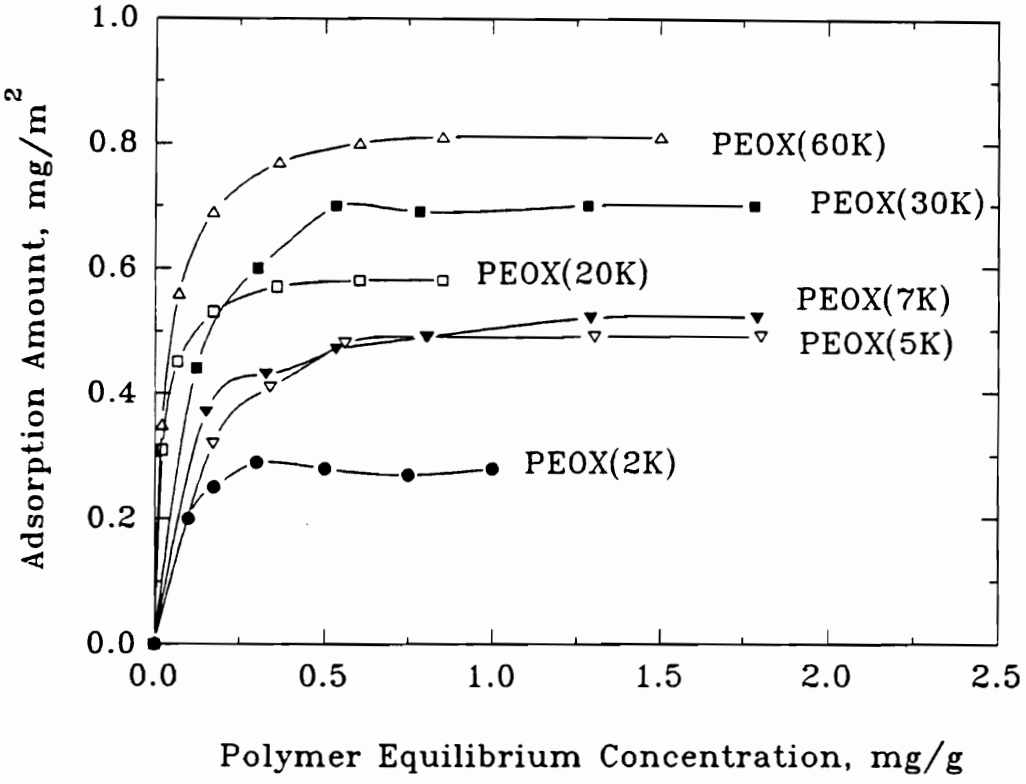

Figure 4.9 (a) PEOX adsorption isotherms from water on Cab-O-Sil silica surface, L-90.

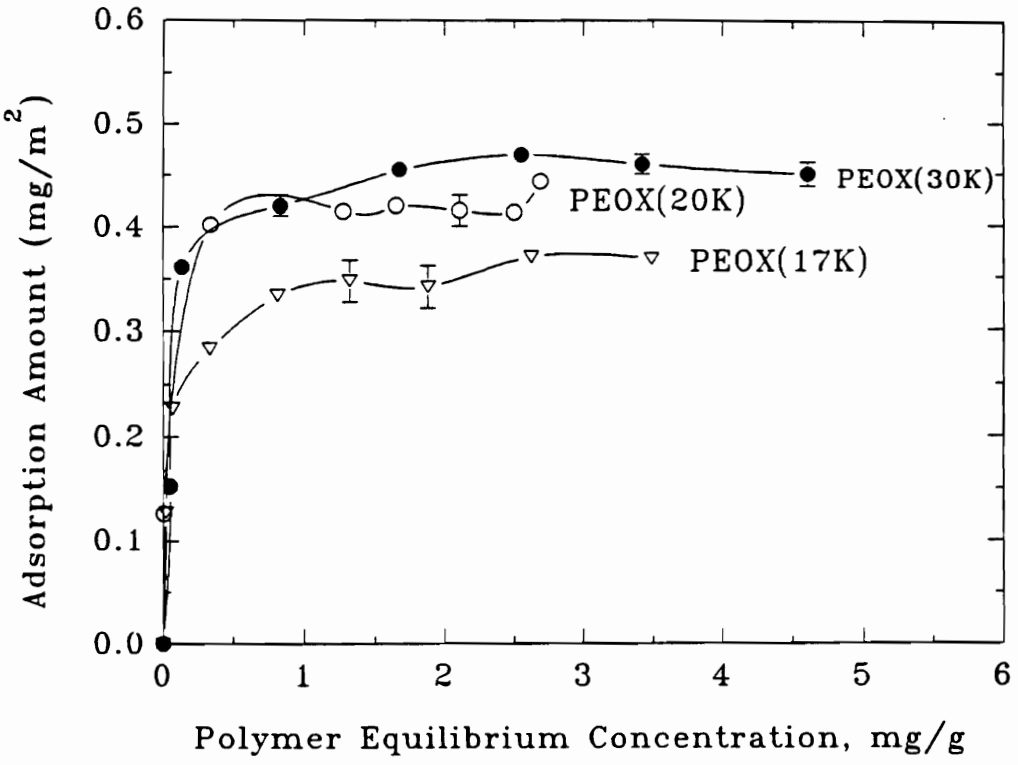

Figure 4.9 (b) PEOX adsorption isotherms from ethanol on Cab-O-Sil silica surface, L-90.

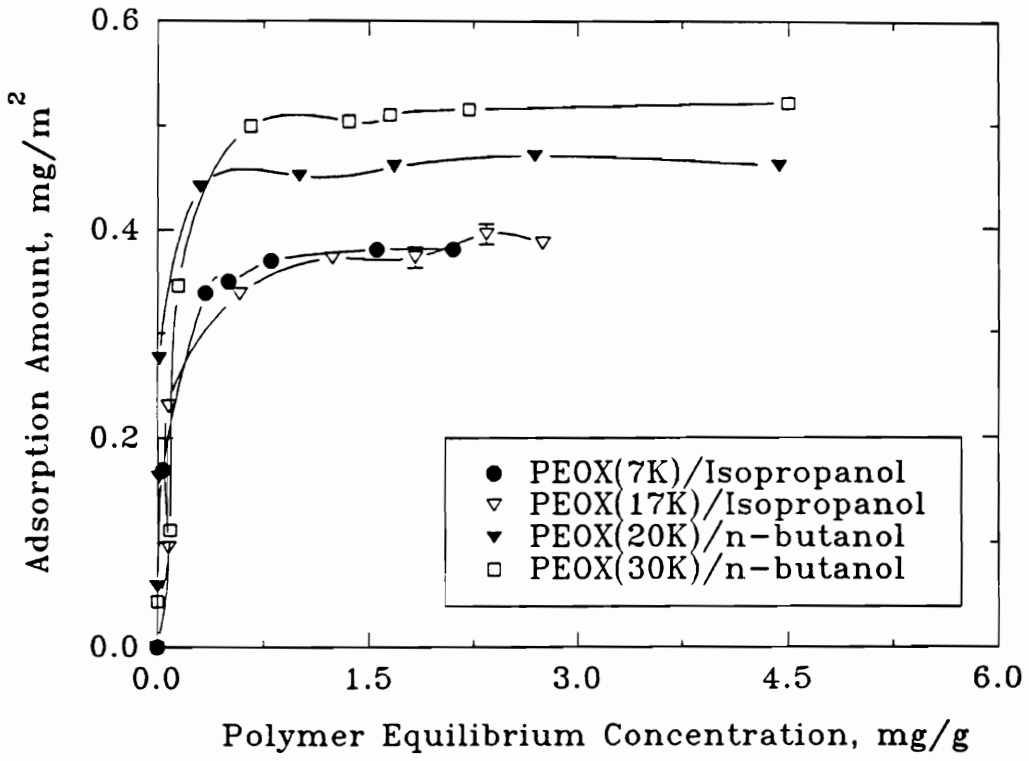

Figure 4.9 (c) PEOX adsorption isotherms from from isopropanol and n-butanol on Cab-O-Sil silica surface, L-90.

All plateau adsorption isotherms are collected in Table 4.3. Values of Γ_p are accurate to $\pm 2\%$. The rapid rise in Γ_p followed by a plateau is consistent with high affinity polymer adsorption behavior. GPC measurements show PEOX to exhibit the polydispersity index in the range of 1.1-1.5 (Chapter 2). The round corner at the turning region near the plateau line is therefore evident. Γ_p is a function of the polymer volume fraction in the solution (ϕ^*), the segment-solvent interaction parameter (χ), the adsorption energy parameter (χ_s), and the degree of polymerization.

Table 4.2 The plateau adsorption amount (Γ_p, mg/m^2) of several PEOX MW from different solvents on Cab-O-Sil silica at 25°C.

PEOX	MW[a] kg/mole	water	ethanol	isopropanol	n-butanol
2K	4.1[b]	0.28			
3K	2.1	0.39			
5K	5.0[c]	0.49	0.28		
7K	7.4[b]	0.52		0.37	
10K	10.0[c]		0.33		
17K	18.5	0.55	0.37	0.37	
20K	22.3	0.58	0.42		0.45
30K	33.2	0.70	0.47		0.50
60K	63.5	0.81			

[a] Water was used as the solvent for the MW light scattering measurement.
[b] MW measurement was done by GPC.
[c] Target MW.

Using an early mean field theory, Hoeve[3] suggested Γ_p in a theta solvent was proportional to $MW^{0.5}$. Scheutjens and Fleer's[8b] lattice theory showed the same result in the limit of high polymer concentration (where $\phi^* \rightarrow 1$, $\theta=\theta_d$), as shown in Equation (4.9b) and Figure 4.3(a). For polymer adsorption at low ϕ^*, a linear relationship of Γ_p against *log* MW was predicted as χ approached 0.5.[4] Also, at the theta condition, Γ_p increased with MW without bound. Our results indeed show a linear relationship of Γ_p

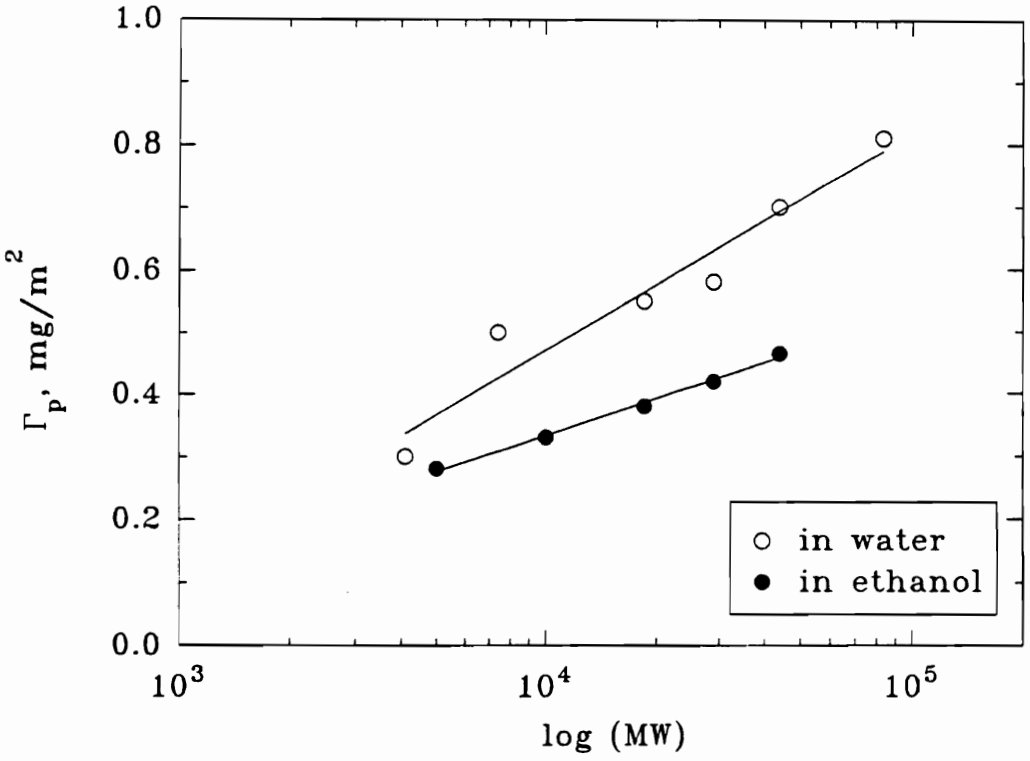

Figure 4.10 A plot of PEOX plateau adsorbed amount against log(Mw) from water and from ethanol on Cab-O-Sil silica surface, L-90.

against *log* MW and are illustrated in Figure 4.10, where $\chi \sim 0.48$ - 0.49 for the PEOX/water solution. A linear relationship of the adsorption of PEOX vs. *log* MW in ethanol, a better solvent (χ=0.32 - 0.35), was also measured. As a result, a lower slope of Γ_p against *log* MW in ethanol is observed. This is fully consistent with the prediction of the S-F theory, *i.e.*, a weaker dependency of polymer adsorption from a better solvent than from a theta solvent.

All PEOX samples displayed a high affinity adsorption isotherm, characterized by a rapid rise followed by a flat plateau. The value of Γ_p always increases with MW. This trend has been observed in many previous studies,[17,27,36] and is attributed to two factors. First, the longer chains possess more possible contacts with the surface, and thus more hydrogen bonding can occur. Second, the Flory-Huggins χ parameter increases with the longer chains. As predicted, poorer solvency leads to an increase in the adsorbed amount.

The Effect of Solvent Type on Γ_p. The slope of Γ_p vs. *log* MW in the S-F theory is a strong function of χ, which is illustrated in Figure 4.2(a). For χ=0, Γ_p is less sensitive to MW.[37] Furthermore, Γ_p increases more gradually at longer chain lengths. Our experimental results agree qualitatively with the S-F theory. The slopes of Γ_p vs. *log* MW of PEOX from water and from ethanol are 0.35 and 0.19, respectively (seen in Figure 4.10). This result shows that the adsorbed amount of PEOX in a better solvent (ethanol) is less affected by the molecular weight than in a poorer solvent (water).

Alcohols are better solvents for PEOX than water according to the second virial coefficient measurements or the corresponding χ values, listed in Table 4.1. Values of Γ_p of PEOX in water are consistently greater than in alcohols. This agrees with the theoretical predictions that better solubility leads to lower Γ_p. This result is accounted for by the decreased dimensions of the polymer chains in a poorer solvent. Consequently, the polymer chain occupies less volume in an aqueous solution. In contrast, the polymer chains in the alcohols expand due to the excluded volume effect leading to greater lateral

interactions in the adsorbed layers. Γ_p is influenced in general by the adsorption energy, $\chi_s kT$, which is positive when the polymer adsorbs preferentially from the solvent. In the previous study of PEOX adsorption on silica in Chapter 3, it was shown that χ_s=5.1 in water and 3.2 in ethanol. The lattice theory predicts that Γ_p increases with χ_s up to χ_s=2 (Figure 4.4).[4] For $\chi_s \geq 2$, Γ_p is relatively insensitive to further increases of χ_s. Consequently, the differences of Γ_p for PEOX in water and the alcohols probably arises mainly from the solvency effects.

Finally, we note that Γ_p of PEOX 60K in water is much lower than in dioxane, shown in figure 4.11. Water and dioxane molecules both can form 2 hydrogen bonds with each segmental unit. Further work needs to be done to measure χ and χ_s of PEOX in dioxane, in order to separate their effects on Γ_p.

pH Effect. The applications of polymer adsorption in the salt and in different pH values are common in the ceramic industry. Therefore, it is of great interest to see how the adsorption of PEOX in water is affected by electrolyte additives. This section concerns the effect of salt concentration and pH values on the adsorption of PEOX 17K.

Figure 4.12 shows the effect of pH on plateau adsorbed amount Γ_p for PEOX 17K. For the majority of the present work we are only interested in the pH range of 2 - 9, where the adsorption on silica is not affected by the dissolution of silica. Above pH 12, dissolution of silica occurs, as reported by Iler.[38] The adsorbed amount of PEOX gradually decreased as pH increased, by a factor of 50% as pH varied from 2.3 to 7. The adsorption vanished as pH>9, consistent with the studies by Blaakmeer *et al.*[9] for the adsorption of PEO and by van der Beek *et al.* for PEO and PVP.[16,40] Blaakmeer attributed this adsorption change to the change of the surface silanol density. The silanol, Si-OH group, is an acidic group. Therefore, increasing pH reduces the surface silanol concentration as shown.

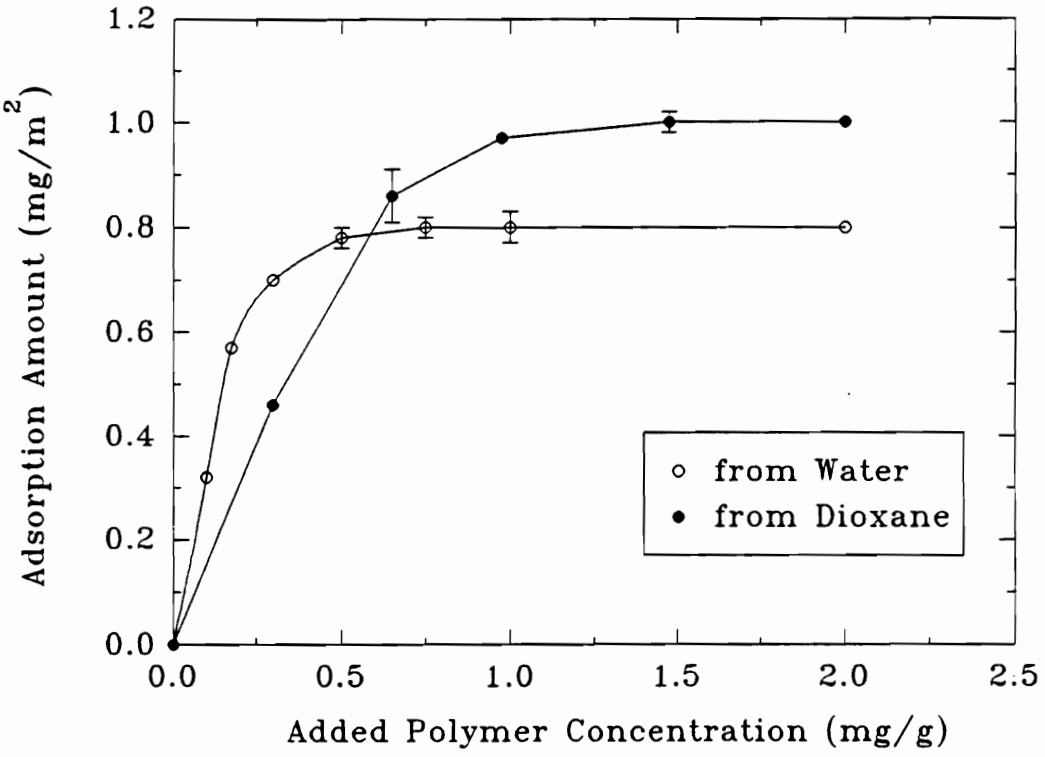

Figure 4.11 The adsorption isotherms of PEOX 60K from water and dioxane on the Cab-O-Sil, L-90, silica surface.

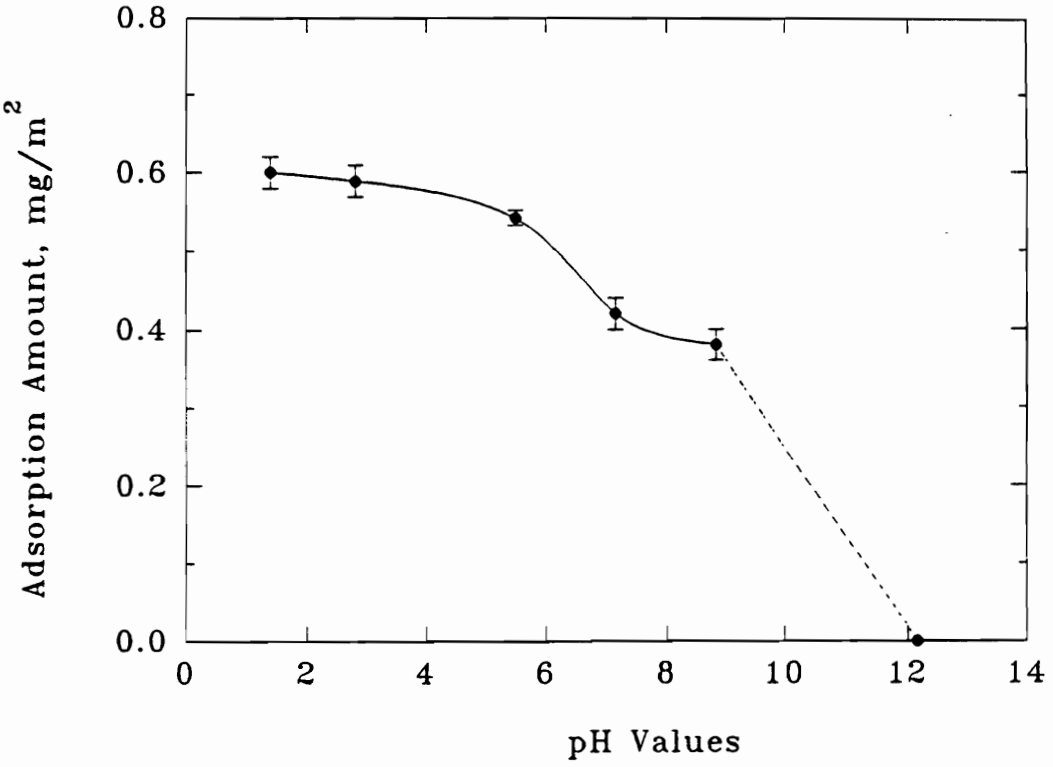

Figure 4.12 The dependence of PEOX 17K adsorption amount upon the pH values from aqueous solution on Cab-O-Sil silica, L-90. PEOX concentration was 3.0×10^{-3} g/g.

$$\equiv SiOH + H_3O^+ \rightleftharpoons \equiv SiOH_2^+ + H_2O \quad (4.15a)$$

$$\equiv SiOH + OH^- \rightleftharpoons \equiv SiO^- + H_2O \quad (4.15b)$$

$$\equiv SiOH + PEOX \rightleftharpoons \equiv SiOH \cdots PEOX \quad (4.15c)$$

By contrast, lowering the pH increases the silanol site density by protonating the Si-O-Si group.[1,16] Joppien[39] reported that the adsorption of PEO (MW=0.4 and 20 kg/mole) on silica dramatically decreased upon increasing pH from 3 to 8. According to Joppien in pH>7, the OH^- ions first adsorbed on existing silanol groups and then dehydrated from the surface (4.15b). Thus, as the silica became progressively more negatively charged with an increase in pH, the adsorption site density decreased. Consequently, the decrease in the adsorbed amount decrease was attributed to the dissociation of the silanol group.

A different view of the effect of pH on the PEO on silica was presented by van der Beek *et al.*[16], who treated the change in Γ_p as a competitive adsorption/desorption process in which ionic species competed with polymer. Polymer desorption may occur by adding components (displacers), such as acids or bases. PEOX can be desorbed from silica at high pH, and so the OH^- anion may be regarded as a displacer. In addition, the effect of pH on polymer solubility could be important as noted earlier. We measured A_2 values for PEOX 17K at pH=2.43 in aqueous solutions (see Table 4.3). We found the solubility dramatically decreased to χ=0.62 for pH=2.43. This reduced solubility increased the adsorption of PEOX on the silica. Therefore, the change in Γ with pH was due to changes in the solubility of PEOX and to changes in the silanol site density.

Table 4.3 The second virial coefficients A_2 and the χ parameters of PEOX 17K in aqueous solutions as a function of pH and NaCl concentration.

Polymer/Solution	A_2 ($x10^{-4}$)[a] cm^3 mole/g^2	χ
PEOX/water	21±3.0	0.46
PEOX/0.22M NaCl	11±3.0	0.47
PEOX/water (pH=2.43)	-60±2.0	0.62

[a] dn/dc=0.174 ml/g for PEOX/water; dn/dc=0.166 ml/g for PEOX/NaCl solution, dn/dc =0.172 ml/g for PEOX/water (pH=2.43), specific volume of PEOX used is 0.87 cm^3/g.

Salt Effect. The adsorption of PEOX 17K from water was measured as a function of NaCl concentration while keeping the bulk concentration of added polymer fixed in the plateau region. The value of Γ increased by 4.1% as NaCl concentration increased from zero to 0.22 M, as demonstrated in Figure 4.13. This increase was well outside of the error bounds of ±2%.

Previous studies have shown that Γ_p for several non-ionic polymers increased with electrolyte concentration at a fixed pH.[15,32,39] The studies generally attributed this increase to two factors: the ionic screening of the partial (local) charge on the C=O group and on the silanol site by the electrolytes, and the decrease of solubility of the polymer. According to Joppien[39], more silanol groups (SiOH) are generated in the presence of NaCl in aqueous solution at pH < 10 because more siloxane groups (Si-O-Si) are broken and protonated. This is due to the screening action of the electrolyte near the SiO^- surface sites. Increasing the silanol group density, as shown in Equation (4.15c), thus results in more PEOX adsorption amount in electrolyte solution is reasonable. The second and more commonly cited reason is that polymer solubility often decreases with increasing electrolyte concentration, which was shown by Einarson *et al.* to be the case for PEO in aqueous electrolyte solutions.[15] This explanation is consistent with the fact that the addition of a non-solvent can decrease the solubility of polymer in solution, as

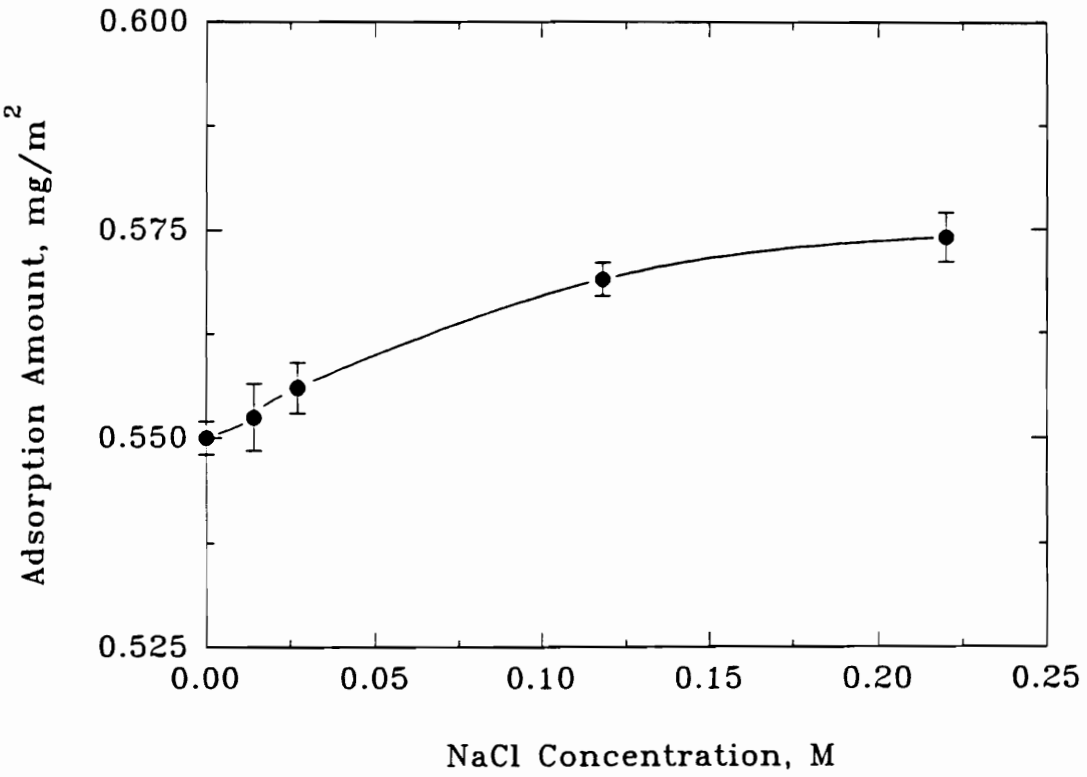

Figure 4.13 The effect of salt (NaCl) concentration to the adsorbed amount of PEOX 17K from water on silica surface, L-90.

noted earlier by Napper[1]. Similar results were reported by Barker and Garvey.[14] In their work on the adsorption of hydrolyzed poly(vinyl alcohol) (PVA) onto polystyrene latex, the sulfate ion SO_4^- lowered the solubility of the polymer. The PVA adsorption amount increased with the sulfate concentration. The thickness of the adsorbed polymer (PVA) layer remained constant, indicating an increased segment density in the adsorbed film. Partyka *et al.*[36] also found the adsorption of surfactants containing ethyl oxide (EO-) on silica increased with NaCl concentration. The salt dependence thus appears to be quite general for nonionic EO- containing systems and not limited to polymers.

The solubility of PEOX 17K was measured at 0.22M NaCl concentration by static light scattering. The values of A_2, shown in Table 4.3, show that the PEOX solubility indeed decreases slightly with increasing NaCl concentration. Thus, the decreasing solubility of PEOX in NaCl solutions accounts for at least part of the increase in PEOX adsorption. Moreover, the added ionic species did not hinder the polymer adsorption since the polymer adsorbed amount did not decrease in the presence of salt in the solution. Therefore, the electrolytes did not act as displacers in our study.

Competitive Adsorption. The adsorption of PEOX from a variety of solvents has been discussed in the previous sections. Another topic which is extremely important for the colloidal scientist is the competitive adsorption between different polymers. Competitive adsorption experiments for binary polymer mixture must be done from a solvent in which both polymers are soluble. PEOX is soluble in all of the solvents studied here while PEO is only soluble in water and PPO is soluble in ethanol and isopropanol. The results of the competitive adsorption for PEOX and these polymers are summarized in Table 4.4. In Table 4.4, the concentrations of added PEOX were all chosen to reach the plateau region based on the earlier adsorption isotherm experiments. The adsorbed amount of PEOX was not significantly affected by the presence of PEO and PPO and all the differences are within the experimental errors. Only for MW ~ 2.1 kg/mole was the PEOX adsorption amount changed slightly by the presence of PEO.

Figure 4.4 A summary of PEOX plateau adsorbed amount and the adsorbed amount of PEOX mixing with other polymers from different solvents. The added weight ratio is 1:1 unless noted.

Polymers	$\frac{DP_{PEOX}}{DP_{polymer}}$	$\frac{\chi_{PEOX}}{\chi_{polymer}}$	$\frac{\text{mole PEOX chains}}{\text{mole other chains}}$	Solvent	Γ_p mg/m^2	Γ_{mix} mg/m^2
PEOX(7K)/PEO(8K)	71[e]/182[g]	<0.46[a]/0.45[b]	2.6	water	0.52	0.50
PEOX(2K)/PEO(2K)	21[f]/46[g]	<0.46[a]/0.45[b]	2.2	water	0.28	0.24
PEOX(20K)/PEO(12K)	225 /284[b]	0.48 /0.41	1.3[d]	water	0.58	0.58
PEOX(20K)/PPO(20K)	225 /326	0.33 /NA[c]	1.5	ethanol	0.42	0.43
PEOX(20K)/PPO(20K)	225 /326	0.20 /0.36	1.5	isopropanol	0.42	0.40

a Based on PEOX(17K)/water SLS measurements.
b Based on PEO(12K)/water SLS measurements.
c Not measured, but it is reminded that χ=0.40 of PVME(16K) in ethanol.
d Different molar ratio of PEOX/PEO have been made, shown in Figure 4.15.
e MW is based on the GPC measurement.
f MW is based on the target MW.
g MW is based on the manufacturer.

This competitive adsorption is of interest as we compare the results with the parameters, χ and χ_s, summarized in Figure 4.14. In a previous section, it was noted that the adsorption amount decreased with χ, *i.e.* increasing solubility. However, the combination of Table 4.3 and Figure 4.14 show that PEOX displaces PEO and PPO in ethanol and isopropanol, even though PEOX had roughly the same or low χ values than these polymers in these solvents. This suggests that competitive adsorption of PEOX was dominated by the adsorption energy parameter χ_s. It is logical to conclude that PEOX has a higher χ_s value than PEO in water and higher than PPO in alcohols.

Some insight into the role of the polymer structure can be obtained from the Hansen solubility parameters[24], which are calculated from the group contribution methods. Table 4.5 shows that the values of the hydrogen bonding parameter δ_h and the dipolar interaction parameter δ_p for PEOX are larger than those for PEO and PPO. This implied that the PEOX segments has higher polarity than the polyether segments. This is consistent with the observation of a stronger affinity of PEOX than PEO and PPO to the polar Si-OH adsorption site.

Table 4.5 The calculated polar (δ_p) and hydrogen bonding (δ_h) parameters of polymer monomers used in this study.

Polymer	repeat unit	$\delta_p(J^{1/2}/cm^{3/2})$	$\delta_h(J^{1/2}/cm^{3/2})$
PEOX	$(C_2H_4NCOC_2H_5)$	12.78	8.97
PEO	(C_2H_4O)	10.2	8.74
PPO	(C_3H_6O)	6.88	7.18

The only exception where PEOX was significantly displaced was for the combination of PEOX(2K) and PEO(2K) where there was a adsorption difference of 16% between PEOX and the polymer mixture from water. This deviation may be due to somewhat similar values of χ_s for PEOX and PEO segments. As stated in equation (4.2),

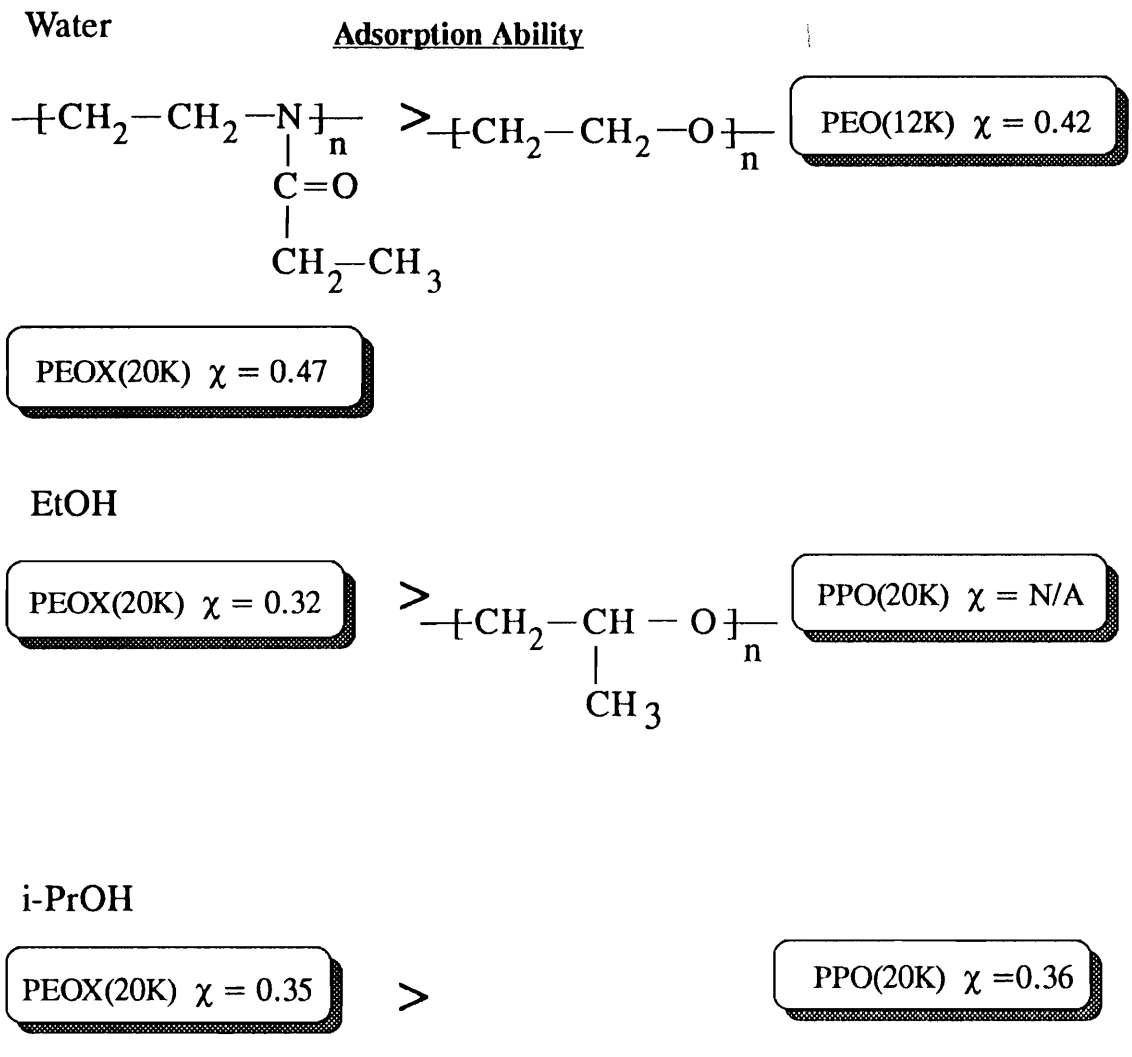

Figure 4.14 A summary of polymer solubilities is listed from different solvents. The PEOX competitive adsorption experiments with other polymers are used in this chapter. All data are based on static light scattering measurements.

the adsorption energy is directly related to the number of the adsorbed train segments n_1 and the segmental energy χ_s. The factor n_1 dominates the adsorption process when χ_s values are similar. In addition, the polydispersity effect is typically more significant at low molecular weight polymers. The net adsorption energy of the PEO 2K sample may be higher than PEOX 2K. In particular, PEO has higher segmental chains (degree of polymerization) relative to PEOX at the same molecular weight. Thus, it is not surprising to find out that, at low MW of PEO and PEOX, PEO can partially displace PEOX on silica.

To further demonstrate this, Γ_{mix} of PEOX(3K) was measured as a function of added PEO(12K) concentration, shown in Figure 4.15. Recalling the conclusion of Kawaguchi *et al*,[21] two factors influence the competitive adsorption: one is the fraction of the train segment in the displaced polymer, which is directly related to χ and χ_s parameters, and the other is the relative molecular weight of the adsorbed and displacer polymers, *i.e.* degree of polymerization differences. The decreasing Γ_{mix} of PEOX(3K) indicates that the polymer chain length dominates the net adsorption energy. At equal weight concentration and high MW, the PEOX adsorbed amount is unchanged in the cases of PEOX(7K)/PEO(8K) and PEOX(20K)/PEO(12K) (seen in Figure 4.15). This again suggests that PEOX has a stronger adsorption affinity than PEO at similar MW's in water. This suggests the amide group adsorbs more strongly onto silica than does the ether group (-C-O-C-). Our finding is consistent with a study by van der Beek *et al.*[16], who reported the displacement of PEO from silica surface by organic compounds, DMSO and DMF, while PVP was not displaced under the same conditions. Our results are very useful for the future design of water soluble diblock copolymer stabilizers. PEOX-PEO diblocks may be an effective steric stabilizer if the block lengths are carefully chosen to avoid displacement of the shorter PEOX anchor block by the longer PEO tail block.

It is observed that PEOX adsorption amount on the silica surface is unaffected by the presence of PEO and PPO with comparable molecular weights from several solvents. The current results imply that polyethers (-C-O-C-) do not bind as strongly to the silica

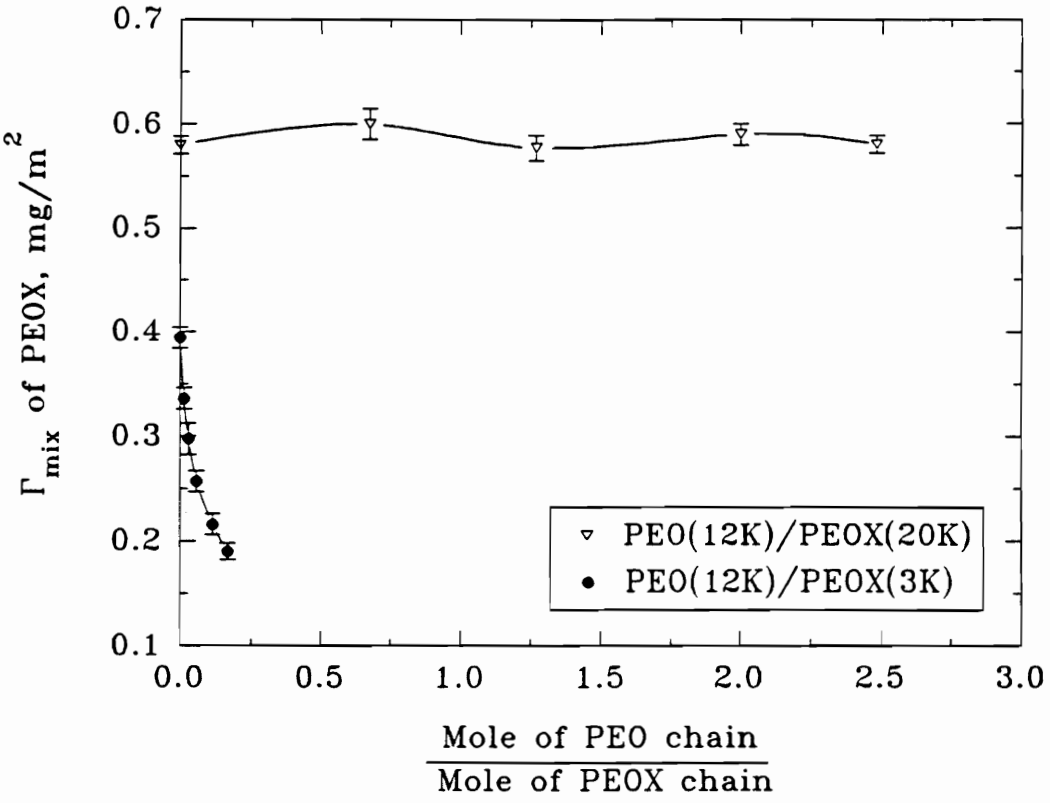

Figure 4.15 The competitive adsorption of PEO(12K)/PEOX(20K) and PEO(12K)/PEO(3K). Both competitive adsorptions were carried out in water.

surface as does the PEOX amide group, but that their χ_s values may be close. This may be proven by further measurement of χ_s for PEO in water by the displacement method.[14] Our experiments illustrate the important role that MW plays when the adsorption energies χ_s kT are similar.

CONCLUSIONS

The adsorption isotherms of a non-ionic polymer, poly(2-ethyl-2-oxazoline) (PEOX), at a hydrophilic silica surface were studied in water and various alcohols. High affinity isotherms were observed in every case. The polymer adsorbed amount increased with the molecular weight in a linear relationship of Γ_p versus *log* MW which agrees qualitatively with Scheutjens-Fleer lattice theory. The differences in the adsorbed amounts at the isotherm plateau, Γ_p, for PEOX in water and alcohols can be attributed primarily to solubility effects at least for water and ethanol given the high values of χ_s for those two solvents, 5.2 and 3.1 respectively. For the PEOX molecular weight equal 63.2 kg/mole, the adsorption process took at least 6 hours to reach equilibrium. Added ionic species probably did not affect PEOX adsorption by acting as displacers since, in the case of added NaCl, this would have resulted in a decrease of adsorption with increasing NaCl concentration. The opposite trend was seen, consistent with the decrease in solubility of PEOX. Increasing pH from 2.4 - 9 lead to a decrease in PEOX adsorption due to a decrease in silanol site density and due to an increase in PEOX solubility.

Competitive adsorption shows that PEOX exhibits a higher adsorption affinity for silica than either PEO or PPO. The χ_s parameter appears to dominate the competitive adsorption. This suggests that the amide group in PEOX has a higher value of χ_s for silica than do the polyethers in this study.

Appendix A. The added PEOX concentrations ($x10^{-3}$, g/g) which reached the plateau adsorption from different solvents.

Polymer	Solvent			
	water	ethanol	isopropanol	n-butanol
2K	0.3			
5K	0.75	1.5		0.80
7K	1.0		1.0	
17K	1.25	2.0	1.5	
20K	0.5	1.2		1.0
30K	0.5	2.0		1.4
60K	0.75			

REFERENCES

(1) Napper, D. H., *Polymeric Stabilization of Colloidal Dispersions*; Academic Press: New York, 1983.

(2) (a) Hunter, R.J., *"Foundations of Colloid Surface"*, Oxford Press, New York, 1989. (b) Israelachvili, J.N., *"Intermolecular and Surface Forces"*, Academic Press, New York, 1985.

(3) Hoeve, C.A.J.; DiMarzio, E.A.; Peyser, P. *J. Phys. Chem.* **1965**, *42*, 2558; Hoeve, C. A. J., *J. Polym. Sci. part C.* **1970**, *30*, 361; *J. Polym. Sci. part C.* **1971**, *34*, 1.

(4) Scheutjens, J.M.H.M.; Fleer, G.J. *J. Phys. Chem.* **1979**, *83*, 1619; **1980**, *84*, 178.

(5) de Gennes, P.,-G., *'Scaling Concepts in Polymer Physics'*, Cornell University Press, Ithaca, N.Y. 1988.

(6) (a) Van der Schee, H.A.; Lyklema, J., *J. Phys. Chem.* **1984**, *88*, 6661. (b) Papenhuijzen, J.; van der Schee, H.A.; Fleer, G.J., *J. Colloid Interf. Sci.* **1985**, *104*, 540.

(7) Evers, O. A., Scheutjens, J. M. H. M., Fleer, G. J. *Macromolecules*, **1991**, *24*, 5558.

(8) (a) Scheutjens, J.M.H.M. Fleer, G.J., Cohen Stuart, M.A. in *Polymers in Colloid Systems*, Tadros, Th. F. (ed.), 1988. (b) Scheutjens, J.M.H.M., Fleer, G.J., in *The Effect of Polymers on Dispersion Properties*, Tadros, Th. F. (ed.) Academic Press, New York, 1982.

(9) Blaakmeer, J.; Bohmer, M. R.; Cohen Stuart, M. A. and Fleer, G. J. *Macromolecules*, **1990**, *23*, 2301.

(10) Howard, G. J.; McConnell, P. *J. Phys. Chem.* **1967**, *71*, 2974.

(11) Perkel, R.; Ullman, R., *J. Polym. Sci.* **1961**, *54*, 127.

(12) Dawkins, J.V.; Guest, M.J.; Taylor, G., in *The Effect of Polymers on Dispersion*

Properties, Tadros, Th. F. (ed.) Academic Press, New York, 1982.

(13) Cohen Stuart, M. A.; Fleer, G. J.; Bijsterbosch, B. H. *J. Colloid Interface Sci.* **1982**, *90*, 310.

(14) Barker, M. C., Garvey, M. J., *J. Colloid Interf. Sci.* **1980**, *74*, 331.

(15) Einarson, M. B.; Berg, J. C., *Langmuir* **1992**, *8*, 2611.

(16) van der Beek, G. P.; Cohen Stuart, M. A., *Langmuir* **1991**, *7*, 327.

(17) Furusawa, K.; Yamashita, K.; Konno, K. *J. Colloid Interface Sci.* **1982**, *86*, 35.

(18) Lipatov, Yu. S.; Todosijchuk, T. T.; Chronaya, V. N.; Khramova, T. S., *J. Colloid Interf. Sci.* **1986**, *110*, 1.

(19) Kawaguchi, M.; Itoh, K.; Yamagiwa, S.; Takahashi, A. *Macromolecules* **1989**, *22*, 2204.

(20) Botham, R.; Thies,C. *J. Colloid Interface Sci.* **1973**, *45*, 512.

(21) Kawaguchi, M.; Sakai, A.; Takahashi, A. *Macromolecules* **1986**, *19*, 2952.

(22) Leonhardt, D. C.; Johnson, H. E.; Granick, S. *Macromolecules* **1990**, *23*, 685.

(23) Kawaguchi, M., *Adv. Colloid Interface Sci.* **1990**, *32*, 1.

(24) van Krevelen, D.W., *'Properties of Polymers'* Elsevier, p. 154, 1976.

(25) Silberberg, A., *J. Chem. Phys.* **1968** *48*, 2835.

(26) Thies, C. *J. Phys. Chem.*, **1966**, *70*, 3783.

(27) Schick, M.J. and Harvey, E. N. *J. Polym. Sci.* Part B, **1969**, *7*, 495.

(28) van der Beek, G.P.; Cohen Stuart, M. A. Fleer, G. J., Hofman, J.E. *Macromolecules*, **1990**, *24*, 6600.

(29) Roe, R.J., *J. Chem. Phys.* **1965**, *43*, 1591; **1966**, *44*, 4264.

(30) Flory, P.J., *'Principles of Polymer Chemistry'*, Cornell University, Ithaca, N.Y., 1953.

(31) van der Beek, G., Ph.D. Dissertation, Agricultural University, Wageningen, 1992.

(32) Kawaguchi, M.; Midura, M.; Takahashi, A. *Macromolecules* **1984**, *17*, 2063.

(33) (a) Liu, Q.; Konas, M.; Riffle, J.S. *Macromolecules* **1993**, *26*, 5572. (b) Liu, Q.;

Wilson, G.R.; Davis, R.M.; Riffle, J.S., *Polymers* **1993**, *34*, 3030.

(34) Franks, F. in *Chemistry and Technology of Water-Soluble Polymers*, Finch, C.A. ed., Plenum, New York (1981).

(35) Howard, G.J., in *"Interfacial Phenomena in Apolar Media"*, Chapter 7, Eicke, H.-F.; Parfitt, G.D. (Ed.) Marcel Dekker Inc., New York, 1987.

(36) Partyka, S.; Zaini, S.; Lindheimer, M.; Brun, B., *Colloids Surf.* **1984**, *12*, 225.

(37) Vincent, B. *Adv. Colloid Interf. Sci.* **1974**, *4*, 193.

(38) Iler, R.K. *The Chemistry of Silica*, Wiley, N.Y. 1979.

(39) Joppien, G. R., *J. Phys. Chem.* **1978**, *82*, 2210.

(40) Cohen Stuart, M.A.; Fleer, G.J.; Scheutjens, J.M.H.M., *J. Colloid Interf. Sci.* **1984**, *97*, 515; 526.

CHAPTER 5

The Solubility and Adsorption of PEOX-PVME and PEOX-PDMS in Organic Solvents

ABSTRACT

Solution properties of the homopolymers poly(2-ethyl-2-oxazoline)(PEOX), poly(vinyl methyl ether)(PVME), poly(dimethyl siloxane)(PDMS), and block copolymers PEOX-PDMS (MW=20.0 kg/mole) and PEOX-PVME (MW=17.6 kg/mole) were investigated in isopropanol and chlorobenzene by static and dynamic light scattering (SLS). Adsorption isotherms for these polymers were also measured on two types of silica. Competitive adsorption experiments showed that PEOX had a stronger adsorption affinity for silica in various solvents, including water, isopropanol and chlorobenzene. The micellization of PEOX-PVME from ethanol/water mixture was examined by dynamic light scattering (DLS). The stability of silica particles in chlorobenzene was characterized using DLS as a function of PEOX-PDMS concentration.

INTRODUCTION

During the last decade, extensive efforts have been made to understand the adsorption of copolymers at interfaces and consequent steric stabilization phenomena in colloidal systems.[1-8] The stabilization of colloidal suspensions is an attractive approach to improve the processability and performance of paints, coatings, inks,[3] and adhesives. According to Napper,[3] non-ionic polymers impart stabilization to dispersions in two ways: the adsorbed polymers can generate repulsive steric force while non-adsorbed polymers at higher concentrations may induce depletion stabilization. Homopolymers form trains, tails, and loops at the solid/liquid interface,[9] whereas the anchor block in

diblock and triblock copolymers can, if properly constituted, mainly form trains, while the solvated block forms tails. In this latter case, the adsorbed layer thickness mainly results from the tail block, which generates the steric repulsive forces.

Homopolymers are not the most efficient steric stabilizers for colloidal systems. Block copolymers are more efficient due to their effective adsorption characteristics resulting from their amphiphilic nature in solutions. Homopolymers strongly adsorbing on a surface can form mostly train fractions with a segment density distribution that decays rapidly away from the surface.[10] This flattened conformation can lead to poor steric stabilization of colloidal particles if the adsorbed layer is not thick enough and the solubility of the layer is sufficiently poor. However, if the polymer-surface interaction energy $\chi_s kT$ is low, the adsorbed layer thickness increases, but the polymer chain does not anchor to the surface well. The χ_s represents the adsorption energy between polymer and surface in the presence of solvent, as defined in Chapter 3. If the particle surfaces are not fully covered, destabilization can occur due to bridging of homopolymers between particles. Thus, an effective polymeric stabilizer requires: 1) high surface coverage; 2) efficient anchoring: the segmental adsorption energy parameter χ_s of trains $> \chi_{sc}$, a critical value of χ_s, beyond which the adsorption may occur; for block copolymers, the adsorption affinity of anchor block is stronger than the tail block, 3) "good" solvency for the tail (loop) segments, $\chi < 0.5$. Again, conditions 2) & 3) are not simultaneously satisfied by homopolymers.[3] Hence copolymers, such as block or graft copolymers, were devised to serve as stabilizers.

Several early reviews of polymer stabilization are available[4-6]. All studies show that polymer adsorption at the consequent stabilization effects are related to several parameters, such as adsorbed amount (Γ_p), adsorbed layer thickness (δ_h)[11], segment density distribution on the surface,[12] and solubility of adsorbed chains.

Recent theories[8,13-16] related to the studies of the adsorbed diblock copolymer at solid/liquid interfaces can be classified into two major groups - scaling concepts[8,16] and mean field lattice theory.[13,15] Both theories agree that the interaction between polymer-

covered particles is related to the adsorbed polymer layer thickness which depended on the polymer composition, polymer solubility (χ), and adsorbed layer affinity (χ_s).[47] Scaling models[8,14,16] focus on the dependence of the layer thickness and the adsorbed amount upon the chain composition and block solubility (see Chapter 6). However, scaling theory provides the functional dependences but does not provide numerical parameters. The self-consistent-field (SCF) copolymer adsorption theory[13,15], which is an extension of the homopolymer adsorption theory by Scheutjens and Fleer[17], accounts for all possible equilibrium copolymer conformations on the surface and particularly focuses on the segmental density distributions of the adsorbed layer. This theory provides functional dependences and numerical factors but is only qualitatively correct. The S-F adsorption theory for homopolymer has been introduced in Chapter 4. At present, no adsorption theories provide quantitative accurate predictions.

Several novel techniques[18] have been developed to characterize the adsorption behavior of copolymers, including photon correlation spectrometry (PCS),[14c] internal reflection interferometry[18a,b] and ellipsometry[18c]. The determination of the anchor or tail block of an adsorbed diblock copolymer can be achieved by the competitive adsorption between the homopolymers.[19] With regard to the copolymer adsorption, general conclusions showed that the adsorbed chain conformation of diblock copolymers was mainly dominated by the solubility of blocks in the solution and the relative affinity of the blocks. Thus, the compositional and sequential variations were important only near the critical adsorption conditions, such as low adsorption energy or solubility limit.[19]

Effect of Block Solubility on Stabilization

Several studies[20,21] demonstrate that the polymer solubility and the steric stabilization effect are closely related. For example, the adsorption of diblock and random copolymers of poly(styrene-methyl methacrylate) (PS-PMMA) on silica from mixtures of carbon tetrachloride and n-heptane and stabilization effect (using volume sedimentation) were investigated by Guthrie and Howard[20]. Both block and random

copolymers showed better stabilization effects than the homopolymer PMMA which had similar molecular weight to the copolymers. The n-heptane is a non-solvent for both blocks. The solubility of the polymers decreases with increasing n-heptane, which is characterized by cloud point titration. In the mixtures of solvents, PMMA reached phase separation at lower heptane concentration than PS, which implies better solubility of PS than PMMA. It is also found that the phased separation of the block copolymers occur at higher n-heptane concentration than the random copolymers and homopolymers. It is found that the silica stability also decreases with increasing n-heptane concentration. The random-type copolymers did not stabilize the silica in a sub-θ condition of PMMA. However, the diblock copolymer still maintained the stabilization ability in the worse than θ-condition of PMMA. The suspension stabilized by diblock copolymer was attributed to the strong adsorption of the anchor block from a micellar solution relative to the random copolymers.

Effect of Block Structure on Adsorption

The adsorbed layer conformation of a diblock copolymer is important for the stabilization effect. The adsorbed amount of diblock copolymers PEO-PS and PDMS-PS on silica from trichloroethylene was studied by Dawkins *et al.*[22]. The PS-PDMS plateau adsorbed amount ($\Gamma_{p,co}$) lay between those of the homopolymers PS ($\Gamma_{p,PS}$) and PDMS ($\Gamma_{p,PDMS}$), both having equivalent molecular weight with the copolymers. This intermdeium adsorbed amount was attributed to both blocks competing on adsorbing the surface. In contrast, the $\Gamma_{p,co}$ of PEO-PS was higher than the Γ_p of PEO and PS homopolymers, both also having the same MW as the copolymers. Dawkins *et al.* concluded that the adsorbed amount of copolymer (PEO-PS) exceeded that of the homopolymers (PS and PEO) due to the formation of an anchor/tail formation, in which the tail block completely protruded into the solution. A more well-defined brush layer is expected for the PEO-PS system compared to the PDMS-PS system. Previously, the displacement adsorption of PS by PEO done by Guest[23a] suggested that PEO had a

stronger adsorption affinity for silica than the other polymers and thus could serve as the anchor block. According to the different adsorbed layer conformation, Dawkins *et al.* predicted that PEO-PS block copolymers should be more suitable than PS-PDMS to stabilize silica dispersions, because PEO can strongly adsorb onto silica surface leaving PS to act as the soluble tail block.

Leermakers *et al.*[13] investigated the kinetics of adsorption of highly asymmetric PEO-PS block copolymer ($DP_{PS}/DP_{PEO} \sim 10$ and 40) on glass from cyclopentane using dynamic scanning angle reflectometry. In the dilute regime, both segments adsorbed on the surface whereas, at higher concentrations, only PEO adsorbed on the surface and PS protruded into solution to act as a brush (tail) layer.

In summary, the use of diblock copolymers[21,22,24] as stabilizers has shown feasible of stabilizing the ceramic powder suspensions for several years. As mentioned, the stabilization of suspensions by polymers significantly depended on the solubility and conformation of the polymer. The characterization of the solubility of the tail block is of importance. The adsorption behavior of a copolymer on the surface can be determined by the competitive adsorption of the homopolymers in the specific solvent. The following sections will briefly introduce the chapter outline and the S-F copolymer adsorption theory.

CHAPTER OUTLINE

This work focuses on the measurements of the solubility and the adsorption of copolymers PEOX-PVME and PEOX-PDMS on silica particles from two organic solvents, isopropanol and chlorobenzene. It is found that chlorobenzene is a good solvent for PDMS but a poor solvent for PEOX, as determined by static light scattering. It is shown that PEOX preferentially adsorbs over PDMS on silica from both isopropanol and chlorobenzene. In addition, the micellization of PEOX-PVME from ethanol/water

mixture was examined by dynamic light scattering. The steric stabilization of near-monodisperse silica by PEOX-PDMS from chlorobenzene was also characterized by measurements of the time rate of change of the particle hydrodynamic diameter.

THEORETICAL BACKGROUND

Copolymer Adsorption Theory

Copolymer adsorption theories can be divided into two principal groups - the mean-field lattice adsorption theory[15] and the scaling models.[8,16] In this chapter, we are mainly concerned with the S-F lattice model predictions of adsorption, and how it is affected by chain composition, surface affinity, and solvency. The scaling model will be introduced in the next chapter.

The statistical S-F copolymer adsorption theory is an extension of the S-F homopolymer adsorption lattice theory,[7] in which all possible adsorbed chain configurations on and near a surface are taken into account and described in terms of chain segment's positions in a lattice. This theory assumes that all lattices are occupied by a segment or a solvent molecule, and all the occupied types have the same volume. A detailed description of the S-F model has been described elsewhere.[15] Thus, we will briefly discuss some details of the model and its principal predictions.

Let $\{\phi_i^f(z)\}$ be the volume fraction profile of polymer chain molecules i in the bulk, *i.e.* the molecules of type *i* which are not in contact with the surface. A segment occupying a lattice site has z nearest neighbors, a fraction λ_0 found in the same layer, and a fraction λ_1 in each of the adjacent layers (in Figure 5.1). The volume fraction profile of adsorbed chains $\{\phi_i^a(z)\}$ is equal to $\{\phi_i(z)-\phi_i^f(z)\}$.[15a] The adsorbed amount θ_i^a (expressed as the equivalent monolayer) is defined as the sum of ϕ_i^a over all layers z, thus:

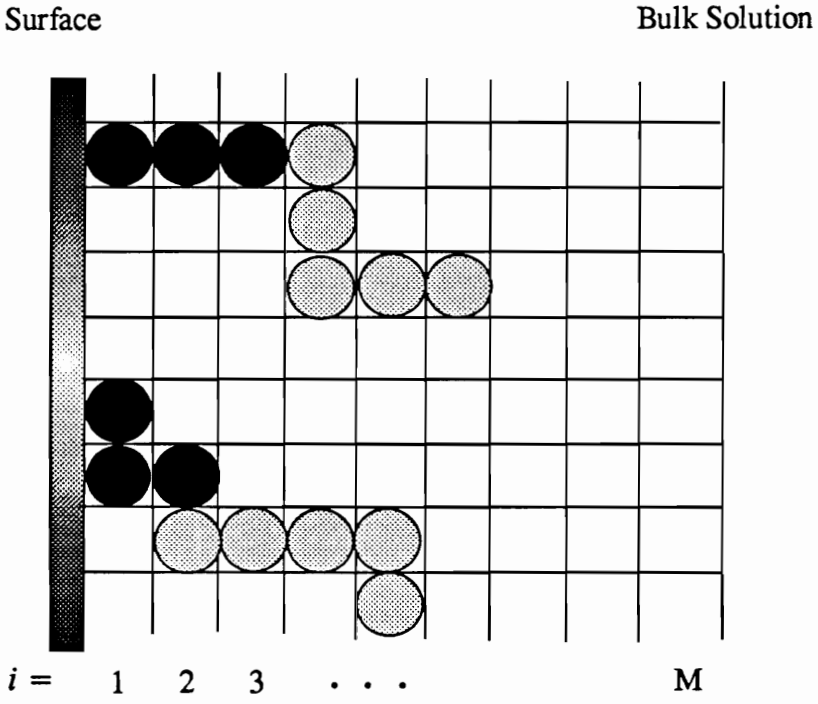

Figure 5.1 Two adsorbed A_3 B_5 diblock copolymer chains adsorbed in a lattice. i =1 when polymer contacts with the surface, i =M represents the bulk solution.

$$\theta_i^a = \sum_{z=1}^{M} [\phi_i(z) - \phi_i^f] \qquad (5.1a)$$

where $z=1$ is the surface layer. The adsorbed amount θ_i^a in number of equivalent *monolayers* per area of the adsorbed polymer can be related to the experimental adsorbed amount according to the expression by

$$\Gamma = \frac{\theta_i^a \cdot MW_{segment}}{A_{segment}} \qquad (5.1b)$$

where Γ is the polymer adsorbed amount, in unit of *mass* per area, $MW_{segment}$ and $A_{segment}$ represent the molecular weight of the anchor block monomer and the molecular adsorbed area of the monomer.[25]

The volume fraction, $\phi_i^a(z)$, of the adsorbed chain in the bulk solution *i.e.*, at $z=M$, approaches zero. If $\theta_i^a=1$, one equivalent monolayer is adsorbed. The quantity ϕ_i^a gives the number of segments of adsorbed molecules i per surface site.

Theoretical Predictions

Effect of chain composition. Some of the salient predictions of the theory are presented below. For an AB block copolymer where block A is defined as the anchor block and B is the non-adsorbing block ($\chi_{BS}=0$, no interaction between block B and surface) and stretched into the solution, ν_A and ν_B are the mole fractions of segments A and B in the whole chain, respectively, *i.e.*, $\nu_A+\nu_B=1$. It is predicted that the adsorbed amount of copolymer (θ^a) reaches a maximum value at a certain specific chain length ratio between A and B. The composition ν_A corresponding to this maximum will be referred to as the 'optimal fraction', ν_A^{opt}. In Figure 5.2(a), each curve represents a constant total chain

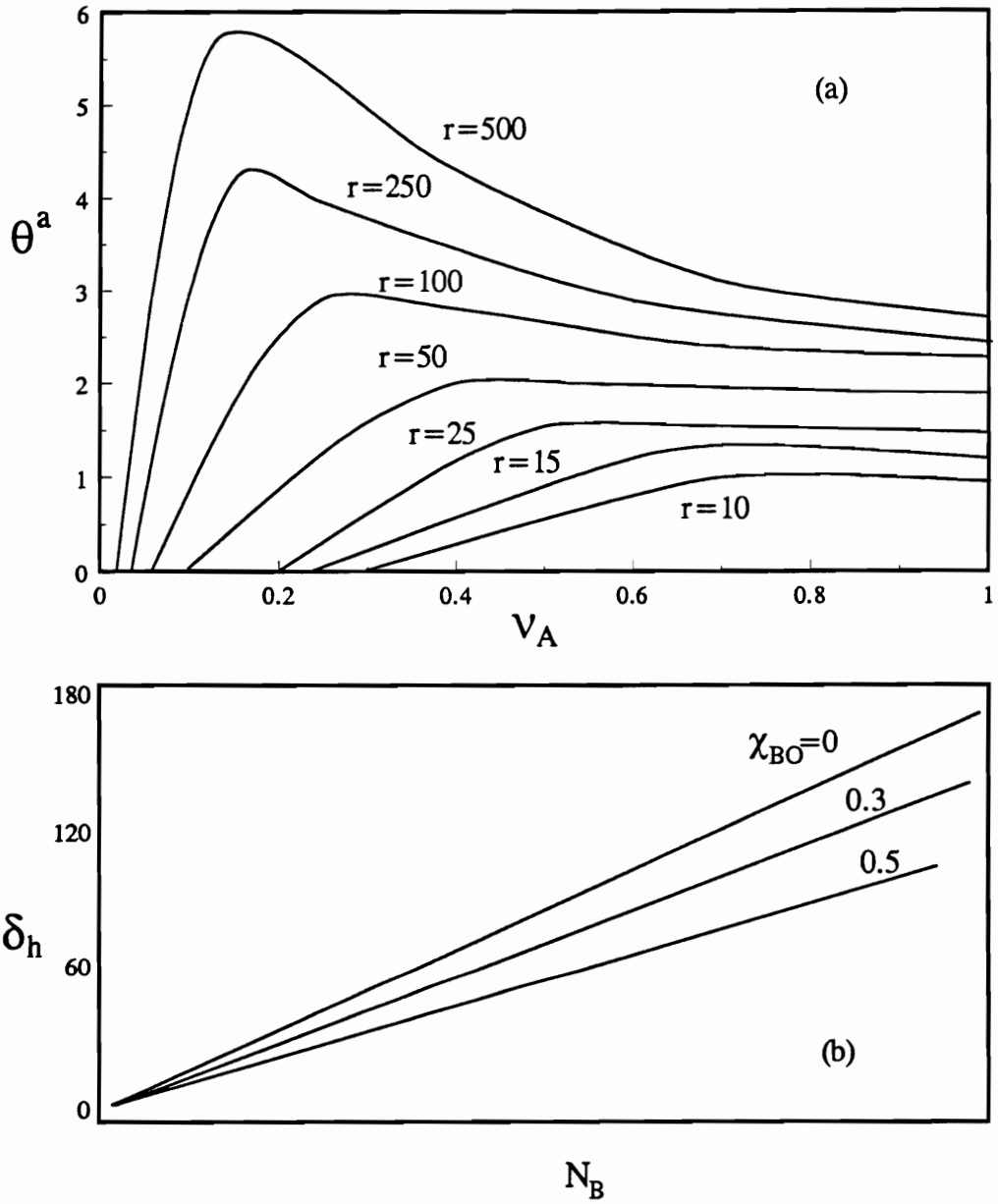

Figure 5.2 (a) Adsorbed amount θ^a (equivalent monolayer) for diblock copolymers against the fraction ν_A of adsorbing A segments. Each curve is for a constant total chain length r (indicated). Parameters: $\phi^*=0.0001$, $\chi_{S,A}=2$, $\chi_{S,B}=0.5$, other χ parameters zero. (b) The hydrodynamic layer thickness as a function of the B block length n at different χ_{BO} values [15].

length (or a constant MW)[15]. At low ν_A, the total adsorbed amount of the polymer is also low because of the small total adsorption energy. As the fraction of A-segments increases, the adsorbed amount correspondingly increases until a maximum adsorbed amount is reached. Beyond ν_A^{opt}, the adsorbed amount gradually decreases because most of the adsorption sites on the surface are occupied by flat A-segments while the B tail blocks become increasingly short. As the adsorbed amount increases, more B block is solvated into solution and the adsorbed conformation changes. When adjacent tail block separation becomes sufficiently small, then repulsive interactions between the blocks lead to chain extension. The S-F lattice theory predicts that the fraction ν_A and adsorbed amount ratio of copolymer and homopolymer, are related by

$$\theta_A^a/\theta_{hA}^a = (1 - \alpha)\nu_A + \alpha \qquad (5.2a)$$

where α is the difference of the segmental adsorption energy of block A and B ($=\lambda_1\cdot(\chi_{BS} - \chi_{AS})$). The term θ_{hA}^a is the adsorbed amount of homopolymer A, which has the same degree of polymerization as the copolymer. At the extreme case for $\nu_A=1$, θ^a ($=\theta_A^a+\theta_B^a$) equals θ_{hA}^a and the ratio θ_A^a/θ_{hA}^a equals unity.

It is useful to rewrite Equation (5.2a) in terms of block length ratio, r_B/r_A. Since $(1-\nu_A)/\nu_A$ ($=\nu_B/\nu_A$) can be replaced by r_B/r_A, Equation (5.2a) then may be written as:

$$\theta^a=\theta_{hA}^a\,(1+\alpha\cdot r_B/r_A). \qquad (5.2b)$$

Equation (5.2b) is valid while the total chain length of the diblock copolymer is longer than 50 and $\nu_A>\nu_A^{opt}$, where ν_A^{opt} is the composition of anchor block at the maximum adsorption. For short chains, the adsorbed amount decreases with decreasing ν_A, because the total adsorption energy per chain becomes too small.

The S-F theory also provides an estimation of ν_A^{opt}, according to the Equation

(5.2a). It is assumed as $\theta_{hA}^{a} \approx 1$, the adsorption of copolymer θ^{a} reached the maximum. Thus, the Equation (5.2a) turns into:

$$\nu_A^{opt} \approx (1/\theta_{hA}^{a} - \alpha)/(1 - \alpha) \qquad (5.3)$$

Equation (5.3) shows an decrease of ν_A^{opt} with increasing adsorption amount of equivalent chain length of homopolymer θ_{hA}^{a}. This estimation is more accurate as the chain is longer than 100, because as r is less than 50, θ^{a} is flat as $\nu_A \geq \nu_A^{opt}$.

Effect of surface affinity. Increasing the surface affinity for the A-segments, *i.e.* increasing χ_{AS}, results in a higher adsorbed amount and a lower optimal fraction ν_A^{opt} since fewer A-segments are necessary to provide sufficient anchoring. At low surface affinity the optimal fraction ν_A^{opt} is almost equal to one. Thus, there is a critical value χ_{AS}, above which an adsorption maximum can be found. Below this critical value the adsorbed amount continues to increase, reaching a maximum adsorbed amount at $\nu_A = 1$.

Effect of solubility. According to the S-F theory, $\delta_h \propto r_B$, in a similar way to θ^{a}, is illustrated in equation (5.2b). As the solvent quality decreases (χ value increases), lower δ_h (dimensionless, in terms of lattice size) values are expected because the adsorbed layer is more compressed. The results are illustrated in Figure 5.2(b) which demonstrates also a linear dependence of the layer thickness on the length of the non-adsorbing block, the chain extension effect. This was also found by Alexander-de Gennes scaling theory[8b] to explain the relationship between the anchored chain length and the adsorption of block copolymers.

While the S-F theory can qualitatively describe copolymer adsorption, it does not rigorously take the concentration-induced excluded volume factor into account. Thus, we do not expect the mean-field to quantitatively predict either adsorbed amount or adsorbed layer thickness. Nevertheless, the S-F lattice is consistent with the prediction of scaling

theory.

In conclusion, the adsorbed amount and the hydrodynamic layer thickness of the block copolymers depend strongly on the composition of the copolymer. When the total length of an AB copolymer and its equilibrium volume fraction remain constant, a maximum of adsorbed amount is found as a function of the fraction of adsorbing segments, ν_A. The optimal fraction (ν_A^{opt}) decreases with increasing total chain length, with increasing surface affinity of the more strongly adsorbing block (anchor) and with decreasing surface affinity for the non-adsorbed blocks (tail). In addition, the S-F theory provides a relation between the adsorbed amount of an AB-block copolymer and the adsorbed amount of an A homopolymer of equal length. A linear relationship is predicted between the adsorbed amount of AB-block copolymer and the block-length ratio, r_B/r_A.

Stabilization

Colloidal particles may be stabilized by four mechanisms, electrostatic (*i.e.*, electrical double layer repulsion), steric stabilization (repulsion from solvated adsorbed layers, seen in Figure 5.3), depletion stabilization (at very high polymer concentrations), and by solvation forces due to adsorbed solvent molecules[26].

The original Deryagain-Landau-Verwey-Overbeek (DLVO) theory, developed in the 1940's, only considered the van der Waals and the electrostatic forces between particles. The pairwise interaction potential V_T included two components - V_R the electrostatic repulsion and V_A the van der Waals attraction (in Figure 5.4). The theory has been modified to take repulsive steric forces into account by adding a term $V_s(h)$[30]:

$$V_T(h) = V_A(h) + V_R(h) + V_S(h) \qquad (5.4)$$

The van der Waals forces are typically attractive and have a relatively short range (1-10 nm) in colloidal suspensions while the electrostatic forces have a variable range (1-50

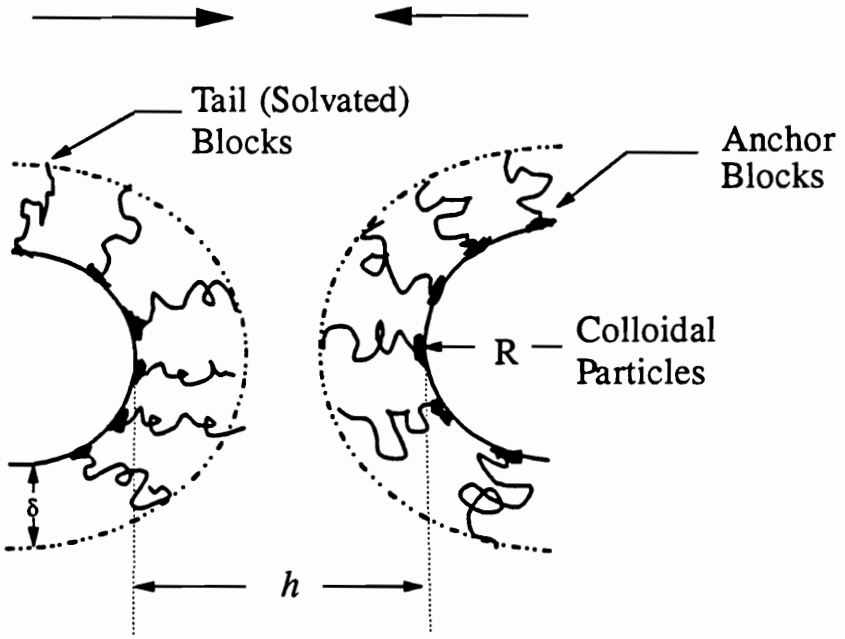

Fig 5.3 Schematically presentative of the steric stabilization effect by adsorbing copolymer chains on the colloidal particle surface, where h is the minimum distance between particle surfaces, R is the radius of the particle. δ is the adsorbed layer thickness.

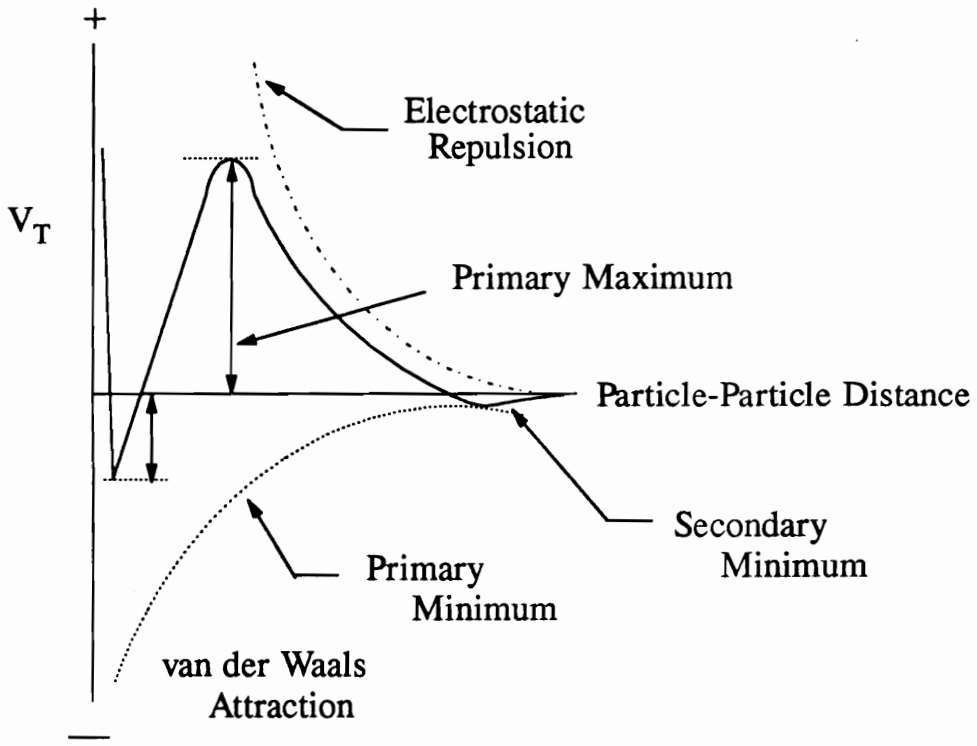

Figure 5.4 Schematic representation of the total potential energy *vs*. distance of separation for a pair of electrostatically stabilized particles. Also shown are the component electrostatic repulsion and van der Waals attraction.

nm) and are repulsive if all particles have the same sign of net charge.

The van der Waals attraction energy between two spherical particles of material (1) in a liquid medium (2) can be expressed in the form:

$$V_A = -\frac{A_{131}}{12}\left[\frac{1}{x^2+2x} + \frac{1}{x^2+2x+1} + 2\ln\left(\frac{x^2+2x}{x^2+2x+1}\right)\right] \qquad (5.5)$$

where $x = h/2 \cdot R$, h is the minimum distance between particle surfaces, R is the particle radius. The quantity 'A_{131}' is the composite Hamaker constant and given by

$$A_{131} = (\sqrt{A_{11}} - \sqrt{A_{33}})^2 \qquad (5.6)$$

where A_{11} and A_{33} are the Hamaker constants of the medium and the solvent, respectively.

The range of the electrostatic forces depends on the thickness of the electrostatic double-layer, κ^{-1}, and is expressed as:

$$\kappa^{-1} = (\varepsilon \cdot kT/2e^2I)^{1/2} \qquad (5.7)$$

where ε = solution dielectric constant and e = electronic charge. The ionic strength I = $\frac{1}{2} \cdot \Sigma n_i(z_i)^2$, where n_i = molarity of ionic species in solution, z_i = valence of ionic species in solution, and the summation is over all the low molecular weight ionic species in solution. V_R is often ignored where the ionic strength of the medium is high or where the dielectric constant of the medium is low such that it will not support ionization.

As for the steric potential, three interaction domains[3,27] are defined as the coated particles approach each other: non-interpenetrational domain ($h > 2\delta_h$), interpenetrational domain ($\delta_h \leq 2h \leq 2\delta_h$) and interpenetrational-plus-compressional domain ($h < \delta_h$). In the range of $h > 2\delta_h$, no steric interaction occurs. The steric interaction[28] between adsorbed

particles in the interpenetrational domain can be expressed as:

$$\frac{V_S}{kT}=4\pi R\frac{\delta^2}{v_1}[f^2(\frac{1}{2}-\chi_1)+1.5\ f^3(\frac{1}{3}-\chi_2)](1-\frac{h}{2\delta})^2 \qquad (5.8)$$

where v_1 is the molecular volume of the solvent, f is the volume fraction of the polymer in the adsorbed layer, χ_2 is the concentration dependence of the Flory-Huggins interaction parameter χ, such that $\chi=\chi_1+\chi_2 \cdot f$. Steric stabilization arises from the sum of osmotic and volume restriction effects. The polymer volume restriction effect arises from the restricted configurations of the polymer chains in the gap between the particles. This results in the loss of configuration entropy. Equation (5.5) describes only the osmotic effect. The contribution of the volume restriction effect, in this domain, is negligible since the volume fraction of the polymer molecules is generally small.

In the interpenetration-plus-compression domain ($h<\delta$), the interaction energy also results from the osmotic and volume restriction effect (V^{El}), according to:[28]

$$V_s/kT = V^M/kT + V^{El}/kT \qquad (5.9)$$

where

$$V^M/kT = 4\pi R(\delta_h^2/v_1)\cdot[f^2\cdot(\tfrac{1}{2}-\chi_1)(h/2\delta_h)(h/2\delta_h - \tfrac{1}{4} - \ln(h/\delta_h)] + f^3/2\cdot(\tfrac{1}{3}-\chi_2)(1+h/2\delta_h+2\delta_h/h - 11/4)] \qquad (5.10a)$$

and

$$V^{El}/kT = 2\pi R\cdot\delta_h^2\cdot(f/v_p)\cdot[h/\delta_h\cdot ln\{h/\delta_h\cdot[(3 - h/\delta_h)/2]^2\cdot\} - 6\ ln[(3-h/\delta_h)/2]+3\cdot(3 - h/\delta_h) \qquad (5.10b)$$

The effect of polymer solubility on steric stabilization is perhaps more clearly seen with the following thermodynamic argument.[1,3,5,29] The theory[29] considered the

overlap range of the steric layers attached to two spheres. Assuming a constant segment distribution density within the steric layer, the steric mixing energy ($\Delta_S G^M$) can be related to the second virial coefficient (A_2) and expressed as [3]:

$$\Delta_S G^M = 2 \int_v RT \cdot A_2 c_2^2 dV \tag{5.11}$$

where V is the overlap volume, and 'c' is the polymer concentration. If the segment density is assumed constant within the steric layer, Equation (5.19) can be converted to:

$$\Delta_S G^M = 2RT \cdot A_2 c_2^2 (\Delta V) \tag{5.12}$$

where the lens shape overlap volume ΔV can be calculated from Equation (5.13):

$$\Delta V = (2\pi/3)(\delta_h - h/2)^2(3a+2\delta_h+h/2) \tag{5.13}$$

where δ_h is the steric layer thickness, h is the minimum distance between the surfaces of the two spheres, and a is the particle radius. The second virial coefficient A_2 can be related to the Flory-Huggins interaction parameter (χ) according to:

$$A_2 = (1/2 - \chi)v_2^2/V_1 \tag{5.14}$$

where v_2 ($=1/\rho$) and V_1 are the polymer specific volume and the molar volume of the solvent, respectively. Thus, the final expression for the $\Delta_S G^M$ can be obtained as:

$$\frac{\Delta_S G^M}{kT} = \left(\frac{4\pi c_2^2}{3V_1\rho_2^2}\right)\left(\frac{1}{2}-\chi\right)\left(\delta_h - \frac{h}{2}\right)^2\left(3a+2\delta_h+\frac{h}{2}\right) \tag{5.15}$$

where ρ_2 is the specific density of polymer. For steric stabilization, $\Delta_S G^M$ must be greater than zero. Thus, steric stabilization requires that the stabilizing chains be in a good solvent, *i.e.*, $\chi < 0.5$.

Kinetics of the Coagulation Process

A theory for the kinetics of coagulation was proposed by von Smoluchowski in 1916.[30b] The initial stage of coagulation is expressed as the disappearance rate of the single particles in the original dispersion:

$$- dN/dt = k \cdot N_0^2 \qquad (5.16)$$

where N_0 is the initial number of particles per unit volume and k is a rate constant. For rapid coagulation (without an energy barrier), the process is diffusion-controlled and $k \equiv k_{smol}$, where k_{smol} is defined by[30]

$$k_{smol} = 8 \cdot kT/3\eta \qquad (5.17)$$

k and T are the Boltzmann's constant and absolute temperature, respectively. If an energy barrier is present,[31] the initial rate of disappearance of the single particles can be written as:

$$- dN/dt = k_{smol} \cdot N_0^2/W \qquad (5.18)$$

where W, is the stability ratio and is related to the total energy V_T by:

$$W = 2R \int_0^{\infty} \frac{\exp(V_T / kT)dh}{(h + 2R)^2} \qquad (5.19)$$

$$= \frac{no.\ of\ collisions}{no.\ of\ collisions\ inducing\ coagulation}$$

where h is the particle separation distance. In the absence of an energy barrier, *i.e.* $V_T=0$; $W=1$. For large V_T, W increases and the rate of coagulation slows down. Generally speaking, the $V_T \sim 25\ kT$ corresponds to a large W of 10^9, the suspension can be stable for several months.[27]

Measurements of the rate of coagulation of particles can be carried out by several ways, including light scattering and particle counting.[32] These techniques give values for the rate constant k_{11}. For the calculation of stability ratio, W, Virden and Berg[32a] proposed an equation by

$$W = k_{smol}/k_{11}. \qquad (5.20)$$

In this technique, the rate constant for doublet formation with the change of the particle radius, at early times, using photon correlation spectroscopy (PCS). The slow coagulation rate constant k_{11} of doublet formation can be calculated from the initial slope of the mean radius change against time by PCS. The expression is written as:

$$k_{11} = \frac{1}{R_{mean,0} \cdot \alpha \cdot N_0} \left(\frac{dR_{mean}}{dt}\right)_{t=0} \qquad (5.21)$$

where $R_{mean,0}$ is the initial mean radius of the particles in the dispersion, R_{mean} is the measured radius, N_0 is the initial particle number concentration, and α is an optical factor

that is a function of initial particle radius, solvent refractive index, and scattering angle. The α can be obtained from a fifth-order polynomial fit at a scattering angle of 90°:[30]

$$\alpha = 0.686+1.545(R/\lambda) - 49.924(R/\lambda)^2+239.07(R/\lambda)^3 - 424.38(R/\lambda)^4+257.104(R/\lambda)^5$$

where λ is the wavelength of light in the air and R ($\sim$35 nm) is the particle radius. In this study α is calculated as 0.63. For the purpose of converting the scattering results to the stability ratio W, the rate constant for fast aggregation can be determined using Smoluchowski's diffusion-limited aggregation model. An important parameter is $t_{1/2}$, the 'half-time', or the time required for the number of particles in the dispersion to be halved, expressed as:

$$t_{1/2} = 2/(k_{smol} \cdot N_0). \qquad (5.22)$$

EXPERIMENTAL

Materials

Polymers. All polymers, including homopolymers and copolymers, were synthesized by Professor Judy S. Riffle's group in the Chemistry Department at Virginia Tech, using ionic living polymerization techniques.[33] Homopolymers were characterized by GPC, which showed that all polymers had polydispersity indices less than 1.50, as described in Chapter 2. To prepare the diblock copolymer PEOX-PDMS, the first step involved the living anionic ring-opening polymerization for making monofunctional PDMS. The PDMS was then terminated with a reactive end-group, benzyl-chloride. Subsequently, PEOX monomers were added for the cationic polymerization with the reactive end-group of PDMS polymer chain, *i.e.*, benzyl chloride acts as an initiator. Then, the copolymers were rigorously extracted with hexane to remove all residual PDMS.[34]

The molecular weight measurements of the monofunctional PDMS were consistent by both low angle laser light scattering (LALLS) in isopropanol and static light scattering

(SLS) in chlorobenzene to be 14.4 kg/mole. The Chromatix KMX-6 LALLS instrument (LDC Analytical Co.) is equipped with 6-7° scattering angle and operated at room temperature. The molecular weight of copolymer was calculated using the elemental analysis data by Atlantic Microlab Inc., Atlantic, GA.. The molecular weight calculation is based on the stoichiometric equilibrium of 'carbon' atoms in the copolymer and in the homopolymer blocks of PEOX and PDMS. The M_w of PDMS (measured by LS) is used to calculate copolymer molecular weight. The total molecular weight of PEOX-PDMS is calculated as 20.2 kg/mole (containing 29 wt.% PEOX).

A well-defined diblock PEOX-PVME was prepared via a living cationic polymerization method[35] using chloroethyl vinyl ether together with HI/ZnI_2 as the initiator and lithium borohydride as the termination reagent. The number-average molecular weight M_n of PEOX-PVME used in this study is 17.6 kg/mole, with a polydispersity of M_w/M_n =1.35, by GPC. A brief summary of the copolymers used in this study was collected in Table 5.1.

Table 5.1 A summary of the copolymer molecular weights used in this chapter.[d]

Copolymer	MW of PEOX (kg/mole)	MW of 2nd block (kg/mole)	Total MW (kg/mole)
PEOX(6K)-PDMS(14K)	5.8	14.4	20.2[a]
PEOX(5K)-PVME(10K)	5.0[c]	10.0[c]	17.6[b]

[a] Calculated by elemental analysis.
[b] Based on the GPC measurements.
[c] Target number-average molecular weight.
[d] see Table 5.2 for data or related homopolymers.

Solvent. The solvents used in this study, including ethanol (200-Proof, Aaper Alcohol and Chemical Co.) and isopropanol (A.C.S. grade, Aldrich Chemical Co.), were purified by distillation using CaH_2. Chlorobenzene (HPLC, Aldrich Chemical Co.) was used as

received. Deionized water with a resistivity of 17 x 10^6 megohm-cm was collected from a four column Barnstead NANOPURE II™ water purification system.

Silica. Cab-O-Sil fumed silica (L-90) was purchased from Cabot Co., IL, which was made by the pyrolysis of silicon tetrachloride vapor in hydrogen and oxygen.[36] This silica was used as the adsorbent for the adsorption experiments. The particles have an equivalent diameter of 0.27 μm and an average surface area of 100 ± 15 m^2/g.[36] Prior to the adsorption experiments, the Cab-O-Sil silica was dried in a convective oven at 115°C for at least 4 hours.

The technique used to synthesize silica particles followed the method described by Stöber *et al.*.[37] Tetraethylorthosilicate (TEOS) was used as the starting reagent in a mixture of ammonia and ethanol. TEOS (Reagent Grade, Fisher Scientific Co.) was vacuum distilled and ethanol (200-proof, Aaper Alcohol and Chemical Co.) was distilled using CaH_2 prior to the synthesis of silica. Both purified solutions were stored in a nitrogen environment. Ammonium hydroxide (containing water 30 wt.%, A.C.S. grade, Fisher Chemical Co.) was used without any further purification. To prepare a batch of 500 ml silica solution with ~2.0 wt/%, the compounds were added in the order of ethanol (455 ml), TEOS (19 ml) and ammonia (26 ml). The synthesis was conducted in a round bottom flask with a stirring bar under nitrogen purge for 48 hours. The size of the precipitated Stöber silica was characterized after 7 days of stirring under nitrogen.

The silica particles (henceforth referred to as "Stöber silica") were transferred to isopropanol for the adsorption experiments. The originally synthesized Stöber silica was centrifuged at 2250 g's for 2 hours. The supernatant was withdrawn and replaced with distilled isopropanol. The silica suspension was then sonicated using a tapered horn at a power of 20 Watts by a Tekmar Sonic Disruptor. At least three minutes (50% duty cycle) were necessary to break the silica agglomerates. Afterwards, the dispersion was centrifuged again. This washing process was repeated three times. Subsequently, the final liquid phase was analyzed by ^1H NMR to confirm that there was no residual ethanol in

the final solution (<0.25%). The same procedure was used to transfer Stöber silica to chlorobenzene.

The size of the Stöber silica was determined by transmission electron microscopy (TEM) and dynamic light scattering (DLS). The sonicated silica suspension was deposited on a carbon-coated copper grid (200 mesh) and dried in air at room temperature overnight. TEM was calibrated using standards to be within an error of 5% at the experimental magnification (x10,500). The size distribution (*i.e.*, polydispersity, PD) of silica was calculated according to:

$$PD = 1 + \frac{\sigma}{<d>} \qquad (5.23)$$

where σ represented the particle size standard deviation and $<d>$ the mean diameter of particle size. Over 120 silica particles were counted to measure the average particle size and particle size distribution. The mean diameter of the silica particles from TEM was 69.0±5.5 nm and the PD value was 1.08 after the sonication process. A typical TEM micrograph is illustrated in Figure 5.5.

Procedure

Light Scattering. The polymer solubility and particle size measurements were performed with a Brookhaven Model BI-2030 light scattering instrument, which consists of a thermostatted sample vat, a 136-channel digital autocorrelator and a photomultiplier tube on a precision goniometer. The light source was a Lexel Model 95 Argon laser operated at 514.5 nm. The scattering angle was fixed at 90°, as described in Chapter 2. The polymer solubility was characterized by measurements of the second virial coefficient (A_2) using static light scattering, which was described previously in Chapters 2 and 4. Silica particle size, copolymer micellization, and the thickness of the adsorbed copolymer

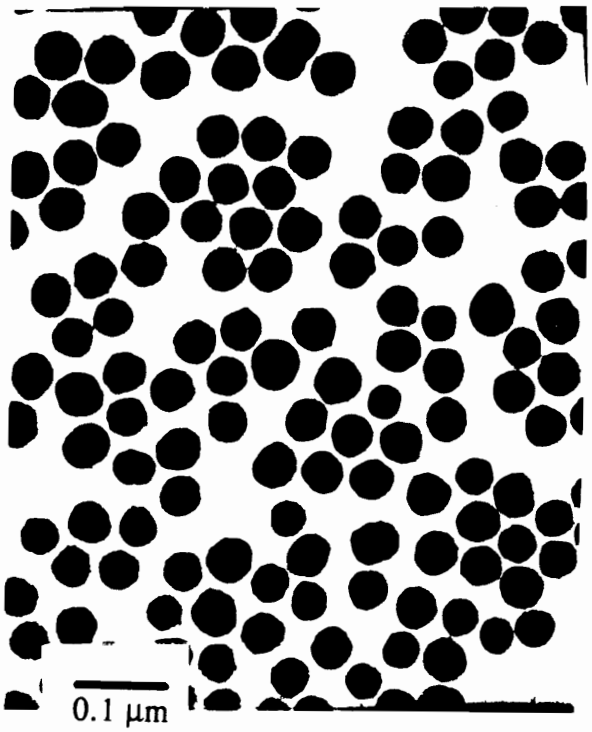

Figure 5.5 Transmission electron micrograph of a typical silica dispersion, prepared by the centrifuge process, see text.

layer on silica were measured using dynamic light scattering.

Static Light Scattering. The second virial coefficient (A_2) measurements were measured by light scattering. A_2 is related to the excess Rayleigh ratio, $\Delta R(\theta)$ by[38]

$$Kc/\Delta R(\theta) = M_w^{-1} + 2 \cdot A_2 c \tag{5.24}$$

where

$$K = \frac{[2\ \pi\ n_0\ (\frac{\partial n}{\partial c})]^2}{N_A\ \lambda_0^4} \tag{5.25}$$

the λ_0 is the wavelength of laser beam in the air (514.5 nm), N_A is Avogadro's number and n_0 is the refractive index of medium at the specific temperature and wavelength. Measurements of the refractive index increment ($\partial n/\partial c$) for PEOX, PDMS and PVME were made using an Abbe Precision refractometer (Bellingham and Stanley Inc.), equipped with an optical filter at a wavelength of 510 nm.

Dynamic Light Scattering. The hydrodynamic diameter of the silica particles was measured by DLS using the second cumulant method,[34,39] The time dependent scattering intensity leads to the first order correlation function $g^{(1)}(\tau)$ which is a function of the delay time τ and is related to the distribution function $G(\Gamma)$ of the characteristic line-width Γ by

$$g^{(1)}(\tau) = \int_0^\infty G(\Gamma) e^{-\Gamma\tau}\, d\Gamma. \tag{5.26}$$

Inversion of Equation (5.25) for $G(\Gamma)$ leads to the size distribution. The cumulant expansion for $G(\Gamma)$ leads to

$$\ln[g^{(1)}(\tau)] = - \Gamma_{avg}\tau + \mu_2\tau^2/2 + \ldots \quad (5.27)$$

where μ_2 is the second cumulant. The average linewidth Γ_{avg} is defined by

$$\Gamma_{avg} = \int_0^\infty \Gamma G(\Gamma)\, d\Gamma. \quad (5.28)$$

The diffusion coefficient D and the scattering vector q are related to Γ_{avg} by $\Gamma_{avg}=Dq^2$, $q=(4\pi n_0/\lambda_0)\cdot\sin(\theta/2)$. The n_0, λ_0 and θ represent the refractive index of solvent, light wavelength and scattering angle, respectively. Using the light scattering, the polydispersity (PD_{LS}) of the solutions can then be defined as

$$PD_{LS} = \mu_2/\Gamma_{avg}^2. \quad (5.29)$$

The PD_{LS} value for a narrow size distribution of spherical particles in suspension is typically less than 0.02.[40] The diffusion coefficient D is related to the equivalent spherical hydrodynamic diameter $D_{h,0}$ with Stokes Einstein equation:[34]

$$D_{h,0} = kT/(3\pi\eta D) \quad (5.30)$$

where η is the viscosity of the medium.

Dynamic light scattering was used to measure the hydrodynamic radius $R_{h,0}$ (or diameter $D_{h,0}$) of polymers and particles. Before measurements, polystyrene latex (149±4 nm Nanosphere™, Duke Scientific Corp., CA) in aqueous solution was used to calibrate the light scattering measurement. We accepted only those autocorrelation functions where the measured base line agreed with the computed base line within several tenths of a percent. This procedure is to insure that dust did not affect the final measurements.

DLS was used to examine the PEOX-PDMS and PEOX-PVME hydrodynamic diameter at 25±0.1°C. Prior to the measurements, the solutions were filtered once with

a 0.2 μm PTFE filter. The laser power was 20-50 mW depending on the scattering intensities. The sample time, sample duration, and pinhole size were adjusted to obtain the optimal signal (S/N ~ 0.30-0.40). Sample durations were typically 20 seconds. The pinhole size for silica aggregation experiments was always set at 50 μm but for copolymer solution experiments, 400 μm was used due to weak scattering intensities.

For the experiments concerning Stöber silica aggregation in chlorobenzene, the mean particle hydrodynamic diameter was measured as a function of time. Prior to the light scattering experiments, the silica suspension in chlorobenzene was exposed to sonication for 3 minutes. The solution was filtered once through a 0.2 μm PTFE filter. The order of this operation is important to minimize the particle loss during filtration. Aggregation data were typically collected for approximately 10 minutes. However, for very slow aggregation data were collected for up to 70 minutes. The elapsed time after the sonication procedure and prior to the light scattering measurement is approximately 3 minutes. The recorded time started at the suspension mounted on the thermostat and ready for light scattering measurements. For polymer steric stabilization experiments, typically 2 g of suspension were prepared by mixing silica/chlorobenzene suspension with different concentrations of PEOX-PDMS in chlorobenzene solutions to make the final silica concentration of 1.03×10^{-3} g/g. The mixed solution was directly examined by DLS after approximately 30 seconds of rigorous shaking by hand. It delayed approximately 5-10 seconds for the first DLS measurement due to computer operation. The silica number concentration (N_0) was estimated to be 5.44×10^{12} particles/ml, as calculated from the mass concentration using a particle diameter of 69 nm and a particle density as 2.20 g/cm^3, similar to amorphous silica.[42] The calculation of the slope of particle diameter as a function of time was taken starting from the onset of measurement, up to 10 minutes.

Adsorption Isotherm Measurements. A total of 10 ml of a mixture of silica and polymer solution was rotated end-over-end for 24 hours at room temperature for the experiments with Cab-O-Sil silica. The concentration of silica was kept fixed at 1.3×10^{-2} g per gram

of the total mixture (g/g). For the experiments with Stöber silica, 5 ml of the total mixture was used. Because chlorobenzene absorbs in the same UV/vis wavelength range as PEOX, the evaporation of chlorobenzene and replacement with non-absorbance (in UV) solvents was necessary, such as water or isopropanol. Evaporation of chlorobenzene was achieved by gently heating the polymer solutions (both before adsorption solutions and after adsorption supernatant) on hot plates. Before the solutions were completely dried, samples were moved to a convective oven (set at $\sim 140°C$) until totally dry. The samples were then stored in a vacuum oven at room temperature for 8 hours. Water or isopropanol was then added to the samples. After 24 hours of mixing, the concentration of the supernatant was examined by UV/vis spectroscopy. An independent study showed that there was no significant polymer loss ($<5\%$) using this heating procedure, *i.e.*, polymer did not decompose in this temperature range.

The adsorption percentage was obtained from the absorbance difference of UV/vis light between bulk solutions and supernatant. The adsorbed amount (in unit of mg/m^2) was calculated according to:

$$\Gamma = M_P(1 - I_S/I_0)/A_S \tag{5.31}$$

where M_P (in mg) is the added polymer mass in the bulk solution, I_S and I_0 respectively represent the absorbance of the supernatant and bulk solution around the UV wavelength 229 nm, and A_S is the total surface area (in m^2). For Cab-O-Sil silica, the total surface area is the product of added silica weight M_S (in g) and the reported surface area per gram, 100 ± 15 m^2/g,[36] which then equals to $100 \cdot M_S$ (in m^2). The total surface area (in m^2) of the Stöber silica was calculated according to:

$$A_S = [6 \cdot 10^3/(D_0 \cdot \rho)] \cdot M_S \tag{5.32}$$

where the Stöber silica density[41] ρ was 2.20 ± 0.05 g/cm^3, and D_0 is the particle diameter

of silica from TEM measurements (=69±5.5 nm). The calculated surface area of Stöber silica according to equation (5.32) is 39.5 m^2/g. Therefore, the silica density plays an important role for the determination of the surface area in Stöber silica.

The competitive adsorption procedure was similar to the procedure described in Chapter 4. PEOX and other polymers were mixed with different weight ratios in several solvents, including isopropanol, ethanol, and chlorobenzene. The spectrophotometer wavelength used to measure polymer solution concentration was in the range 238-241 nm. The concentration of PDMS could be measured by this method because the PDMS chain end group, benzyl chloride, absorbed strongly light at wavelengths lower than 245 nm.

RESULTS AND DISCUSSION

Solution Properties

Homopolymers. The solubility of a tail block is critical to the steric stabilization effect. In a good solvent, the tail block penetrates into the liquid phase, forming a layer that generates repulsive steric forces. The second virial coefficients and molecular weights of PVME, PDMS and PEOX in different solvents were measured by SLS and are discussed next.

The PEOX-PVME diblock was originally designed in the belief that PVME would serve as the stabilizing tail block in water. Thus, the solubility of PVME in water was examined by SLS. For SLS experiments at polymer concentration, $C_P \leq 1x10^{-3}$ g/ml, the calculated mass-average molecular weight exceeded 40 kg/mole, which is much higher than the target MW of 16 kg/mole and larger than the value measured in ethanol (17.4 kg/mole). This suggested that PVME associated in water. At higher concentrations, PVME in water formed precipitates. The precipitates could not be removed by heating (~75°C) and cooling (~4°C) cycles. These observations indicate that PVME was not fully soluble in water and thus was unable to act as a steric stabilizer in aqueous solution.

Further, scattering experiments show that ethanol is a good solvent for PVME and the results are shown in Table 5.2. Thus, ethanol was chosen as a solvent to test the stabilizing capability of PEOX-PVME.

PEOX-PDMS was also studied as a copolymer stabilizer in this work. Thus, the solubilities of PEOX and PDMS in isopropanol and chlorobenzene were examined by light scattering techniques. The second virial coefficient measurements of polymers in different solvents are summarized in Table 5.2. The negative value of A_2 for PEOX in chlorobenzene shows that PEOX is in a sub-θ state.

Table 5.2 Summary of the solubility and MW of selected homopolymers from different solvents at 25°C and at λ_0=514.5 nm.

Polymer	Solvent	$\partial n/\partial c$ ml/g	MW kg/mole	$A_2(x10^{-4})$ cm^3 mole g^{-2}	χ
PEOX(3K)	isopropanol	0.155±0.003[b]	2.1±0.5	17.1±1	0.32
PEOX(17K)	isopropanol	0.155±0.003	14.5	29.6±2.0	0.20
	chlorobenzene	0.022	16.8±1.0	-13.4±0.5	0.53
	water	0.176±0.002	18.5±0.3	21±3	0.46
PDMS(14K)	isopropanol	0.029±0.001[c]	14.4±1.0	9.98±0.5[a]	0.42
	chlorobenzene	-0.123±0.004	15.5±2.0	4.0±0.2	0.46
PVME(16K)	ethanol	0.136±0.003	17.4	16.2±2.0	0.41
	water	0.129[d]	>400	2.7	~0.5

[a] Obtained by the low angle laser light scattering (LALLS), by T. Brady.
[b] Based on the $\partial n/\partial c$ value of PEOX(17K) in isopropanol.
[c] Using Chromatix KMX-16 Laser Differential Refractometer with wavelength 632.8 nm.
[d] Based on the report by J. E. Wilson using wavelength of 589 nm.
[e] All $\partial n/\partial c$ values except PDMS 14K in isopropanol are measured at 510 nm.
[f] For the conversion of A_2 to χ (Eqn.(5.14)), polymer specific volume v_p of PEOX=0.87 cm^3/g, and PDMS=1.01 cm^3/g, and PVME=0.97 cm^3/g, the last two values from ref.[42].

Copolymers Solutions of PEOX-PDMS (MW=20.2 kg/mole) in chlorobenzene was evaluated at 25±0.1°C by DLS. Micelles were not observed even though the PEOX block (~6 kg/mole) was not soluble. This suggests that the critical micelle concentration (CMC) of PEOX-PDMS in chlorobenzene must be higher than the highest experimental concentration, $3.4x10^{-3}$ g/g. The relatively low MW of PEOX in the diblock (~6 kg/mole) also leads to be more solubility in chlorobenzene than the PEOX 17K homopolymers. This is consistent with the adsorption isotherms of PEOX 3K and PEOX 17K in chlorobenzene which will be introduced in the subsequent sections.

Copolymer in Mixed Solvents. Water is not a good solvent for PVME at 25 °C but PVME and PEOX are fully soluble in ethanol. Therefore, solutions of PEOX-PVME in mixtures of water and ethanol were studied by DLS to determine the concentration of water at which micelles would form. This is important to determine the solvent composition range over which a PEOX-PVME diblock might conceivably serve as an effective steric stabilizer. The hydrodynamic size of PEOX-PVME in ethanol at different water concentrations was measured by DLS.

The hydrodynamic diameter of PEOX 5K-PVME 16K (~1.0 wt.%) in ethanol is ~3.6±1.0 nm, as shown in Figure 5.6. Based on the DLS measurements, the hydrodynamic size of PEOX-PVME remained constant as water content increased to 4 wt.% (~0.10 water mole fraction). The parameters used in these calculations were listed in the Appendix. As shown, the copolymer size abruptly increased to approximately 55.9±2.0 nm as the water concentration increased to 7.0 wt.% (0.19 water mole fraction). At this water concentration, PEOX-PVME forms micelles in the water-ethanol mixture. Thus, the effective solvent composition over which the diblock is expected to function as a steric stabilizer is water mole fraction = 0 - 0.1. This is important for the future applications of PEOX-PVME in alcohol/water mixture.

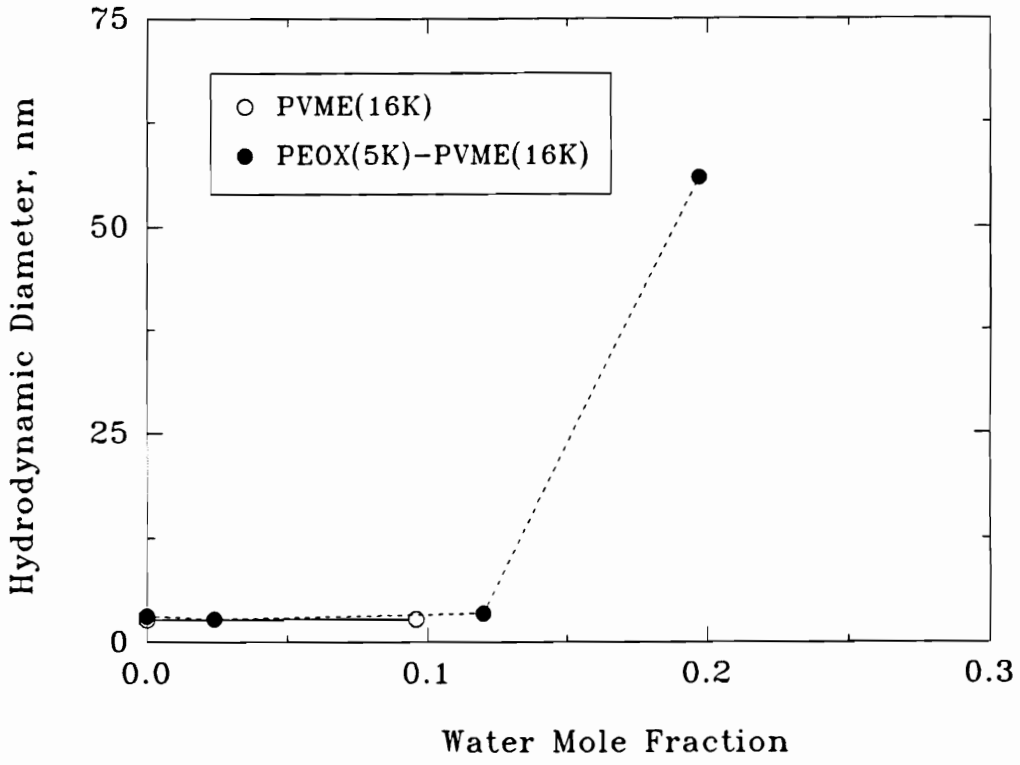

Figure 5.6 The hydrodynamic diameter of PEOX 5K-PVME 10K and PVME 16K homopolymer in ethanol as a function of water mole fraction. The diameter was measured by DLS at 25°C, copolymer concentration=1.0 wt.%.

Adsorption Studies

Stöber Silica Characterization. The resulting hydrodynamic particle diameter of silica in isopropanol at 25±0.1°C was 92.0±3.0 nm. The difference between particle diameters determined by TEM and DLS is attributed to some slight particle aggregation.[11] The particles were stable against further aggregation in isopropanol solution due to a residual surface charge given isopropanol is relatively high dielectric constant (~18).[18,42] The surface area calculations and the adsorbed layer thickness measurements in this chapter are based on the TEM micrograph diameter of 69 nm.

Adsorption Isotherms. The plateau adsorption amount (Γ_p) of polymers on Cab-O-Sil silica surface from different solvents are listed in Table 5.3.

Table 5.3 Polymer plateau adsorption amount (Γ_p) on Cab-O-Sil silica, L-90. The MW values and degree of polymerization (DP) were measured by light scattering unless indicated otherwise.

Polymers	MW (kg/mole)	DP	Solvent	Γ_p (mg/m^2)
PEOX(2K)	2.0[c]	20	water	0.28
PEOX(3K)	2.1[d]	21	chlorobenzene	0.5
PEOX(7K)	7.4[a]	75	isopropanol	0.38
PEOX(17K)	18.5[b]	187	water	0.55
			isopropanol	0.38
			ethanol	0.36
			chlorobenzene	1.0
PEOX(20K)	22.3[b]	225	isopropanol	0.42
PDMS(14K)	14.4	195	isopropanol	0.10
PEOX 6K-PDMS 14K	20.0		isopropanol	0.9
PEOX 5K-PVME 10K	15.0[c]		n-butanol	1.2

[a] From GPC measurement.
[b] Water as the solvent.
[c] Target MW.
[d] Isopropanol as the solvent.

PEOX Adsorption. Figure 5.7(a) shows that Γ_p for PEOX 7K from isopropanol is higher than that of PDMS 14K. The magnitude of the adsorbed amount in general is affected by several factors, including polymer molecular weight (MW), adsorption energy parameter (χ_s), and polymer solubility (χ). The higher MW of a polymer usually results in a higher adsorption amount, which has been discussed in Chapter 4. In addition, a higher adsorption energy (*i.e.* large χ_s) or lower polymer solubility (low χ) in the solution leads to a higher adsorbed amount. Based on the solubility measurements by SLS, PEOX ($\chi \sim 0.20$ - 0.30) is more soluble in isopropanol than PDMS ($\chi \sim 0.42$). Thus, we concluded that the adsorbed amount of PEOX is greater than that for PDMS due to a higher value of χ_s for PEOX. More evidence for this will be discussed in the later competitive adsorption section.

For PEOX 17K in chlorobenzene, the adsorbed amount Γ did not reach a plateau but rather increased with polymer concentration, as shown in Figure 5.7(b). This is consistent with the formation of multilayers on the surface[43] due to the poor solvency of PEOX in chlorobenzene. This multilayer adsorption results from the net attractive interactions between PEOX segments. Comparing the Γ_p values of PEOX 17K in water (0.55 mg/m^2) and chlorobenzene (>1.0 mg/m^2), the higher Γ_p of PEOX in chlorobenzene than in water is also consistent with multilayer formation. The adsorption plateau for PEOX 3K in chlorobenzene is likely due to this polymer's greater solubility due to its lower molecular weight. Thus, multilayer adsorption did not occur. Both isotherms are consistent with the polymer adsorbing primarily by hydrogen bonding.

Competitive Adsorption. The competitive adsorption experiments (illustrated in Figure 5.8) of PEOX in the presence of other polymers, *i.e.* PVME and PDMS, on Cab-O-Sil silica (L-90) from several solvents are summarized in Table 5.4. These polymers were mixed with PEOX in chlorobenzene and in isopropanol. The concentrations of PEOX in

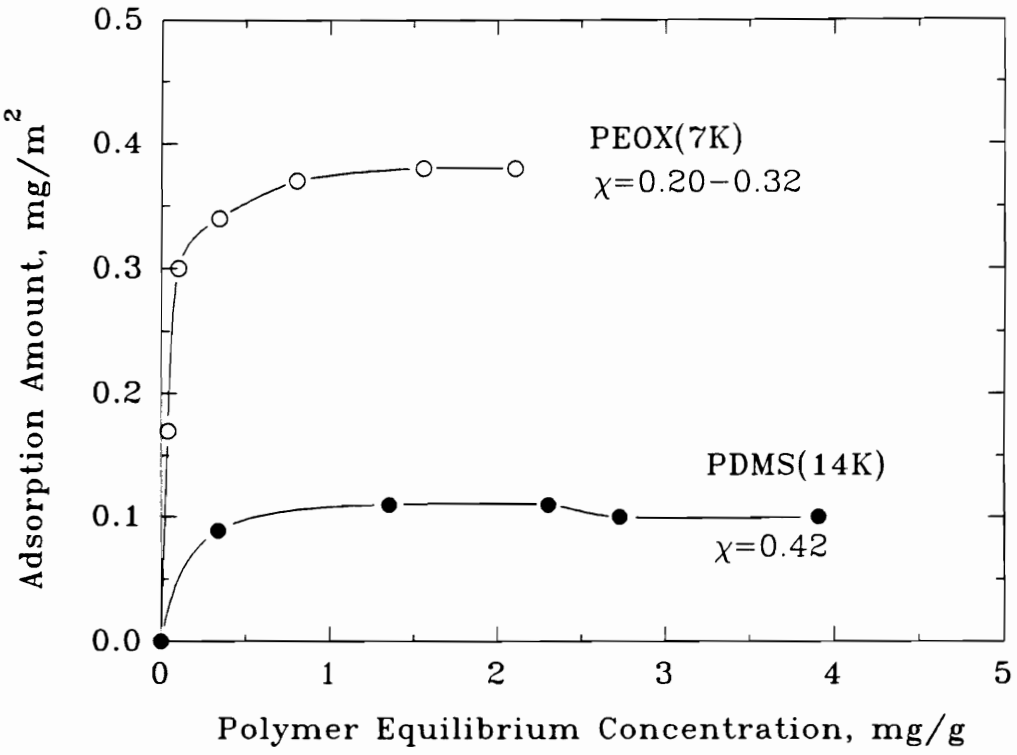

Figure 5.7(a) The adsorption isotherms of PEOX and PDMS on Cab-O-Sil silica surface, L-90, from isopropanol.

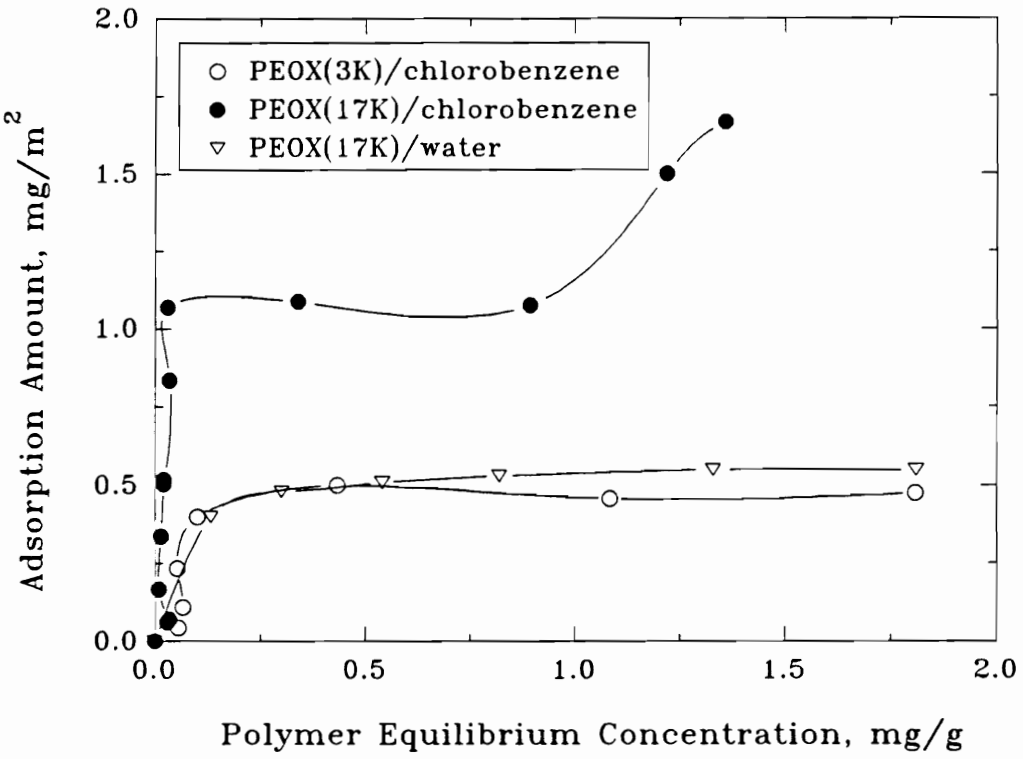

Figure 5.7(b) PEOX adsorption isotherms on Cab-O-Sil silica surface from chlorobenzene. The uproaring adsorbed amount is attributed to the poor solvent of PEOX in the solvent.

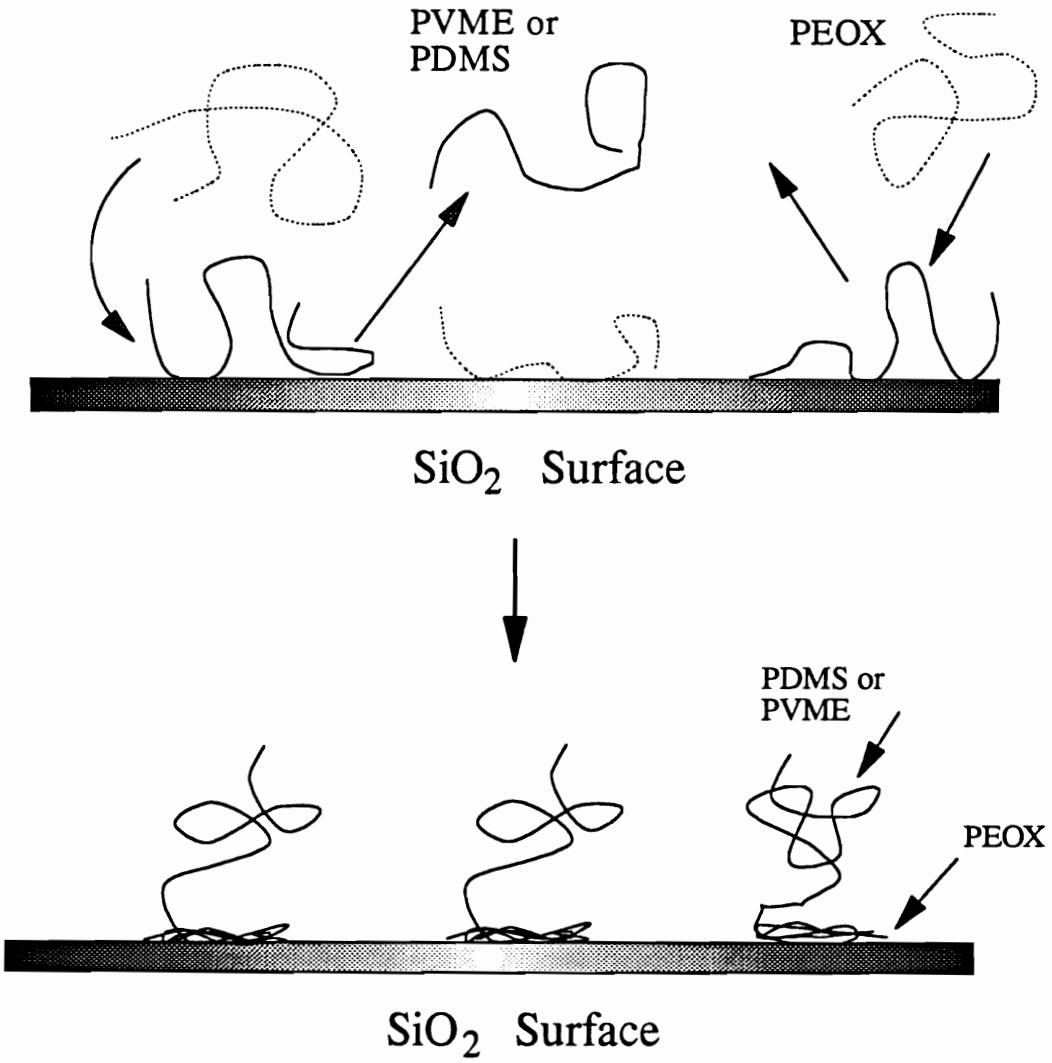

Figure 5.8 An illustration of the competitive adsorption between polymers and PEOX on silica surface. Based on the homopolymer competitive adsorption experiments, the anchor block and tail block of the corresponding molecular weights in a copolymer can be estimated.

all of the mixtures were fixed at the concentrations which, for pure PEOX, resulted in a plateau of the isotherm, which was previously determined.

(1) *PEOX/PDMS*

(a) *in isopropanol.* Mixtures of PDMS 14K and PEOX 7K at various concentration ratios were performed in isopropanol for the competitive adsorption experiments. Figure 5.9 shows that the Γ_{mix} values (PEOX adsorbed amount in the polymer mixture) are similar to the Γ_p values of PEOX alone from isopropanol for all concentrations of added PDMS. This suggests that PEOX has a higher adsorption affinity to silica surface than does PDMS. The strong adsorption ability of PEOX is consistent with the previous results that PEOX has a higher Γ_p value than PDMS in isopropanol. A separate experiment associated with the competitive adsorption between PDMS 14K and PEOX 20K from isopropanol again showed that the PEOX adsorbed amount was not affected by the presence of PDMS in the solution. The higher adsorption amount of PEOX on silica surface is due to its χ_s parameter since the solubility and MW's of PEOX and PDMS studied hinders the adsorption of PEOX on the surface; the result is shown in Table 5.4. The higher adsorption affinity of PEOX than PDMS (in isopropanol) suggests that PEOX serves as the anchor block and PDMS as the tail block in the PEOX-PDMS copolymer adsorption conformation.

(b) *in chlorobenzene.* Figure 5.9 shows the competitive adsorption between PEOX 3K and PDMS 14K from chlorobenzene. Γ_{mix} of PEOX was not significantly affected by the presence of PDMS for PDMS/PEOX concentration ratio up to 0.3. There was a slight increase of the measured adsorption value in the high PDMS concentrations. This was probably due to the absorbance contributions of benzyl chloride (the end group of PDMS), which also adsorbed in the same UV wavelength range as PEOX. Moreover, due to the poor solubility of PEOX in chlorobenzene, the stronger adsorption of PEOX than PDMS in chlorobenzene is reasonable.

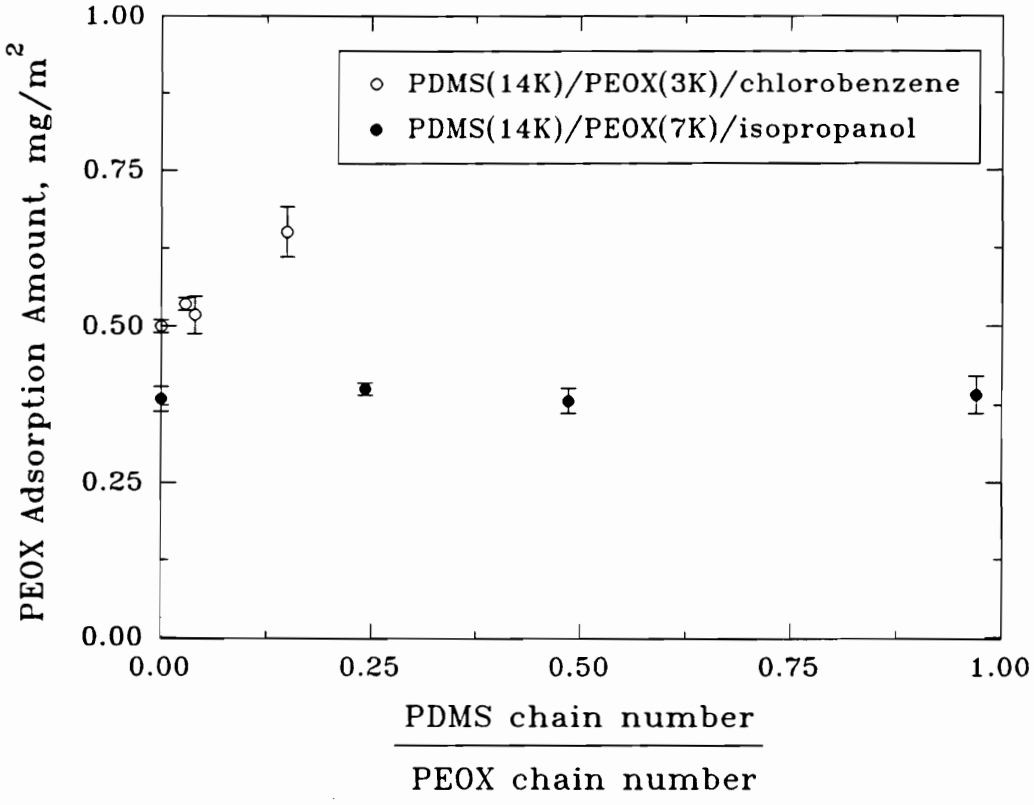

Figure 5.9 The competitive adsorption between PDMS and PEOX from isopropanol and chlorobenzene on silica surface. The adsorbed amount of PEOX is not affected by the presence of PDMS, implying a stronger affinity of PEOX than PDMS on silica. PEOX concentration is ~2.0 mg/g.

However, another explanation for the increasing adsorbed amount in the above case is that PEOX 3K and PDMS 14K may both adsorb on silica from chlorobenzene. As mentioned in Chapter 4, the adsorption ability of a homopolymer is also a function of the relative molecular weight. At such a low molecular weight of PEOX (MW=2.1 kg/mole), PEOX chains may not be able to compete with the long PDMS chain (MW = 14.4 kg/mole). Thus, the co-adsorption of PDMS and PEOX on silica surface is possible. To be more certain, the competitive adsorption between PEOX and PDMS of comparable degrees of polymerization on silica surface from chlorobenzene needs to be measured.

In PEOX-PDMS diblock copolymer case, benzyl groups on PDMS ends are reacted with PEOX monomers during copolymerization and positioned at the middle of copolymer chain. Thus there may be no significant contribution to UV/vis absorbance. Also, the residual PDMS was extracted by hexane. In addition, no end group effect was detected by the UV analysis in the mixture of PDMS 14K with PEOX 7K case. This was because, at equal chain number ratio, the ratio of (benzyl group/PEOX repeat unit) was lower for the PDMS 14K/PEOX 7K case than for the PDMS 14K/PEOX 3K case. Thus, the end groups are not that significant in PEOX 7K/PDMS 14K as in PEOX 3K/PDMS 14K.

(2) PEOX/PVME

(a) *in water.* As shown in Table 5.4, the plateau adsorption amount of PEOX alone is the same as the Γ_{mix} of PEOX 2K and PVME 2K mixture in water. Due to the poor solubility of high MW of PVME in water, we could not measure the competitive adsorption at high MW of PVME in water. The competitive adsorption is only done using the low MW of PVME with PEOX. The PVME is terminated by the chloride, and thus did not contribute to the UV absorbance.

(b) *in ethanol.* Competitive adsorption of PEOX(17K) and PVME(16K) mixture from ethanol is next examined. No significant difference was found between the adsorbed

Figure 5.4 Competitive adsorption between PEOX and PDMS or PVME from different solvent, the added weight ratio 1:1, unless noted.

Polymers	$\frac{DP_{PEOX}}{DP_{polymer}}$	$\frac{\chi_{PEOX}}{\chi_{polymer}}$	$\frac{\text{mole PEOX chains}}{\text{mole other chains}}$	Solvent	Γ_p mg/m^2	Γ_{mix} mg/m^2
PEOX(7K)/PDMS(14K)	75[f]/195	0.20[a]/0.42	1.9[d]	isopropanol	0.38	0.38
PEOX(20K)/PDMS(14K)	225 /195	0.21 /0.42	0.7	isopropanol	0.40	0.42
PEOX(3K)/PDMS(14K)	21 /195	0.50[c]/0.46	6.9[d]	chlorobenzene	0.50	0.50
PEOX(2K)/PVME(2K)	20[g]/35[g]	0.45[b]/0.50[c]	1.0	water	0.28	0.28
PEOX(17K)/PVME(16K)	187[g]/300	0.35[a]/0.41	0.9	ethanol	0.36	0.36

a SLS measurements of PEOX(20K) in ethanol, in Chapter 4.
b SLS measurements of PEOX(3K) in ethanol, in Chapter 4.
c estimated due to the poor solubility of PVME in water.
d different weight ratios were measured.
e MW based on SLS measurements in water.
f MW based on GPC measurement.
g target MW.

amount of the PEOX alone and the polymer mixture. Based on the above discussion, it is concluded that $(\chi_s)_{PEOX} > (\chi_s)_{PVME}$ for silica in ethanol.

Combining the results of Chapter 4 and the results in Table 5.4, we summarize in Figure 5.10, the competitive adsorption results of PEOX with the polymers, PEO, PPO, PDMS and PVME from several solvents. For all studies, PEOX showed the strongest adsorption ability to silica surface with respect to other polymers in all solvents. In general, PEOX also exhibited comparable or greater solubility than the other polymers tested in a given solvent. As discussed in Chapter 4, the adsorbed amount increases with χ due to the shrinkage of polymer dimensions on the surface in a poor solvent. Therefore, the strong adsorption of PEOX relative to other polymers strongly suggests that PEOX must have a higher adsorption energy parameter, χ_s, relative to other polymers in solvents. This result is very important for the design of diblocks that contain PEOX. These results suggest that PEOX could act as the anchor block in copolymers of PEOX made with these other polymers. This general result is reasonable given that the carbonyl groups (C=O) in PEOX forms a more polar hydrogen bond with the silanol group on silica than the other polymers containing either ester groups (C-O-C) or siloxane Si-O-Si groups. This is consistent with the results in Chapter 4. To be more quantitative, the segmental adsorption energy parameters χ_s of PEO, PPO, and PVME should be measured using the displacement technique developed by Cohen Stuart *et al.*[44], as described in Chapter 3.

PEOX-PDMS Copolymer. The adsorption of the diblock copolymer PEOX 6K-PDMS 14K on silica from isopropanol was measured using the depletion method. The value Γ_p on Cab-O-Sil silica was 0.95 ± 0.05 mg/m^2 and plotted in Figure 5.11 (a). For comparison, the adsorption isotherm of PEOX 6K-PDMS 14K was also measured on Stöber silica, leading to Γ_p 0.72 ± 0.04 mg/m^2. The differences of Γ_p between these silica surfaces may be attributed to several factors, including (1) the state of hydration of the

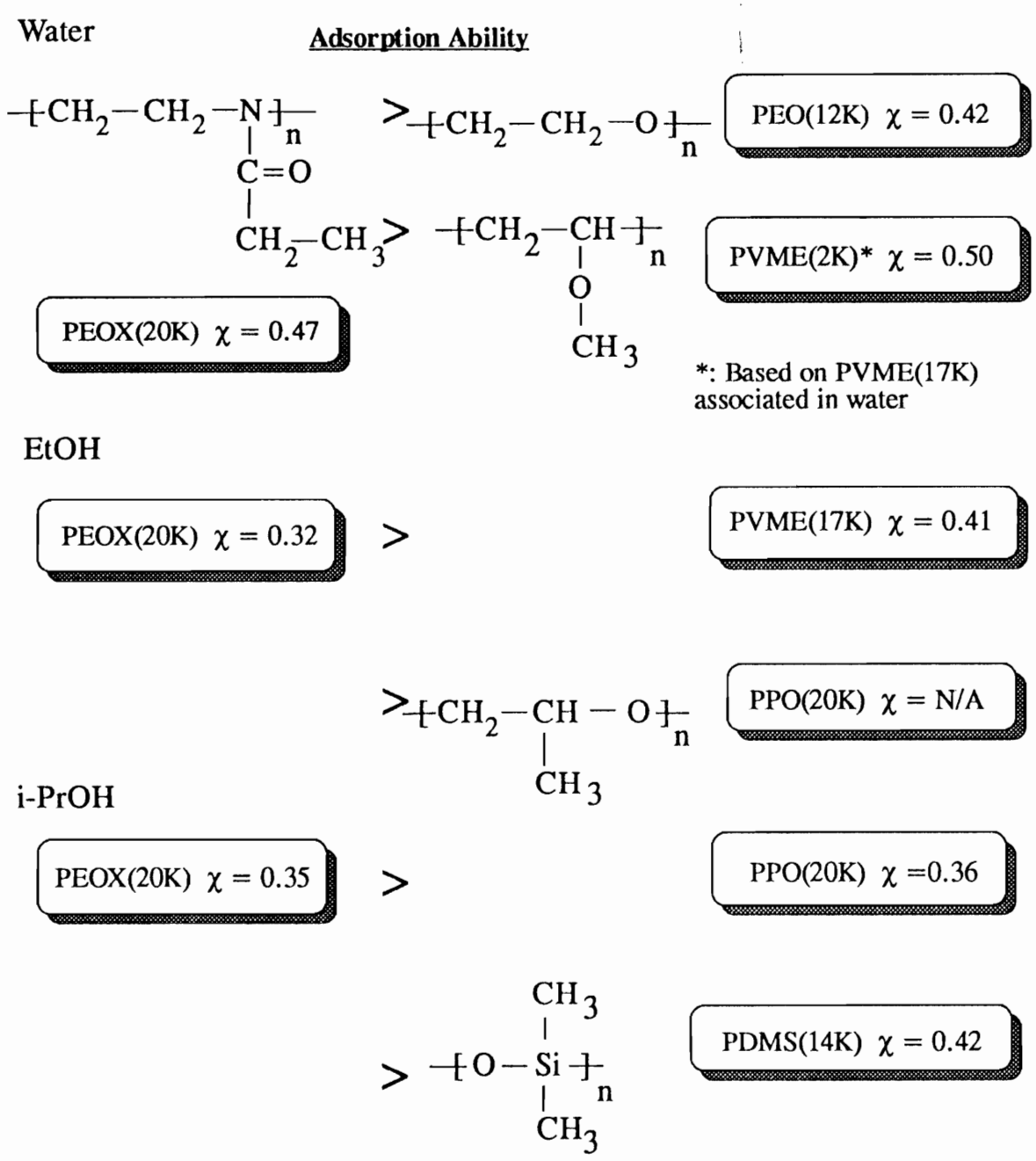

Figure 5.10 A summary of the competitive adsorbed amount of PEOX relative to the other polymers in the corresponding solvents. The PEOX adsorption ability is not reduced by the higher Flory-Huggins parameter χ of other polymers. This suggests that χ_s may dominate the adsorption behavior.

particles' surface, (2) uncertainties in the density of Stöber silica, and (3) differences in porosity. It is unlikely that factor (2) is relevant here since using a higher density than 2.2 (closer to the amorphous value of 2.5 - 3.0)[36,42] would in greater discrepancy with the data.

The adsorption isotherm of PEOX-PDMS on Cab-O-Sil silica from chlorobenzene does not reach a plateau, as seen in Figure 5.11(b). The adsorbed amount increases with the added polymer concentration upto $C_P=6.0x10^{-3}$ g/g which suggests multilayer adsorption. This was unexpected since chlorobenzene is a good solvent for the PDMS 14K block. It was expected that the good solubility of PDMS and the poor solubility of PEOX in chlorobenzene would lead to the establishment of a brush layer and a plateau in the adsorption isotherm. It is not clear at present why a plateau was not reached.

Steric Stabilization.

To study the steric stabilization of dispersions, copolymer PDMS-PEOX was used as the stabilizer in two solvents, chlorobenzene and isopropanol. In chlorobenzene, we could not measure adsorbed layer thickness δ_h due to rapid aggregation of the Stöber silica particles. Therefore we characterized the particle stability in terms of aggregation rate as functions of silica and polymer concentrations. By contrast, the Stöber silica was itself stable in isopropanol due to electrostatic stabilization from the partially ionized silanol groups. Thus we could only measure the hydrodynamic thickness δ_h in isopropanol case.

Stability Ratio in Chlorobenzene. The particle flocculation rate in chlorobenzene was examined by measuring the hydrodynamic diameter of particles in the solution as a function of time using DLS, as shown in Figures 5.12 (a and b). Due to the low dielectric constant of chlorobenzene ($\sim$5.71), ionization of surface silanol groups was suppressed, leading to negligible electrostatic stabilization effects. The apparent

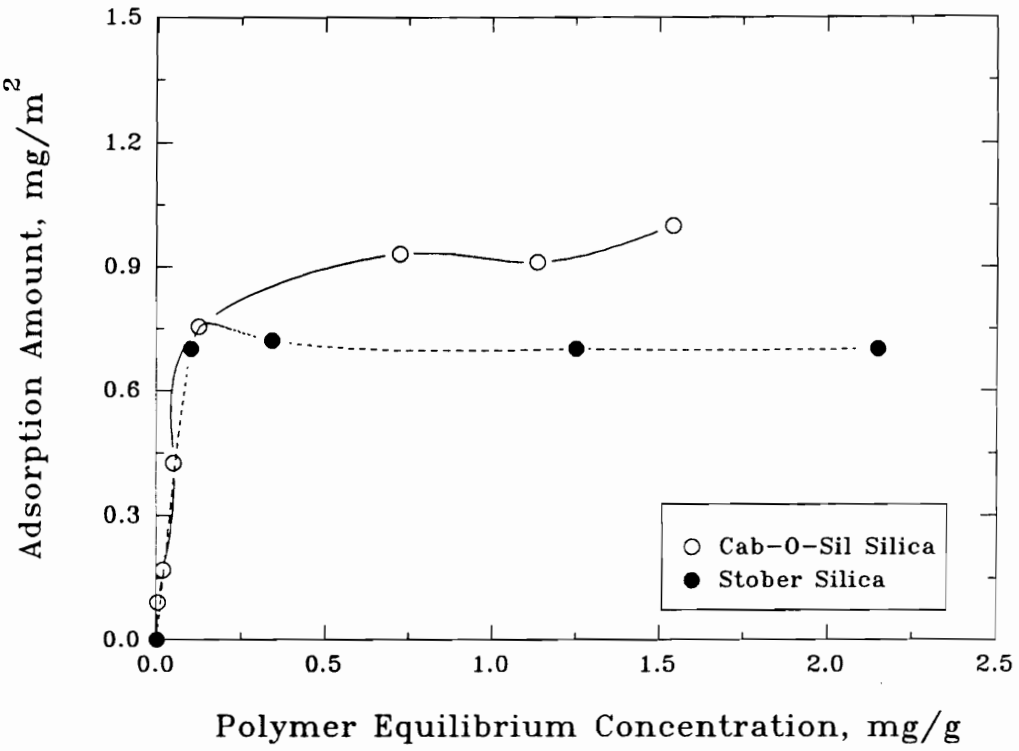

Figure 5.11(a) The adsorption isotherms of copolymer PEOX 6K-PDMS 14K on silica surfaces from distilled isopropanol. Silica particle diameter is 69.0 nm and density is 2.2 g/cm^3. The Stöber silica surface area is 39.5 m^2/g.

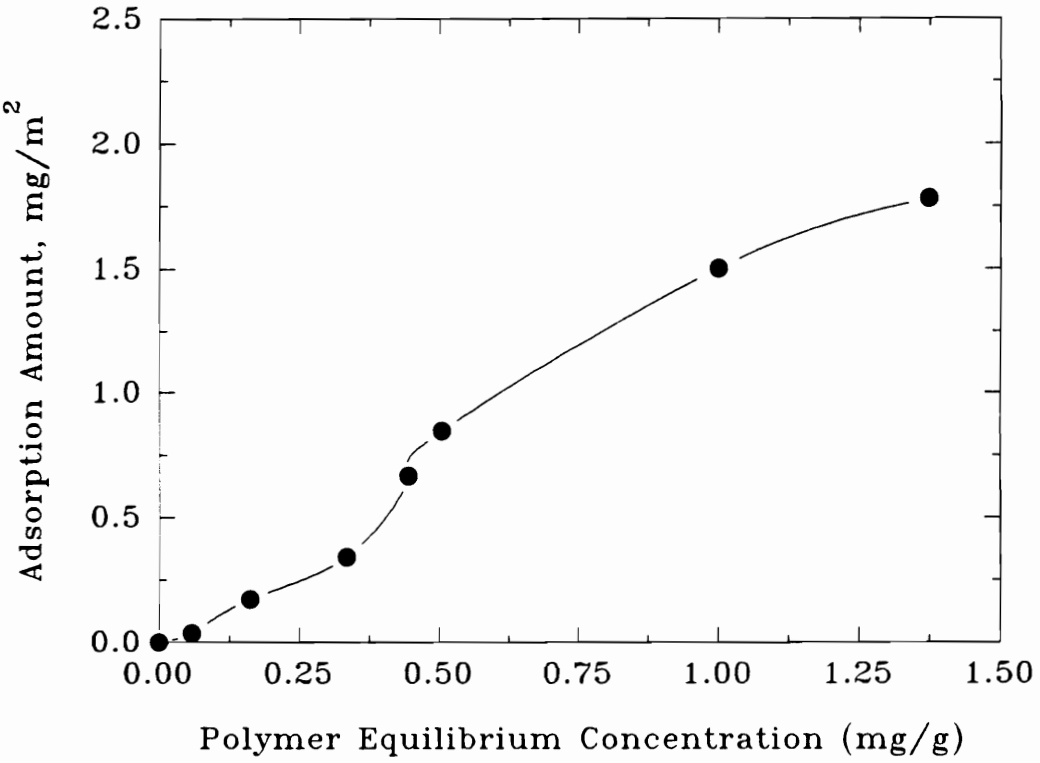

Figure 5.11(b) The adsorption isotherm of copolymer PEOX 6K-PDMS 14K on Cab-O-Sil silica from chlorobenzene. The adsorption did not reach plateau region.

flocculation rates increase significantly with silica particle concentration due to the increasing frequency of collision (Figure 5.12(a)).

The hydrodynamic size versus time as a function of PEOX-PDMS polymer concentration was measured, seen in Figure 5.12(b). The mean hydrodynamic diameters of aggregates in the dispersions increase with time. Obviously, the rate of flocculation decreased as the copolymer concentration increased. Owing to the lack of plateau adsorption information by PEOX 6K-PDMS 14K isotherm from chlorobenzene, we are unable to report if this concentration reaches the plateau region. Based on DLS results, the PDMS layer does not generate sufficiently strong steric repulsion forces to overcome the van der Waals attractive force. This is attributed to the thin steric layer formed due to the low MW (PDMS 14.4 kg/mole) of the tail block (PDMS). Nevertheless, the concentration dependence of the added polymer qualitatively showed the effects of polymer steric stabilization.

Quantitatively, the stability ratio W (defined in equation (5.19)) is an indication of the dispersion stability in the medium. A higher stability ratio indicates more stable particles in the suspension. The stability ratio of silica in copolymer solutions can be calculated according to the method developed by Virden *et al.*.[32a] The coagulation rate constant in the presence of energy barrier k_{11} of doublet formation can be related to the particle diameter (or radius) growth as a function of time, as shown in equation (5.21). Smoluchowski's diffusion-limited rate constant in the absence of energy barrier can then be obtained from equation (5.17). Thus, the stability ratio, W, can be measured experimentally by[32a]

$$W = k_{smol}/k_{11} \qquad (5.20)$$

The stability ratio W of silica with different concentrations of copolymer in chlorobenzene is summarized in Table 5.5. The slopes of particle hydrodynamic radius vs. time for each measurement were calculated from the data in the first 10 minutes.

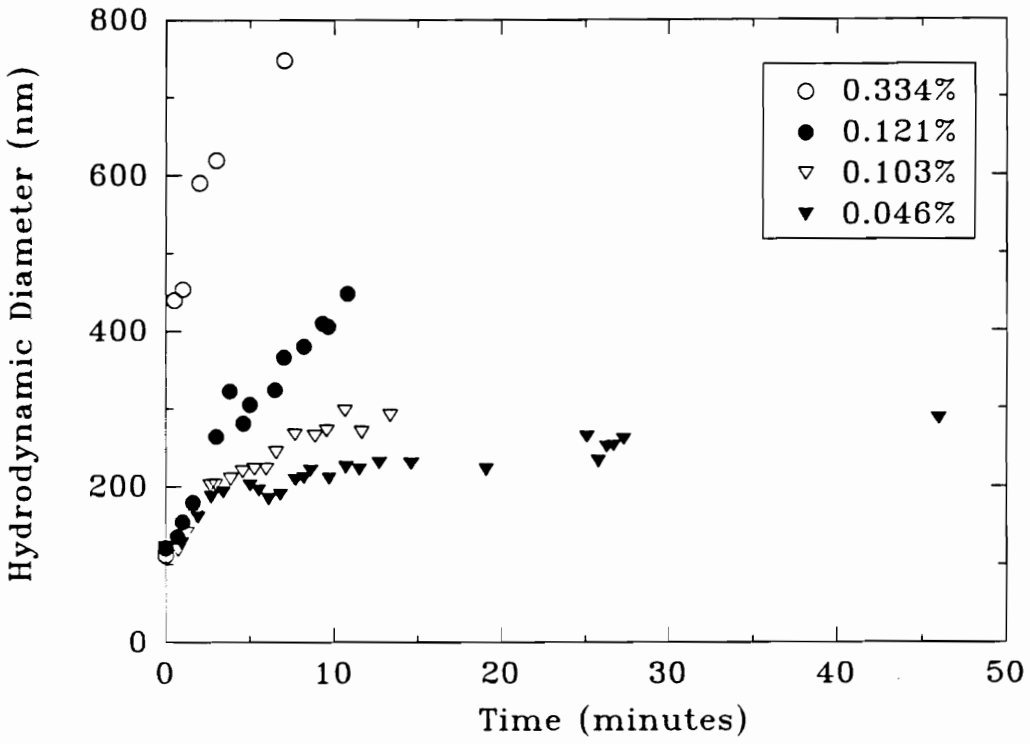

Figure 5.12(a) The hydrodynamic size of Stöber silica particle against time at different particle concentrations in chlorobenzene.

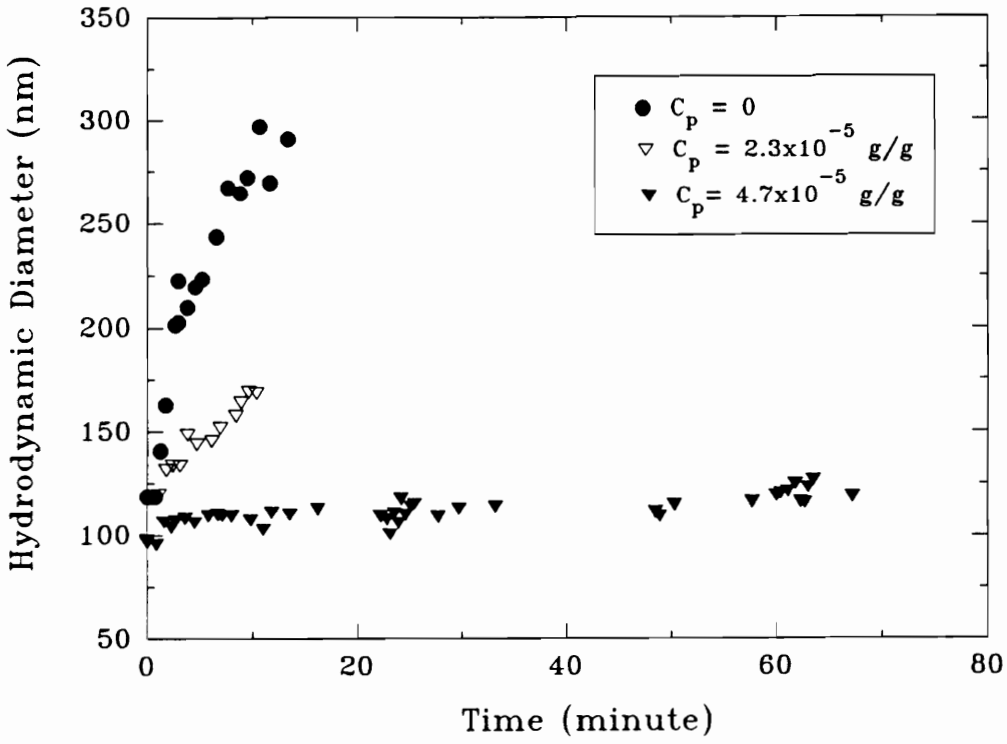

Figure 5.12(b) The Stöber silica is sterically stabilized by PEOX 6K - PDMS 14K from chlorobenzene. The suspension concentration in solution is 1.03 mg per gram of total solution. The diameter change calculation was taken at the first 10 minutes.

Based on the calculations, the stability ratio of the sterically stabilized silica increased by about 44 times (in Table 5.5) compared to the polymer-free solution.

Table 5.5 The stability ratio of silica (1.03×10^{-3} g/g) coated by PEOX-PDMS from chlorobenzene at 20°C.

Added Polymer conc. (g/g)	dR_{mean}/dt (nm/sec)	W
0	0.167	95
2.5×10^{-5}	0.1	160
4.68×10^{-5}	0.0038	4200

Layer Thickness Measurements in Isopropanol. The layer thickness was calculated from the hydrodynamic diameter difference between the bare and polymer-coated particles. Based on the competitive adsorption results, PDMS was expected to be excluded from the silica surface by PEOX. Thus, PDMS should act as the tail block which penetrated into the solution and formed a steric layer. The attempts to measure the hydrodynamic thickness (δ_h) of PEOX 6K - PDMS 14K on the Stöber silica from isopropanol by DLS were complicated due to the following reasons: (1) the relatively large ratio of the diameter of the silica particle (69 nm) to the size of the PDMS tail block, (2) the significant uncertainties of the thickness by DLS measurements due to the small molecular weight of the PDMS block. PDMS is known to have a very flexible chains. Due to the relatively low MW in our study, a small hydrodynamic thickness was expected. Thus, a small adlayer thickness of the copolymers on silica (about 4 nm) is subjected to high error. The future work is suggested to synthesize the smaller silica diameter which may increase the accuracy of thickness measurement. However, it is also warned that the decrease of particle size might increase the particle polydispersity.

For the block molecular weight used in this study, the measured hydrodynamic thickness is expected to be comparable to the theoretical values of the hydrodynamic

diameter $D_{h\theta}$ of PDMS in isopropanol, which can be calculated from

$$D_{h\theta}=1.33\ R_{g\theta} \tag{5.34}$$

and

$$R_{g\theta} = (L_k \cdot L_c/6)^{1/2} \tag{5.35}$$

L_c is the contour length and L_K is the Kuhn length which characterizes the effective stiffness of the polymer backbone. The above Equations (5.34 and 5.35) are valid for non-draining Gaussian coils at the theta state. For such conditions, values of L_k can be determined by the following form:[45]

$$L_k=(M_{Mon}/L_{Mon})*(6R_g^2/MW) \tag{5.36}$$

where M_{Mon} and L_{Mon} are the monomer molecular weight and length, respectively. In this case, the Kuhn length L_k of PDMS is 1.1 nm,[34] and L_c (contour length, nm)=DP·L_{Mon}. L_{mon} is 0.30 nm (equals twice of Si-O bond length),[46] and the MW of PDMS is 14.4 kg/mole. Thus, L_c=194·0.3 = 58.3 nm and R_g=3.3 nm. DLS can not accurately measure such a small thickness on particles that are 10 times larger.

The S-F theory provides an important information for the designing block length for the diblock stabilizers. In the present case, the total degree of polymerization of PEOX 6K - PDMS 14K is about 252 and the λ_A of this copolymer is 0.227. As shown in Figure 5.2(a), the λ_A^{opt} in this degree of polymerization is approximately 0.18. This shows that the current λ_A is not in the best block length ratio. However, the copolymer indeed shows some steric stabilization for the silica suspension in chlorobenzene.

CONCLUSIONS

The solution properties and adsorption behaviors of the homopolymers PEOX, PVME, PDMS, and the respective diblock copolymers, poly(ethyl oxazoline-*b*-dimethyl siloxane) (PEOX 6K-PDMS 14K) and poly(ethyl oxazoline-*b*-vinyl methyl ether) (PEOX 5K - PVME 10K) were studied. Based on competitive adsorption experiments of PEOX with PVME and with PDMS from several organic solvents, it was found that PEOX has the strongest adsorption affinity to the surface among the polymers in the study. The strongest adsorption is due to the high segmental adsorption energy ($\chi_s kT$) of PEOX. This suggests that diblocks containing PEOX with these other blocks should function such that PEOX will be the anchor block. Sterically stabilized silica in chlorobenzene was also examined by observing the hydrodynamic particle size change with time. It was found that the stability ratio increased by approximately 44 times upon the addition of various concentrations of PEOX-PDMS. The hydrodynamic adsorbed layer thickness of PEOX 6K - PDMS 14K on Stöber silica in isopropanol could not be precisely measured by DLS mainly due to the small MW of PDMS. Based on the Marques-Joanny model for non-selective solvent systems, this PEOX-PDMS chain composition does not reach the optimum of block ratio yet, therefore the current adsorbed layer thickness does not represent the maximum extension of the tail block. The adsorbed amount of PEOX 6K - PDMS 14K on Cab-O-Sil silica (0.95 mg/m^2) was greater than that on Stöber silica (0.72 mg/m^2) from isopropanol. This deviation may be attributed to the different surface preparations and surface area calculation parameters (such as particle density).

Appendix A

Some parameters used for the calculation of hydrodynamic diameter diameters by DLS.

Solvent	Temperature (°C)	Refractive index n_D	Viscosity η (mN·s·m^{-2})	density ρ (g/cm^3)	Ref.
chlorobenzene	20	1.5337	0.799		a
water	25	1.3333	0.8903	0.997	a
ethanol	20	1.3614	1.20	0.789	b
	25	1.3610	1.078		b
isopropanol	25	1.3787	2.038	$0.786^{20°C}$	a

a: Lange's Chemistry Handbook
b: CRC Handbook of Chemistry and Physics, Chapter D

REFERENCES

(1) (a) Th.F. Tadros, *"The Effect of Polymers on Dispersion Properties,"* Academic Press, London, 1982. (b) Fontana, N.J., in *"Chemistry of Biosurfaces,"* Vol. I, Hair, M.L. ed., Dekker, New York, 1971.

(2) (a) Price, in *"Developments of Block Copolymers I,"*, Goodman, I., (Ed.) *Appl. Sci.*, London, 1982. (b) Bluhm, T.L., Malhotra, S.L., *Eur. Polym. J.* **22**, 249 (1986). (c) Brown, D. S., Dawkins, J. V., Farnell, A. S., Taylor, G., *Eur. Polym. J.*, **23**, 463 (1987).

(3) Napper, D. H. *"Polymeric Stabilization of Colloidal Dispersions,"*, Academic Press, New York, 1983.

(4) Ash, S.G. in *"Colloid Science,"* Vol I, Everett, D.H. ed., The Chemical Society, London, 1973.

(5) Vincent, B. and Whittington, S. in *"Surface and Colloid Science,"* Vol 12, Matijevic, E. ed., Plenum, New York, 1981.

(6) Takahashi, A. and Kawaguchi, M., *Adv. Polym. Sci.* **46**, 1 1982.

(7) (a) Scheutjens, J. M. H. M., Fleer, G. J. *Macromolecules* **18**, 1882 (1985). (b) Fleer, G.J., Scheutjens, J.M.H.M. *J. Colloid and Interf. Sci.* **111**, 504 (1986). (c) van Lent, B., Scheutjens, J.M.H.M. *Macromolecules* **22**, 1931 (1989).

(8) (a) Alexander, A. *J. Phys.* **38**, 983 (1977). (b) Patel, S., Tirrell, M., Hadziiouannou, G. *Colloids Surf.* **31**, 157 (1988). (c) Marques, C., Joanny, J.F., Leigler, L. *Macromolecules* **20**, 1692 (1987). (d) Marques, C., Joanny, J.F., *Macromolecules* **22**, 1454 (1989).

(9) Fleer, G.J., Scheutjens, J.M.H.M. *Adv. Colloid Interface Sci.*, **16**, 341 (1982).

(10) de Gennes, P-.G. *Adv. Colloid Interface Sci.*, **27**, 189 (1987).

(11) Killmann, E., Maier, H., Kaniut, P. and Gutling, P. *Colloids and Surf.*, **15**, 261 (1985).

(12) Cosgrove, T., Vincent, B., Crowley, T.L., Barnett, K.G., King, T.A., Tadros,

Th.F., Burgess, A.N. *Polymer* **75**, 4115 (1981).

(13) Leermakers, F. A. M., Gast, A. P. *Macromolecules* **24**, 718 (1991).

(14) (a) Guzonas, D, Boils, D., Hair, M.L., *Macromolecules* **24**, 3383 (1991). (b) Guzonas, Hair, M.L., Cosgrove, T., *Macromolecules* **25**, 2777 (1992). (c) Wu, D. T., Yokoyama, A., Setterquist, R. L. *Polymer J.* **21**, 709 (1991).

(15) (a) Evers, O.A., Scheutjens, M.M.H.M., Fleer, G.J., *J. Chem. Soc. Faraday Trans.*, **86**, 1333 (1990). (b) Evers, O.A., Scheutjens, M.M.H.M. and Fleer, G.J., *Macromolecules*, **24**, 5558 (1991). (c) Fleer, G.J., Scheutjens, M.M.H.M. *Colloids and Surfaces* **51**, 281 (1990).

(16) (a) Ploehn, H.J., Russel, W.B. *Advances in Chemical Engineering* **15**, 137 (1990); (b) Munch, M.R., Gast, A.P. *Polymer Communication* **30**, 324 (1989).

(17) Scheutjens, J.M.H.M., Fleer, G. J. *J. Phys. Chem.* **83**, 1619 (1979); **84**, 178 (1980).

(18) (a) Munch, M.R., Gast, A.P. *J. Chem Soc. Faraday Trans.* **86**, 1341 (1990). (b) Chittur, K.K., Fink, D.J., Leininger, R.I., Hutson, T.B. *J. Colloid Interface Sci.*, **111**, 419 (1986). (c) Lee, J-J., Fuller, G.G. *J. Colloid Interface Sci.*, **103**, 569 (1985).

(19) Howard, G.J. in *"Interfacial Phenomena in Apolar Media,"* Eicke, H.,-F. and Parfitt, G.D. (Ed.), Marcel Dekker, Inc. N.Y., 1987.

(20) Guthrie, I. F., Howard, G. J. in *'Polymer Adsorption and Dispersion Stability'*, Goddard and B. Vincent (Ed.), ACS Symposium Series 240, Washington, D.C., 1984.

(21) Kerkar, A.V., Henderson, R.J.M., Feke, D.L. *J. Am. Ceram. Soc.* **73**, 2879; 2886 (1990).

(22) Dawkins, J.V., Guest, M.J. and Taylor, G., in *"The Effect of Polymers on Dispersion Properties,"* Tadros, Th.F., (Ed.) Academic Press, London, 1982.

(23) (a) Guest, M.J. Ph.D. Thesis, Loughborough University of Technology (1979). (b) Fontana, B.J. *J. Phys. Chem.*, **67**, 2360 (1963).

(24) Cesarano, J. III, Aksay, I.A., Bleier, A. *J. Am. Ceram. Soc.* **71**, 250 (1988).

(25) Snyder, L.R. in *"High-performance liquid chromatography"*, 3 rd ed. Horvath, C. (ed.)Academic Press, New York, 1983.

(26) Israelachvili, J.N. *'Intermolecular and Surface Forces, With Applications to Colloidal and Biological Systems'* Academic Press, New York, 1985.

(27) Hunter, R. J., *"Foundations of Colloid Science,"*, Vol I, Oxford University Press, Oxford, 1989.

(28) Ruckenstein, E., Rao, I. V., *Colloids and Surfaces* **17**, 185 (1986).

(29) Fischer, E.W., *Kolloid-Z.* **160**, 120 (1958).

(30) (a) Overbeek, J.T.G., in *'Kinetics of Flocculation'* H.R. Kruyt (Ed.). Elsevier, Amersterdam, 1952. (b) von Smoluchowski, M., *Phys. Z.* **17**, 557 (1916).

(31) (a) Fuchs, N., *Z. Phys.*, **89**, 736 (1934). (b) Overbeek, J. Th. G., *Colloid Science*, Vol 1, H.R. Kruyt (ed.), Elsevier, Amsterdam (1952).

(32) (a) Virden, J. W. and Berg, J. C. *J. Colloid and Interf. Sci.* **149**, 528 (1992). (b) Ottwell, R.H. and Shaw, J.N., *Disc Faraday Soc.*, **42**, 154 (1966).

(33) Liu, Q., Wilson, G.R., Davis, R.M., Riffle, J.S. *Polymer* **34**, 3030 (1993).

(34) Nagpal, V.J., Davis, R.M., Liu, Q., Facinelli, J., Riffle, J.S. *Langmuir*, 1994.

(35) Liu, Q., Konas, M., Davis, R.M., Riffle, J.S. *J. Polymer Science: Part A: Polymer Chemistry* **31**, 1709 (1993).

(36) *CAB-O-SIL Fumed Silica Properties and Functions*; Cabot Corporation, Tuscola IL, 1991.

(37) Stöber, W. and Fink, A. *J. Colloids and Interf. Sci.* **26**, 62 (1968).

(38) Hiemenz, P.C., *Polymer Chemistry The Basic Concepts*, Marcel Dekker Inc., N.Y., **1984**, Chapter 10, p.709.

(39) (a) Pusey, P.N., Tough, R.J.A. in *'Dynamic Light Scattering'*, Pecora, R., Ed. Plenum Press, N.Y., 1985, Chapter 4. (b) Chu, B. *'Laser Light Scattering'*, 2nd Ed., Academic Press, 1991. p.248.

(40) *Instruction Manual for Model BI-2030 AT Digital Correlator*; Brookhaven

Instruments Corporation, N.Y., 1986.

(41) Jelinek, L, Dong, P., Rojas-Pazos, C., Taibi, H., Kovats, E. sz., *Langmuir* **8**, 2152 (1992).

(42) van Krevelen, D.W. *'Properties of Polymers, their estimation and correlation with chemical structure.'* Elsevier Sci. 1976.

(43) A. Silberberg in *'Polymer Adsorption and Dispersion Stability'*, E.D. Goddard and B. Vincent (ed.), ACS Symposium Series Vol 240, Washington, D.C., 1984.

(44) Cohen Stuart, M.A., Fleer, G.J., Scheutjens, J.M.H.M., *J. Colloid Interf. Sci.* **97**, 515; 526 (1984).

(45) Tanford, C. *Physical Chemistry of Macromolecules* John Wiley & Sons, Inc., N.Y., 1961; Chapter 6. (b) Brandrup, J., Immergut, E.H. *Polymer Handbook*; John Wiley & Sons Inc., N.Y., 1975.

(46) Weast, *CRC Handbook of Chemistry & Physics* Section F, 68th Ed. 1988.

(47) Siffert, B., Li, J.F. *Colloids and Surfaces*, **62**, 307 (1992).

CHAPTER 6

The Adsorption of Copolymer Poly(dimethyl amino ethyl methacrylate-*b*-n-butyl methacrylate) (DMAEM-BMA) from Isopropanol

ABSTRACT

For diblock copolymers to perform as stabilizers, it is important to understand the relationship between surface coverage, layer thickness and block size. In isopropanol, we studied the polymer amount adsorbed (Γ_p) and the adsorbed layer thickness (δ_h), of poly(dimethyl amino ethyl methacrylate-*b*-n-butyl methacrylate) (DMAEM-BMA) on Cab-O-Sil silica and Stöber silica, respectively. The adsorbed amount was measured by a depletion method, and the thickness by dynamic light scattering (DLS). A dimensionless surface density (σ) was proposed to be a unique function of the copolymer block size asymmetry ratio (β). We compared our measured values of Γ_p and δ_h with those from the Marques and Joanny (MJ) adsorption model in a nonselective solvent and found the MJ model a powerful tool for predicting copolymer adsorption from a nonselective solvent.

INTRODUCTION

Stabilization of colloids by polymers[1,2] requires the formation of a polymer layer around each particle sufficiently thick to create a repulsive force which shields van der Waals attraction. The choice of a good solvent can allow a layer to form thickness on the order of the radius of gyration of the isolated polymer chains. A well-solvated polymer chain forms a thicker layer since the chains stretch normal to the surface, thus increasing the range of the repulsive steric force. It is recognized that an effective way to sterically

stabilize particles is to end-graft polymers on the surface, either by terminals chemical grafting or by diblock copolymer adsorption. In the latter method the anchor block (A) adsorbs strongly onto the surface while the buoy or tail block (B) does not interact with the surface but penetrates into the solution to form a protective layer around the colloidal particles.

Marques and coworkers,[1,3] developed scaling theories to predict block copolymer adsorption at the interface. In a non-selective solvent for both blocks (both blocks are soluble), the adsorption was strongly related to an asymmetry factor, β ($=R_B/R_A$ which is the ratio of the radii of gyration of the two blocks) and $\beta = (N_B/N_A)^{3/5}$). The theory is henceforth called MJ model.[3] In this model, the tail block is assumed to have no interaction with the surface. That is, only the anchor block adsorbs, completely displacing the tail block.

For diblock copolymers with small β values in a non-selective solvent[3], the adsorbing block forms a layer swollen by the solvent and the nonadsorbing block forms a polymer brush extending into the bulk solution. When the tail block is much larger than the anchor block, $\beta > N_A^{0.5}$, the adsorbed layer breaks into individual, discontinuous chains, which form 'flat pancakes' on the particle surface. The buoy chains still form a grafted layer. Another important case is that of a selective solvent for the anchor block, *i.e.* a good solvent for the stabilizing block but a poor solvent for the anchoring block, $\beta = N_B^{3/5}/N_A^{1/2}$, which was described by Marques, Joanny and Leibler (MJL model).[1] In MJL model, the copolymer chains form micelles in solution above the critical micelle concentration.

The design of diblock copolymers for stabilization of colloidal dispersions requires knowledge of the optimal sizes of both A and B blocks to give the greatest Γ_p and δ_h. The two scaling models (MJ and MJL) for the adsorption of diblock copolymers along with the mean field lattice theory of Scheutjens and Fleer described in Chapter 5 have proven quite useful in correlating diblock adsorption data with the block lengths and solubility. Some of these experiments will be reviewed after the scaling theory for non-

selective solvents is briefly reviewed.

GOAL OF THIS CHAPTER

This chapter concerns the measurements of the adsorbed amount and layer thickness of the diblock copolymers dimethyl amino ethyl methacrylate and n-butyl methacrylate (DMAEM-*b*-BMA) with three block ratios on silica in isopropanol. The isopropanol is known to be a good solvent for both blocks. The data are correlated with the MJ theory for non-selective solvents.

Scaling Theory for Non-selective Solvents

The MJ adsorption model for a non-selective solvent gives expressions for the polymer surface density σ (number of adsorbed chains per unit area) in terms of the degrees of polymerization N_A and N_B of the anchor and buoy (tail) blocks, respectively. Detailed descriptions of the theory are mentioned in Ref [3]. When both blocks are in a good solvent, a characteristic asymmetry ratio β can be defined in terms of the radii of gyration of the component polymers, $\beta=(R_A/R_B)^{3/5}\sim(N_A/N_B)^{3/5}$. The above relation assumes the repeat units have similar sizes, which is the case for DMAEM-BMA. The adsorption behavior of the copolymer depends on β according to:

$$\sigma \sim N_A^{-1} \qquad \text{for } \beta < N_A^{1/2} \qquad (6.1)$$

and

$$\sigma \sim \beta^{-2} \qquad \text{for } \beta > N_A^{1/2} \qquad (6.2)$$

The adsorbed layer thickness (L), illustrated in Figure 6.1, follows from the Alexander-de Gennes expression[4]

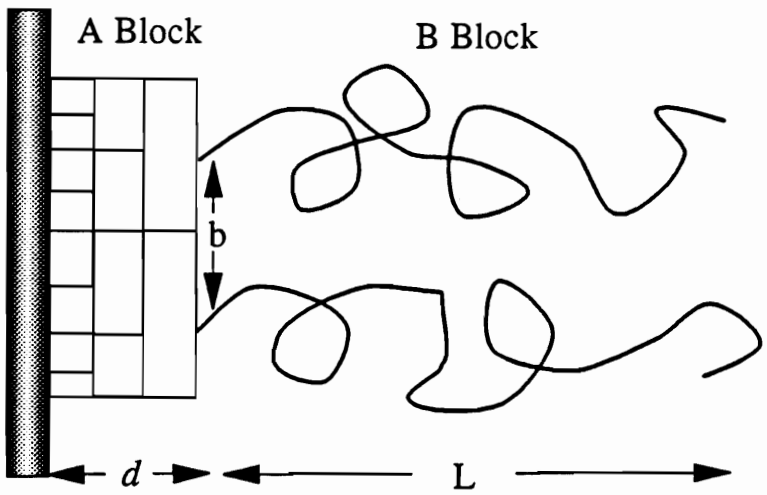

Figure 6.1 A model of AB block copolymer adsorbed from a non-selective solvent, *i.e.*, both blocks are soluble in the solvent. *d* is the thickness of the adsorbed anchor block, L is the thickness of the tail block. (after Marques and Joanny [3])

$$d \sim N_A^{1/2}/\beta \quad (6.3a)$$

$$\sigma \sim 1/N_A \quad (6.3b)$$

$$L \sim N_B \cdot \sigma^{1/3} \quad (6.3c)$$

where d is the thickness of the anchoring layer. Applying Equations (6.2) into Equation (6.3c) gives:

$$L \sim N_B N_A^{-1/3} \qquad \text{for } \beta < N_A^{1/2} \text{ (regime I)}, \quad (6.4)$$

for polymer adsorption dominated by the anchor block, *i.e.*, the anchor block is longer than optimum. For the case where adsorption is dominated by the tail block, *i.e.*, where the tail block is longer than optimum,

$$L \sim N_B^{3/5} N_A^{2/5} \qquad \text{for } \beta > N_A^{1/2} \text{ (regime II)}. \quad (6.5)$$

A simple expression of the surface density σ was used by Guzonas *et al.*, which is related to the adsorbed amount and copolymer molecular weight (MW), and can be expressed as: $\sigma = (\Gamma_p/MW)N_{Av} \cdot 10^{-21}$, where Γ_p is in units of mg/m^2 and σ is in units of nm^{-2}. N_{Av} is Avogadro's number. An important prediction of this theory is that a maximum in the adsorbed amount Γ_p and the thickness L are predicted at $\beta \sim N_A^{1/2}$. This is discussed in the next section which briefly reviews relevant experimental studies.

Reviews of Adsorption Experiments

Wu and coworkers[5] experimentally correlated the adsorbed layer thickness (δ_h) and the plateau adsorbed amount Γ_p to seek an optimum length ratio for adsorption. The authors used eleven poly(dimethyl amino ethyl methacrylate-*b*-butyl methacrylate) (DMAEM-BMA), including homopolymers and copolymers, with various β values to adsorb on narrow particle size distribution of Stöber silica in isopropanol, a good solvent

for both blocks. DMAEM served as the anchor block and BMA as the tail block because BMA did not adsorb on silica surface from isopropanol. The copolymers were classified, according to the total degree of polymerization N_T ($=N_A+N_B$), into $N_T=200$ and 700. The maximum adsorbed amount occurred when in the mole fraction of the anchor block was about 0.04-0.05 and 0.10-0.15 for $N_T=200$ and 700, respectively. The ratio of the tail length (N_B) to the anchor length (N_A), N_B/N_A, was in the range of 20-25. However, this composition in the maximum adsorbed amount somewhat deviated from the prediction of self-consistent field (SCF) lattice theory[6], as described in Chapter 5. Evers *et al.*[6] predicted that this composition should locate in the anchor molar fraction approximately 0.20. The authors also compared the measured hydrodynamic thickness with scaling theory. They found the slope of a *log-log* plot of δ_h to N_B to be 0.53, and attributed this low value to the packing of the non-adsorbing block in this case.

Recently, Guzonas *et al.* tested the MJ model using the measurements of Γ_p and δ_h for DMAEM-BMA by Wu *et al.*,[5] as well as their own PEO-PS results. The authors found that the MJ scaling model was very useful in predicting the adsorption of copolymers in these systems. For copolymers with a constant total degree of polymerization, an optimal composition β^* can be calculated to predict the maximum adsorption amount and layer thickness. The optimal composition can be obtained from the simple relation: $\beta^*=N_A^{1/2}$. This simple prediction equation of the MJ model may simplify the design of copolymers for stabilization applications.

Munch and Gast[7] summarized the relationships of the adsorbed thickness from the selective solvent studies of poly(2-vinylpyridine-*b*-polystyrene)(P2VP-PS)[8], PEO-P2VP[9], PS-X[10], and P2VP-PBS[11] on mica in toluene. The slopes of a *log* δ_h versus *log* N_B revealed the adsorption mode. A slope of unity suggested that the anchor block dominated the adsorption. A slope less than unity indicated that the tail block dominated the adsorption.

EXPERIMENTAL

Materials

Copolymers. Three block length ratios of poly(dimethyl amino ethyl methacrylate-*b*-butyl methacrylate) (DMAEM-BMA) were kindly donated by Dr. D.T. Wu at Du Pont Chemical Co.. The copolymer chemical structure is shown in Figure 6.2, and the chain compositions are summarized in Table 6.1. The copolymers were synthesized using the group transfer living polymerization[12] to produce narrow molecular weight distribution copolymers, with all polydispersity indice normally < 1.4 (by GPC).[5] The polymers were stored in a vacuum oven at room temperature for 24 hours prior to use.

The solvent, isopropanol (99% ACS grade, Aldrich Chemical Co.), was distilled once with CaH_2 in a nitrogen environment, as mentioned in Chapter 5.

Table 6.1. Characterization of three copolymers used in this study.

$N_{DMAEM}(N_A)$	$N_{BMA}(N_B)$	ν_A	$\beta=(N_B/N_A)^{3/5}$	$\beta^*(=N_A^{1/2})$
27	157	0.15	2.9	5.2
31	528	0.06	5.5	5.6
36	342	0.10	3.9	6.0

Adsorbent. Two silica particles were used as adsorbents in this study. Cab-O-Sil fumed silica was purchased from Cabot Co., IL, which was made by hydrolyzing silicon tetrachloride vapor in a flame of hydrogen and oxygen.[13] This silica was used as the adsorbent for the adsorption experiments. The particles have an equivalent diameter of 0.27 μm and an average surface area of 100 ± 15 m^2/g.[13]

The technique used to synthesize silica particles for layer thickness measurements follows the method described by Stöber *et al.*[14] and described in earlier Chapter 5.

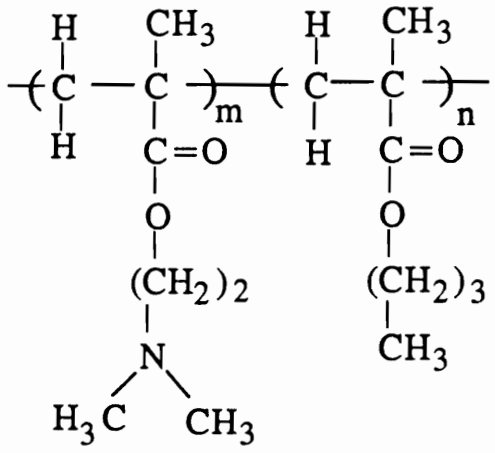

Figure 6.2 The chemical structure of the repeat unit of poly(dimethyl amino ethyl methacrylate-*b*-butyl methacrylate) (DMAEM-BMA).

Tetraethylorthosilicate (TEOS) was used as the starting reagent in a mixture of ammonia and ethanol. TEOS (Fisher Scientific Co., Reagent Grade) was vacuum distilled and ethanol (200-proof, Aaper Alcohol and Chemical Co.) was distilled using CaH_2 prior to the synthesis of silica. Both purified solutions were stored in a nitrogen environment. Ammonium hydroxide (containing water 30 wt.%, A.C.S. grade, Fisher Chemical Co.) was used without any further purification. To prepare a batch of 500 ml silica suspension, the compounds were added in the order of ethanol (441.4 ml), TEOS (19 ml) and ammonia (39.6 ml). The synthesis was performed in a round bottom flask with a stirring bar under a nitrogen environment for 48 hours. The size of the precipitated Stöber silica was characterized one week after synthesis.

The silica particles (henceforth referred to as "Stöber silica") were transferred to isopropanol for the adsorption experiments. The synthesized Stöber silica was centrifuged at 2250 g's for 12 minutes. The supernatant was withdrawn and replaced with distilled isopropanol. The silica suspension was then sonicated using a microtip at a power of 20 Watts by a Tekmar Sonic Disruptor. At least three minutes were necessary to break the silica agglomeration, induced by the centrifugation. Afterwards, the dispersion was centrifuged again. This washing process was repeated three times. ^1H NMR confirmed that there was no residual ethanol in the final liquid solution.

The size of the Stöber silica was determined by transmission electron microscopy (TEM) and dynamic light scattering (DLS). The sonicated silica suspension was deposited on a carbon-coated copper grid (200 mesh) and dried in air at room temperature overnight. The size distribution (*i.e.*, polydispersity, PD) of silica was calculated according to:

$$PD = 1 + \frac{\sigma}{<d>} \qquad (6.6)$$

where σ represented the particle size standard deviation and $<d>$ the mean diameter of

particle size. Over 100 silica particles were counted to measure the average particle size and particle size distribution. The mean diameter of the silica particles from TEM was 240±12 nm and the PD value is 1.05 after the sonication process. A typical TEM micrograph is shown in Figure 6.3.

Procedure

Dynamic Light Scattering. The polymer solubility and size measurements were performed with a Brookhaven Model BI-2030 light scattering instrument, which consists of a thermostatted sample vat, a 136-channel digital autocorrelator and a photomultiplier tube on a precision goniometer. The light source was a Lexel Model 95 Argon laser operated at 514.5 nm. The scattering angle was fixed at 90°, as described in Chapter 5. Dynamic light scattering was used to measure the silica particle size and thickness of the adsorbed copolymer layer.

The hydrodynamic diameter (D_h) of the Stöber silica particle in isopropanol was measured by dynamic light scattering as well, which was based on the Einstein-Stokes equation (in Chapter 5). A series of known concentrations of polymer solutions were mixed with 0.1 wt.% Stöber silica in isopropanol. After 24 hours of end-over-end rotation, the suspension was diluted to approximately 100 times for the particle size measurement. The particle concentration was kept low ($<8\text{x}10^{-5}$ g/ml) to eliminate the inter-particle interactions. The difference between the diameters of the bare and coated particles was twice the layer thickness, $2\cdot\delta_h$. During the measurements, the measured base-line and the calculated base-line were within a few tenths of a percent, which indicated the negligible effect of dust. The final δ_h values were the average of four polymer concentrations. Also, at least ten measurements were recorded for each polymer concentration. All DLS measurements were performed at 25°C.

The average measured D_h of bare silica was 267.9±10.8 nm. The hydrodynamic diameter of the bare particle was measured each time before the measurements of coated

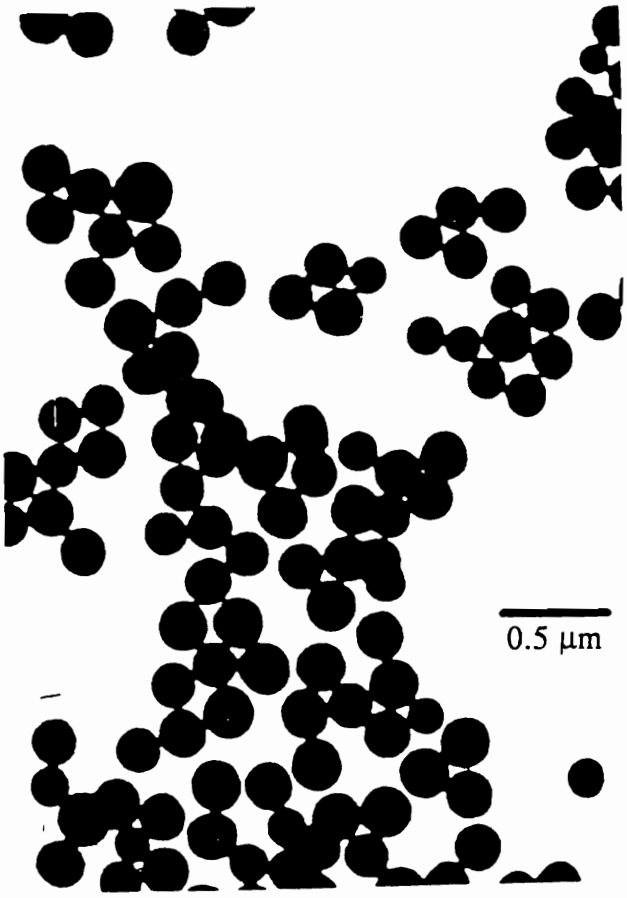

Figure 6.3 Transmission electron micrograph of a typical precipitated Stöber silica particle.

particles in each copolymer adsorption, which was used to calculate the hydrodynamic thickness δ_h.

Adsorption Isotherm. Cab-O-Sil silica (L-90) was used as the adsorbent. Prior to the adsorption experiment, silica was dried in a convection oven at 110-120 °C for 12 hours. Copolymers were dissolved in isopropanol for 24 hours before mixing with silica. For the adsorption experiment, 50 ml of the polymer solution was mixed with 0.25 g silica. After 24 hours of stirring, the solutions were centrifuged at 2250 g's for 10 minutes. Due to the copolymer polydispersity and the difficulty of distinguishing between carbonyl groups (C=O) and amino groups (-N<) by UV/vis spectroscopy (both adsorb in the same wavelength range 210 - 250 nm). It was not possible to measure the supernatant concentration by UV/vis spectroscopy. Thus it was necessary to measure the polymer concentration by gravimetry. Typically, 25 ml of supernatant was placed in a flask and gently dried in the air on a hot plate. The flask was then stored in a vacuum oven at room temperature for 8 hours. The polymer weight difference in the flasks before and after adsorption was used to calculate the supernatant concentration and hence the adsorption amount. The adsorption measurements were normally made twice at each polymer concentration.

RESULTS AND DISCUSSION

Hydrodynamic Thickness. To prevent particles from aggregating, the adsorbed layer thickness should be sufficiently large to shield the van der Waals attractive forces. Several groups have experimentally measured the hydrodynamic thickness δ_h using DLS.[4,5,7] Our measurements of δ_h are summarized in Table 6.2. Note that these polymers all have $\beta < \beta^*(=N_A^{1/2})$, *i.e.*, adsorption was dominated by the tail block (regime I in Guzonas *et al.*[4]).

δ_h vs. $N_B N_A^{-1/3}$ Our thickness measurements of DMAEM-BMA, for the copolymer studied by Wu *et al.*[5], the β values are between 2.9 and $N_A^{1/2}$. According to Guzonas *et al.*[16], in this range the thickness of the adsorbing block is negligible relative to the tail block thickness ($d << L$ in Equation (6.3)).

A plot of δ_h against $N_B N_A^{-1/3}$ is illustrated in Figure 6.4. Several data points were compared to Wu's results.[4,5] It can be seen that our data are quite consistent with Wu's. The linear relationship between the δ_h value and $N_B N_A^{-1/3}$ fully agreed with the prediction of the MJ model. It was also found that as the asymmetry factor β approaches β^*, a larger δ_h value was obtained. This suggests that the tail block expanded into solution. According to Figure 6.4, the slope of 0.12 for DMAEM-BMA of δ_h against $N_B N_A^{-1/3}$ is obtained. This empirical value is important for predicting the thickness of DMAEM-BMA copolymer adsorption in isopropanol, while in $\beta < \beta^*$ range.

Table 6.2. Hydrodynamic thickness of DMAEM-BMA on Stöber silica in isopropanol

N_A-N_B	Thickness, nm	$N_B N_A^{-1/3}$	β	β^*
27-157	7.3±0.5	52.3	2.9	5.2
36-342	17.1±1.5	103.6	3.9	6.0
31-528	20.2±2.0	168.1	5.5	5.6

Adsorption Isotherms. The plateau adsorption amount (Γ_p) of our three copolymers was measured on Cab-O-Sil silica, L-90. The adsorption isotherms of DMAEM-MBA copolymers from isopropanol were shown in Figure 6.5 and Table 6.3. The adsorbed amount increased with the BMA fraction in the copolymers. The result was consistent with the increasing thickness for longer tail blocks, as described in Chapter 5. Thus, we analyzed the results using Equation (6.1) and the result was plotted in Figure 6.6(a). A linear relationship of the σ value as a function of N_A^{-1} was obtained, which agreed well with the prediction of the MJ model. We found that our data are consistent with the

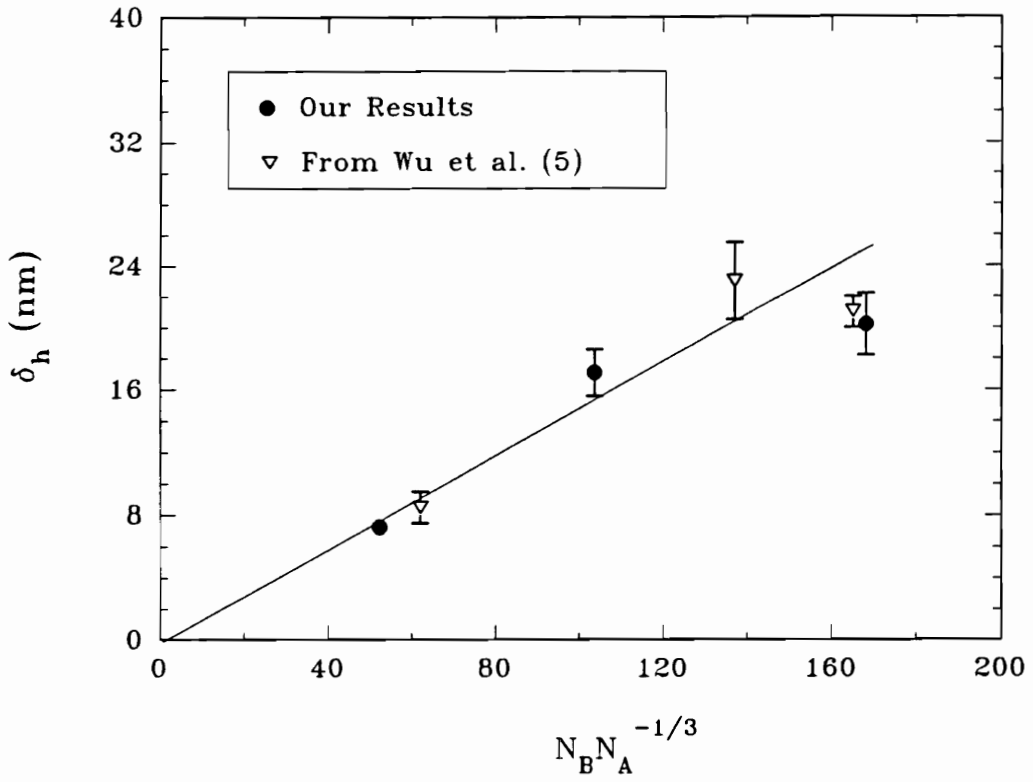

Figure 6.4 The adsorbed layer thickness of DMAEM-BMA in the regime I against $N_B N_A^{-1/3}$ of block length.[4] Some data points are referred to Wu *et al.*.[5]

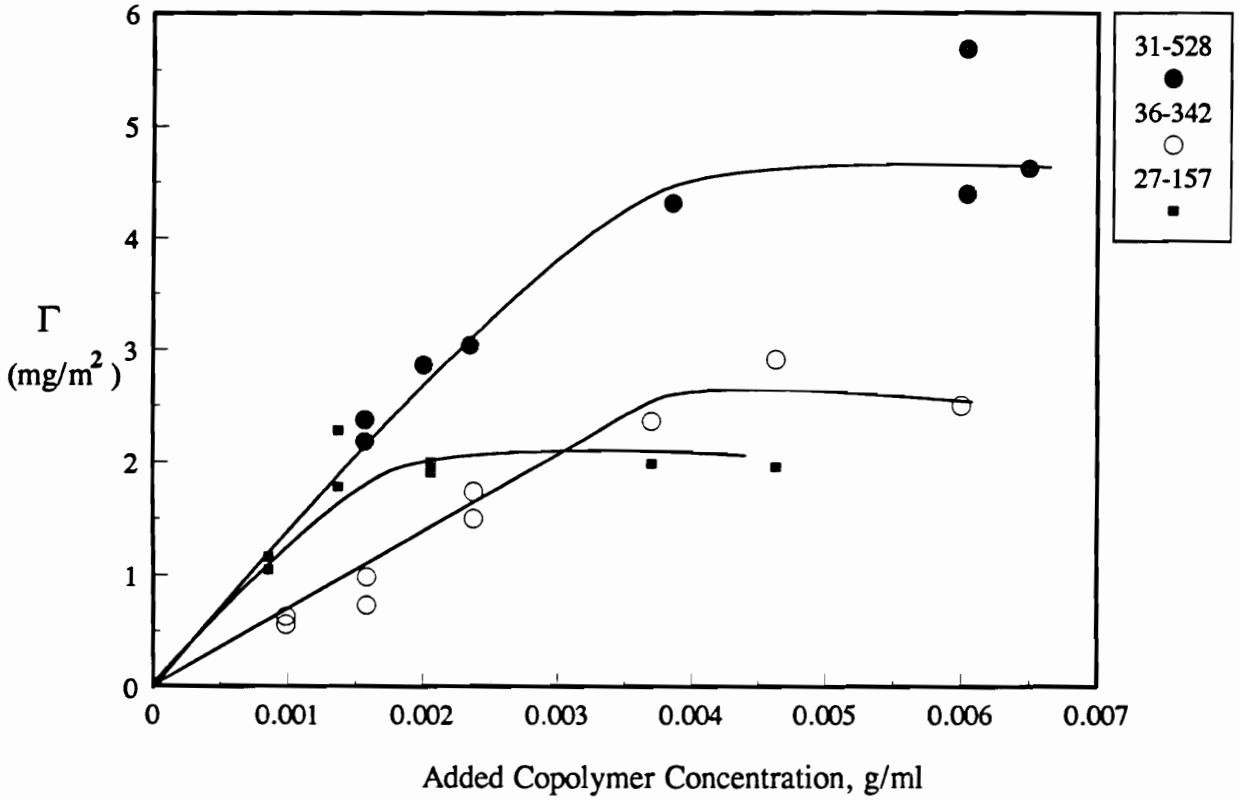

Figure 6.5 The adsorption isotherms of copolymer DMAEM-BMA on Cab-O-Sil silica, L-90 from isopropanol. The adsorbed amount Γ as a function of copolymer concentration.

adsorption amount data by Wu *et al.*[5], as shown in Figure 6.6(b).

Comparing the β values of these copolymers with the optimum asymmetric ratio β^*, we found that when β was closest to the optimal β^*, such as for the 31-528 sample, the values for both the adsorbed thickness and adsorbed amount were the largest obtained.

Wu *et al.*[5] addressed that BMA served as the tail block in isopropanol due to no adsorption on silica. As the length of DMAEM increased, the adsorption energy also increased due to the increase of the acid-base interactions (*i.e.* between *acidic-type* silica surface and *basic-type* DMAEM). The increase of the adsorption energy compensated the repulsion between the BMA blocks and induced a greater amount of adsorption. With increasing adsorbed amount, the interactions between the buoy blocks became significant and a stretching conformation occurred (thus, hydrodynamic thickness increases). However, as the chain fraction of DMAEM increases further (beyond the β^*), the anchor block of the copolymer molecule occupies a larger area on the surface due to the flat formation of DMAEM on the surface. This large occupied area per molecule corresponds to the small copolymer adsorbed amount. The increased DMAEM block length leads to a short BMA chain length when the total degree of polymerization is constant. This decreased BMA block length may be responsible for a decrease in the hydrodynamic layer thickness.

Table 6.3. Adsorption amount of DMAEM-BMA on silica surface from isopropanol

Name	M_n(kg/mole)	Γ,mg/m^2	DMAEM mole%	σ(nm^{-2}, x10^3)
27-157	26.6	2.0	14.7	45.3
36-342	54.3	2.5	9.5	27.7
31-528	80.0	4.5	5.5	33.8

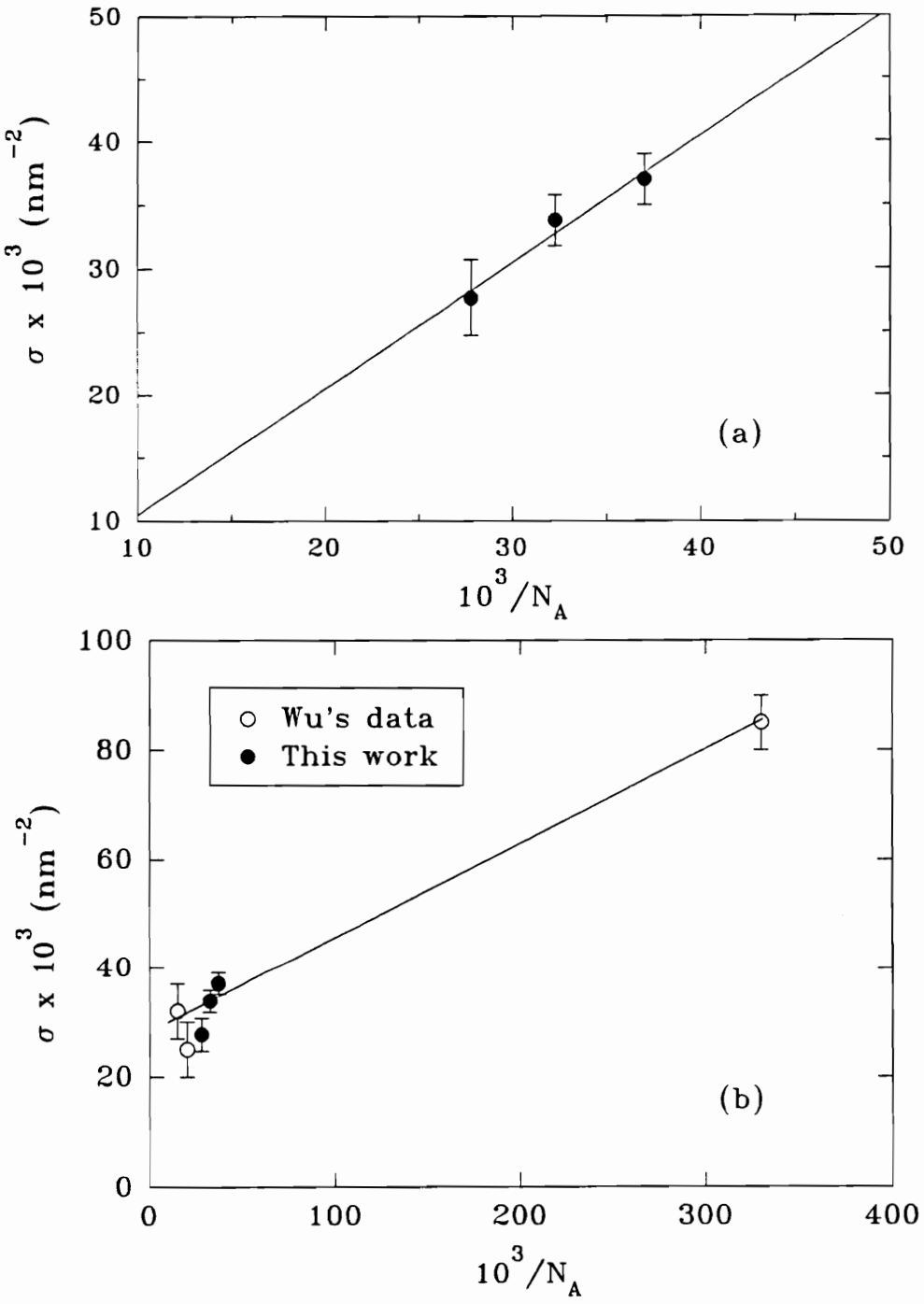

Figure 6.6 (a) Linear relationship of surface density (σ) vs. N_A^{-1} of DMAEM-BMA, adsorption on Cab-O-Sil silica, L-90, from isopropanol. (b) Comparison with Wu's data.[5]

CONCLUSIONS

The adsorbed layer thickness and the plateau adsorbed amount of poly(dimethyl amino ethyl methacrylate-*b*-n-butyl methacrylate) (DMAEM-BMA) diblock copolymers on a silica surface from a non-selective solvent, isopropanol, were studied. A linear relationship between layer thickness and tail block length was found. With an application of the surface density (σ), defined by Guzonas *et al.*, plots of the adsorbed amount of copolymers on Cab-O-Sil silica surface versus the reciprocal of the anchor block length (N_A^{-1}) show a linear relationship. The results are quite consistent with Wu *et al.*. This study confirms that the Marques-Joanny (MJ) adsorption theory can effectively explain the copolymer adsorption behavior.

REFERENCES

(1) Marques, C., Joanny, J.F., Leibler, L. *Macromolecules*, **21**, 1051 (1988).

(2) Rossi, G., Cates, M.E., *Macromolecules*, **21**, 1372 (1988).

(3) Marques, C., Joanny, J.F. *Macromolecules*, **22**, 1454 (1989).

(4) (a) de Gennes, P.-G. *Macromolecules* **15**, 492 (1982). (b) Alexander, S. *J. Phys.* (Paris) **38**, 983 (1977).

(5) Wu, D.T., Yokoyama, A., Setterquist, R.L. *Polymer J.*, **23**, 709 (1991).

(6) Evers, O.A., Scheutjens, J.M.H.M., Fleer, G.J. *Macromolecules*, **23**, 5221 (1990).

(7) Munch, M.R., Gast, A.P., *Polym. Comm.*, **30**, 324 (1989).

(8) Patel, S., Tirrel, M. *Colloids and Surfaces*, **31**, 157 (1988).

(9) Taunton, H., Toprakcioglu, C.; Fetters, L. J.; Klein, J. *Macromolecules* **23**, 571 (1990).

(10) Taunton, H.J., Toprakcioglu, C.; Fetters, L.J.; Klein, J. *Nature* **332**, 712 (1988).

(11) Ansarifar, M.A., Luckham, P.F. *Polymer*, **29**, 329 (1988).

(12) Sogah, D.Y., Hertler, W.R., Webster, O.W., Cohen, G.M. *Macromolecules*, **20** 1473 (1987).

(13) *'Cab-O-Sil Silica Fumed Silica Properties and Functions'* Cabot Corporation, 1990.

(14) Stöber, M.R., Fink, A., Bohn, E., *J. Colloid Interface Sci.* **26**, 62 (1968).

(15) Guzonas, D., Hair, M.L., Cosgrove, T. *Macromolecules*, **25**, 2777 (1992).

(16) Guzonas, D., Boils, D., Hair, M.L., *Macromolecules*, **24**, 3383 (1991).

CHAPTER 7
Conclusions and Future Work

SUMMARY

Water-soluble homopolymers PEOX and PEO, homopolymers PPO, PVME, and PDMS, and PEOX-containing copolymers were studied in this work. The thermodynamic properties of the water-soluble polymer PEOX were investigated by light scattering and cloud point measurements. The adsorption experiments of polymer on silica surface from different solvents were accomplished using the depletion method. The results are consistent with some of the theoretical predictions by the lattice theory of Scheutjens and Fleer. In this work, several achievements and conclusions can be stated:

(1) The thermodynamic studies of PEOX in water reveal that the polymer solubility is related to the specific interaction of hydrogen bonding. Measurements of the second virial coefficients as a function of temperature show that the thermodynamic excess properties of dilution of water, *e.g.* enthalpy (Δh^E) and entropy (Δs^E), both have negative values. This suggests that the entropy factor ($T \cdot \Delta s^E$) dominates the polymer dilution (or mixing) properties in water. In addition, the Kuhn length of PEOX chains was estimated as 0.77 nm, which is less than two monomer units, indicating PEOX to be quite flexible in water. The cloud point measurements are consistent with the light scattering which suggest that the specific hydrogen bonding plays an important role in the dilution process. The lower critical solution temperatures (LCST) decrease with increasing PEOX molecular weights. This is attributed to the decreasing solubility as the molecular weights increase. A trend of larger second virial coefficients of PMOX relative to the same molecular weight of PEOX may be due to a more hydrophobicity of the repeat unit of PEOX than that of PMOX.

(2) To assess the capacity for PEOX to function as an anchor block, we quantitatively measured the PEOX segmental adsorption energy, $\chi_s^{po}kT$, in water and ethanol. The segmental adsorption energy was calculated based on the lattice theory, developed by Cohen Stuart, Scheutjens, and Fleer. The relatively high χ_s values of PEOX in water and ethanol were 5.1 and 3.2, respectively. This significant difference between water and ethanol did not change as the hexagonal lattice structure in the model was changed to a simple cubic lattice structure. Based on the high adsorption energy in water, the bridging effect of water in the adsorption of PEOX on silica surface was proposed.

(3) The adsorption of PEOX from water and several alcohols onto silica was compared with qualitative predictions from the Scheutjens-Fleer lattice theory. The adsorbed amount of PEOX increased with molecular weight in water and ethanol with a high affinity shape. Linear relationships between the amount of adsorbed polymer and the logarithm of polymer molecular weight were obtained in both water and ethanol. In addition, the adsorption of PEOX was increased by the concentration of electrolyte (NaCl), but decreased with an increase of pH values. This increase of adsorption in salt was partially due to the decrease of the polymer solubility in water. The decrease of adsorption that occurred with the increase of pH value may result from both the decrease of polymer solubility and the increase of the silanol site density.

(4) As two polymers with different chemical structures are mixed, the one with the higher χ_s will preferentially adsorb on the surface while the other remains in the solution. In the competitive adsorption, PEOX shows exclusive adsorption affinity to the surface in the mixtures of PEOX with polyethers and with PDMS. The conclusion shows that the χ_s may dominate the polymer adsorption. It was also found that the adsorption affinity depended on the polymer molecular weight. Low molecular weight PEOX 3 K in water was replaced by higher molecular weight PEO 12K, but this replacement did not occur for high molecular weight PEOX 20K. Thus, the relative block length ratio is important for the design of the diblock copolymer stabilizers.

(5) The steric stabilization of Stöber silica suspension in chlorobenzene is significant when PEOX-PDMS diblock copolymer was present. This effect was evidenced by the low aggregation rate. The stability ratio W increased by about 45-fold when the particles were stabilized with the diblock copolymer.

(6) The adsorption of three DMAEM-BMA copolymers from a non-selective solvent, isopropanol, on silica surfaces followed the predictions of the Marques-Joanny (MJ) scaling theory. The surface coverage and layer thickness were linearly dependent upon the block length, which was consistent with the prediction by the MJ theory.

FUTURE WORK

Future research will emphasize the adsorption of the homo/copolymers on different adsorbents to provide more detailed information. Current theories poorly explain water-soluble polymer solution properties in water. The establishment of an experimental expression for polymers in dilute aqueous solution is important, especially in the connection of the adsorption behavior. Further, verification of the lattice theory to understand the effect of χ and χ_s is of importance for the application of particle stabilization. The following is suggested to extend the current work:

(1) The use of water-soluble stabilizers in the aqueous solution can circumvent environmental problems. To prevent micellization, both blocks should be soluble in water. A very promising diblock copolymer is PEO-PEOX. PEO is a proven steric stabilizer as a homopolymer.

A high adsorption energy (χ_s) of PEOX on silica from water was measured in this study. Using the same technique, the adsorption energy (χ_s) of PEO can be measured. These data along with homopolymer adsorption data can be used to specify the optimum block length ratios of the PEOX-PEO diblock system. Diblock adsorption experiments can be used to verify the scaling theory and Scheutjens-Fleer lattice theory for the

optimal composition.

(2) The adsorption energy measurement of polymers (PEOX and PEO) on metal oxides from water, such as Al_2O_3 and TiO_2 particles, can be used to build a useful database. These particles are widely used in ceramic, pigment, and paper industries. Due to the difficulty of measuring polymer χ_s in water by the conventional calorimetry technique, the displacement method developed by Cohen Stuart *et al.* may benefit both academic interest and industrial applications. The displacement technique is able to measure the polymer adsorption energy in water and organic solvents. Under this condition, the adsorption process was controlled by the entropy terms.

(3) Additives may affect both the surface and green body of ceramic particles, where polymers or surfactants can stabilize the particles in the media. Further work is needed to understand the role that electrolytes play in controlling adsorption of polymers like PEOX and PEO. This is needed for both scientific and technological reasons. In this study, the increase of PEOX adsorption with electrolyte concentration but the decrease of the adsorption with pH value have been observed. Nevertheless, the determining factor (*e.g.* χ or χ_s) to the polymer adsorption is still unclear. It is interesting to determine the major consideration (either χ or χ_s) for the polymer adsorption, and the stabilization effect, in the presence of electrolytes and acid/base compounds.

(4) Concentrated suspension that are sterically stabilized have much better rheological properties than unstabilized suspensions. Future work should include the stabilization of highly concentrated silica suspensions and other metal oxides.

(5) It is recognized that hydrogen bonding plays an important role in the solubility of nonionic water-soluble polymers in water. However, the structure of the water molecules around the polymer repeat unit is not clear. This puzzle can be attacked by computer simulation to understand the relationship between polymer monomer and water molecules in aqueous solution.

VITA

Chiahong Chen

Chiahong Chen was born on August 18, 1962 in Taipei County, Taiwan, Republic of China to Shan-Chung and Shiou-Yu Chen. His college began in 1980 when he was admitted to the Chemical Engineering Department of Tunghai University in Taichung, Taiwan. In 1984, he received his B.S. degree and went to the Chinese Navy as a secondary lieutenant for two years. Upon finishing his M.S. degree in Chemical Engineering from Tufts University in 1989, the author continued his graduate study at Virginia Polytechnic Institute and State University. His interest in polymer colloidal science led him to study under Dr. Richey M. Davis in Chemical Engineering Department. His current research interest includes the steric stabilization of the ceramic particles by water-soluble polymers and the adsorption behavior of polymer on solid surface.